INNERVATION OF THE UPPER ALIMENTARY AND RESPIRATORY TRACTS: A LIGHT AND ELECTRON MICROSCOPIC STUDY OF THE MEDULLA OBLONGATA OF THE RAT.

by

Dale William Saxon

Submitted in partial fulfilment of the requirements for the Degree of Doctor of Philosophy at Dalhousie University, September, 1992.

at

Department of Anatomy and Neurobiology
Dalhousie University
Halifax, Nova Scotia.

National Library
of Canada

Acquisitions and
Bibliographic Services Branch

395 Wellington Street
Ottawa, Ontario
K1A 0N4

Bibliothèque nationale
du Canada

Direction des acquisitions et
des services bibliographiques

395, rue Wellington
Ottawa (Ontario)
K1A 0N4

Your file Votre référence

Our file Notre référence

ISBN 0-315-60168-9

Canada

Name DALE W. SAXON

Dissertation Abstracts International is arranged by broad, general subject categories. Please select the one subject which most nearly describes the content of your dissertation. Enter the corresponding four-digit code in the spaces provided.

Neuroscience — SUBJECT TERM

0317 — SUBJECT CODE

U·M·I

Subject Categories

THE HUMANITIES AND SOCIAL SCIENCES

COMMUNICATIONS AND THE ARTS
Architecture 0729
Art History 0377
Cinema 0900
Dance 0378
Fine Arts 0357
Information Science 0723
Journalism 0391
Library Science 0399
Mass Communications 0708
Music 0413
Speech Communication 0459
Theater 0465

EDUCATION
General 0515
Administration 0514
Adult and Continuing 0516
Agricultural 0517
Art 0273
Bilingual and Multicultural 0282
Business 0688
Community College 0275
Curriculum and Instruction 0727
Early Childhood 0518
Elementary 0524
Finance 0277
Guidance and Counseling 0519
Health 0680
Higher 0745
History of 0520
Home Economics 0278
Industrial 0521
Language and Literature 0279
Mathematics 0280
Music 0522
Philosophy of 0998
Physical 0523
Psychology 0525
Reading 0535
Religious 0527
Sciences 0714
Secondary 0533
Social Sciences 0534
Sociology of 0340
Special 0529
Teacher Training 0530
Technology 0710
Tests and Measurements 0288
Vocational 0747

LANGUAGE, LITERATURE AND LINGUISTICS
Language
- General 0679
- Ancient 0289
- Linguistics 0290
- Modern 0291

Literature
- General 0401
- Classical 0294
- Comparative 0295
- Medieval 0297
- Modern 0298
- African 0316
- American 0591
- Asian 0305
- Canadian (English) 0352
- Canadian (French) 0355
- English 0593
- Germanic 0311
- Latin American 0312
- Middle Eastern 0315
- Romance 0313
- Slavic and East European 0314

PHILOSOPHY, RELIGION AND THEOLOGY
Philosophy 0422
Religion
- General 0318
- Biblical Studies 0321
- Clergy 0319
- History of 0320
- Philosophy of 0322

Theology 0469

SOCIAL SCIENCES
American Studies 0323
Anthropology
- Archaeology 0324
- Cultural 0326
- Physical 0327

Business Administration
- General 0310
- Accounting 0272
- Banking 0770
- Management 0454
- Marketing 0338

Canadian Studies 0385
Economics
- General 0501
- Agricultural 0503
- Commerce-Business 0505
- Finance 0508
- History 0509
- Labor 0510
- Theory 0511

Folklore 0358
Geography 0366
Gerontology 0351
History
- General 0578
- Ancient 0579
- Medieval 0581
- Modern 0582
- Black 0328
- African 0331
- Asia, Australia and Oceania 0332
- Canadian 0334
- European 0335
- Latin American 0336
- Middle Eastern 0333
- United States 0337

History of Science 0585
Law 0398
Political Science
- General 0615
- International Law and Relations 0616
- Public Administration 0617

Recreation 0814
Social Work 0452
Sociology
- General 0626
- Criminology and Penology 0627
- Demography 0938
- Ethnic and Racial Studies 0631
- Individual and Family Studies 0628
- Industrial and Labor Relations 0629
- Public and Social Welfare 0630
- Social Structure and Development 0700
- Theory and Methods 0344

Transportation 0709
Urban and Regional Planning 0999
Women's Studies 0453

THE SCIENCES AND ENGINEERING

BIOLOGICAL SCIENCES
Agriculture
- General 0473
- Agronomy 0285
- Animal Culture and Nutrition 0475
- Animal Pathology 0476
- Food Science and Technology 0359
- Forestry and Wildlife 0478
- Plant Culture 0479
- Plant Pathology 0480
- Plant Physiology 0817
- Range Management 0777
- Wood Technology 0746

Biology
- General 0306
- Anatomy 0287
- Biostatistics 0308
- Botany 0309
- Cell 0379
- Ecology 0329
- Entomology 0353
- Genetics 0369
- Limnology 0793
- Microbiology 0410
- Molecular 0307
- Neuroscience 0317
- Oceanography 0416
- Physiology 0433
- Radiation 0821
- Veterinary Science 0778
- Zoology 0472

Biophysics
- General 0786
- Medical 0760

EARTH SCIENCES
Biogeochemistry 0425
Geochemistry 0996
Geodesy 0370
Geology 0372
Geophysics 0373
Hydrology 0388
Mineralogy 0411
Paleobotany 0345
Paleoecology 0426
Paleontology 0418
Paleozoology 0985
Palynology 0427
Physical Geography 0368
Physical Oceanography 0415

HEALTH AND ENVIRONMENTAL SCIENCES
Environmental Sciences 0768
Health Sciences
- General 0566
- Audiology 0300
- Chemotherapy 0992
- Dentistry 0567
- Education 0350
- Hospital Management 0769
- Human Development 0758
- Immunology 0982
- Medicine and Surgery 0564
- Mental Health 0347
- Nursing 0569
- Nutrition 0570
- Obstetrics and Gynecology 0380
- Occupational Health and Therapy 0354
- Ophthalmology 0381
- Pathology 0571
- Pharmacology 0419
- Pharmacy 0572
- Physical Therapy 0382
- Public Health 0573
- Radiology 0574
- Recreation 0575
- Speech Pathology 0460
- Toxicology 0383

Home Economics 0386

PHYSICAL SCIENCES
Pure Sciences
Chemistry
- General 0485
- Agricultural 0749
- Analytical 0486
- Biochemistry 0487
- Inorganic 0488
- Nuclear 0738
- Organic 0490
- Pharmaceutical 0491
- Physical 0494
- Polymer 0495
- Radiation 0754

Mathematics 0405
Physics
- General 0605
- Acoustics 0986
- Astronomy and Astrophysics 0606
- Atmospheric Science 0608
- Atomic 0748
- Electronics and Electricity 0607
- Elementary Particles and High Energy 0798
- Fluid and Plasma 0759
- Molecular 0609
- Nuclear 0610
- Optics 0752
- Radiation 0756
- Solid State 0611

Statistics 0463

Applied Sciences
Applied Mechanics 0346
Computer Science 0984
Engineering
- General 0537
- Aerospace 0538
- Agricultural 0539
- Automotive 0540
- Biomedical 0541
- Chemical 0542
- Civil 0543
- Electronics and Electrical 0544
- Heat and Thermodynamics 0348
- Hydraulic 0545
- Industrial 0546
- Marine 0547
- Materials Science 0794
- Mechanical 0548
- Metallurgy 0743
- Mining 0551
- Nuclear 0552
- Packaging 0549
- Petroleum 0765
- Sanitary and Municipal 0554
- System Science 0790

Geotechnology 0428
Operations Research 0796
Plastics Technology 0795
Textile Technology 0994

PSYCHOLOGY
General 0621
Behavioral 0384
Clinical 0622
Developmental 0620
Experimental 0623
Industrial 0624
Personality 0625
Physiological 0989
Psychobiology 0349
Psychometrics 0632
Social 0451

This Thesis is dedicated to:

My Mother and Father.

TABLE OF CONTENTS

CHAPTER 2. SUBNUCLEUS CENTRALIS OF THE NUCLEUS OF THE TRACTUS SOLITARIUS: ULTRASTRUCTURE AND SYNAPTOLOGY OF ESOPHAGEAL AFFERENTS IN THE RAT.

CHAPTER 3. SUBNUCLEUS INTERSTITIALIS OF THE NUCLEUS OF THE TRACTUS SOLITARIUS OF THE RAT: CYTOARCHITECTURE, ULTRASTRUCTURE, AND SYNAPTOLOGY OF PRIMARY AFFERENTS.

CHAPTER 5. EFFERENT AND COLLATERAL ORGANIZATION OF NEURONS IN THE PARATRIGEMINAL NUCLEUS: AN ANTEROGRADE AND RETROGRADE FLUORESCENT NEUROANATOMICAL TRACER STUDY IN THE RAT.

LIST OF FIGURES

CHAPTER 5

ABSTRACT

This thesis provides a comprehensive light and electron microscopic analysis of the ultrastructure of two subnuclei of the nucleus of the tractus solitarius (NTS) (i.e., subnucleus centralis and subnucleus interstitialis) and the paratrigeminal nucleus (PTN). In addition, the synaptology of primary afferents originating in the upper alimentary and respiratory tracts and terminating in these areas was investigated. The efferent connectivity and collateral organization of PTN neurons to regions of the medulla oblongata, pons and thalamus was elucidated.

The transganglionic transport of horseradish peroxidase conjugated to wheat-germ agglutinin or cholera-toxin (ß-subunit) was utilized to label anterogradely afferent terminals in the NTS and PTN which originated in the esophagus, pharynx and larynx. The esophagus has projections to the subnucleus centralis of the NTS, while the pharynx and larynx project to the subnucleus interstitialis of the NTS and the PTN. Regardless of the viscus of origin, primary afferents terminating in the NTS and PTN were all found to have similar synaptic morphology. Anterogradely labeled primary afferent terminals all contained round, agranular vesicles and formed asymmetric synaptic contacts (RA) with small diameter dendrites. A second type of synaptic terminal containing pleomorphic, agranular vesicles and forming symmetric synaptic contacts (PS) did not contain HRP reaction product. Complex synaptic arrangements involving axon terminals, dendrites and dendrites containing vesicles were encountered in the NTSis and PTN but not the NTScen.

The efferent connectivity and collateral organization of the PTN was elucidated in a series of fluorescent anterograde and retrograde tracing experiments. The PTN was found to have a diverse array of efferent projection sites including the contralateral PTN and thalamus and the NTS and parabrachial nucleus, bilaterally. Retrograde double-labeling experiments indicated that the PTN was highly collateralized to several of these sites and as such may have a general role in the modulation of these regions in response to primary afferent input received in the PTN.

ACKNOWLEDGEMENTS

I would like to thank Dr. David A. Hopkins for all the support and guidance he has given me over the past five years. I would also like to express my appreciation to the following people for their advice and assistance in the preparation of this thesis: Dr. J.A. Armour, Dr. J.G. Rutherford, Dr. D.G. Gwyn, A. Losier, and D. Grantham.

CHAPTER 1

This thesis documents experiments designed to further our understanding of the underlying anatomical substrates related to the primary afferent innervation of the upper alimentary and respiratory tracts. The results contained herein are an extension of a comprehensive light microscopic study of primary afferents originating in the upper alimentary and respiratory tracts and terminating in the medulla oblongata carried out by Altschuler and colleagues ('89).

LITERATURE REVIEW

The Subnucleus Centralis of the Nucleus of the Tractus Solitarius

Historically, many investigations into the topographical representation of the viscera in the medulla oblongata have relied on degeneration techniques. This was for the most part a successful enterprise (see Bieger and Hopkins, '87 for a review) but only with respect to motor innervation (Getz and Simes, '49; Bell and Lawn, '55; Kerr et al., '70). Understanding of the organization of visceral afferents lagged because of the lack of sensitive and reliable techniques for tracing anterograde degeneration. As a result there was little information regarding the sensory innervation of viscera. With the introduction of neuroanatomical tracing techniques based on retrograde and anterograde axoplasmic transport considerable information has accumulated about the organization of motoneuronal pools innervating various viscera (Coil and Norgren, '79; Kalia and Mesulam , '80b; Leslie et al., '82a, Connors et al., '83; Bieger and Hopkins, '87,) and about the viscerotopic organization of afferent projections from the viscera to sites in the medulla oblongata (Gwyn et al., '79; Kalia and Mesulam, '80a, '80b; Leslie et al., '82a; Altschuler et al., '89). These studies and others have demonstrated that the nucleus of the tractus solitarius

(NTS) is the primary site of termination for primary visceral afferents carried in the glossopharyngeal and vagus nerves and have shown that there is a high degree of specificity to the viscerotopic representation in the NTS. The subnucleus centralis (NTScen) of the NTS consists of a longitudinal cell column which was first described by Ross et al. ('85). The NTScen is the primary site of termination for afferent fibers conveyed in the vagus nerve and originating in the esophagus (Altschuler et al. '89).

Afferent Connections. It has been established that a significant number of afferents conveying information to the NTS via the vagus originate in the esophagus (Fryscak et al., '84 ; Altschuler et al., '89). Esophageal afferents originating in branches of the subdiaphragmatic, thoracic and cervical vagus terminate in a discrete subnucleus of the medial NTS named the subnucleus centralis (NTScen) by Ross et al. ('85) by virtue of its central location in the NTS. The cell bodies giving rise to esophageal primary afferents in the NTScen lie primarily in the inferior vagal (nodose) ganglion (Altschuler et al., '89) and terminate peripherally in myenteric ganglia of the tunica muscularis, in the tunica mucosa and to a lesser degree on more superficial layers of the esophagus (Rodrigo et al., '82; Neuhuber, '87; Cunningham and Sawchenko, '90). Myenteric terminations may act as mechanoreceptors or tension receptors while those in the submucosal or muscular layers may respond not only to mechanical but also to chemical and thermal stimuli (Clark and Davison, '78; Mei, '85; Clerc and Condamin, '87; Cunningham and Sawchenko, '90). Altschuler et al. ('89) observed that the rostral NTScen received afferent projections from the cervical esophagus and that progressively more caudal esophageal locations (i.e., thoracic and subdiaphragmatic), although overlapping with cervical terminal fields, showed a distinct rostral to caudal topographical organization.

Very little is known about the neurotransmitters in esophageal afferents terminating in the NTScen other than that a small number of the esophageal sensory neurons in the

nodose ganglion contain substance P and calcitonin gene related-peptide (Green and Dockray, '87). Two recent publications are very suggestive that nitric oxide may play a role in esophageal afferent transmission. The first by Herbert et al. ('90) reported that in sections reacted for nicotinamide adenine dinucleotide phosphate (NADPH)-diaphorase activity the NTScen stood out from the surrounding NTS subnuclei by virtue of the intense staining of its neuropil. The second study by Aimi et al. ('91) in which double staining for NADPH-diaphorase histochemistry and peptide immunohistochemistry revealed that NADPH-diaphorase is colocalized with substance P and calcitonin gene-related peptide in primary sensory neurons of the nodose ganglion, many of which have terminations in the NTS. Other than the primary afferent input from the esophagus, there is no evidence identifying any other afferent input of peripheral or central origin terminating in the subnucleus centralis.

Efferent Connections. The NTScen does not appear to give rise to ascending projections in a manner characteristic of most other subnuclei in the NTS (Herbert et al., '90). Most notable is the absence of a projection from the NTScen to the parabrachial nucleus: a primary site for efferents from all other subnuclei of the NTS (Herbert et al., '90). The only established efferent connection of the NTScen is a projection to the ventral lateral medulla in the area corresponding to the compact formation of the nucleus ambiguus (Bieger, '84; Ross et al., '85; Moyles and Hopkins, '88; Cunningham and Sawchenko, '89, '90) which provides motor innervation to the esophagus (Bieger and Hopkins, '87; Herbert et al., '90). Cunningham and Sawchenko ('89, '90) revealed in a double-labeling PHA-L/ immunocytochemical study that the projection from the NTScen to the ventrolateral medulla was predominantly ipsilateral and that some of these fibers were somatostatinergic.

Neurochemistry. Although the NTS as a whole has been extensively studied with regard to its neurochemistry and has been identified as containing more than thirty potential neuroactive substances (see Leslie, '85 for review) many of these studies are very general and do not provide much needed information about the specific locations of the substances as they relate to the various subnuclei of the NTS. Furthermore, confusion about the different nomenclatures (see Cottle, '64; Kalia and Sullivan, '82) has led to the inclusion of well-established subnuclei like the NTScen (Ross et al., '85; Altschuler et al., '89) in broader and often largely unrelated subnuclei. For example, the NTScen is most commonly included in the larger subdivision of the NTS referred to as the medial NTS. This having been said, a number of potential neurotransmitters have been specifically localized to the NTScen and more generally to the medial NTS.

With regard to neuroactive substances specifically localized to the NTScen, Cunningham and Sawchenko ('89, '90) reported that neurons projecting to the esophageal portion of the nucleus ambiguus from the NTScen were somatostatinergic and enkephalinergic. More recently Herbert et al. ('90) showed that in NADPH-diaphorase stained preparations the NTScen is well circumscribed by the dense staining of the neuropil relative to surrounding NTS subnuclei. Other possible neuroactive substances which have been identified in the medial part of the NTS include substance P, enkephalin, somatostatin, neurophysin-oxytocin (Armstrong et al., '81; William and Dockray, '83; Kalia et al., '84a; Björkland and Hökfelt, '85; Velley et al., '91), galanin (Skofitsch and Jacobowitz, '85; Melander et al., '86), cholecystokinin (Kubota et al., '83), and neuropeptide Y (Blessing et al., '86). There is also the possibility that catecholamine- (Armstrong et al., '81, '82; Blessing et al., '86; Reiner and Vincent, '86) and bombesin- (Björkland and Hökfelt, '85) containing neural elements are present in the NTScen.

Functional Considerations. By virtue of its connections and physiological properties the NTScen has been implicated in the regulation of esophageal reflex activity and peristalsis (Bieger, '84; Jean, '84; Altschuler et al., '89; Cunningham and Sawchenko, '90). Jean ('84) suggested that since the NTScen appears to be the only central nuclear structure interposed between the primary afferent limb and the efferent output to the esophagus it likely plays a crucial role in the normal physiological function of the esophagus. It is generally accepted that the central regulation of swallowing which is a primary function of the pharynx and esophagus is intimately related to the sensory information conveyed via nerves in the afferent limb of innervation from these viscera (Miller, '82; Jean, '84; Miller, '86; Diamant, '89).

The Subnucleus Interstitialis of the Nucleus of the Tractus Solitarius

The nucleus of the tractus solitarius is the primary site of termination for peripheral afferent projections originating in visceral and gustatory structures. Primary afferent transmission to the NTS is via four cranial nerves: the trigeminal, facial, glossopharyngeal and vagus nerves (Torvik, '56; Kerr, '62; Cottle, '64; Rhoton et al., '66; Beckstead and Norgren, '79; Kalia and Mesulam, '80a; Contreras et al., '82; Kalia and Sullivan, '82; Nomura and Mizuno, '82; Hanamori and Smith, '89). In recent years, considerable evidence has shown that the NTS is comprised of several distinct subnuclei which receive topographically organized projections from the viscera (Kalia and Mesulam, '80a; Altschuler et al., '89) including the upper alimentary and respiratory tracts. Nonetheless, some areas of the NTS receive overlapping projections from the periphery, especially the pharynx and larynx which require coordinated action during swallowing and respiration. For example primary afferent projections from the pharynx and larynx converge in the subnucleus interstitialis (NTSis) of the NTS (Altschuler et al., '89).

The NTSis over most of its rostral to caudal extent lies embedded within the tractus solitarius (TS) except where the tract opens ventrolaterally to merge with the surrounding NTS subnuclei. The NTSis has been identified in a number of mammalian species including the rat (Hamilton and Norgren, '84; Kalia and Fuxe, '85; Altschuler et al., '89), the rabbit (Von Euler et al., '73; Nomura and Mizuno, '82; '83), the cat (Cajal, '09), the lamb (Sweazy and Bradley, '86), the monkey (Maley et al., '87) and human (Paxinos, '90). Some investigators do not regard the NTSis as a unique subnucleus of the NTS and as such include it as part of other subnuclei of the NTS depending on the nomenclature used (see Cottle, '64; Kalia and Sullivan, '82; Whitehead, '88 for review).

Afferent Connections. The NTS receives numerous afferent inputs of peripheral and central origin. Peripheral afferents terminating in the rostral NTS originate in sensory structures associated with special visceral function, (i.e., taste). Gustatory information is transmitted via the facial, glossopharyngeal and vagus nerves (Norgren, '85; Whitehead and Frank, '83 ; Hamilton and Norgren, '84). The remainder of the NTS , the caudal two thirds, is largely dedicated to general visceral function and is a primary site for the termination for afferents important in cardiovascular, respiratory and alimentary functions (Panneton and Loewy, '80 ; Kalia and Mesulam, '80a ; Ciriello et al., '81; Kalia and Richter, '85 , '88; Altschuler et al., '89).

The NTSis receives afferent input via the glossopharyngeal (Ciriello et al., '81; Contreras et al., '82; Nomura and Mizuno, '82; Hamilton and Norgren, '84; Bradley et al., '85; Sweazy and Bradley, '86; Altschuler et al., '89) and vagus (Contreras et al., '82; Hanamori and Smith, '89; Kalia and Mesulam, '80a; Leslie et al., '82; Kalia and Sullivan, '82; Chazal et al., '91) nerves. The glossopharyngeal nerve conveys afferent information originating in the pharynx while the vagus nerve provides afferent conduction from the larynx back to the NTSis. The pharyngeal and laryngeal terminal fields overlap in the

subnucleus interstitialis along with afferent terminations originating in the soft palate (Altschuler et al., '89) and trachea (Kalia and Mesulam, '80b). The modalities conveyed by afferents to the NTSis are at present not known. However the convergence of afferent information from these two structures clearly underscores the importance of this subnucleus in the relay of primary afferent information to other parts of the neuraxis.

The literature has not clearly defined the inputs to the NTSis from other sites in the central nervous systemto this region of the NTS. Review of the literature provided an indication of at least a few possible inputs of central origins to the NTSis. Hopkins and Holstege ('78) following ^{3}H-leucine injections into the central nucleus of the amygdala showed a small number of labeled terminals in the NTS in the area of the NTSis. Willet et al. ('86) placed large HRP injections into the frontal cortex of the cat and reported light anterograde labeling in the NTSis. A similar result was obtained by van der Kooy et al. ('84). In two autoradiographic studies of the connections of the hypothalamus Saper et al. ('76) and Willet et al. ('87) suggest that the hypothalamus might innervate the NTSis.

Efferent Connections. Specific information regarding the efferent connections of the NTSis is lacking in the literature. However, the NTSis probably follows the efferent connectivity of most other subnuclei of the NTS with the exception of the NTScen and thus can be discussed loosely in terms of the NTS as a whole. Neuroanatomical and electrophysiological studies have demonstrated efferent projections from the NTS to a number of areas of the central nervous system implicated in autonomic function. These projections can be to the spinal cord (Von Euler et al., '73; Loewy and Burton, '78); to relay nuclei in the brainstem (Loewy and Burton, '78; Norgren, '78; King, '80; Ross et al., '85; Ciriello and Caverson, '86; Cunningham and Sawchenko, '89; '90; Herbert et al., '90;) to the midbrain periaqueductal gray (Bandler and Tork, '87); the hypothalamus (Saper et al., '76; Ricardo and Koh, '78; Willett et al., '87) and amygdala (Ricardo and

Koh, '78; Cechetto and Calaresu, '85; Danielsen et al., '89), all of which have been shown to receive afferent projections from the NTS. Relay of primary afferent information via the NTS to higher levels of the neuraxis provides the anatomic substrate for the integration of visceral and gustatory information at the level of the forebrain and possibly influencing autonomic function and behavior (Norgren, '76; Loewy and Burton, '78; Saper and Loewy, '80; Fulwiler and Saper, '84; Cechetto and Calaresu, '85). The NTSis has been shown in retrograde tracer experiments to have efferent projections to the ventrolateral medulla (Ross et al., '85; Herbert et al., '90) and parabrachial nucleus of the dorsolateral pons (Loewy and Burton, '78; Cechetto et al., '85; Herbert et al., '90).

Neurochemistry. Much of the neurochemical information about the NTSis is of a general nature and relates to the NTS as a whole and the mapping as it relates to the subnuclear organization is at present inadequate and awaits careful analysis. An immunohistochemical study by Henderson et al. ('91) revealed that there are high levels of nerve growth factor receptors in the NTSis. Kalia et al. ('84b) identified a number of peptides in the NTSis, including, substance P, met-enkephalin, somatostatin and neurophysin-oxytocin. Maley et al. ('87) reported dense immunoreactivity in the NTSis for substance P but only light staining for enkephalin. Kalia et al. ('85) identified catecholaminergic neurons and fiber plexus within the NTSis of the rat.

Functional Considerations. Altschuler et al. ('89) suggested that since it is generally accepted that regulation of visceral activities is intimately dependent on afferent information, it is likely that primary afferents innervating the NTSis convey important information about the state of the viscus, that will permit the initiation and coordination of neural activity related to the normal physiological function of the structure. The convergence of afferents carried in the glossopharyngeal and vagus nerves in the NTSis

provides some support for the idea that the NTSis is an important site for the integration of sensory information from a number of areas including the caudal tongue, respiratory and alimentary tracts. It has been speculated that through these convergent afferent inputs, the NTS is able to influence oropharyngeal and laryngeal reflexes (Sweazy and Bradley, '86). It is interesting to note that the NTS serves the viscera generally and yet each has its own territory and distinct central projections. On the other hand, almost every visceral function has consequences for another; for example the inability to breathe and swallow at the same time or the change in heart rate as a result of a change in breathing.

The Paratrigeminal Nucleus

The patchy or reticulated network of neuropil which makes up the PTN was identified by Cajal ('09) in Golgi material prepared from the medulla oblongata of the cat, and referred to as the cellules interstitielles of the spinal trigeminal tract. Subsequently, a variety of terminologies have been used to identify what is essentially the same anatomical structure in different species. The term interstitial nucleus has been used in the rabbit (Hanamori and Smith, '89; Phelan and Falls, '89) and the cat (Gobel and Purvis, '72; Arvidsson and Thomander, '84; Shigenaga et al., '86). The interstitial gray matter of the spinal trigeminal tract has also been designated the promontorium in mouse (Åstrom, '53) and rat (Cechetto et al., '85); the ectotrigeminal nucleus in rat (Campbell et al., '74); and paratrigeminal nucleus in muskrat (Panneton, '91), cat (Chan-Palay, '78a,b; Panneton and Burton, '81, '85; Menétrey and Basbaum, '87; Menétrey et al., '87); opossum (Oswaldo-Cruz and Rocha-Miranda, '68); and monkey (Chan-Palay '78a, b; Beckstead et al., '80) and the nucleus trigeminocuneatus lateralis (Fuse, '19) the nucleus insulae cuneati lateralis (Olszewski and Baxter, '54) in human. Although there are variations in the dorsal-ventral and rostral-caudal locations of the PTN in different species (see Phelan and Falls, '89 for review), it generally lies dorsolateral to the rostral one third of the subnucleus pars caudalis

and caudal two thirds of the subnucleus pars interpolaris among the descending myelinated fibers of the spinal trigeminal tract.

There is considerable divergence of opinion in the literature as to whether or not the PTN is a distinct neuroanatomical and/or functional entity or merely a rostral extension of more caudally located structures, particularly laminae I and/or II of the spinal trigeminal nucleus pars caudalis (Torvik, '56). This line of reasoning has lead to the argument that cytoarchitectural similarities between the spinal trigeminal nucleus pars caudalis and the dorsal horn of the spinal cord imply a functional homology (Gobel and Hockfield, '77). A similar argument has been put forward for the PTN which may be considered a rostral extension of laminae I and/or II of the rat spinal trigeminal nucleus pars caudalis since it is generally agreed that these laminae contribute to the neuronal complement in the PTN (Torvik, '56). By contrast Phelan and Falls ('89) present evidence based on Nissl and Golgi preparations that there are differences between the PTN and the superficial laminae of the spinal trigeminal complex. However, some similarities, with regard to connections and immunocytochemical characteristics of the PTN and superficial layers of spinal trigeminal nucleus pars caudalis do exist and thus, provide some support for functional homology (Marfurt, '81; Panneton and Burton, '85; Shigenaga et al., '86; Lucier and Egizii, '86; Chan-Palay, '78b; Finley et al., '81; Shults et al., '84, '85), although such evidence cannot be taken as definitive proof of functional parallels (Phelan and Falls, '89). Clearly, there are discrepancies in the literature regarding the cytoarchitecture and connectivity of the PTN as well as ambiguity regarding the functional homologies between the PTN and the superfical laminae of the spinal trigeminal complex.

Afferent Connections. Degeneration techniques and, more recently, sensitive transganglionic neuroanatomical tracers have made it possible to study the afferent terminal distribution of peripheral nerves and individual viscera within the medulla oblongata. A

number of retrograde and anterograde studies in which the neuroanatomical tracer horseradish peroxidase (HRP) was used have elucidated primary afferent input to the PTN from a variety of cranial nerves. It has been shown that the trigeminal (Panneton and Burton, '81; Hamilton and Norgren, '84; Shigenaga et al., '86; Pfaller and Arvidsson, '88; Panneton, '91), the glossopharyngeal (Nomura and Mizuno, '82; Hamilton and Norgren, '84; Bradley et al., '85; Housley et al., '87; Altschuler et al., '89; Panneton, '91) and vagus nerves (Hamilton and Norgren, '84; Arvidsson and Thomander, '84; Hanamori and Smith, '89; Altschuler et al., '89) project to the PTN. Two other cranial nerves, the facial (Rhoton et al., '66; Beckstead and Norgren, '79; Arvidsson and Thomander, '84) and hypoglossal (Nazruddin et al., '89) have been identified as containing afferent fibers terminating in the PTN although the primary cell bodies of these afferents lie in the nodose and petrosal ganglia. Dorsal root ganglia as far caudal as C7 and associated nerves have been shown to innervate the PTN region (Abrahams et al., '84; Pfaller and Arvidsson, '88; Neuhuber and Zenker, '89; Arvidsson and Pfaller, '90).

Specific structures including the soft palate, pharynx and larynx (Altschuler et al., '89), cornea (Panneton and Burton, '81), and muscles of mastication (Nishimori et al., '86; Shigenaga et al., '86, '88) have been shown to be sites for the origin of topographically overlapping inputs to the PTN. With such tremendous overlap from widespread regions of the body surface and upper alimentary and respiratory tracts one would have to conclude that the PTN is probably involved in integrative activity related to external and internal sensitivity although the exact nature of such integration is not known.

Surprisingly, only two central sites have been identified as providing afferent projections to the PTN. Shapiro and Miselis ('85a) suggested that the area postrema projected to the PTN although injection of retrograde neuroanatomical tracers into the medullary dorsal horn including the PTN does not support this conclusion (Craig and Burton, '81; Hockfield and Gobel, '82; Cechetto et al., '85). The only other reported

source of central afferents to the PTN was the rostral nucleus of the tractus solitarius (NTS) (Beckstead et al., '80).

Efferent Connections. The efferent connections of the PTN have been, for the most part, identified through the use of retrogradely transported tracers (Cechetto et al., '85; Panneton and Burton, '85; Granum, '86; Menétrey et al., '87). The PTN has connections with a number of extratrigeminal areas of the brainstem and with the thalamus. Within the brainstem, PTN efferents project to the nucleus of the tractus solitarius (NTS) (Menétrey et al., '87; Menétrey and Basbaum, '87), the parabrachial nucleus (PBN) (Cechetto et al., '85; Panneton and Burton, '85; Menétrey et al., '87; Herbert et al., '90), Kölliker-Fuse nucleus (Cechetto et al., '85; Panneton and Burton, '85), the thalamus (Burton et al., '79; Granum, '86; Yoshida et al., '91), and cerebellum (Somana and Walberg, '79). Specific data regarding the termination of PTN efferents in the various nuclei or subnuclei are scarce, and refinement of information concerning the distribution of terminal sites may provide valuable insight into the potential functional significance of the PTN.

Neurochemistry. In light of the numerous neurochemical and neuropharmacological studies focused on the spinal trigeminal complex it is surprising that very little has been reported regarding the PTN. This probably stems from the common practice of lumping the PTN in with the superficial laminae of the spinal trigeminal nucleus. Nevertheless there is a small amount of information available in the literature which presents indirectly some of the neurochemical characteristics of the PTN (Jennes et al., '82; Kubota et al., '83; Björklund and Hökfelt, '85; Skofitsch et al., '85; Skofitsch and Jacobowitz, '85; William and Dockray, '83; Blessing et al., '86; Melander et al., '86; Matthews et al., '89; Bennett-Clark et al., '92).

Skofitsch et al. ('85) probably provide the most complete information about the potential neurotransmitters and neuromodulators in the PTN. Their evidence based on immunocytochemistry and radioimmunoassay revealed that the PTN contained immunoreactivity for substance P (SP), somatostatin (SOM), vasoactive intestinal polypeptide (VIP), cholecystokinin (CCK), enkephalin (ENK), and corticotrophin releasing factor (CRF). In addition they established that CRF immunoreactivity is colocalized with SP, SOM, and ENK in primary sensory neurons of the trigeminal ganglion and dorsal root ganglia and in fibers located in the PTN and superficial laminae of the spinal trigeminal nucleus pars caudalis. They suggested that at least some of these plexuses in the PTN and superficial laminae are derived from projections originating in the trigeminal (Pfaller and Arvidsson, '88) and dorsal root ganglia (Neuhuber and Zenker, '89; Arvidsson and Pfaller, '90). Other potential neurotransmitters identified by immunohistochemical methods include Neuropeptide Y (Blessing et al., '86), galanin (Melander et al., '86), neurotension (Jennes et al., '82), calcitonin gene-related peptide (Kawai et al., '85), met-enkephalin (Fallon and Leslie, '86; William and Dockray, '83; Matthews et al., '89), GABA (Björklund and Hökfelt, '85) and serotonin (Matthews et al., '89). Bennett-Clark et al. ('92) reported the PTN and subjacent spinal trigeminal complex contained dense staining for cytochrome oxidase.

Functional Considerations. Although information is accumulating regarding the connectivity of the PTN there is little in the literature as to the function of the nucleus and where present it must be viewed carefully since the PTN is often not identified but mistakenly clumped with more general terms such as medullary dorsal horn or superficial laminae and thus information must be extrapolated from photographic and diagrammatic evidence. Salt et al. ('83) in a combined physiological and immunocytochemical study in the rat provided evidence that there were neurons in the rat that were unimodal and

polymodal in a region corresponding to the location of the PTN in Chan-Palay ('78a). They identified two distinct groups of neurons: one group which responded exclusively to noxious (thermal and/or mechanical) stimuli and a second polymodal group which were responsive to noxious and non-noxious thermal and mechanical cutaneous stimuli. The location of nociceptive neurons was coextensive with the distribution of substance P immunoreactivity (Salt et al., '83), a known putative neurotransmitter associated with pain pathways. Hayashi and Takata ('89) reported that a small number of neurons in the cat PTN were responsive to thermal and mechanical cutaneous stimuli and that some of these neurons projected to the parabrachial nucleus. Further support of the possible involvement of the PTN in pain pathways was provided in Altschuler et al. ('89) who reported a positive histochemical reaction for fluoride-resistant acid phosphatase (FRAP), a marker for nociceptive or C-fiber axon terminals (Knyihar and Csillik, '77). The distribution of the FRAP reaction very closely corresponds to the distribution of afferent terminals originating in the pharynx and larynx (Altschuler et al., '89). The PTN has also been implicated in a thermosensory role in hibernating rodents. Kilduff et al. ('83) showed in a 2-deoxyglucose autoradiographic study that the PTN is a metabolically significant area relative to other brain structures during entrance into and during deep hibernation in the golden mantle ground squirrel. They speculated that the PTN might participate in the regulation of the hibernating state by monitoring thermoreceptive inputs from the periphery.

The efferent projections of the PTN to such autonomic centers as the NTS and PBN implicate the PTN in autonomic regulation (Cechetto et al., '85; Menétrey and Basbaum, '87; Menétrey et al., '87). The medial and ventrolateral subnuclei of the PBN receive gustatory, mechanosensitive and thermosensitive inputs from the palate and tongue (Ogawa et al., '82; Travers and Smith, '84) and are major target sites for PTN efferents (Cechetto et al., '85). The PBN maybe a site for the convergence of information of gustatory and vagal hepatic origin (Gerlinda and Rogers, '85) suggesting a visceral-vagal modulation of taste

perception which might further be modified by convergent visceral and somatic information relayed from the PTN to this region. The lateral PBN receives afferent information related to cardiovascular and respiratory function (Cohen, '79; Hamilton et al., '81; Cechetto et al., '85), and also information relayed through the PTN (Cechetto et al., '85). The NTS is an important brainstem site for termination of primary gustatory and visceral afferents as well as afferent input from the PTN (Menétrey and Basbaum, '87). These anatomical and physiological studies show a high degree of interconnectivity and functional interrelatedness between the PTN and important brainstem autonomic centers.

CHAPTER 2

SUBNUCLEUS CENTRALIS OF THE NUCLEUS OF THE TRACTUS SOLITARIUS: ULTRASTRUCTURE AND SYNAPTOLOGY OF ESOPHAGEAL AFFERENTS IN THE RAT.

INTRODUCTION

The esophagus is a muscular tube composed of varying degrees of striated and smooth muscle along its length depending on the species investigated. In the rat the esophagus is predominantly made up of striated muscle organized with an outer longitudinal layer and an inner circular layer. Sensory information from the esophagus is conveyed centrally via the vagus nerve (Christensen, '84; Clark and Davison, '78; Fryscak et al., '84; Clerc and Condamin, '87; Cunningham and Sawchenko, '90; Diamant, '89; Neuhuber, '87; Altschuler et al., '89). There is also evidence to suggest that sensory information passes via sympathetic nerves to the spinal cord at levels T3 through T12 (Christensen, '84). Based on neuroanatomical tracer studies it is known that afferents originating in the cervical, thoracic and subdiaphragmatic esophagus terminate in a roughly overlapping topography in the NTS (Altschuler et al., '89). Esophageal afferents terminate in a specific cell column of the NTS referred to as the subnucleus centralis (NTScen) (Ross et al., '85). Current knowledge of the afferents to the NTScen suggests that the esophagus supplies the only peripheral input to the NTScen. Central afferent connections to the NTScen have not been reported.

The NTScen has an efferent connection to the ventrolateral medulla to a region containing esophageal motor neurons (Bieger and Hopkins, '87). Cunningham and Sawchenko ('89, '90) put forth a proposal of a disynaptic reflex-loop control of esophageal

motility in which the NTScen is the intermediate between primary afferents originating in the esophagus and esophageal motor neurons in the compact formation (Bieger and Hopkins, '87) of the nucleus ambiguus.

In light of the pivotal role the NTScen plays in the control of esophageal motility, it is surprising that there is no information in the literature regarding the ultrastructure and synaptology of the NTScen. It is also of considerable interest to investigate the centrally located anatomical substrates which subserve the afferent innervation of the esophagus.

The present chapter presents the results of an ultrastructural study of the NTScen as well as a study of the synaptology of esophageal afferent projections to the NTScen. These studies are designed to extend the information available regarding the NTScen and provide a foundation for future investigations.

MATERIALS AND METHODS

Subjects and Surgery

The subjects were 22 male Wistar rats weighing 250-350 grams. In preparation for surgery and prior to perfusion, rats were anaesthetized with sodium pentobarbital (40-65 mg/kg, i.p.).

The cervical esophagus was exposed by a ventral incision in the neck followed by the retraction of the strap muscles of the neck and the lateral displacement of the trachea with a strip of umbilical tape. A length of the cervical esophagus was freed from the overlying trachea by careful dissection of the fascia adhering the two structures. The subdiaphragmatic esophagus was exposed by a midline incision through the skin and linea alba followed by carefully displacing the stomach in a caudal direction with cotton swabs and elevating the lobes of the liver anteriorly in the abdominal cavity with gauze pads. Once the esophagus was exposed, it was isolated from surrounding structures by the strategic placement of absorbent gauze to prevent or reduce tracer spread to adjacent structures.

Injections of horseradish peroxidase (HRP) conjugates, either wheat-germ agglutinin-HRP (WGA-HRP, Sigma) or cholera toxin-HRP beta subunit (CT-HRP, List Laboratories) were made into the cervical esophagus (n = 11), subdiaphragmatic esophagus (n = 9) or both (n = 2). Aqueous solutions of WGA-HRP (2-5 %) and CT-HRP (0.1-0.25%) were pressure-injected in small aliquots at a series of sites around the exposed length of the esophagus until the entire volume (3-5 μl) of tracer was expelled. Any spillage of tracer was absorbed with sterile cotton swabs. Injections of neuroanatomical tracer into the wall of the esophagus were accomplished by means of glass micropipettes (tip diameters 40-80 μm) attached to a 25 μl Hamilton syringe.

Fixation and HRP Histochemistry

Preliminary experiments established that the ultrastructure of the NTScen was not deleteriously affected or altered by procedures for histochemical detection of HRP. For this reason and because the NTScen can be identified with certainty by virtue of the anterograde labeling in experimental animals the ultrastructural results reported herein are based on cases in which neuroanatomical tracing was carried out.

Animals, were allowed to survive 48-72 hours before they were sacrificed, and their brains processed for electron microscopy. Transcardial perfusion with a cannula through the left ventricle into the ascending aorta was carried out with 500 ml of pre-rinse (0.15 M phosphate buffer, pH 7.3-7.4) followed by 1 liter of fixative (0.5% paraformaldehyde - 2.5% glutaraldehyde, pH 7.3-7.4) in the same buffer for one hour at room temperature.

Fixed brains were removed and placed in 0.15 M phosphate buffer prior to cutting 100-μm-thick vibratome (Lancer) sections through the medulla oblongata in the transverse plane. Vibratome sections were processed for HRP histochemistry using tetramethylbenzidine (TMB) (Mesulam, '78) as the chromogen. Vibratome sections containing the NTScen were blocked out and osmicated in 1% osmium tetroxide in 0.15 M phosphate buffer, stained *en bloc* with saturated aqueous uranyl acetate, dehydrated in graded solutions of acetone and embedded in epoxy resin (TAAB, Marivac) as described elsewhere (see Chapter 3). In order to optimize the labeling and detection of HRP reaction product in neural elements, the HRP reaction product was stabilized by means of a 10 -15 minute incubation in 5% ammonium molybdate (Marfurt et al., '86) in acetate buffer (pH 5). This procedure produced distinctive electron-dense crystalline structures in primary esophageal afferent and axon terminals in the NTScen. Motoneurons of the compact formation of the nucleus ambiguus also contained reaction product. These histochemical procedures have the advantage of producing electron-dense labeling that rarely obscures the ultrastructural features of neuronal elements labeled and produces

superior results in comparison to procedures in which stabilization of TMB reaction product is achieved with sequential incubation in DAB (Lemann et al., '85; Allen and Hopkins, '89).

HRP histochemistry was carried out at pH levels between 4.8 and 6.0 rather than the standard light microscopic pH of 3.3 in order to optimize the preservation of normal ultrastructure of the tissue. At the higher pH's there may have been only a slight decrease in the degree of labeling, (i.e., a small reduction in sensitivity) but as the size of the HRP crystals formed tended to be larger they were easier to detect at the electron microscopic level. With higher pH's in the range of 5.5 to 6.0, the ultrastructure was well-preserved and HRP crystals were easy to find in terminals due to their larger size as compared to HRP histochemical procedures carried out at pH 3.3. A minor drawback to using higher pH levels was identified and was directly related to the increased size of reaction crystals. On rare occasions, larger reaction crystals disrupted the plasma membranes of terminals and extended beyond the boundaries of the terminal and into adjacent structures. Nonetheless, there did not appear to be changes in the basic ultrastructure of the material.

To date, there is no universally-accepted cytoarchitectonic parcellation of the nucleus of the tractus solitarius for the rat and the terminology to be used herein is based on the NTS subdivisions or subnuclei identified by Altschuler et al. ('89), which is a combination of terminologies taken from studies both of the cytoarchitectonic features and connections of the NTS.

Light Microscopy

For cytoarchitectonic studies 1-μm-thick plastic sections were cut in the transverse plane from four rats and stained with toluidine blue for two minutes at 40 $^{\circ}$C on a hot plate. Sections were coverslipped with DPX mountant and studied with a Leitz Dialux 20 microscope. Plastic sections were prepared from experimental animals in order to correlate

the location of esophageal afferent terminal label with cytoarchitectonic boundaries of the NTScen. Photomicrographs were taken of stained and unstained sections under bright- and dark-field optics. Semi-thin sections were chosen for cytoarchitectonic study rather than thicker frozen sections because of the superior resolution of neuronal elements which can be obtained without obscuring the image by structures in other planes of focus.

ABBREVIATIONS

D	dendrite
G	glial cell
m	mitochondrion
mvb	multivesicular body
NTS	nucleus of the tractus solitarius
NTScen	subnucleus centralis of NTS
Nu	nucleolus
PS	pleomorphic symmetrical synaptic terminal
RA	round asymmetric synaptic terminal
TS	tractus solitarius

RESULTS

Light Microscopic Observations

Cytoarchitecture. In the rat the NTScen was most prominent medial to the TS at and rostral to the level of the area postrema. In the transverse plane a distinctive clustering of small neurons which made up the subnucleus was easily distinguished from surrounding neuronal populations. In relation to other subnuclei of the NTS, the NTScen is located medial to a region of larger neurons belonging to the subnucleus intermedialis of the NTS intervening between the NTScen and TS. The subnucleus gelatinosus of the NTS lies dorsal to the NTScen while the dorsal motor nucleus of the vagus nerve nerve lies ventral to it. The NTScen began caudally as a small group of neurons which became more prominent and distinct at and rostral to the area postrema. It could be clearly identified cytoarchitectonically as extending from the obex to approximately 450 μm rostral to the area postrema although afferent labeling showed that it was more extensive, covering approximately 700 μm in total caudal to rostral length. At its most rostral extent the small neurons characteristic of the nucleus tend to be more scattered and less easily identified as a distinct subnuclear entity without the presence of esophageal afferent labeling.

Neurons and Neuropil The NTScen was comprised of small (7-12 μm) diameter neurons which were tightly clustered medial to the TS (Fig. 1A). Around the periphery of the centrally clustered NTScen neurons was a relatively cell-poor region composed of dendritic and unmyelinated axonal profiles. NTScen neurons were distinctly smaller (averaging approximately 8 μm in diameter) than neurons in the surrounding NTS and dorsal motor nucleus of the vagus nerve. Because of the clustering of neurons in the NTScen, neurons were rarely found more than a few microns from another neuronal profile and it was not uncommon to find as many as four or five neuronal somata in close spatial relation to one and another. These somata were in very close apposition with little

Fig. 1. Photomicrographs of adjacent transverse 1 μm-thick plastic sections through the NTScen at the level of the area postrema. **A**: Toluidine blue-stained section showing the clustering of small neurons and the surrounding cell-sparse region. The TS is located to the left (i.e., lateral). **B**: Dark-field photomicrograph of an unstained section showing anterograde labeling in the NTScen following injection of CT-HRP into the cervical esophagus. Arrowheads point to three of many HRP labeled primary afferent elements. The asterisk indicates the same blood vessel in both sections. Calibration bar: 50 μm.

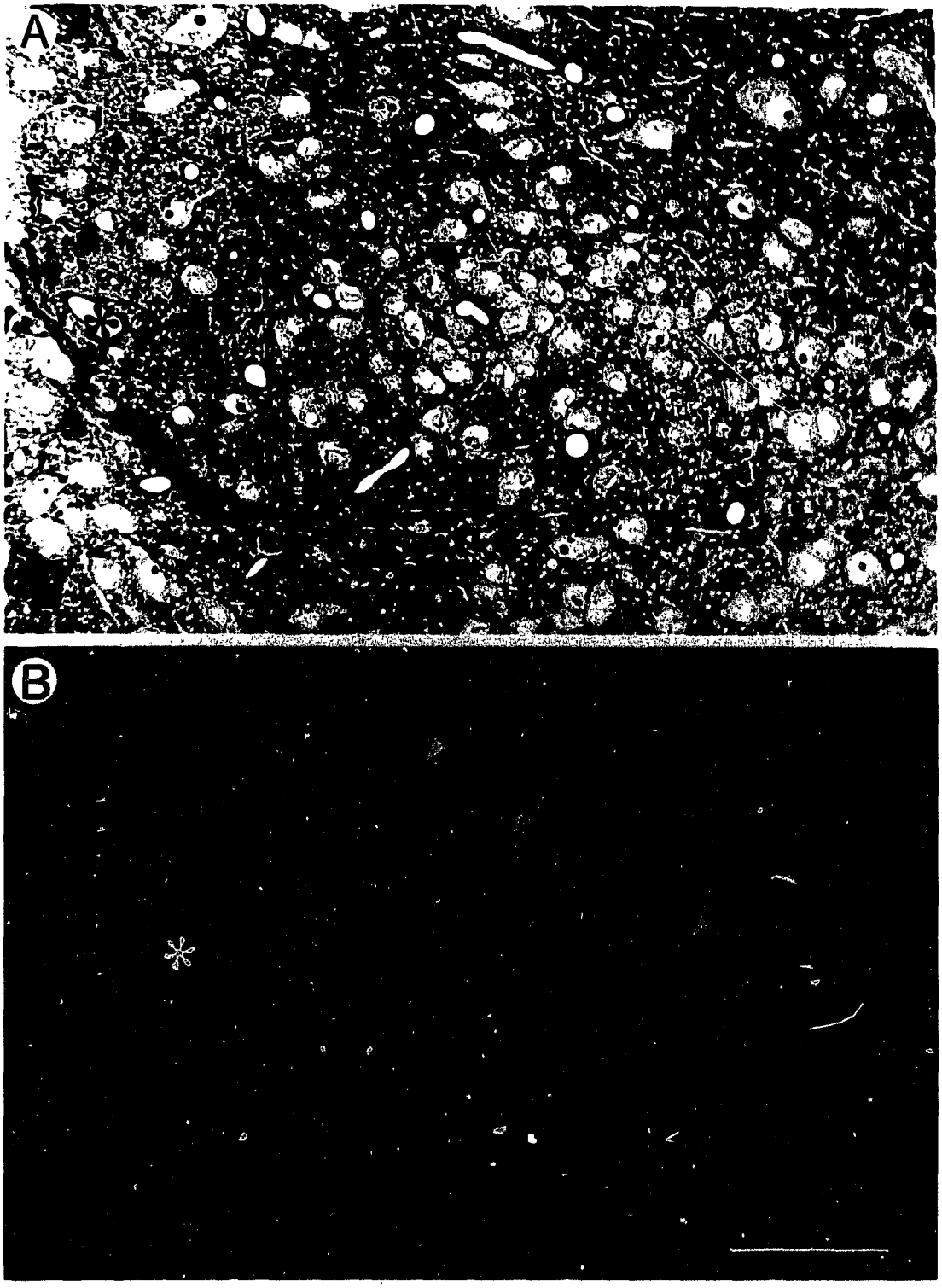

Figure 1

evidence of intervening neuropil or glia. The absence of intervening neuropil or glia between these neuronal somata was confirmed at the electron microscopic level.

Neurons were very homogeneous in morphology throughout the NTScen. Neurons were small, round, and contained a large nucleus surrounded by sparse cytoplasm. Nissl substance could not be discerned in the cytoplasm of NTScen neurons. The nucleus was remarkably similar in each neuron in that the nuclear membrane typically was deeply invaginated at one or more points. Most nuclei contained a single prominent nucleolus which was located eccentrically within the nucleoplasm and in many instances the nucleolus occupied a position immediately adjacent to the nuclear membrane. In a small proportion of NTScen neurons the nucleus was found to contain a second, smaller darkly staining extranucleolar element in addition to a nucleolus . Because of its structural similarity to the nucleolus at the light microscopic level it was referred to as the extranucleolar body. These structures were also typically located eccentrically in the nucleus and often near the nucleolus or the nuclear membrane. In plastic sections it could not be determined if the extranucleolar body was attached to the nucleolus although a very close association was frequently noted.

Glial cells in the NTScen were similar in size to nearby neuronal somata but were easily distinguished from neurons by virtue of their granular, darkly-staining cytoplasm and nucleus. Nuclei of glial cells rarely showed deep nuclear invaginations. When nuclear invaginations were present in glial nuclei, there was usually only one and it was shallow when compared to the deep infoldings in most NTScen nuclei.

The neuropil of the NTScen was made up of many unmyelinated processes with an occasional myelinated profile. The cluster of neurons in the center of the subnucleus was encompassed by a circular zone which was largely devoid of somatal profiles. This cell-poor zone was most evident in the transverse plane. In sections which contained esophageal afferent labeling, the cell-poor zone also contained labeling and in some

instances the labeling was more dense in this region.(Fig. 1B). At the light microscopic level it was not possible to identify definitively axonal and dendritic elements. However, it was possible to determine the overall orientation of elements making up the neuropil. In general, transverse sections revealed that most elements making up the neuropil were cut in cross-section. This suggests that these fibers are predominantly oriented along the long axis of the NTScen (Fig. 1A).

Electron Microscopic Observations

Neurons. In confirmation of the light microscopic results, neurons contained deeply invaginated nuclear membranes and dark-staining nucleoli (Figs. 2, 3). At the electron microscopic level the nucleolus and extranucleolar body often appeared distinctly different in morphology. The round nucleolus was typically larger and had a more heterogeneous appearance (Fig. 2) as a result of light regions distributed in the dark matrix. This vacuolated appearance is believed to be due to entrapped masses of karyoplasm which is less dense than the granular material making up the rest of the nucleus (Peters et al., '91). The extranucleolar body was smaller and of a different texture to that of the nucleolus (Fig. 2). Typically, it was granular and very dense in appearance with infrequent light and dark regions evident.

The very close apposition between neurons in the NTScen was verified in electron micrographs (Fig. 3) which demonstrated that for many of the neurons in close spatial apposition with adjacent neurons there was no discernible neuropil or glial elements intervening between the plasma membranes of the two adjacent neurons (Fig. 3). Many such examples of close soma-soma appositions were examined for membrane specializations that might be associated with such close appositions, but none was evident. These close appositions between neurons were observed to include up to five neuronal profiles in a row or cluster. Interestingly, such close appositions did not occur exclusively

Fig. 2. Electron micrograph of a neuronal soma and a glial cell (G) body closely apposed (arrowheads) in the NTScen. N_1 represents the nucleolus and N_2 an extranucleolar body contained in the nucleus which has two deep membrane invaginations. Note the paucity of cytoplasmic organelles in the neuron and the dark appearance of the glial cell nucleus and cytoplasm. Calibration bar: 3 μm.

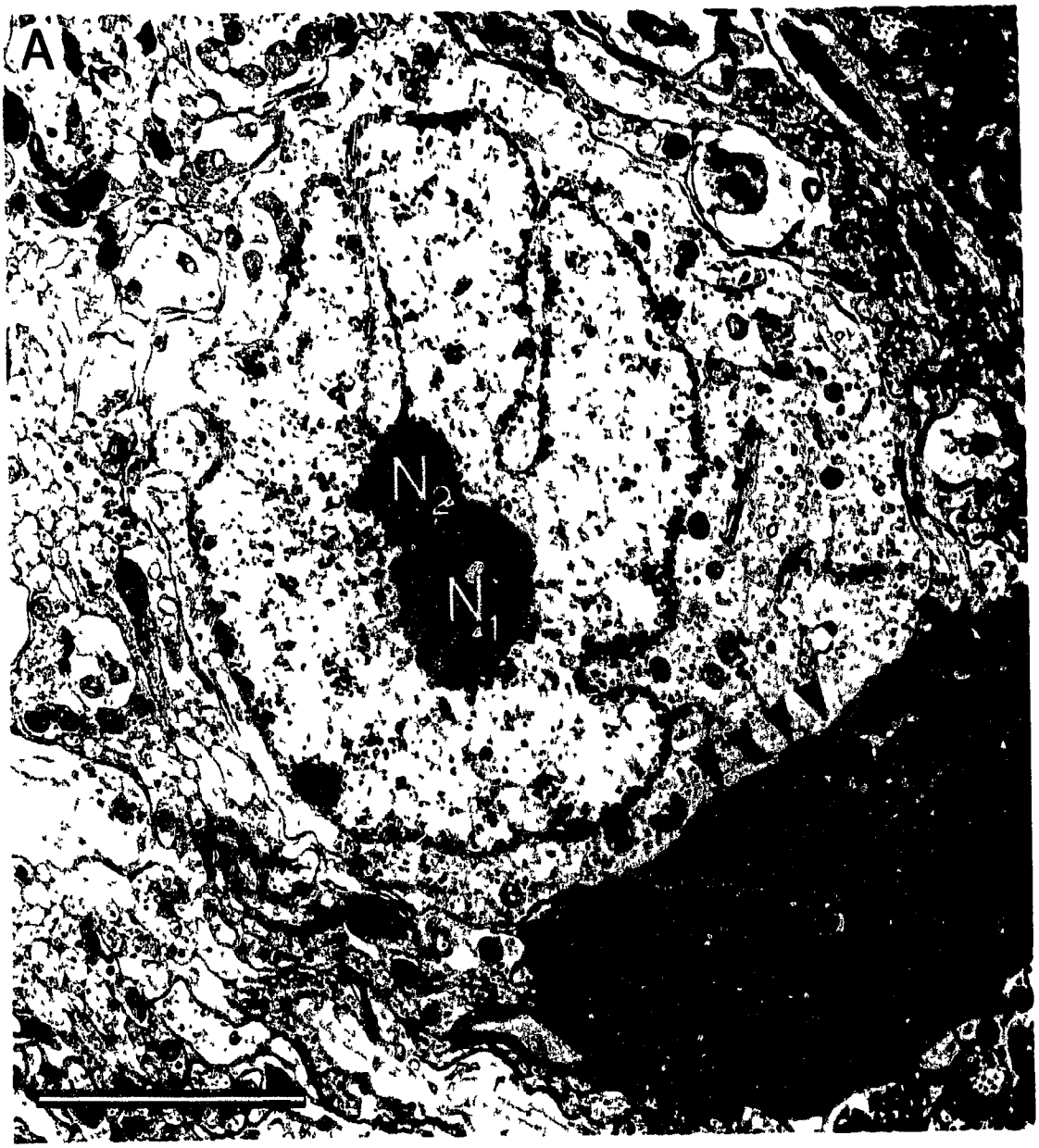

Figure 2

Fig. 3. Electron micrograph of two NTScen neuronal somata in close apposition (arrows) to one another. Note the large number of transversely cut dendritic and axonal profiles in the neuropil around each neuron. T_1 indicates an unlabeled axon terminal synapsing (arrowhead) on a dendrite and T_2 a labeled esophageal afferent terminal synapsing on a small dendrite (arrowhead).
Calibration bar: 4 μm.

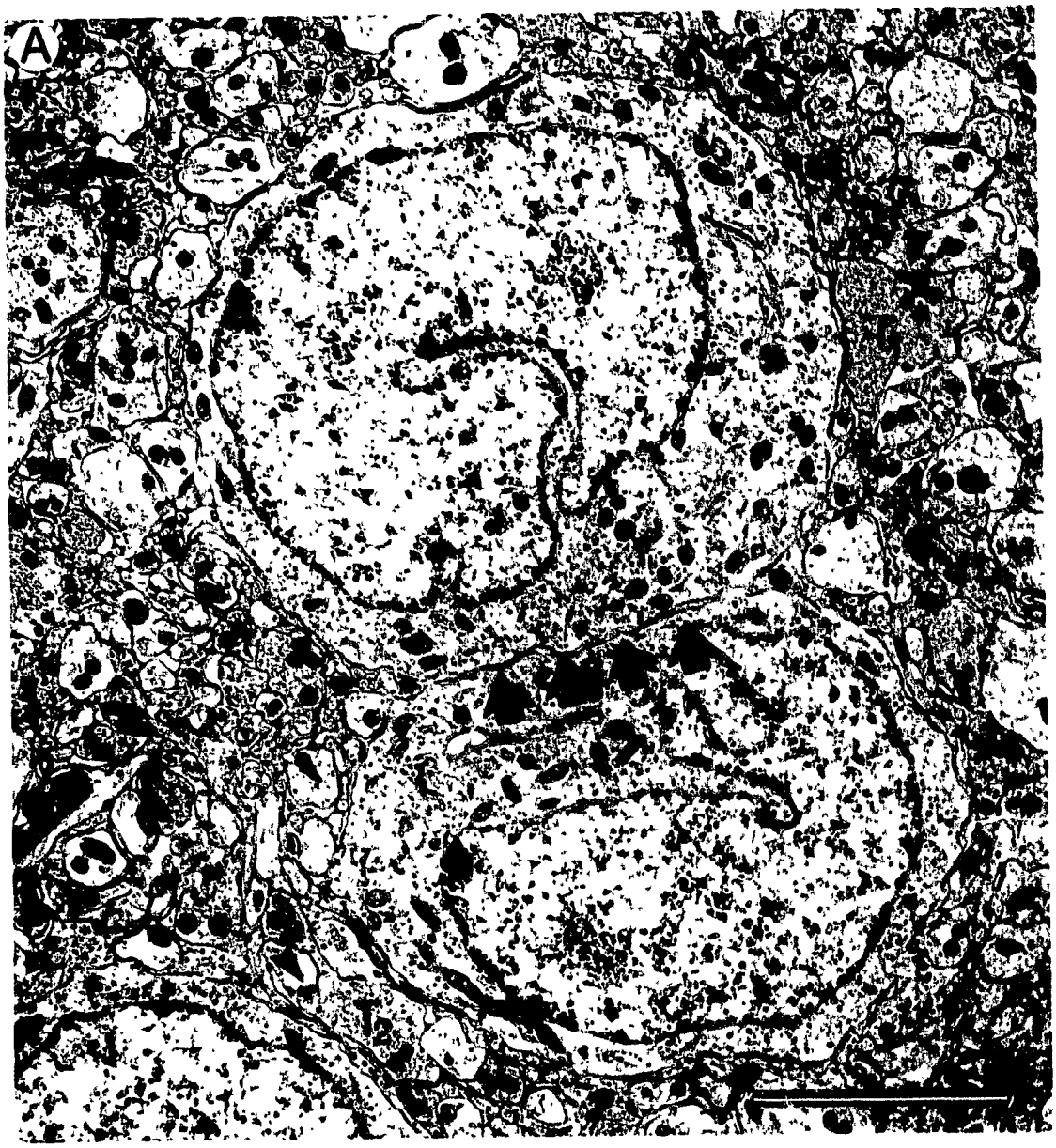

Figure 3

between neurons of the NTScen. It was not uncommon to find a single NTScen neuron in close association with a darkly-staining glial cell (Fig. 2). The appositions between a glial cell and a neuronal somata were similar in the length of contact (2-4 μm) to that observed between adjacent neurons. Glial coverage of neuronal somata was sparse and if glial coverage was present it usually was in the form of the glial-neuron association mentioned above. Occasionally a dark, glial process could be seen adjacent to a neuronal somata but more often the plasma membrane of NTScen neurons were apposed to numerous preterminal axons, dendrites and non-synaptic axon terminals of various sizes.

The paucity of Nissl substance evident at the LM level was confirmed at the ultrastructural level. Rough endoplasmic reticulum (RER) was sparse in the cytoplasm of NTScen neurons (Figs. 2, 3). The cytoplasm of NTScen neurons typically contained a small golgi apparatus consisting of several agranular sacs stacked in a laminar fashion, small round or oval mitochondria, short segments of RER, multivesicular bodies (MVB) and dark-staining lysosomes. It was apparent that basophilic staining of the cytoplasm observed in 1-μm-thick plastic sections was not due to RER but rather to the presence of numerous free ribosomes and ribosomal rosettes distributed throughout the cytoplasm. Such ribosomal structures were the only organelles observed in the cytoplasm that extended into the nucleus as a result of nuclear membrane infolding (Fig. 2,3).

Neuropil The neuropil consisted of numerous dendrites, preterminal axons and axon terminals of various sizes. Myelinated axons were occasionally found and were generally only lightly myelinated.

Dendrites were distinguished from surrounding neuronal and non-neuronal elements by a number of features. Firstly, the cytoplasm of dendrites was conspicuously light in appearance and typically contained microtubules arranged in an evenly spaced fashion along the long axis of the dendrite (Figs. 4C, 5, 6A, 8). The contours of dendrites in

Fig. 4. Electron micrographs of small RA synaptic terminals on dendritic profiles in the NTScen. **A**: RA terminal containing two large dense-cored vesicles (curved arrows) displaced from the active zone (arrowheads). **B**: Two RA synaptic terminals (RA_1, RA_2) making contact with the same dendrite (D). m indicates a long mitochondrial profile. **C**: Two RA terminals making synaptic contact with separate dendrites (D_1, D_2). Note the clustering of vesicles at the cytoplasmic face of the presynaptic membrane at the active zone. Calibration bars: 0.5 μm.

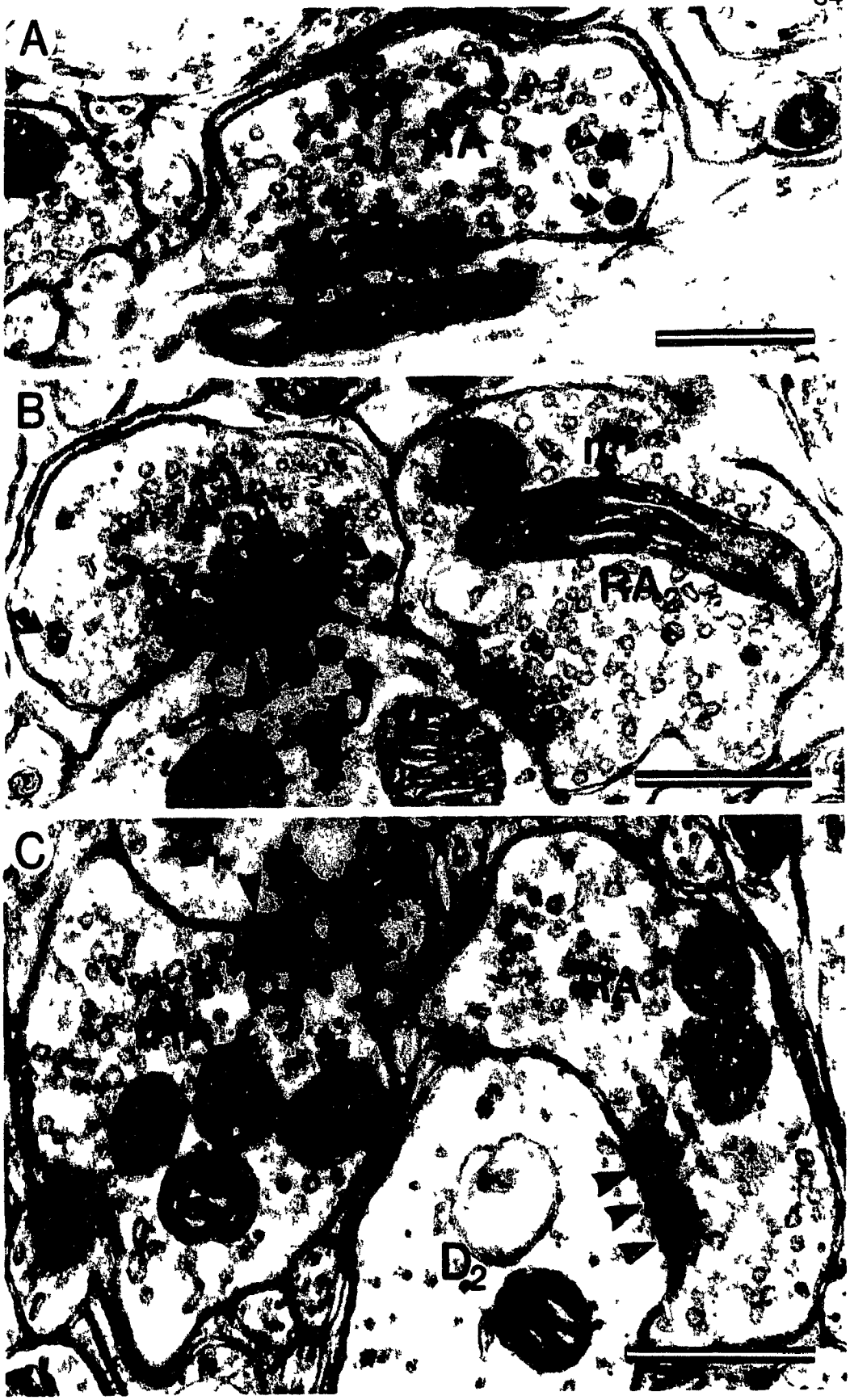

Figure 4

cross-sectional profile tended to be more irregular when compared to axonal profiles. Smooth endoplasmic reticulum (SER) could be identified within the pale matrix of some small dendrites while RER was evident in dendrites greater than 2 μm in diameter. Free ribosomes could be seen in small numbers in some but not all elements that displayed dendritic characteristics. Proximal dendrites were rarely observed leaving the soma, indicating that proximal dendrites are oriented in a rostral-caudal direction and therefore would be difficult to identify in the transverse preparations used here.

Axons were predominantly unmyelinated and distributed throughout the neuropil. The contours of axons were smooth and they were cylindrical in shape indicating that they were for the most part oriented parellel to the long axis of the subnucleus. The axonal matrix was generally more darkly-staining than that of dendrites and contained small numbers of mitochondria, and microtubules which were less regular in spacing than those seen in dendrites. Occasionally a preterminal axon was seen to contain small groups of agranular vesicles similar to those found in synaptic terminals.

Synaptology Within the boundaries of the NTScen two types of synaptic terminals were identified. The first type of terminal contained predominantly round, agranular vesicles and formed asymmetric synaptic (RA) contacts with the postsynaptic element (Fig. 4). The second terminal type contained agranular vesicles which varied greatly in shape from round to flattened and formed symmetric synaptic contacts with the postsynaptic element (Fig. 5.) and were, therefore, designated pleomorphic symmetrical synaptic terminals (PS). Both RA and PS synaptic terminals were also found to contain small numbers of dense-cored vesicles. Dense-cored vesicles were larger than the more numerous agranular vesicles and contained a membrane bound dense particle (Figs. 4A, 4B, 5B, 6). Dense-cored vesicles were not present in all synaptic profiles, however, serial sections through three initially found not to contain DCV revealed that in most cases dense-cored vesicles were present but at a different level in the terminals. Typically, dense-cored

Fig. 5. Electron micrographs of axon terminals containing pleomorphic vesicles (PS) and forming symmetric synaptic contacts (arrowheads) with dendrites. **A**: Note the clustering of vesicles at the cytoplasmic face of the synaptic contact and the evenly spaced microtubules (arrows) cut in cross-section in the postsynaptic dendrite (D). **B**: Two axon terminals containing pleomorphic agranular vesicles. The one on the right makes a symmetric synaptic contact with a dendrite (D). The one on the left contains a single dense-cored vesicle but does not make synaptic contact in this plane of section. Calibration bars: 0.5 μm.

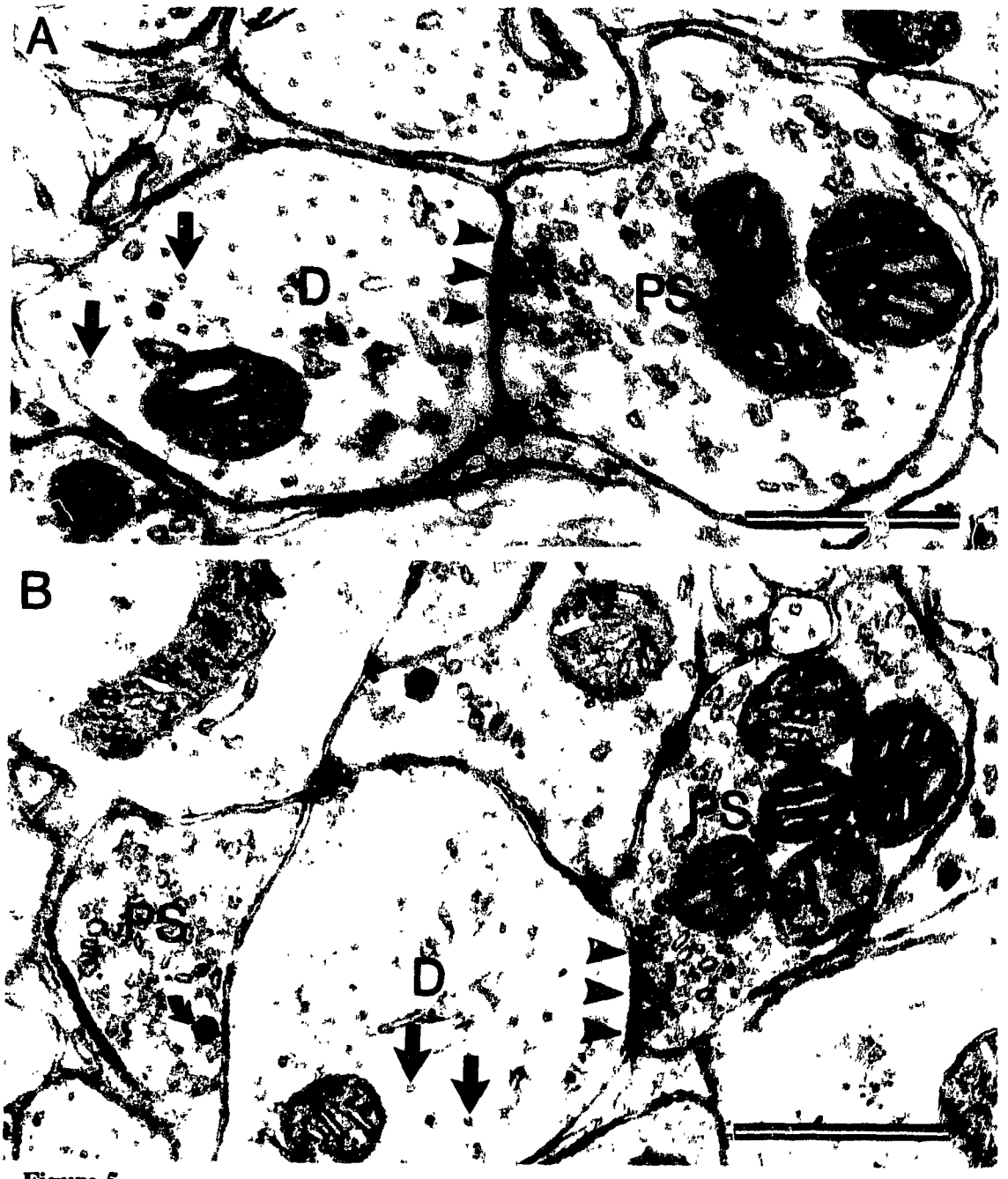

Figure 5

vesicles were located some distance from the synaptic contact and, in many cases, were near the periphery of the agranular vesicles which clustered near the presynaptic membrane at the active zone (Figs. 6A, 8). The only other organelle frequently encountered in axon terminals making synaptic contacts were small numbers of mitochondria. In a small number of instances, postsynaptic dendrites were also found to contain one or two dense-cored vesicles (Fig. 7B).

RA synaptic terminals were the predominant type of terminal in the NTScen while PS synaptic terminals were relatively rare in the neuropil . Both synaptic types produced axo-dendritic synaptic contacts (Figs. 4, 5). Axo-dendritic synaptic contacts were predominantly with small (< 1μm) diameter dendrites although synaptic contacts with dendrites greater than 1 μm in diameter were observed in the NTScen. Postsynaptic dendrites greater than 2 μm in diameter were only occasionally found to have synapses. No axo-somatic or axo-axonic arrangements were observed in the NTScen. In a photomontage of approximately 2200 μm^2 taken from the core of the NTScen at the level where the nucleus is most prominent (i.e., at the level of the rostral area postrema) a total of 16 neuronal profiles containing a nucleus (average somal diameter of 7.79 μm) and 6 which did not contain a nucleus (average diameter of 4.3 μm) were found. Since NTScen neurons and profiles were predominantly round the total area of the neurons and profiles was calculated using the formula for the area of the circle and the total used to calculate the percentage of the total area which constituted neuronal somata. The result of these calculations indicate the NTScen is 38.6% neuronal somata and 61.4% neuropil. Calculations were not done for the cell sparse region around the periphery but it can be assumed that these percentages would lean farther toward the neuropil. The same photomontage was used to calculate approximate percentages of axon boutons (synaptic and nonsynaptic) containing each of the two types of agranular vesicles. Of a total of 454 boutons identified, 86% contained agranular round vesicles and of the remaining 14%,

11% contained agranular pleomorphic vesicles and the other 3% could not be identified for various technical reasons.

As a result of comparing unlabeled RA synaptic terminals with labeled esophageal RA synaptic terminals it was decided that two populations of RA terminals existed based on the size of the terminal. Calculations from the above photomontage indicate that synaptic terminals which were RA and had diameters 1 μm or greater constituted less than 9% of the total number of RA synaptic terminals and that only 3% of these terminals were labeled after cervical and subdiaphragmatic injections of WGA-HRP. The most numerous RA's were those which were less than 1μm (usually 0.5-0.75 μm) in diameter and made synaptic contacts with small dendritic profiles (Fig. 4). These RA synaptic terminals typically made synaptic contact with a single dendritic profile but two adjacent RA terminals frequently made synaptic contact with the same dendrite (Fig. 4B). Large RA terminals, 1μm in diameter or larger, made synaptic contact with small diameter (< 2 μm) postsynaptic dendrites and as the afferent results suggested correspond to esophageal primary afferent terminals (Figs. 6, 7, 8)(see afferent section).

Esophageal Afferent Projections.

Light microscopic observations. Following injections of WGA- or CT-HRP into the musculature and mucosa of the cervical and/or subdiaphragmatic esophagus, anterograde axonal and axon terminal labeling was evident in the NTS. Light to moderate labeling was largely restricted to the NTScen (Fig. 1B) and extended into the cell poor zone around the centrally located cluster of neurons (Fig. 1). The densest labeling in NTScen appeared at a level in which the nucleus was just medial to the tractus solitarius beginning at the level of the obex and continuing rostrally for some 700 μm as visible in 100 μm vibratome sections in rats receiving injections in both the cervical and subdiaphragmatic

Fig. 6. Electron micrographs of anterogradely labeled esophageal afferent terminals (RA) in the NTScen contacting (arrowheads) small dendrites following injection of WGA-HRP into the cervical esophagus. **A**: A labeled RA terminal containing electron-dense HRP reaction product and contacting a dendrite (D) which also receives input from a PS terminal. The curved arrows indicate dense-cored vesicles. **B**: Labeled RA synaptic terminal contacting a dendrite (D). Calibration bars: 0.5 μm.

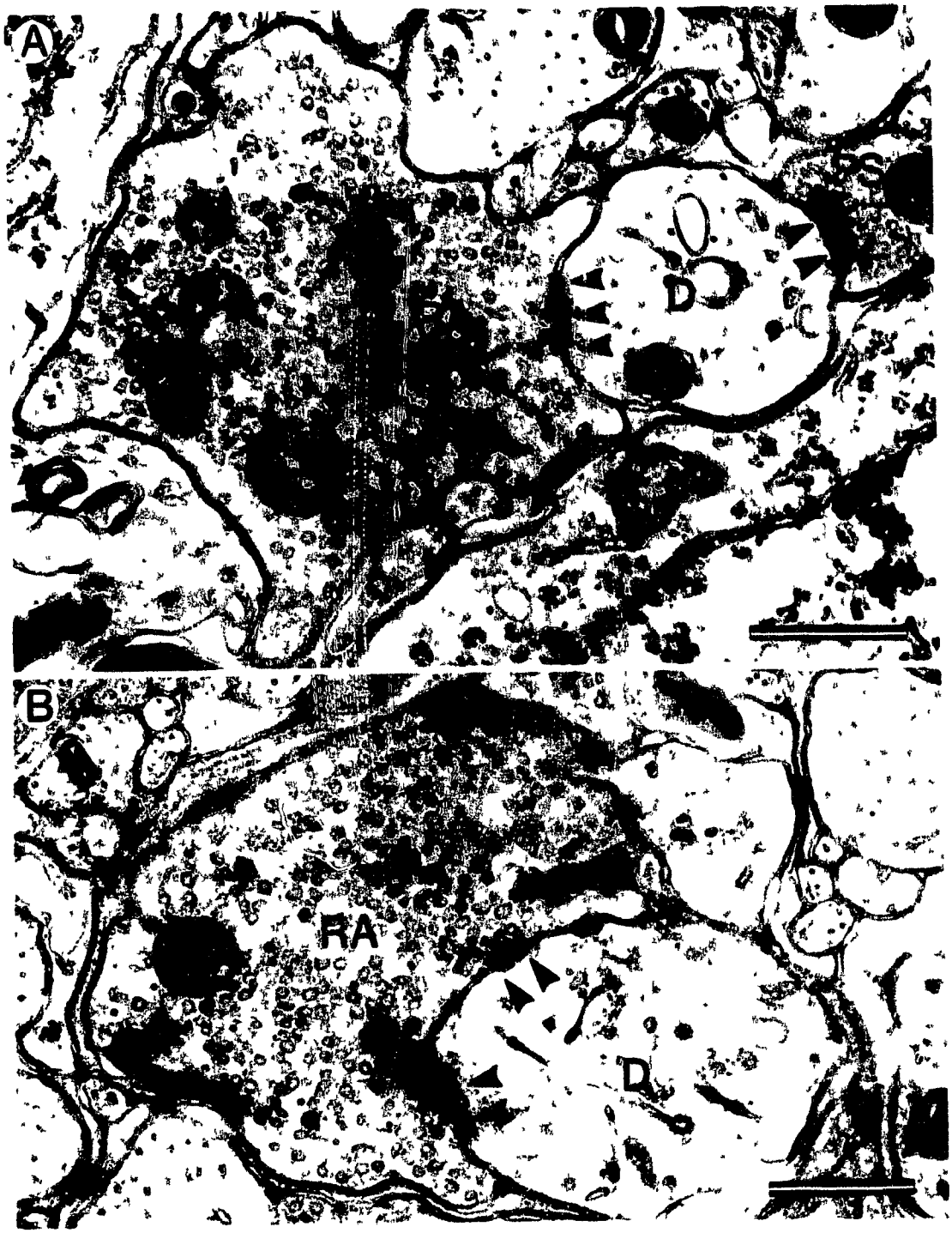

Figure 6

Fig. 7. Electron micrographs of anterogradely labeled esophageal afferent terminals in the NTS following subdiaphragmatic injection of CT-HRP into the esophagus. **A**: A large esophageal afferent terminal (right) making multiple synaptic contacts (arrowheads) with two dendrites (D_2, D_3) and a small unlabeled terminal (left) synapsing (arrowheads) on a dendrite (D_1). **B**: Labeled esophageal terminal synapsing on two small dendrites (D_1, D_2). Note D_2 contains a single dense-cored vesicle (arrow). Calibration bars: 0.5 μm.

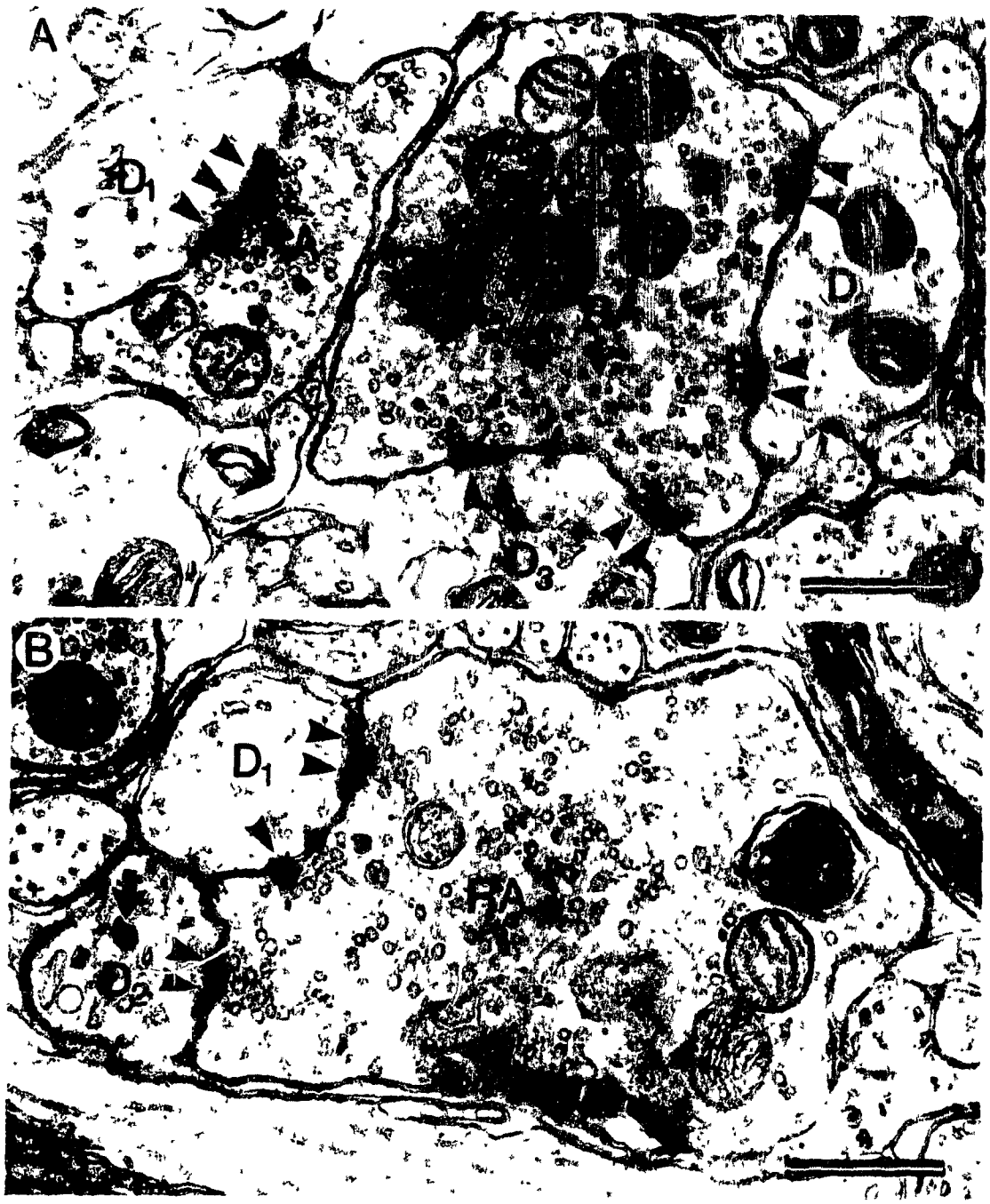

Figure 7

esophagus. Afferent labeling following cervical esophageal injection extended farther rostral in the NTScen than labeling resulting from subdiaphragmatic esophageal injections. However, cervical terminal fields overlapped caudally with subdiaphragmatic labeling as evidenced by the continuum of labeling in the NTScen following injection of both the cervical and subdiaphragmatic esophagus in the same rat. In confirmation of the injection site, the nucleus ambiguus was found to contain many retrogradely labeled neurons located in the compact formation (Bieger and Hopkins, '87). Neurons of the compact formation are a distinct population of vagal efferent motor neurons previously identified as innervating the esophagus (Bieger and Hopkins, '87). In two cases in which the subdiaphragmatic esophagus was injected a small number of neurons in the dorsal motor nucleus of the vagus nerve were retrogradely labeled indicating spread of the tracer to the stomach. This spread of tracer was of little consequence since the stomach has no afferent input to the NTScen (Altschuler et al. '89).

Electron microscopic observations. Anterogradely labeled terminals containing predominantly agranular round synaptic vesicles were surveyed in the NTScen. HRP reaction product took the form of prominent, dark, crystalline structures within the matrix of labeled axon terminals (Figs. 6-8). Often more than a single crystal was present in one bouton (Fig. 6). Even in those instances where several HRP crystals were present in a single bouton, the morphology of the synapse and the contents of the bouton were easily identified.

Typically the largest concentration of synaptic vesicles was near the presynaptic membrane at the active zone of the synapse. This feature has been used as a morphological criterion for identifying synapses (Ramon-Moliner, '77). Labeled esophageal afferent terminations were exclusively axo-dendritic, although different axo-dendritic arrangements were found (Figs. 6-8). Labeled boutons were typically 1 μm or larger in diameter and represented the subpopulation of large RA synaptic terminals defined in the section on

Fig. 8. Electron micrograph of a large (>1.5 μm in diameter) esophageal primary afferent terminal containing numerous dense-cored vesicles (curved arrows) and making synaptic contact (arrowheads) with two dendrites (D_1, D_2). The terminal was anterogradely labeled after an injection of CT-HRP into the subdiaphragmatic esophagus. A multivesicular body in D_2 is indicated by mvb. Calibration bar: 0.5 μm.

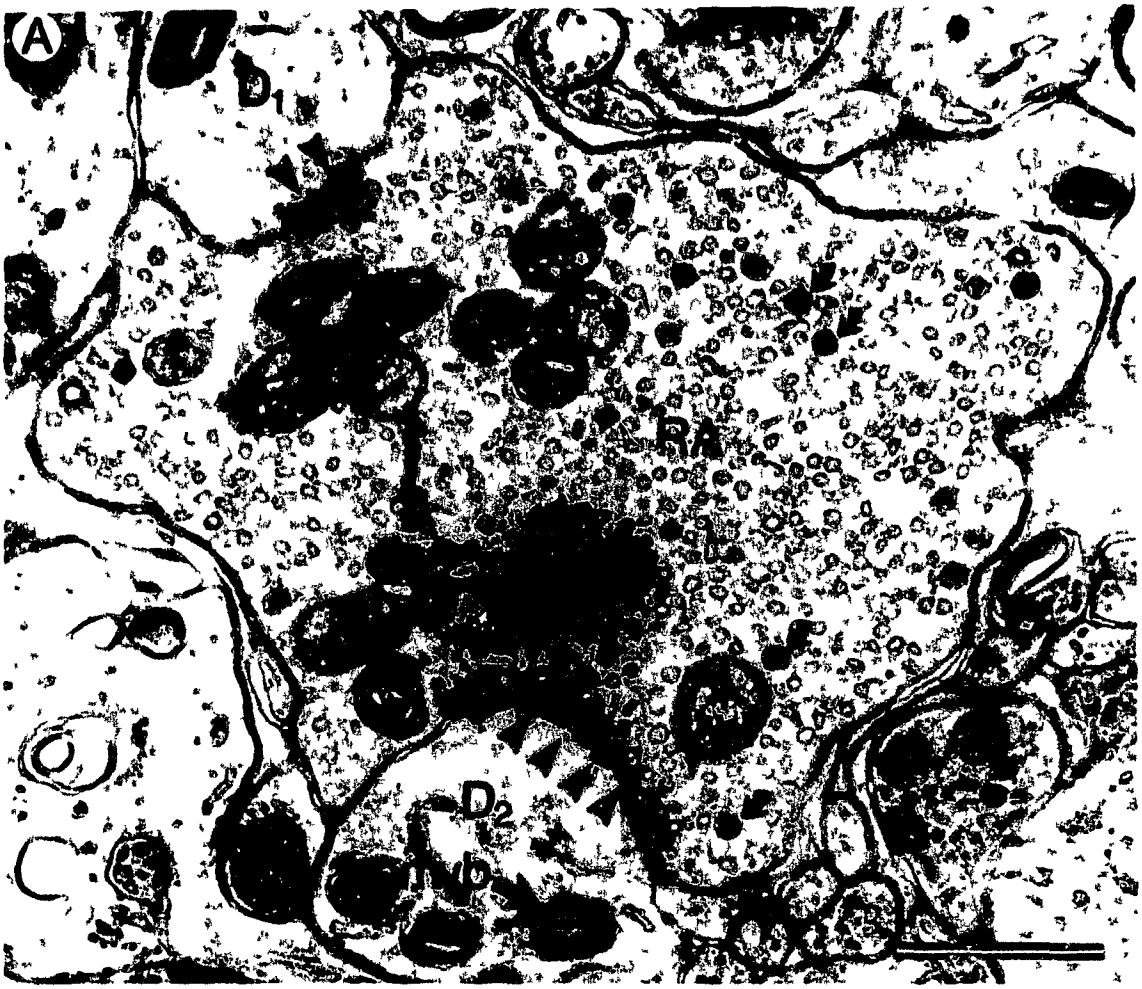

Figure 8

synaptology. The most common relationship observed was one in which a single large, labeled primary afferent terminal synapsed on a small diameter dendrite (< 1 μm) (Fig. 6A). A variation on the above basic arrangement is that of a labeled terminal making multiple synaptic contacts with a single postsynaptic dendrite (Fig. 6B). Another common arrangement was that of a primary afferent terminal making synaptic contact with two small dendritic elements (Figs. 7, 8). Multiple synaptic contacts on dendrites were also common (Figs. 6B, 7A). Esophageal afferent terminals also contained varying numbers of dense-cored vesicles distributed among the more numerous agranular vesicles (Figs. 6, 8). Dense-cored vesicles were not restricted to axon terminals and in a number of instances postsynaptic dendrites were identified as containing one or two dense-cored vesicles (Fig. 7B). Multivesicular bodies lying in the cytosol of the postsynaptic element were encountered (Fig. 8).

In summary, the results indicate that primary esophageal afferents form a number of different synaptic arrangements on small diameter dendrites in the NTScen. Furthermore, these terminals can be classified on the basis of size as a distinct subpopulation of RA synaptic terminals, the terminal type found to be most abundant in the NTScen.

DISCUSSION

This is, to our knowledge, the first electron microscopic study to be centered on esophageal afferents to the NTScen, where possible comparisons will be made between the ultrastructural features of esophageal afferents in the NTScen and features reported for other visceral afferents originating in upper alimentary and respiratory structures which have terminations in subnuclei of the NTS.

Previous cytoarchitectonic (Kalia and Sullivan, '82) or neurochemical (Kalia et al., '84b) studies of the rat NTS did not recognize the NTScen as a distinct entity, including it only in a larger medial subdivision of the NTS. Indications that there is a distinct part of the medial NTS corresponding to the NTScen was provided by Reiner and Vincent ('86) and Reiner et al. ('86) who noted that a region of the medial NTS was typically devoid of immunoreative staining for catecholamines. A similar area can be discerned in the neurochemical study of Kalia and colleagues ('84b). Most of the subsequent documentation confirming the NTScen as a distinct subnucleus was derived from neuroanatomical tracing studies which demonstrated NTScen projections to the ventrolateral medulla (Bieger, '84; Ross et al., '85) and anterograde studies of the sensory innervation of the esophagus (Altschuler et al., '89) and a study of NTS projections to the PBN (Herbert et al., '90).

Our studies in 1-μm-thick plastic sections containing anterograde labeling as a result of cervical and abdominal esophageal injections indicate that the NTScen extends for approximately 700 μm caudal to rostral, of which one quarter of the subnucleus lies caudal to the level of the obex. The present light and electron microscopic results show that the NTScen contains a distinct population of small, round neurons (7-12 μm in diameter). This contrasts with the results reported in Ross et al. ('85) who found NTScen neurons to be similar in shape but somewhat larger (12-17 μm in diameter). It is not clear from their

results whether measurements were taken from HRP or Fast Blue-labeled neurons or both. If measurements were made on fluorescent tracer-filled neurons, the fluorescent flare associated with such labeling could have obscured the true borders of the cell making it considerably more difficult to make accurate measurements, thus introducing an element of error that might translate into measurements which would be significantly greater than those obtained in the present study. However, Herbert et al. ('90) reported NTScen neurons of 10-12 μm in diameter in 40 μm-thick-sections which are closer to that of the present study The use of plastic sections (present study) enabled measurements to be made with a higher magnification (100x) and therefore greater resolution as a result of the thinness of the section. A second important cytoarchitectonic feature of the NTScen that has not been reported previously is the relationship which the centrally clustered neurons of the NTScen have with a rather cell-poor region at the peripheral boundaries of the nucleus in the transverse plane. This feature is most clearly evident in thin plastic sections cut in the transverse plane through the subnucleus just rostral to the level of the area postrema. On review of photographs of the NTScen in Altschuler et al. ('89) and Herbert et al. ('90) this feature is present, but in 40-μm-thick Nissl stained sections was less distinct possibly due to the greater thickness of the sections or to the staining of numerous glial cells. Interestingly, primary esophageal afferent labeling is prominent in this region of the subnucleus. Unfortunately, there are no specific Golgi studies of the NTScen in the rat which might shed some light on the organization of processes in this boundary region. Whitehead ('88) in a Golgi study of the rostral and caudal NTS in the hamster included an area that could correspond to the NTScen, in his central caudal subdivision. The cells in the central caudal subdivision were slightly larger than those in the rat NTScen and it was evident from the Golgi reconstructions of this area that neuronal cell bodies appear to be located centrally with dendritic processes predominantly oriented in a radial pattern out from the center of the subnucleus. Golgi preparations revealed neurons of the central

caudal subdivision to have 1-5 primary dendrites which branch to form aspinous secondary and tertiary branches within the peripheral zone around the subdivision. One interpretation of the present results and Whitehead's ('88) Golgi results might be that some neurons in the rat and hamster NTScen have preferential dendritic orientation in a radial fashion and that these dendrites (secondary and tertiary) are an important site for contact between centrally located neurons and primary afferent projections originating in the esophagus. The cytoarchitectonic arrangement of neurons and neuropil in the NTScen differs from that of the subnucleus interstitialis in which the neuronal somata concentrate around a peripheral core of longitudinally oriented neuropil (see Chapter 3). The function of the apparent segregation of neurons and neuropil is not known although it may imply integration of information at distal regions of the neurons.

Although there is considerable information regarding the cytoarchitecture (Ross et al., '85; Herbert et al., '90), connectivity (Fryscak et al., '84; Ross et al., '85; Cunningham and Sawchenko, '89; Altschuler et al., '89; Herbert et al., '90) and neurochemistry (Cunningham and Sawchenko, '89; Cunningham et al., '90; Herbert et al., '90) of the NTScen there is no information about the ultrastructure and synaptology of the NTScen or about the fine structural detail as it pertains to the main afferent input to this subnucleus from the esophagus. In spite of the pivotal role the NTS plays as a relay nucleus for sensory information related to gustatory and visceral sensations it has received very little attention with regard to the ultrastructural and synaptic organization within the individual subnuclei. Only a very few fine structural studies have been carried out in the NTS and most of these were in the cat (Chiba and Doba, '75, '76; Leslie et al., '82b; Chazal et al., '91). A similarly small number of investigations have looked at the synaptology of primary vagal afferents (Gwyn et al., '82; Velley et al., '91; Chazal et al., '91) and of these only two have addressed the question of vagal afferents of specific visceral origin, in particular slow and fast adapting pulmonary mechanoreceptors (Kalia and Richter, '85, '88).

Since the NTScen is most prominent at and just rostral to the level of the area postrema, the present electron microscopic survey was mainly carried out in sections from this region. Neuronal somata shared many of the morphological characteristics of neurons observed in the subnucleus interstitialis of the NTS (see Chapter 3). Both subnuclei contained neurons which were small in size, round or oval in shape and had a large nucleus set in a sparse cytoplasm. The nuclear membrane often contained numerous invaginations and organized Nissl substance was not present. The similarities in morphology between sensory neurons in the NTScen and those of the NTSis, both of which receive primary afferents from the upper alimentary tract, suggest that these neurons may perform similar functions. It is worth noting that electron microscopic surveys of the subnucleus gelatinosus (Leslie et al., '82b) and subnucleus commissuralis (Chiba and Doba, '76) revealed neurons of remarkably similar morphology to that of the NTScen. Both the NTScen and NTSis are known to have direct connections with the ventrolateral medulla (Ross et al., '85) including the region in and around the rostral part of the nucleus ambiguus where motoneurons innervating the pharynx and esophagus are located (Bieger and Hopkins, '87). However, while the NTSis also has connections with the PBN (Herbert et al., '90), the NTScen lacks any apparent connections with other brainstem regions outside the ventrolateral medulla (Ross et al., '85; Altschuler et al., '89; Herbert et al., '90). The lack of connections between the NTScen and the PBN is consistent with the disynaptic closed-loop reflex theory of esophageal motility presented by Cunningham and Sawchenko ('89, '90) in which primary afferent information from the esophagus converges on neurons in the NTScen which have direct connections (Moyles and Hopkins, '88) with neurons of the compact formation of the nucleus ambiguus innervating the musculature of the esophagus. There is evidence that NTScen neurons participating in the disynaptic closed-loop pathway of esophageal innervation (Cunningham and Sawchenko, '89) contain somatostatin and/or enkephalin (Cunningham and Sawchenko, '90). Both transmitters have been suggested to

be important inhibitory transmitters in the CNS (Siggins and Gruol, '86). Further evidence of somatostatin's role in inhibition comes from physiological work by Kalia et al. ('84a) which showed somatostatinergic NTS neurons to be involved in reflex circuits which inhibit respiratory efferent centers. It should also be mentioned that in a study of the synaptology of NTScen projections to the compact formation of the nucleus ambiguus following focal HRP injection into the NTScen all anterogradely labeled synaptic boutons were of a morphology consistent with excitatory inputs (Moyles and Hopkins, '88). This underscores the tenuous nature of the structure-function hypothesis if the two neurotransmitters mentioned above do, in fact, have inhibitory effects on neurons in the nucleus ambiguus.

An interesting and distinct feature of the NTScen was the clustering of neuronal somata centrally in the subnucleus and the tendency of small groups of neurons to be in close apposition to one another. Observations at the electron microscopic level revealed no membrane specializations (i.e., puncta adhaerentia or gap junctions) between these neurons. The functions of such close appositions is not clear; however, they may permit the exchange of small molecules directly between neurons.

The synaptic organization of the NTScen included axo-dendritic contacts involving RA and PS synaptic terminals. Of the two types of synaptic terminals identified PS synaptic terminals were extremely rare. One interpretation of the rarity of the PS type might be that these terminals play only a minor role in the function of the subnucleus. Conversely, the populous nature of RA synaptic terminals in the NTScen implicates this synaptic arrangement as being very significant in relation to NTScen function. Because the morphology of synaptic terminals has been linked to function, such that terminals containing round clear vesicles and forming asymmetric synapses (i.e., the present RA type) are excitatory and those containing pleomorphic or flattened clear vesicles and forming symmetric synapses (i.e., PS) are inhibitory (Eccles, '64; Uchizono, '65; Gray,

'69; Peters et al., '91) it would appear that the neurons of the NTScen are largely dependent on excitatory circuits with only a small inhibitory contribution. Although the hypothesis of a structure-function relationship has been invoked here, it need not necessarily be a valid correlation in every instance. This is particularly true in light of the fact that certain neurotransmitters (e.g., acetylcholine) can have two different functions (i.e., excitatory or inhibitory) depending on its location in the nervous system (Peters et al., '91). Therefore, even though neurotransmitters and neuromodulators have been identified in the NTScen (Kalia et al., '84b; Cunningham and Sawchenko, '90; Herbert et al., '90), it cannot be concluded that the vast majority of synapses in the NTScen are excitatory based only on synaptology. Without knowledge of neurotransmitters specifically localized to these terminals and their effect on neurons in the NTScen it is purely speculation as to their functional significance in the subnucleus. With respect to primary afferents it is generally accepted that their effect on centrally located second order neurons is excitatory. Therefore esophageal afferent projections to the NTScen excite postsynaptic neurons whose projections to the nucleus ambiguus influence motor outflow to the esophagus. In a pharmacological study Bieger ('84) was able to elicit esophageal motility as a result of the application of muscarinic cholinergic agonists to the NTScen.

Electron microscopic survey of the somata of the NTScen revealed that there is an absence of axo-somatic synaptic contacts in the subnucleus. This is similar to the situation in other NTS subnuclei including the subnucleus interstitialis (see Chapter 3) and the subnucleus commisuralis (Chiba and Doba, '76). The absence of axo-somatic contacts has some functional implications. It is generally accepted that synaptic contacts on the soma or on dendrites proximal to the cell body are (all other things being equal) more effective than similar synapses located at more distal sites on dendrites. The predominant synaptic arrangement in the NTScen regardless of the origin of the input involves a synaptic bouton

contacting a small diameter dendritc profile, presumably a distal dendrite since no dendritic spines were found on the somata or proximal dendrites in the NTScen.

The present study indicates that primary esophageal afferent terminations in the NTScen only make up a proportion of the total population of RA terminals within the subnucleus. Presumably unlabeled RA synaptic terminals which are larger than 1 μm in diameter correspond to primary afferents of esophageal origin, likely from thoracic regions of the esophagus which was not investigated in this study. The origin of the abundant small RA terminals is uncertain. However, there is some evidence that the rostral ventrolateral medulla has a light projection to the region of the NTScen (Herbert et al., '90; Ross et al., '85). The significance of a possible reciprocal connection between the ventrolateral medulla to the NTScen is not known nor is it clear from where specifically in the ventrolateral medulla such projections arise. It is unlikely, however, that this projection originates in the esophageal motor part of the nucleus ambiguus, since out of the many studies investigating the afferent inputs to the NTS there is no evidence of such a projection. Other than esophageal afferent inputs and possibly a projection from the ventrolateral medulla, no other part of the brain or spinal cord has been identified as giving rise to afferent fibers innervating the NTScen.

The present study of the synaptic organization of the NTScen has enabled the distinction of two main synaptic terminal types (i.e., RA and PS) based on the morphology of the vesicles and symmetry of synaptic contacts. In addition, two classes of RA synapses were identified: small and large. Following analysis of labeled esophageal RA synaptic terminals it was concluded that esophageal terminals differed in size from most unlabeled RA terminals in the NTScen and, thus, constituted a subpopulation of synaptic terminals. Esophageal afferent terminals in the NTScen are morphologically similar to vagal afferent terminals identified in other subnuclei of the NTS (Gwyn et al., '82; Kalia and Richter, '85, '88; Chazal et al., '91; Velley et al., '91). NTScen neurons, some of

which are somatostatinergic, serve as premotor neurons which project to the esophageal part of the nucleus ambiguus which supplies motor innervation to the musculature of the esophagus. The neurotransmitter or neurotransmitters contained in esophageal afferent projections are not known. Two putative neurotransmitters have been suggested based on histochemical and immunocytochemical studies. Cunningham and Sawchenko ('90) identified a small number of CGRP and substance P fibers in the NTScen although they could not establish their origin. The presence of neurons positive for CGRP and substance P in the nodose ganglion (Green and Dockray, '87) suggests that at least some of the fibers in the NTScen might be of primary afferent origin. Substance P has also been identified in fibers innervating the circular muscle layer, myenteric and submucosal plexus of all levels of the gastrointestinal tract, including the esophagus (Schultzberg et al., '80). Some of these fibers may be the peripheral endings of CGRP positive sensory neurons located in the nodose ganglion.

Functional Considerations

The act of deglutition (i.e., swallowing) requires the coordinated action of muscles in the mouth, pharynx, larynx and esophagus. Dysfunction of muscles during any phase of deglutition can result in difficulty in moving liquid and/or solid material from the mouth into and along the esophagus to the stomach. Swallowing is a complex sequence of events involving the coordination of a number of muscles located in the upper alimentary and respiratory tracts. It is generally accepted that the central regulation of the pharyngeal as well as esophageal stage of swallowing is dependent upon the sensory input of receptors located in the mucosa and submucosal regions of these structures (Miller, '82; Diamant, '89). Mei ('83) classified the viscerosensory receptors of the esophagus into muscular mechanoreceptors, mucosal and serosal mechanoreceptors as well as mucosal chemosensitive and thermosensitive receptors. Sensory information is conveyed centrally

to the medulla oblongata from the esophagus via the vagus nerve but sensory pathways are also believed to be present in sympathetic nerves which enter the spinal cord (T3-T12) (Diamant, '89). Vagal sensory fibers have been described as originating primarily in the muscular layers of the esophagus in and around the myenteric plexus with only a few fibers in the submucosal and mucosal layers (see Cunningham and Sawchenko, '90 for review). Esophageal afferent projections terminate in a discrete subnucleus of the NTS lying medial to the TS (Altschuler et al., '89) termed the subnucleus centralis of the NTS (Ross et al., '85) but it is not known at present what modalities are carried by afferents to the NTScen. Esophageal afferent projections have a topographical arrangement within the NTScen such that cervical levels terminate in slightly more rostral parts and successively more caudal esophageal locations (i.e., thoracic and abdominal) have more caudal terminal fields in the NTScen (Altschuler et al., '89). There is, however, a high degree of overlap in the terminal fields of afferent projections from these three levels of the esophagus

Most of the current knowledge about the neural basis of esophageal motility has been derived from studies carried out in a variety of species including, cat, dog, sheep, opossum and rodent. The present study of the sensory innervation of the rat esophagus is a continuation of a number of light microscopic studies of the distribution of esophageal afferent projections to the NTScen (Fryscak et al., '84; Altschuler et al., '89). The NTScen has been implicated both anatomically (Fryscak et al., '84; Altschuler et al., '89) and physiologically (Jean, '84; Bieger, '84) as subserving reflex control of esophageal motility. According to the disynaptic closed-reflex loop theory of esophageal motility (Cunningham and Sawchenko, '89) the NTScen contains neurons which receive afferent sensory information from mechanoreceptors located in the wall and mucosa of the esophagus. Jean ('84) identified three regions of the medulla oblongata of sheep which are important to deglutition activity; of which one group's location corresponded to the NTScen. In further support of these data, Bieger ('84) was able to elicit the esophageal

stage of swallowing following injection of the excitatory amino acid glutamate into the area of the NTScen.

Vagal sensory information from the esophagus appears to originate primarily from the peripheral endings located between the longitudinal and circular muscle layers of the esophageal tube and from in and around the myenteric ganglia (Clerc and Condamin, '87; Christensen, '84; Neuhuber, '87). Although myenteric ganglia are more numerous and probably play a larger role in the motor activity of smooth muscle such ganglia do exist in the striated musculature of the esophagus and have been suggested to play a sensory rather than a motor role (Diamant, '89; Nelson and Richter, '89). The significance of sensory ganglia in the striated esophagus has not been clearly established although they probably play a role in the local sensory activity, and in this capacity mediate and/or modulate mechanoreceptive information, possibly as a result of distortion of the ganglion (see Cunningham and Sawchenko, '90 for review). Centrally directed vagal fibers innervating the esophageal ganglia probably convey information collected directly through distortion of their peripheral endings or possibly indirectly through contacts with ganglion cells.

Two types of esophageal peristalsis have been identified. The first, primary peristalsis is elicited in response to pharyngeal swallowing while secondary esophageal peristalsis occurs in response to distension of the organ whether or not it is preceded by a swallow (Hwang, '54; Cunningham and Sawchenko, '90). The reflex peristaltic response of the esophageal musculature to distension of the esophageal wall in a disynaptic reflex loop must be dependent on central relay of information about the status of the viscus, particularly in light of the paucity of identified inputs to the NTScen from elsewhere in the periphery or centrally. It would seem likely that in order for smooth, orderly peristaltic waves to occur, sensory input must also be organized sequentially. This is supported by the observation that esophageal terminal fields in the NTScen are topographically organized (Altschuler et al., '89) as are esophageal motoneurons (Bieger and Hopkins, '87). This

arrangement might provide the anatomical substrate for the recruitment of neurons in the NTScen responsible for influencing distinct populations of motoneurons in the compact formation of the nucleus ambiguus. In other words, local sensory events are transmitted sequentially from cervical, thoracic and abdominal parts of the esophagus to specific regions of the NTScen where premotor neurons can sequentially affect motoneurons in the compact formation of the nucleus ambiguus thus producing organized cranial to caudal waves of motor activity. At this time it is not clear whether the effect of NTScen neurons on NA motoneurons is excitatory or inhibitory or both. However, it is known that relaxation of muscle tone in the esophageal wall is necessary prior to bolus movement (Diamant, '89). This suggests that at least part of the input to motoneurons is likely to be inhibitory in nature. This is consistent with the identified somatostatinergic and enkephalinergic inputs to the nucleus ambiguus from the NTScen (Cunningham and Sawchenko, '90). On the other hand Moyles and Hopkins ('88) found anterogradely labeled boutons in the nucleus ambiguus which morphologically corresponded to excitatory terminals following injection of HRP into the medial NTS. It might be that both excitatory and inhibitory inputs from the NTScen are present and that these are also sequentially activated by some as yet unidentified mechanism. Such a mechanism might be related to the many small unlabeled RA synaptic terminals identified in the present study. The origin, central or peripheral, of these apparently non-esophageal synaptic terminals is not known. Perhaps these are excitatory inputs of central origin responsible for the activation of neurons in the NTScen, responsible for sequentially activating motoneurons which will produce contraction of the esophageal musculature. Although a considerable body of information has been reported in the literature related to esophageal motility, it is far from clear how sensory afferent information conveyed to the NTScen is organized to produce sequential effects on motoneurons producing muscular contractions. Clearly, further study of the neurochemical properties of esophageal afferent projections, their effects on NTScen

neurons, and the origin of non-esophageal RA terminals in the NTScen would greatly extend our understanding of interactions within the NTScen.

CHAPTER 3

SUBNUCLEUS INTERSTITIALIS OF THE NUCLEUS OF THE TRACTUS SOLITARIUS OF THE RAT: CYTOARCHITECTURE, ULTRASTRUCTURE, AND SYNAPTOLOGY OF PRIMARY AFFERENTS.

INTRODUCTION

Deglutition is a complex sequence of muscular contractions and relaxations which involve the coordinated efforts of oral, pharyngeal, laryngeal and esophageal musculature. The pharynx and larynx are anatomically and embryologically closely related. Furthermore, these structures are linked in function such that certain physiological processes like respiration, deglutition, coughing, and phonation require reflex changes in one or both of these viscera in order for smooth effective results to occur. Dysphagia (i.e., difficulty in swallowing) is an example of a motility disturbance that is often localized to the pharynx and can cause distressing symptoms such as disturbances of speech and regurgitation (Nelson and Richter, '89). The pharynx acts as a conduit for air movement into and out of the larynx and for liquids and solids diverted to the esophagus. The larynx on the other hand forms the upper end of the tracheopulmonary tree and functions in phonation and reflexive defense responses which prevent the incidental influx of solids and liquid into the trachea as a result of respiration or deglutition.

Sensory information from the pharynx and larynx is conveyed to the brainstem via the glossopharyngeal and vagus nerves, respectively (Kalia and Mesulam, '80b; Nomura and Mizuno, '83; Jean, '84; Bradley et al., '85; Sweazey and Bradley, '86; Hanamori and Smith, '86, '89; Altschuler et al., '89). Interestingly, although the pharynx and larynx are

separate structures they provide convergent afferent input to a small circumscribed subnucleus of the NTS called the subnucleus interstitialis (NTSis) (Kalia and Mesulam, '80b; Altschuler et al., '89) The NTSis is closely associated with the tractus solitarius along its rostrocaudal length and within the NTSis pharyngeal and laryngeal afferent terminal fields overlap extensively (Altschuler et al., '89).

The NTSis has efferent connections with the ventrolateral medulla (Ross et al., '85; Herbert et al., '90) and with the parabrachial nucleus of the dorsolateral pons (Herbert et al., '90). In the ventrolateral medulla the semicompact formation of the nucleus ambiguus (Bieger and Hopkins, '87) contains the motoneurons which innervate the striated musculature of the pharynx while the loose formation contains motoneurons supplying innervation to the muscles of the larynx. The parabrachial nucleus receives an ascending projection from the NTSis although the specifics of this projection have not been clearly demonstrated.

Very little is known about the function and fine structural detail of the NTSis. With the exception of a recent report by Chazal et al. ('91) on the ultrastructure of vagal afferents in the NTSis of the cat, no information is available with regard to the fine structural detail of afferents originating in specific structures and terminating in the NTSis.

The present chapter presents the results of a transganglionic tracer study, investigating the synaptology of pharyngeal and laryngeal afferents terminating in the NTSis. In addition it provides a description of the neurons, neuropil and synaptic organization of the NTSis.

MATERIALS AND METHODS

Subjects and Surgery

The subjects were 48 male Wistar rats (250-350g) anaesthetized with sodium pentobarbital (40-60 mg/kg, i.p.) for all surgical procedures and prior to sacrifice.

In 30 of the 48 rats used in this study, wheat germ agglutinin-horseradish peroxidase (WGA-HRP, Sigma) or cholera toxin-HRP, beta subunit, (CT-HRP, List Laboratories Ltd.) were injected into the pharynx or larynx.

The pharynx and larynx were exposed through a ventral approach. A ventral midline incision was made in the neck and the underlying superficial neck muscles were exposed, and the muscles were carefully dissected along fascial planes using a blunt probe and scissors so as to minimize hemorrhage. Deep to these muscles, the trachea and esophagus were displaced laterally with umbilical tape looped under both structures to expose the retropharyngeal space and permit visualization of the dorsal aspect of the pharynx and the lateral part of the larynx. Microinjections (2-8 μl) of WGA-HRP or CT-HRP were made into the musculature and mucosa of the pharynx or larynx under the visual guidance of a Leitz surgical microscope. Tracer injections into the dorsal aspect of the larynx were accomplished by freeing the trachea and larynx from the underlying esophagus and placing sterile gauze over the esophagus to prevent incidental uptake due to tracer spillage.

To make injections, glass micropipettes (tip diameter 50-75 μm) were attached with dental sealing wax to polyethylene tubing and a mineral oil-filled 50 μl Hamilton syringe. WGA-HRP was administered at a concentration of 5% and CT-HRP at 0.1 or 0.5% in distilled water. The micropipettes were inserted into the wall of the viscus and single or multiple penetrations were made with small aliquots of tracer being delivered by pressure injection. In order to limit tracer spillage and spread to adjacent structures, sterile gauze was placed around adjacent structures and visible leakage was absorbed with sterile cotton

swabs. Following injections, the neck muscles were reapposed and sutured. The skin incision was closed with surgical staples and a topical antibacterial was applied to prevent infection.

The specificity of each of the injection sites was verified by identifying the distribution of retrogradely labeled motoneurons in the nucleus ambiguus. Pharyngeal motoneurons were found to be located in the semicompact formation, while the loose formation of the nucleus ambiguus contained discontinuous clusters of motoneurons characteristic of motoneurons innervating the musculature of the larynx (Bieger and Hopkins, '87). Spread of tracer to the esophagus, particularly during pharyngeal injections, did occur but could be easily identified by the presence of afferent labeling in the subnucleus centralis of the NTS and retrogradely labeled neurons in the compact formation of the NA (Bieger and Hopkins, '87; Altschuler et al., '89). In those cases where retrograde labeling in the compact formation indicated spread to the esophagus it was not necessary to eliminate these from the study since the esophagus does not project to the NTSis (Altschuler et al., '89).

Light Microscopy

The cytoarchitectonic analysis of the NTSis was carried out on semithin (1 μm-thick) sections in 10 normal rats. Rats were perfused transcardially with a fixative suitable for electron microscopy, were processed for electron microscopy and embedded in epoxy resin (see section on electron microscopy). Representative semithin plastic sections in the transverse (n=6) or horizontal (n=4) planes were cut from the NTSis. Sections were floated onto chrome alum-coated slides and stained with toluidine blue. Stained sections were studied and photographed with a Leitz Orthoplan microscope.

Electron Microscopy

Thirty-eight male Wistar rats were used to study the ultrastructure and synaptology of primary afferent projections of the NTSis. The rats were perfused transcardially over a period of 1 hour with a prerinse of 500 ml of 0.15 M phosphate buffer containing 0.1% sodium nitrite followed by 1 L of aldehyde fixative (0.5% paraformaldehyde and 2.5% glutaraldehyde) in 0.15 M phosphate buffer giving a final osmolarity of 777-800 mosmol (pH 7.3; 20°C). Following perfusion the brains were left in situ for 1-2 hours before craniotomy and removal of the brain. Each brain was placed in 0.15 M phosphate buffer prior to cutting 100-μm-thick vibratome (Lancer) sections through the medulla oblongata. Vibratome sections were cut from each brainstem in either the transverse (n=28) or horizontal (n=10) plane. Blocks of tissue containing the NTSis and adjacent NTS subnuclei were trimmed with a razor blade to a trapezoid shape with a standardized orientation. Tissue blocks were secondarily fixed in 1% osmium tetroxide in 0.15 M phosphate buffer for 1-2 hours (20°C), stained *en bloc* with saturated aqueous uranyl acetate for 1 hour (4°C), dehydrated through a graded series of acetone baths (5 min. each) and embedded in epoxy resin for 48 hours at 60°C. Semi-thin plastic sections (1 μm-thick) were cut on a Reichert OMU3 ultramicrotome. Sections were either stained with toluidine blue for orientation purposes prior to electron microscopic analysis or left unstained as was the case when dark-field illumination was necessary to identify afferent terminal fields. Ultrathin sections of silver interference color were cut with a diamond knife and floated onto slotted grids coated with pioloform (Marivac, R 1275) or 400 mesh grids. Ultrathin sections were stained with Reynolds lead citrate at room temperature for 1-2 minutes. Electron microscopic observations were carried out on a Zeiss EM 10A electron microscope.

HRP Histochemistry

After survival periods of 2-4 days, rats were sacrificed and the brains processed for HRP histochemistry with tetramethylbenzidine as the chromogen (Mesulam, '78). Serial 100-μm-thick vibratome sections were cut in either the transverse or horizontal plane through the medulla oblongata. Sections were incubated in medium containing the chromogen for twenty minutes, followed by a further twenty minutes in the same medium after the addition of 6 ml of substrate (1% H_2O_2) per 300 ml of medium. Once the crystalline reaction product was developed, it was stabilized for 10-15 min. in 5% ammonium molybdate in acetate buffer (pH 5.0) (Marfurt et al., '86). Following stabilization, blocks of tissue containing afferent labeling in the NTSis were processed for electron microscopy according to methods described for electron microscopy above. This procedure yielded HRP reaction product which was easily identified in 1 μm-thick plastic stained or unstained sections. At the electron microscopic level, HRP reaction product was readily located in axonal and terminal profiles and appeared as a distinct electron-dense crystal which rarely obscured the ultrastructure of synaptic boutons (Allen and Hopkins, '90). This histochemical procedure was found to be more sensitive than the diaminobenzidine technique of Itoh et al. ('79) and the tetramethylbenzidine sequential incubation in diaminobenzidine technique (Allen and Hopkins, '90).

Quantitative Analyses

A camera lucida was used to make drawings of neuronal somata in the NTSis in plastic sections stained with toluidine blue. Drawings were made with a 100x oil immersion objective. Sections were taken from representative rostral to caudal parts of the NTSis in the transverse plane, and from representative dorsal to ventral sections in the horizontal plane. Measurements of the maximum and minimum diameter, and nucleus to cytoplasm ratio were made from the camera lucida drawings with a Zeiss IBAS image analysis

system. A total of 607 neuronal profiles containing a nucleolus were included in the analyses.

ABBREVIATIONS

A	axon
D	dendrite
DCV	dense-cored vesicles
G	glia cell
Go	golgi apparatus
mt	mitochondrion
N	nucleus
NTS	nucleus of the tractus solitarius
NTSis	subnucleus interstitialis of NTS
PD	proximal dendrite
PS	pleomorphic symmetric
pt	preterminal axon
RA	round asymmetric
RER	rough endoplasmic reticulum
SER	smooth endoplasmic reticulum
sp	dendritic spine

TS tractus solitarius

RESULTS

Light Microscopic Observations

Cytoarchitecture. The NTSis was a distinct subnucleus (Fig. 1) closely related to the tractus solitarius (TS) with an overall length ranging from 1100 to 1400 μm. Caudally, the NTSis, which closely follows the length of the TS, is located dorsomedially in the caudal brainstem. At more rostral levels the NTSis and the tract move progressively more laterally as the fourth ventricle opens. The major portion of the subnucleus lies rostral to the obex with approximately one third of its length located caudal to the obex. Except for its rostral and caudal limits, the NTSis is easily identified as a circumscribed region of grey matter with a characteristic neuropil lying within the crescent of the TS which encompasses the subnucleus on all sides except for a ventrolateral area that merges with the adjacent nuclei (Fig. 1). At its caudal extreme the NTSis consists of a very small number of neurons and sparse neuropil dispersed among tightly packed, myelinated fibers of the TS. At its rostral pole the NTSis gradually expands to form diffuse moderately cell-rich regions among the heavily myelinated fibers of the TS. At this level the TS consists of dispersed bundles of myelinated fibers that have yet to form the discrete bundles that are characteristic of the TS over most of its length.

Neurons. In the transverse plane small neurons, typically 9-16 μm in diameter, were conspicuously located around the periphery of the subnucleus with few neurons in the core of the subnucleus (Fig. 1A). Neurons of similar size and morphology were found embedded among the bundles of myelinated fibers of the TS that surround the NTSis and were considered to be part of the subnucleus (c.f., Cajal, '09). Neurons in the ventrolateral part of the subnucleus where the TS opens to adjacent subnuclei, merge with the larger neurons of the subnucleus ventrolateralis. The profiles of neuronal somata in the

Fig. 1. Photomicrographs of NTSis cut in the transverse (A) and horizontal (B) plane. **A**: In the transverse plane most of the processes in the NTSis appear to be cut in cross section. The core of the subnucleus is surrounded by peripherally located neurons (arrowheads) and myelinated fibers of the tractus solitarius (TS). **B**: In the horizontal plane many of the processes making up the neuropil are longitudinally or obliquely cut. Note the fusiform-shaped neuron with two proximal dendrites originating from opposite poles of the cell body (arrowheads). Calibration bars: 50 μm.

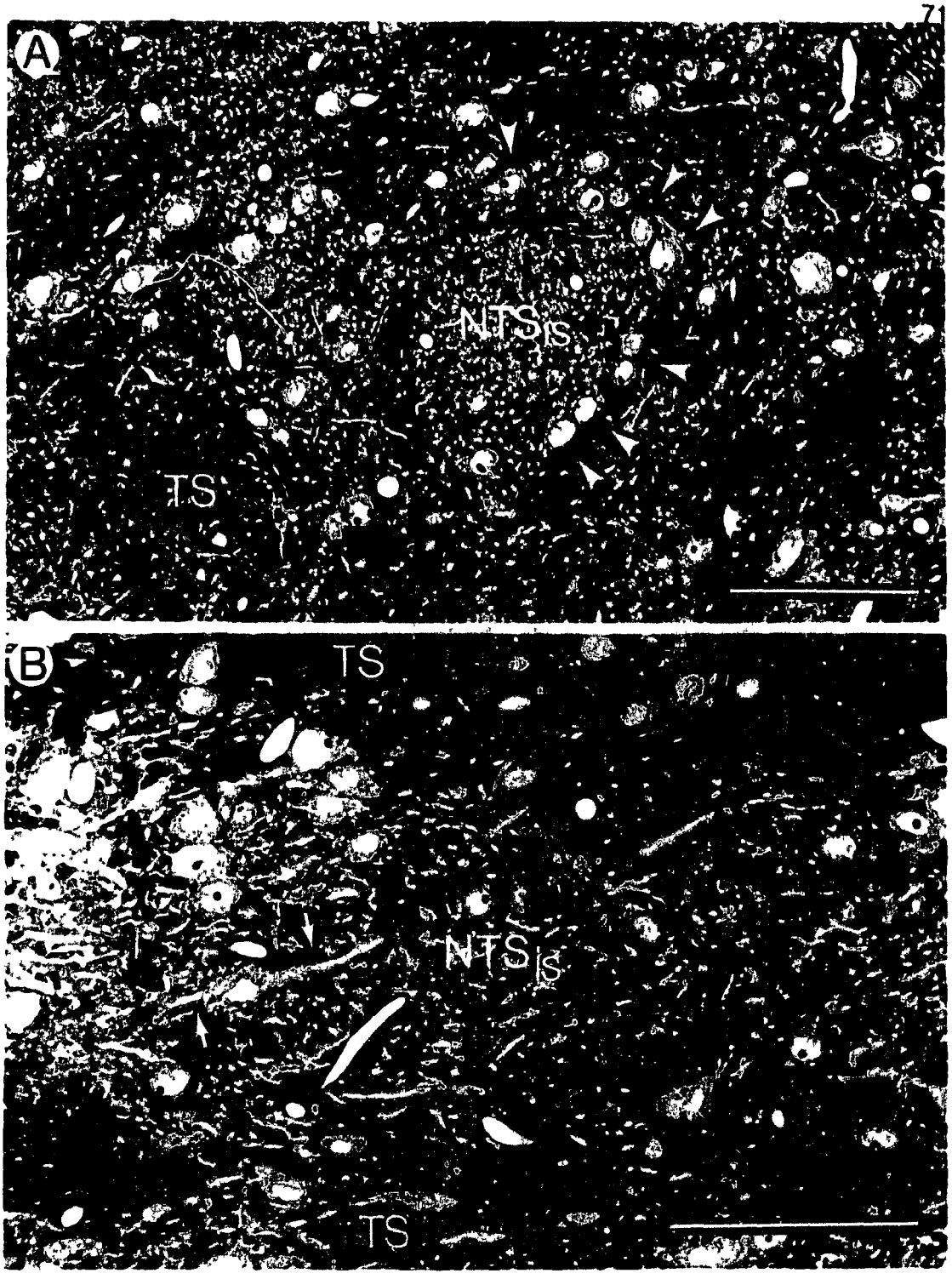

Figure 1

NTSis were round or oval when cut in the transverse plane and were characterized by a nucleus to cytoplasm ratio of 1:2, and a paucity of cytoplasmic organelles. In particular, there was little in the way of clumped or organized Nissl substance. The nucleus frequently had numerous deep infoldings in the nuclear membrane and a prominent, eccentric nucleolus. It was not unusual to see an extranucleolar mass located some distance from the larger nucleolus.

Neuropil. The neuropil consisted predominantly of unmyelinated processes. Small-diameter, lightly myelinated fibers occasionally coursed through the subnucleus. When the NTSis was cut in the transverse plane the majority of processes had a distinct orientation as evidenced by the many cross-sectional profiles in the neuropil. Thus the fibers making up the neuropil of the NTSis were oriented predominantly along the long axis of the subnucleus (Fig. 1A). Glial cell bodies, slightly smaller in size than neuronal profiles, were easily distinguished by their homogeneous darkly-stained cytoplasm and nucleus with dense chromatin.

The appearance of neurons and neuropil in horizontal sections through the NTSis were consistent with the features of the cytoarchitecture identified in transverse sections and provided additional information about the orientation and shape of neurons. In horizontal sections the NTSis was small and indistinct at its caudal extreme with a greatly reduced number of neurons and scant neuropil while at the rostral pole, the subnucleus gradually dissipated as the longitudinal bundles of the TS became less organized. At middle levels the NTSis reached its largest extent and this is the level from which the description and ultrastructural analysis of the nucleus is primarily based. Numerous neuronal somata were more fusiform in shape when observed in horizontal sections (Fig. 1B). In optimal sections one and sometimes two proximal dendrites could be seen emanating from opposite poles of the soma (Fig. 1B). Nissl substance was typically very sparse even though considerably more cytoplasm, particularly at the poles of the cells, could be seen in the

horizontal plane. The neuropil consisted of many longitudinally or obliquely cut profiles of axons and dendrites of various sizes. Glial cell morphology appeared similar in both the transverse and horizontal planes.

Electron Microscopic Observations

In order to ensure that the ultrastructural analysis was restricted to the NTSis and did not include adjacent subnuclei, blocks of tissue for electron microscopy were trimmed so that only the TS and grey matter making up the NTSis were present. As a consequence, the most rostral and caudal portions of the subnucleus were not investigated for the normal ultrastructural studies. However, in experiments in which primary afferent labeling was present, it was possible to identify and study the ultrastructure and synaptology of rostral and caudal regions with considerable certainty. Examination of caudal and rostral regions did not reveal ultrastructural or synaptological differences from the more easily delineated intermediate regions, which formed the bulk of the subnucleus.

Neurons. Round to fusiform neuronal profiles (Figs. 2, 3) were most numerous around the periphery of the NTSis. Occasionally, two neurons were in close apposition with no intervening neuropil, but no plasma membrane specializations were observed in any of these instances. A survey of many neurons in both transverse and horizontal preparations revealed several characteristic features of NTSis neurons. In general, the nucleus occupied most of the soma and was surrounded by a thin band of cytoplasm (Figs. 2, 3). Most nuclei were centrally located and contained at least one and often several invaginations in the nuclear membrane. These invaginations often imparted a lobular appearance to the nucleus (Fig. 2C). Each nucleus contained a prominent, darkly-stained nucleolus and occasionally, an extranucleolar body. The extranucleolar body was located either in close association with the nucleolus or some distance removed in the nucleoplasm (Fig. 2A, C). The extranucleolar body was typically smaller in size than the nucleolus and

Fig. 2. Electron micrographs of typical NTSis neurons. **A**: Two nuclei (N_1 and N_2) in adjacent somata which are closely apposed to each other (arrowheads) and to a darkly-stained glial cell (G). Note the extranucleolar body (arrow) in N_1. **B**: NTSis neuron exhibiting a prominent nucleolus, highly invaginated nuclear membrane and sparse reticulated RER (arrowheads). **C**: Neuron exhibiting a lobulated nucleus and extranucleolar body (arrow).
Calibration bars: 3 μm.

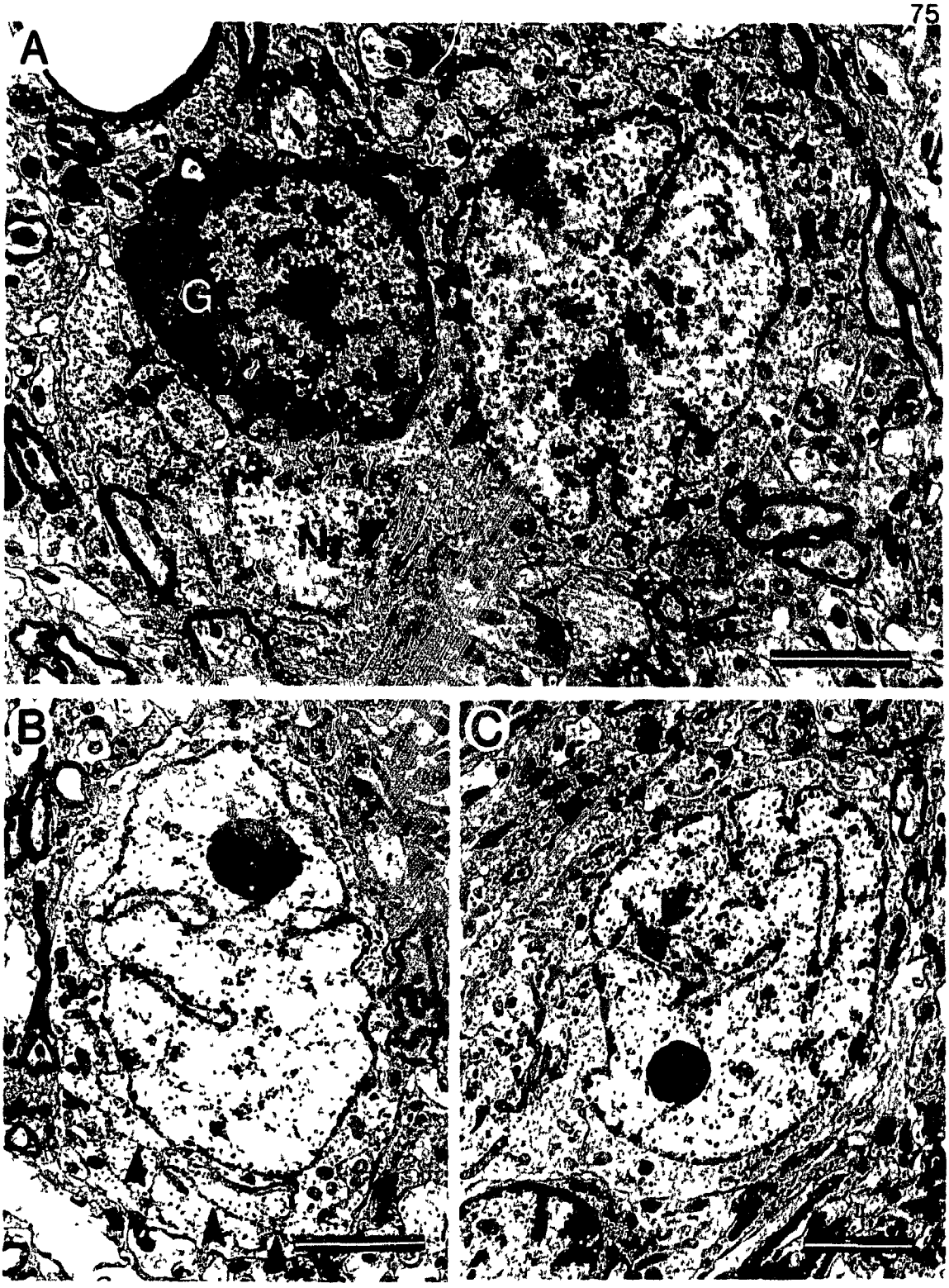

Figure 2

appeared to correspond to a coiled body, or accessory body of Cajal (see Peters et al., '91 for review).

Neuronal somata contained the normal complement of cytoplasmic organelles although most were relatively few in number. Rough endoplasmic reticulum (RER) in perikarya was particularly sparse although strands of RER were seen. In many instances RER appeared to take origin from the nuclear membrane and extended out into the cytoplasm. Single strands of RER coursing in the cytoplasm often bifurcated to give off short segments that ended near but not in contact with the plasma membrane. Free ribosomes and ribosomal rosettes were numerous throughout the soma and extended into proximal dendrites (Fig. 3). Well-developed Nissl bodies were observed in only two neurons and these neurons were deeply embedded in the TS and may, therefore, have represented neurons belonging to another subnuclear group. Other organelles present in the cytoplasm of somata and proximal dendrites included: mitochondria, golgi apparatuses and dark lysosomal profiles. Rarely, the golgi apparatus was found in the proximal dendrites but numerous free ribosomes and elongated mitochondria were commonly found in this location (Fig. 3). Occasionally, dense-cored vesicles (DCV) 70-100 μm in diameter and similar in morphology to those found in axon terminals in the NTSis were seen in the cytoplasm of NTSis neurons.

Darkly-stained glial cell bodies and glial processes were widely distributed among the neural elements of the NTSis. Glial cells were often in close apposition to neuronal profiles with no apparent intervening neuropil (Fig. 2A). Fine glial processes permeated the space between dendrites, unmyelinated axons and axon terminals.

Neuropil. At the electron microscopic level the neuropil in the NTSis contained many dendritic, axonal and axon terminal profiles with the orientation of most processes being consistent with the observations made at the light level where processes were oriented along the long axis of the subnucleus. Occasionally one and sometimes two

Fig. 3. Electron micrograph of a NTSis neuron with a single PS terminal synapsing on a proximal dendrite (PD). **A:** Note the nucleus (N), mitochondrion (mt) and golgi complex (Go). **B:** High magnification of boxed area in (A) showing a PS synaptic terminal making two contacts (arrowheads) with a proximal dendrite. Calibration bars: A, 2 μm; B, 1 μm.

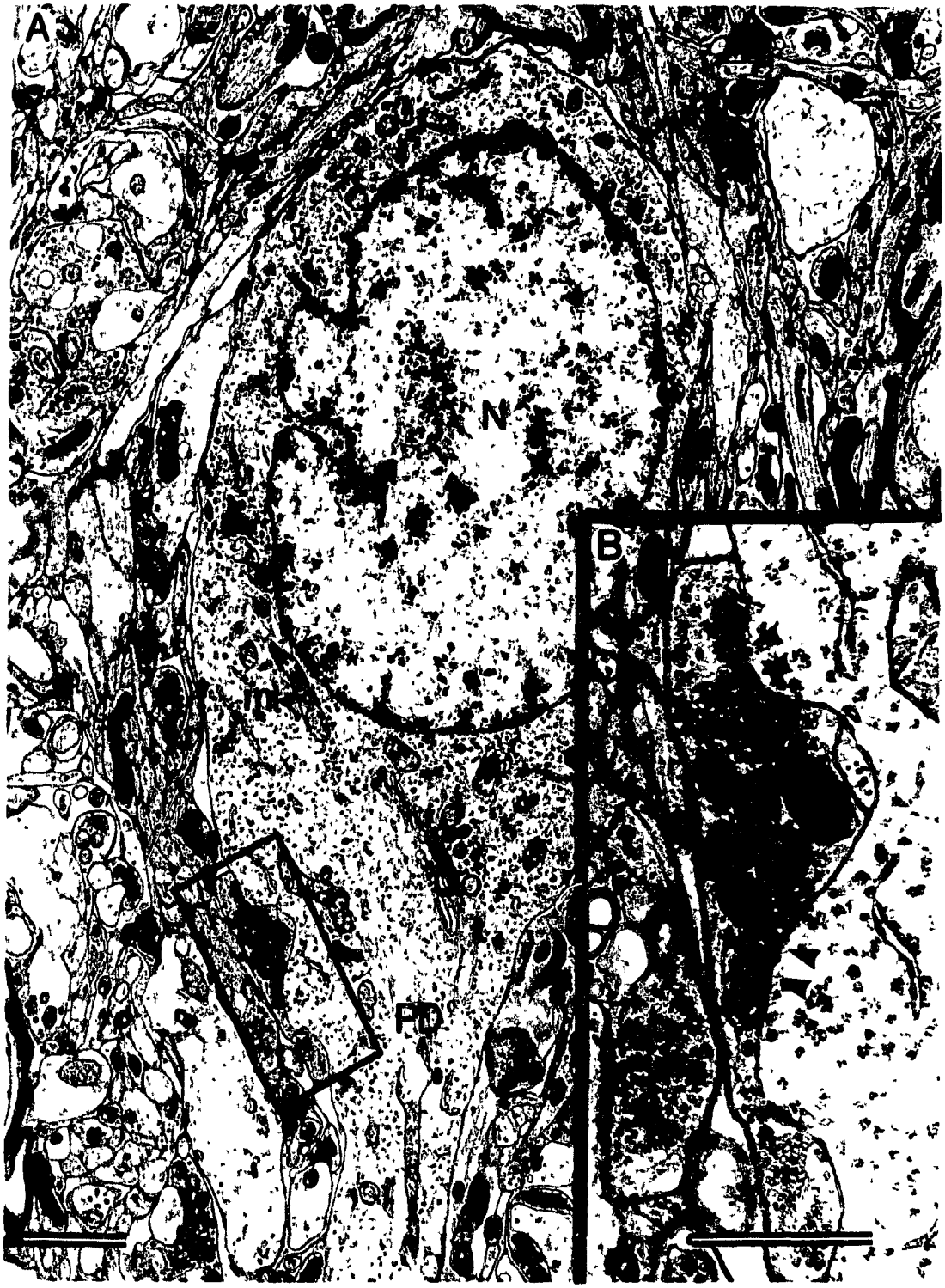

Figure 3

primary dendrites could be observed arising from a neuronal cell body. When two dendrites were present in a single profile they usually were located at opposite poles of the cell. Proximal dendrites were between 2.0-3.5 μm in diameter and tapered rapidly within a short distance (10-20 μm) from the soma. Numerous dendritic profiles ranging in size from less than 0.5 μm in diameter to that of proximal dendrites were intermingled with preterminal axons and axon terminals.

Proximal dendrites were pale or flocculent in appearance and contained numerous evenly spaced microtubules. Organelles present in large proximal dendrites included: mitochondria, numerous free ribosomes, smooth endoplasmic reticulum (SER) and/or RER. Axo-dendritic contacts on proximal dendrites were infrequent, and predominantly contained clear pleomorphic vesicles and formed symmetric synaptic junctions (Fig. 3). Smaller (< 1.5 μm in diameter) pale profiles, presumably representing secondary and tertiary dendrites made up the bulk of the dendritic profiles in the NTSis. These dendrites displayed a paucity of organelles such as RER and free ribosomes. However, evenly spaced microtubules and dark mitochondrial profiles could be seen in most small dendritic elements greater than 1 μm in diameter (Figs 5, 7). Pale dendritic profiles lacking any distinct organelles were common (Fig. 5B). Occasionally, multivesicular bodies and DCV were found in dendritic profiles adjacent to synaptic contacts. Near the periphery of the NTSis, adjacent to the TS, dendritic elements outnumbered axonal profiles and often formed small bundles containing 4-7 dendrites. Synaptic contacts were most numerous on dendritic profiles of small diameter (< 1.0 μm) in the neuropil. Dendritic spines were not observed on primary and secondary dendrites although some small (< 1 μm diameter) dendritic profiles in some instances could not be reliably distinguished from dendritic spines because of a lack of evidence that would suggest that a profile was dendritic or spinous.

Fig. 4. Electron micrograph of two neurons and a glial cell (G) in the NTSis. Note the axon bundles (A_1 and A_2) running in different orientations through the neuropil. Calibration bar: 4 μm.

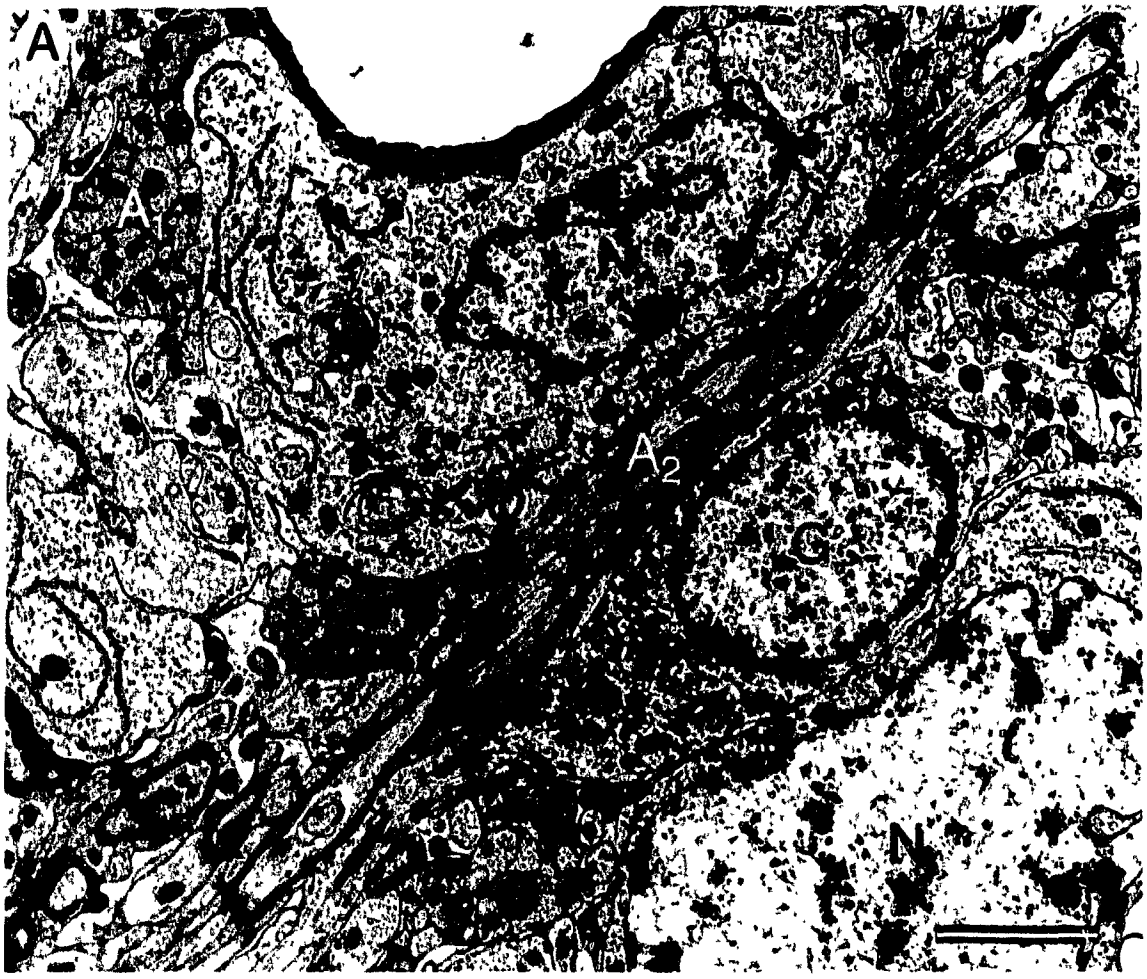

Figure 4

Other constituents of the neuropil included unmyelinated preterminal axons and axon terminals. The cytosol of preterminal axons was characteristically darker in appearance than dendritic profiles and contained numerous microtubules although they were usually less well organized than those in dendrites. Vesicles with similar morphology to those found in axon terminals (see synaptology) were observed in small numbers in preterminal segments of axons. Unmyelinated axonal profiles coursed among neuronal somata, dendrites and other axons. A striking feature of the NTSis was the presence of unmyelinated axonal bundles (Fig. 4). Bundles contained twenty or more morphologically similar axons. In addition to microtubules, axonal elements contained small numbers of dark mitochondria. Occasionally, puncta adhaerentia were observed between adjacent axons in axonal bundles or between two adjacent axons in the neuropil. Unlike the majority of processes in the neuropil which were oriented along the long axis of the subnucleus, axonal bundles could be seen running parallel as well as perpendicularly to the more general orientation of the neuropil (Fig. 4).

Synaptology. Within the NTSis, two major classes of synaptic terminals were distinguished based on the morphology of the synaptic vesicles and synaptic contacts. The first terminal type contained predominantly agranular, round vesicles and formed an asymmetric synaptic contact (RA) with postsynaptic elements (Figs. 5, 6). Vesicles in RA synaptic terminals were generally uniform in shape and size. The second terminal type contained a mixture of agranular vesicle ranging in shape from flattened to round and therefore were pleomorphic in appearance. Terminals containing pleomorphic vesicles formed symmetric contacts (PS) (Figs. 6, 7). On rare occasions axon terminals containing round vesicles appeared to form symmetric synaptic contacts, although serial sections through a number of these profiles revealed this to be due to the plane of section through the synapse. Frequently, postsynaptic dense bodies were encountered when RA synaptic terminals contacted small dendrites (Fig. 10). In both RA and PS synaptic terminals the

Fig. 5. Electron micrographs of RA synaptic terminals. **A:** RA terminal making a single asymmetric contact (arrowheads) with a dendrite (D). Note the microtubules (arrows) in the axon terminal and dendrite. **B:** Small unmyelinated preterminal axon (pt) expanding to form a RA synaptic terminal which makes four asymmetric contacts (arrowheads) with four different dendritic profiles (D). The arrow indicates a multivesicular body. Calibration bars: A, B, 0.5 μm.

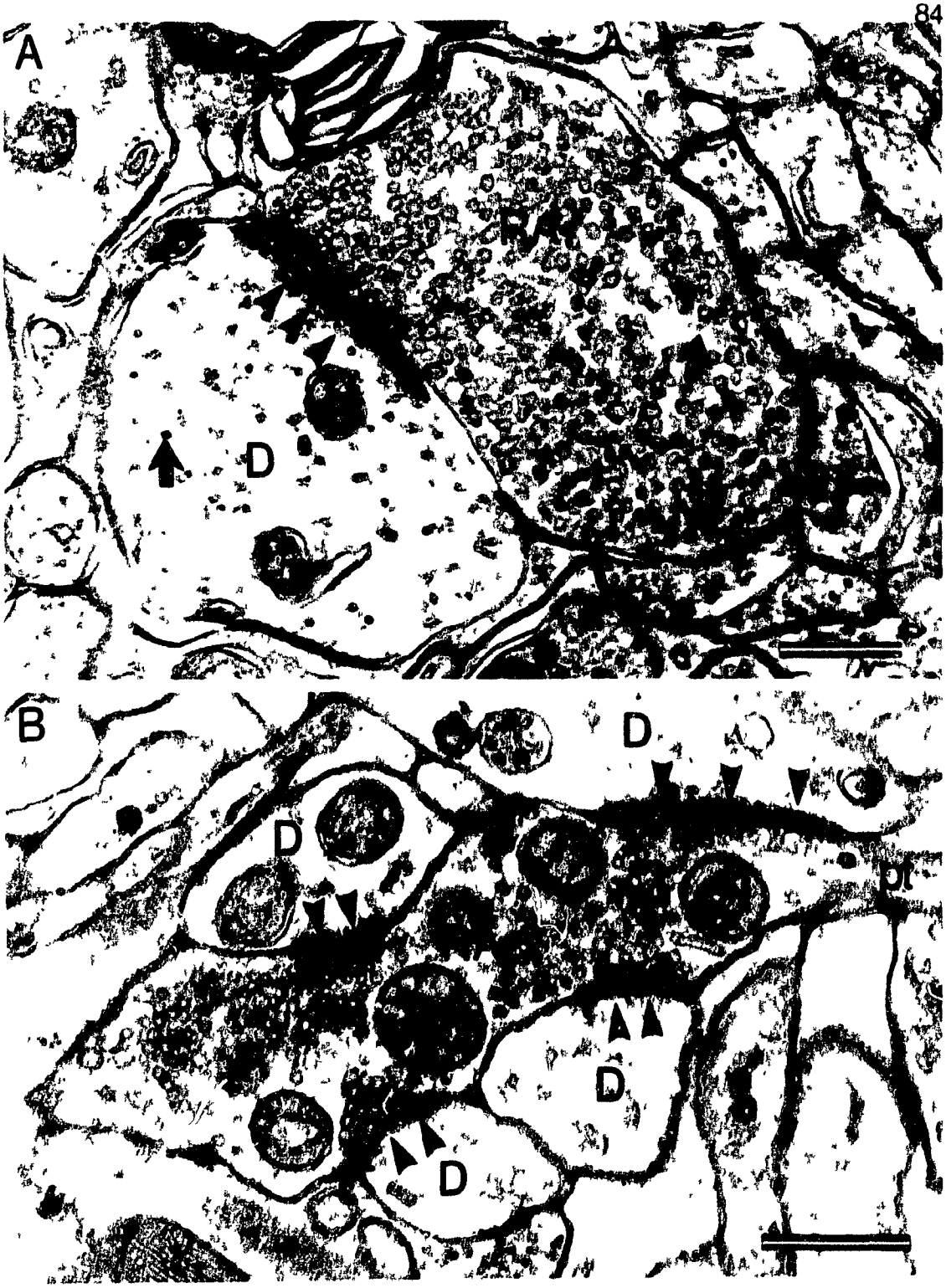

Figure 5

Fig. 6. Electron micrographs illustrating synaptic terminals, puncta adhaerentia and a dendritic spine in the NTSis. **A:** Two adjacent synaptic terminals (RA_1 and RA_2) each forming a single contact (arrowheads). RA_1 is forming a contact with a dendrite (D) and RA_2 a synaptic contact with a dendritic spine (sp) on D. Note the puncta adhaerentia (large arrows), the location of DCV (small arrows) and the clustering of synaptic vesicles at the presynaptic membrane of the active zone. **B:** A PS terminal containing many clear pleomorphic vesicles and number of DCV (arrows) and forming a symmetric contact with a dendritic profile (D). Calibration bars: A, B, 0.5 μm.

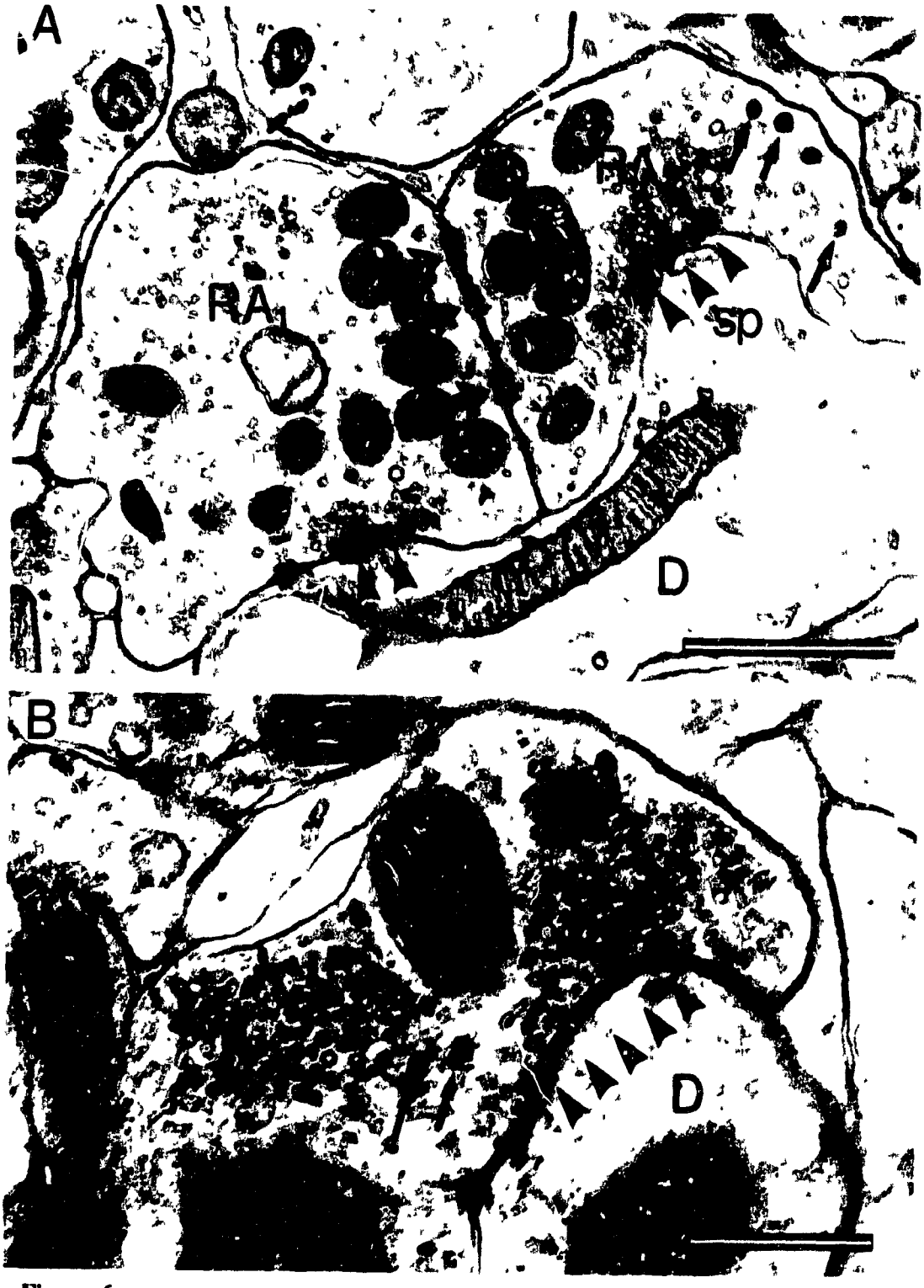

Figure 6

distribution of vesicles within the synaptic bouton was variable. In some profiles there was a relatively even distribution of vesicles throughout (Fig. 5A) while others exhibited a prominent clustering of vesicles near the presynaptic membrane (Fig. 6A) with small clusters some distance from the active zone (Figs. 5, 6, 7). The clustering of vesicles near the active zone was most prominent when a single synaptic terminal was presynaptic to multiple dendritic targets (Fig. 5). Small darkly-staining mitochondria and longitudinal profiles of microtubules (Fig. 5A) were evident in many RA and PS synaptic terminals (Figs. 5B, 6, 7).

In the present study a definitive classification of synaptic type was made only when a clear synaptic junction was present. For instance RA synaptic arrangements showed a distinctive asymmetry in junctional contact and in favorable sections an obvious widening of the adjacent plasma membranes to form the synaptic cleft. PS synaptic terminals, on the other hand, formed symmetric junctions. In serial sections the symmetry remained uniform with regard to pre- and postsynaptic density. Clustering of vesicles near the presynaptic membrane at the active zone was characteristic of most terminals when a synaptic junction was present. Terminal profiles were encountered which contained either round or pleomorphic agranular vesicles but formed no clear synaptic junction although puncta adhaerentia were frequently associated with these profiles (Fig. 8). This was particularly evident in the neuropil bordering the TS.

Axo-dendritic synapses were the predominant type of contact in the NTSis. RA and PS synaptic terminals made contact with dendrites of small diameter although PS synaptic terminals were rare relative to RA contacts (Fig. 5-7). PS synaptic terminals tended to be on large diameter dendrites (Fig. 3) probably corresponding to proximal dendrites and rarely on somata. Synaptic contacts on the somata of NTSis neurons were always of the PS type. In the few cases where axo-somatic synaptic contacts were encountered only a single terminal profile was found per somal profile. PS synaptic terminals were most likely

Fig. 7. Electron micrographs of two PS terminals, one from a normal animal (A) and the second from an animal processed for HRP histochemistry (B). **A:** PS terminal containing many pleomorphic vesicles and exhibiting clustering of vesicles presynaptic to the active zone (arrowheads). **B:** PS terminal making a contact (arrowheads) with a dendritic profile (D) lying immediately adjacent to a preterminal axon containing HRP reaction product. Note the arrows indicating microtubules in the preterminal axon. Calibration bars: A, B, 0.5 μm.

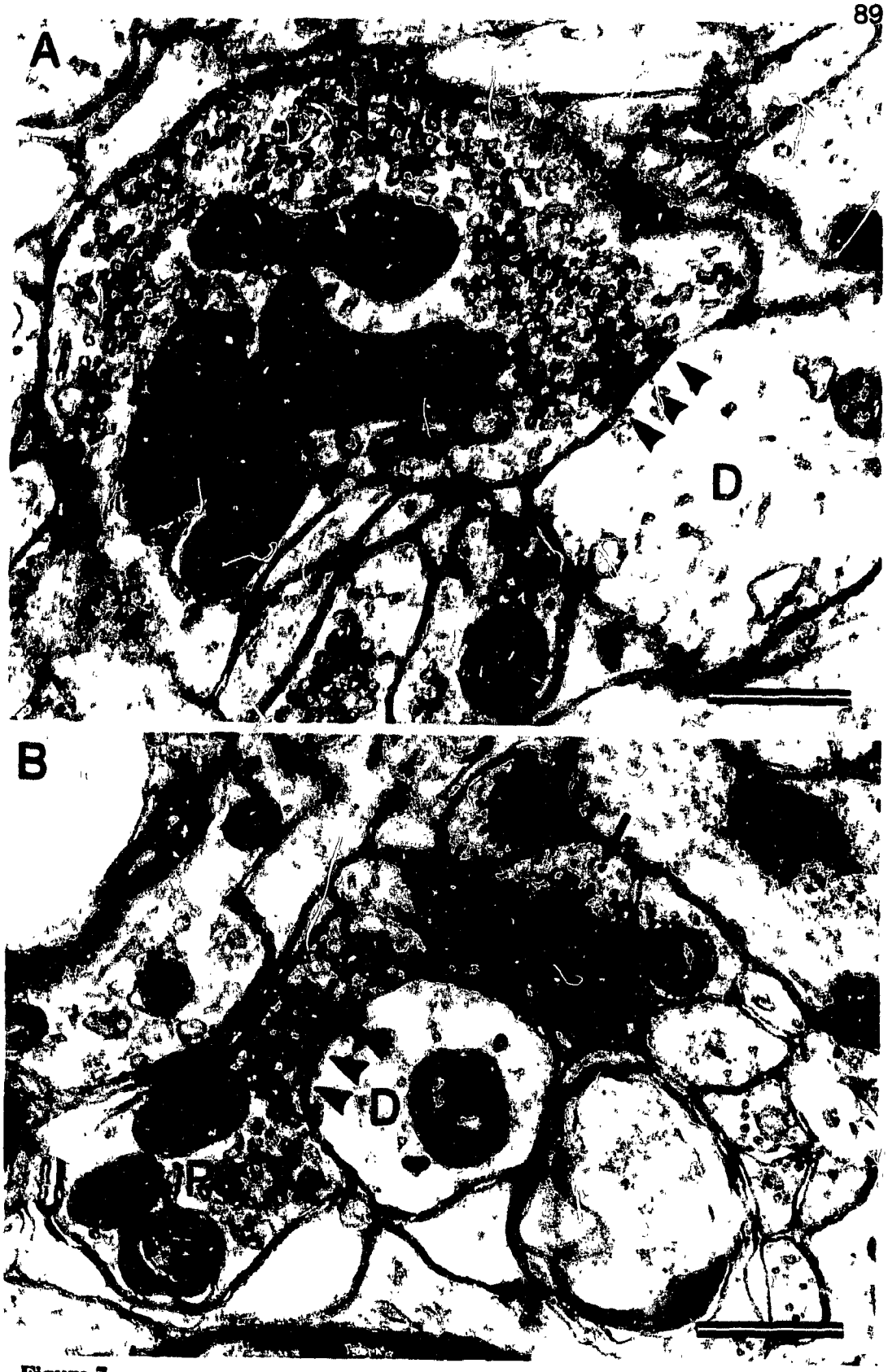

Figure 7

to be seen on large diameter dendrites and were never observed to make contact with more than one postsynaptic profile.

A number of different synaptic arrangements were identified for RA synaptic terminals The most frequent synaptic arrangement observed involved a single axon terminal synapsing on a small dendrite; both structures were typically less than 1 μm in diameter. Synaptic contacts with one or more postsynaptic dendrites were common (Fig. 5B, 11C). In such cases a narrow unmyelinated preterminal axon expanded to form an elongated terminal which made contact with as many as four separate small dendritic elements (Fig. 5B). Both RA and PS synaptic terminals usually formed a characteristic concave curvature over the region of membrane specialization at the synaptic junction. Puncta adhaerentia between two adjacent RA synaptic terminals synapsing on the same dendritic profile were frequently observed (Fig. 6A).

Another feature which varied with respect to synaptic terminals of either type was the number of dense-cored vesicles (DCV) present. Typically, DCV were round or oval in shape and bore a darkly-staining core region, and were distinctly larger (60-100 nm in diameter) than the abundant agranular vesicles (30-50 nm in diameter) in the terminal. Both RA and PS synaptic terminals were found to contain DCV in variable numbers (Fig. 6). Some presynaptic boutons were devoid of DCV while others contained significant numbers of dense-cored vesicles. In two terminals in which DCV were not present, subsequent serial sections revealed the presence of DCV in other planes through the terminals. In the NTSis, DCV tended to be located some distance from the concentration of clear vesicles which characteristically clustered at the presynaptic membrane (Fig. 6).

Complex synaptic arrangements involving three distinct profiles were identified in the neuropil of the NTSis. These arrangements often took the form of synaptic triplets in which three profiles, two containing vesicles and a third, a dendrite, were joined by two synaptic junctions. The first element (as established by its lack of an incoming synapse) in

Fig. 8. Electron micrographs illustrating puncta adhaerentia in the NTSis. **A:** Note the large number of DCV and that no vesicles granular or agranular cluster near the puncta adhaerens (arrowheads). **B:** A small axon terminal containing numerous round agranular vesicles and a single, large DCV. The terminal forms a puncta adhaerens (arrowheads) with a neighboring profile containing round agranular vesicles. Calibration bars: A , B, 0.5 μm.

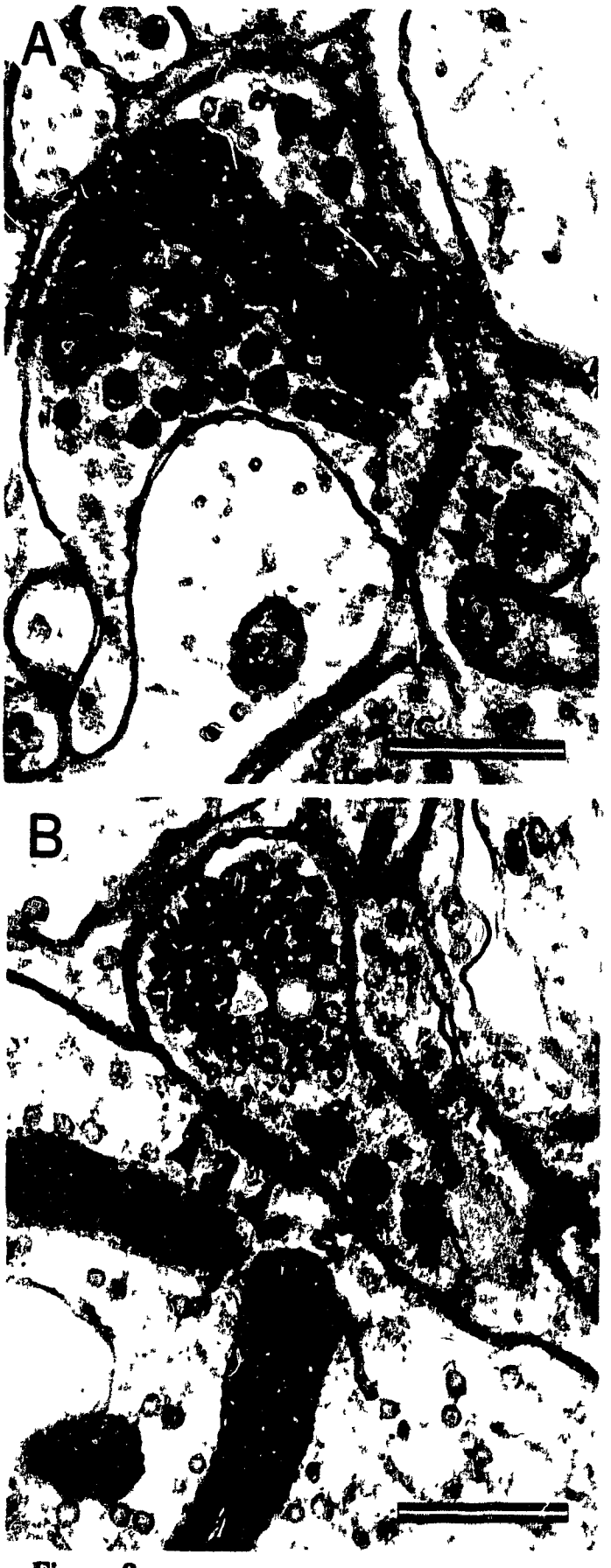

Figure 8

Fig. 9. Electron micrographs of complex synaptic arrangements encountered in the NTSis. **A:** An example of a synaptic triplet where a RA is presynaptic to a (arrowheads) second vesicle containing profile (PS) which in turn makes synaptic contact with a dendritic profile (D). The small arrows denote smooth endoplasmic reticulum. **B:** A synaptic triplet where a PS is presynaptic to (arrowheads) a RA contacting a dendrite (D). Calibration bars: A, B, 0.5 μm.

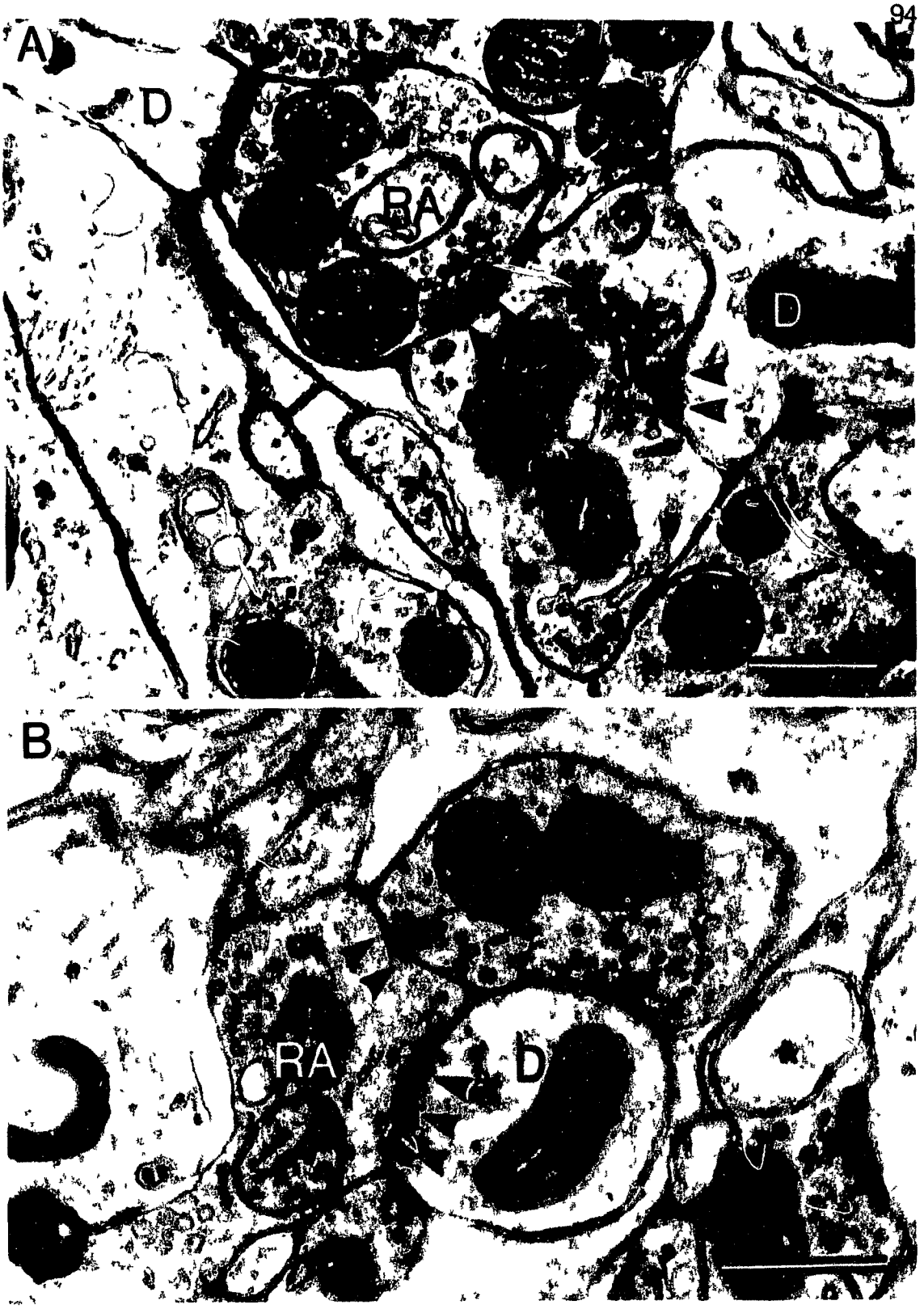

Figure 9

Fig. 10. Electron micrographs of serial sections through an RA terminal containing a large DCV (arrow) and forming an asymmetric synaptic contact with subsynaptic dense bodies (arrowheads) on a second profile containing numerous agranular pleomorphic vesicles. Note the gradual disappearance of the subsynaptic dense bodies and the darker appearance of the cytosol in RA as compared to the postsynaptic profile. Calibration bars: A-C, 0.5 μm.

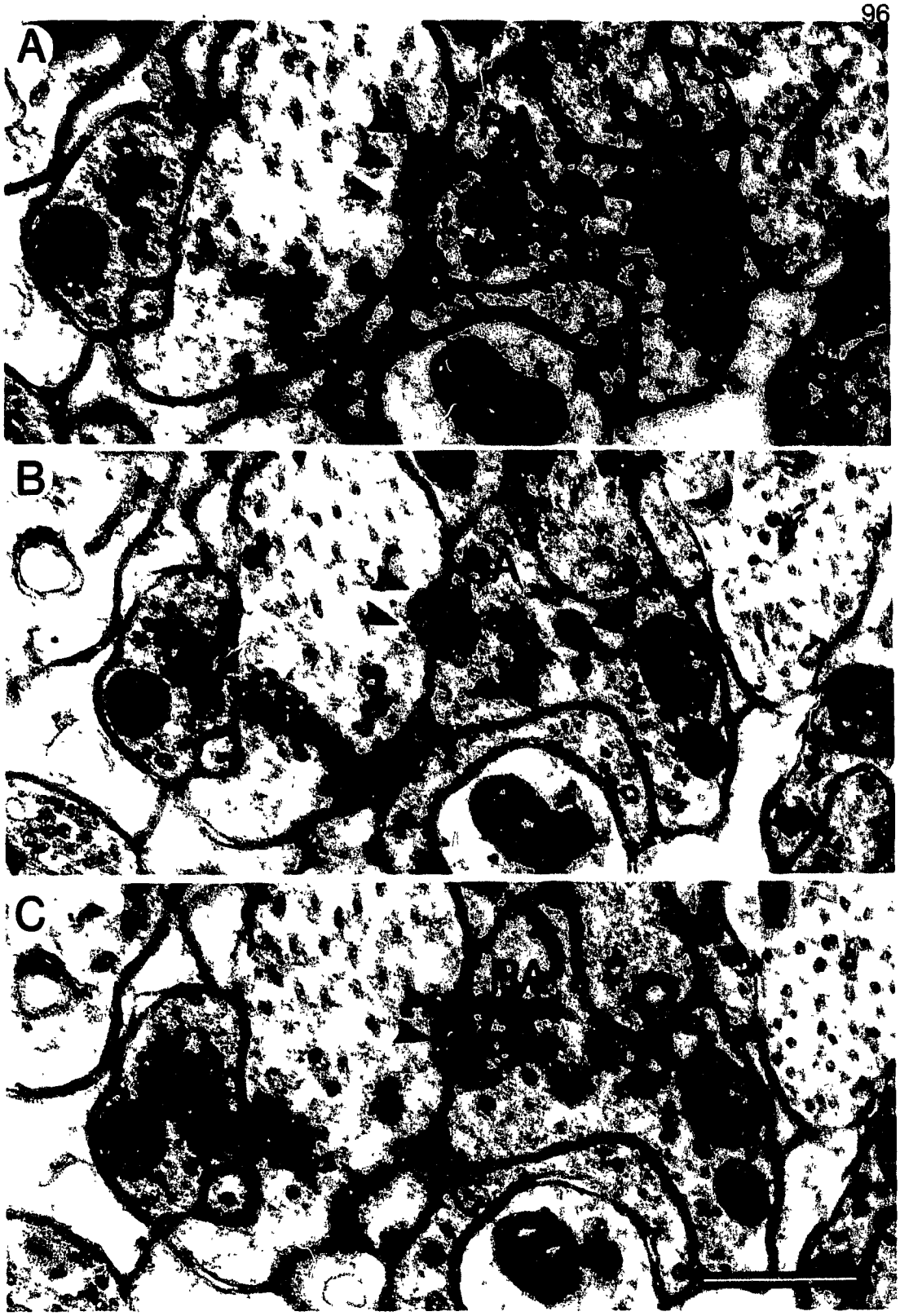

Figure 10

the triplet usually contained round agranular vesicles and was presynaptic to a second vesicle-containing profile. Morphologically the first element was typically RA while the second profile of the triplet most often contained pleomorphic vesicles and corresponded to the PS synaptic terminal (Figs. 9, 10). The symmetry of the synaptic contact was consistent for each type of terminal previously described. The third element of the triplet lacked vesicles, contained pale cytosol and often a small amount of SER (Fig. 9). Most of the triplets observed in the NTSis consisted of a RA synaptic terminal contacting a second PS synaptic terminal, although in two instances a PS synaptic terminal was seen to make a symmetric synaptic contact with an RA synaptic terminal which in turn made a asymmetric synaptic contact with an adjacent small dendrite (Fig. 9B).

Synaptology of Pharyngeal and Laryngeal Afferent Projections

Light microscopic observations. Injections of WGA-HRP or CT-HRP into the pharyngeal or laryngeal musculature and mucosa resulted in anterograde and retrograde labeling in the medulla oblongata in patterns characteristic for each viscus. Anterograde labeling in the NTS, including the NTSis and subnucleus intermedialis after pharyngeal or laryngeal injection overlapped extensively but was heaviest following pharyngeal injections (see Fig. 12, Chapter 4). Pharyngeal labeling was relatively heavier and extended more rostrally in the NTSis. Retrograde labeling in the ventrolateral medulla in the nucleus ambiguus (NA) verified that the injections were appropriately placed in that the pattern of labeling in the subdivisions of the NA was consistent with the patterns previously reported for each structure (Bieger and Hopkins, '87), thereby providing a reliable verification of the location of tracer injections. In two of the pharyngeal cases, light anterograde labeling was observed in the subnucleus centralis and a small number of retrogradely labeled

neurons were observed in the compact formation of the NA, indicating the spread of tracer to the esophagus.

At the light microscopic level, anterograde and retrograde labeling was easily identified in wet vibratome sections and in stained and unstained 1-μm-thick plastic sections. Intense anterograde labeling was seen in the NTSis and in the paratrigeminal nucleus overlying the spinal trigeminal complex following both pharyngeal and laryngeal injections (see Fig. 12, Chapter 4). Primary afferents terminating in the NTSis were most evident at and rostral to the level of the area postrema (AP). Laryngeal terminal fields largely overlapped pharyngeal in the NTSis, however, laryngeal labeling extended approximately 200 μm caudal to the level of the AP where pharyngeal terminal label was sparse. Both pharyngeal and laryngeal afferent labeling in the NTSis become progressively more diffuse at rostral levels of the NTS where the TS begins as dispersed bundles of myelinated axons. There was a small afferent projection to the subnucleus intermedius of the NTS following most pharyngeal and laryngeal injections. This subnucleus intermedialis of the NTS was not labeled in every case or was so lightly labeled that it was not evident in 100 μm-thick vibratome sections.

Electron microscopic observations. Following injections of WGA- HRP or CT-HRP into either the pharynx or larynx, anterogradely labeled axons and axon terminals were identified in the NTSis at the electron microscopic level.

The synaptic morphology of identified pharyngeal and laryngeal primary afferent terminals was not noticeably different in that both were characterized by round agranular vesicles and formed asymmetric synaptic junctions with small (< 1 μm in diameter) postsynaptic dendritic profiles (Figs. 11, 12). Labeled terminals typically made a single synaptic contact with a small diameter dendrite, although it was not uncommon to find a terminal making synaptic contact with two dendritic profiles. Synaptic boutons containing reaction product were only rarely identified synapsing on large (> 1.5 μm in diameter)

Fig. 11. Electron micrographs of transganglionically labeled pharyngeal axon terminals in the NTSis following injection of WGA-HRP into the pharynx. **A:** RA terminal containing three darkly-staining, crystalline structures corresponding to HRP reaction product formed at pH 5.5. The terminal forms a synapse (arrowheads) with a small dendrite (D). **B:** Labeled RA terminal contacting (arrowheads) a small dendrite (D). The axon terminal contains two DCV (arrows) and a group of small HRP crystals (reaction at pH 4.0). **C:** Labeled RA terminal making contacts (arrowheads) with two dendritic profiles (D). **D:** A labeled preterminal axon containing a small number of agranular, round vesicles (arrows) adjacent to a small, labeled axon (A). Note that the preterminal axon appears to be making synaptic contact (arrowheads) but no clustering of vesicles are visible in this plane of section. Calibration bars: A-D, 0.5 μm.

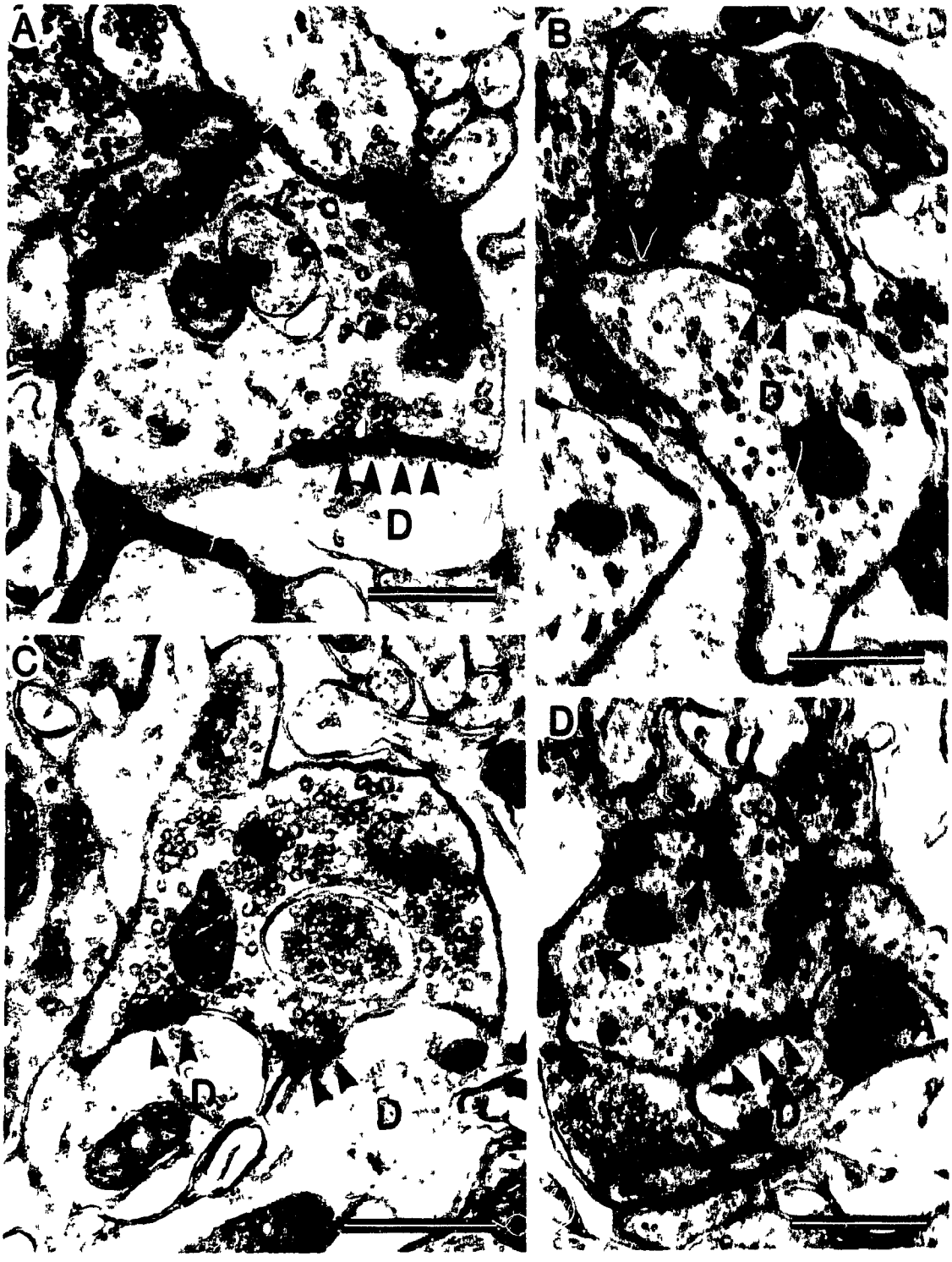

Figure 11

Fig. 12. Electron micrographs of transganglionically labeled laryngeal primary afferent axon terminals within the NTSis following injection of WGA-HRP in the larynx. **A:** RA terminal containing a single darkly-stained HRP crystal and making two contacts (arrowheads) with the same dendrite (D). **B:** Labeled RA terminal containing DCV (arrows) and forming a contact (arrowheads) with a small dendritic profile (D). Calibration bars: A, B, 0.5 μm.

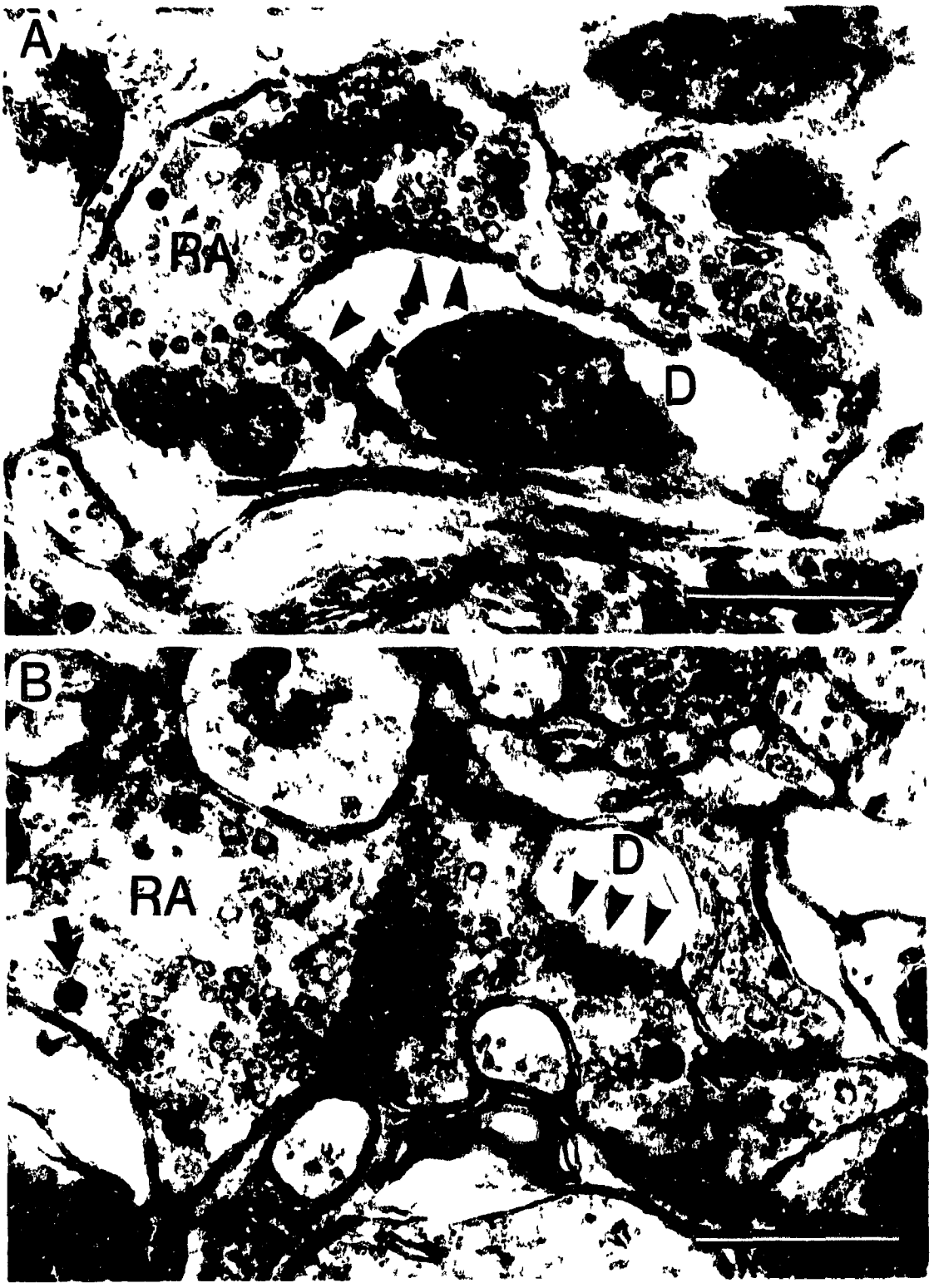

Figure 12

dendrites. Dense-cored vesicles were observed in labeled terminals (Figs. 11B, 12B). Both unmyelinated preterminal axons, usually less than 0.75 μm in diameter (Fig. 7B), and larger myelinated fibers containing HRP reaction product were present in the NTSis. Labeled myelinated elements were typically located near the periphery of the nucleus in or near the TS. Small unmyelinated preterminal axons containing reaction product were common in the neuropil and were often in close association with labeled terminals, although continuity between these two structures was rarely detected.

RA synaptic terminals involved in complex synaptic arrangements were never observed to contain label, indicating that RA synaptic terminals participating in complex synaptic arrangements are not primary afferent in origin. No axo-somatic synapses or terminals containing pleomorphic vesicles were found to be labeled. With the survival times used in the present study there was no evidence of transsynaptic labeling. Reaction product rarely disrupted the terminal plasma membrane and invaded nearby structures including the postsynaptic dendrite but the bulk of the reaction product was contained within the presynaptic profile and the disrupted membranes were clearly evident.

DISCUSSION

The NTS is the primary site for termination of sensory afferents originating in viscera located at cervical, thoracic and abdominal levels. As such the NTS contains the first centrally located neurons that function to transfer or relay sensory information conveyed by cranial nerves V, VII, IX and X. Of particular interest in the present study were those afferents originating in the pharynx (Altschuler et al., '89) and larynx (Kalia and Mesulam, '80b; Altschuler et al., '89) which terminate in the subnucleus interstitialis of the NTS. On the basis of results from anatomical and physiological studies the NTSis has been implicated in reflex activities such as deglutition, gagging, phonation and respiration (Bieger, '84; Miller, '82, '86; Hashim and Bieger, '87; Altschuler et al., '89). In the rat, much like that of the cat (Chazal et al., '91), the NTSis is nestled in the center of the tractus solitarius over most of its caudo-rostral length. In rat however, there is a distinctive organization that becomes readily apparent in thin plastic sections cut in the transverse plane through the subnucleus. Neuronal somata tend to be organized such that they are located around the periphery of the subnucleus with the central core being composed primarily of unmyelinated axons, axon terminals and dendrites. Interestingly in Golgi preparations, Cajal ('09) recognized this neuronal organization in the cat, although it was not mentioned by Chazal et al.('91) in their study of the cat. Based on the present study and earlier descriptive and connectivity studies, the NTSis is clearly a unique and distinct subnucleus of the NTS, yet it has often been overlooked or lumped in with other subnuclear components of the NTS. The NTSis has been included in the subnucleus magnocellularis in rabbit (Meesen and Olszewski, '49), the ventral sensory nucleus in man (Olszewski and Baxter, '54), the lateral nucleus in cat and rat (Torvik, '56), the ventral subdivision of cat (Taber, '61) and the ventrolateral subnucleus in rat (Herbert et al., '90). On the other hand, a number of early investigators did identify the subnucleus interstitialis as a distinct

subdivision of the NTS. Cajal ('09) identified it as the ganglion interstitial in mouse, cat, and guinea pig and Papez ('29) recognized an interstitial subdivision near the TS in cat. In addition to its unique cytoarchitecture, the connectivity of the NTSis also supports the notion that it is a distinct subnucleus. The NTSis is a major site for the termination of specific primary visceral afferents conveyed via the glossopharyngeal and vagus nerves. The tongue (Bradley et al., '85), soft palate, pharynx, and larynx (Altschuler et al., '89; Kalia and Mesulam, '80b) are all known to have dense projections to the NTSis. It has been suggested on the basis of the diverse, convergent inputs to the NTSis that the NTSis plays an important role in integrating visceral sensory information related to deglutition, phonation and defensive reflexes such as coughing and gagging (Altschuler et al., '89).

Neuronal somata in the NTSis of rat share ultrastructural features with somata in a number of other subnuclei of the NTS including the subnucleus gelatinosus (Leslie et al., '82b), dorso-medial NTS (Chiba and Doba, '75), subnucleus commissuralis (Chiba and Doba, '76) and subnucleus interstitialis (Chazal et al., '91) all of which were studied in the cat. These subnuclei were described as containing neurons which were round to fusiform in shape and falling in a size range of 9-19 μm in diameter with the average soma diameter being 10 μm. Other morphological features consistently reported included a large nucleus to cytoplasm ratio, prominent eccentrically located nucleolus, organelle sparse cytoplasm, little or no organized Nissl substance and infrequent axo-somatic contacts. This being the case it could be suggested that the morphological similarities between the neurons in the different subnuclei of the NTS and that of the NTSis might reflect cross species similarities in the overall function of these neurons as secondary relay neurons sending information to other levels of the neuraxis, in particular, the parabrachial nucleus (Herbert et al., '90) and ventrolateral medulla (Ross et al., '85; Herbert et al., '90). Rare myelin-like ensheathments like those encountered in the subnucleus gelatinosus (Leslie et al., '82b) were not found in the NTSis and appear to be unique to that subnucleus of the NTS.

The neuropil of the NTSis consisted of unmyelinated axons, axon terminals and dendritic profiles. Consistent with the light microscopic observations, the electron microscopic survey revealed that most of the neural elements in the neuropil are oriented along the caudo-rostral axis of the subnucleus. Bundles of 15-25 small, unmyelinated axons were frequently encountered in the NTSis. Axonal bundling was also a prominent feature of the subnucleus gelatinosus of the NTS in the cat (Leslie et al., '82b). It was not determined in the present study or in Leslie et al., ('82b) if these axons represent primary afferents entering the subnucleus or efferent projections leaving, perhaps on course to the parabrachial nucleus or ventrolateral medulla. However, in the present study of pharyngeal and laryngeal afferents, axons contained in bundles were never seen to contain HRP reaction product, indicating that afferents originating in the pharynx or larynx do not contribute to the formation of axon bundles in the NTSis. Axonal profiles found to contain reaction product, were small in diameter (< 0.5μm) and typically unmyelinated. However, because a small number of myelinated axons near the TS were labeled, the possibility arises that unmyelinated axons found in the NTSis might represent preterminal axons which have lost their myelin sheath shortly after leaving the TS. Kalia and Richter ('88), in a study of rapidly adapting pulmonary receptors in the dorsal and intermediate subnuclei of the NTS, were able to follow the central projections of physiologically identified primary afferent axons in the NTS and demonstrated that pulmonary afferents lose their myelin sheath when the afferent diameter ranged between 0.4-1.0 μm.

The numerous dendrites in the NTSis varied greatly in morphology. The most frequently encountered dendritic profile was small (< 1 μm in diameter) and had irregular contours. Dendritic spines in the present electron microscopic survey were very rare but a few were identified (Fig. 6A). This fact, combined with the description of a small number of spines in the Golgi preparations in the cat NTSis (Cajal, '09), suggests that at least some proportion of nondescript dendritic elements in the NTSis of rat might correspond to

dendritic appendages (i.e., spines). Although criteria have been established (Ralston, '71; Peters et al., '91) for differentiating dendrites and dendritic spines these criteria were difficult to apply to such small processes because of the absence in many instances of any defining features. Dendritic shafts, less than 1 μm in diameter, were typically distinguished from smaller elements of the neuropil by the presence of parallel arrays of microtubules, small amounts of RER and/or ribosomes. Smaller presumed dendritic structures often lacked microtubules and even in serial sections ribosomes, were extremely rare. Some of these might correspond to dendritic spines since Cajal ('09) described small numbers of spine-like structures in the cat ganglion interstitialis, the equivalent of the NTSis in the present study. Spines are identified at the electron microscopic level as typically containing undifferentiated cytoplasm with smooth endoplasmic reticulum and elaborate agranular cisternae (i.e., spine apparatus) (Ralston, '71; Peters et al., '91). Characteristics of spines were often absent from structures with lucent cytoplasm and thus the identification of these elements as spines or dendrites proper was difficult. The remaining small dendritic elements correspond to small dendrites which lack many of the cytoplasmic organelles characteristic of larger dendrites or spines of similar size.

Another interesting feature of the neuropil was the presence of vesicle-containing profiles which are more similar in morphology to dendrites than axons. Following comparison of these profiles in the NTSis with similar dendritic structures in the subnucleus gelatinosus (Leslie et al., '82b) and NTSis (Chazal et al., '91) in the cat, it was evident that these vesicle-containing processes described herein were morphologically similar to and corresponded to dendrites containing pleomorphic clear vesicles. Dendrites containing vesicles have been described elsewhere in the central nervous system including the thalamus (Harding, '71; Lieberman, '73), substantia nigra (Groves and Linder, '83), NTS (Gwyn et al., '82; Chiba and Doba, '76), and superficial region of the spinal trigeminal complex and dorsal horn of the spinal cord (Ralston, '71; Gobel, '74; '76). In

the NTSis of the rat, vesicle-containing dendrites participate in complex synaptic arrangements where they are pre- or post- synaptic to axon terminals or presynaptic to a dendritic profile lacking vesicles. Definitive identification of vesicle-containing structures was possible in most cases. However, not all axon terminals or vesicle-containing dendrites exhibited a sufficient number of defining characteristics to permit absolute identification and therefore the possibility of dendro-dendritic contacts could not be totally ruled out. Dendro-dendritic synapses have been reported in the subnucleus gelatinosus of the NTS (Leslie et al., '82b). In such an arrangement, a dendrite containing pleomorphic vesicles was presynaptic to a second dendrite lacking vesicles. Leslie et al. ('82b) suggested that although the functional significance of dendro-dendritic synapses is not known for certain, they probably play only a minor role in the NTS since they typically are rare. Further study of the synaptic relationships as they relate to the neurochemistry of the NTSis may provide insight into the origins of dendrites containing vesicles and their possible role in NTSis.

With regard to the synaptology in the NTSis, there were many simple synaptic arrangements involving a single axon terminal and a postsynaptic dendrite and, less frequently, synaptic arrays (triplets) involving an axon terminal, vesicle-containing profile (i.e., axonal or dendritic) and a typical dendrite containing no vesicles.

Axo-somatic synaptic contacts were extremely rare, which contrasts with observations in the NTSis of the cat in which axo-somatic Gray's type I and II synapses were found (Chazal et al., '91). However, PS synaptic terminals making symmetric synaptic contacts close to the cell body on proximal dendrites did occur with considerable frequency. Axo-somatic contacts were absent in the subnucleus commissuralis (Chiba and Doba, '76) and in the subnucleus gelatinosus (Leslie et al., '82b) of the NTS they were very rare, but when present were of the PS morphology. The absence of axo-somatic contacts in the NTSis has functional implications. Presumably, inputs synapsing directly on the soma can

transfer information immediately to the postsynaptic neuron with little diminution in effect whereas synapses on more distal dendrites probably have less influence all other things being equal since the resultant potential moving toward the soma via the postsynaptic dendrite is not self-potentiating and is therefore subject to the cable properties of that dendrite. Consequently, the resultant changes that occur due to synaptic activity at more distal points are somewhat diminished by the time it reaches the cell body. Thus, responses (i.e., action potentials) in the postsynaptic neuron might require many distal inputs to initiate an action potential while fewer proximal inputs on the neuronal perikarya might produce the same effect as the cumulative effect of many distal inputs. It has been suggested that contacts on distal dendrites and spines provide the substrate for exerting modulatory influences on postsynaptic neurons (Kalia and Richter, '88). This being the case, primary pharyngeal and laryngeal afferent terminals which synapse on small dendrites of second order neurons in the NTSis may produce modulatory effects on these neurons. On the other hand, it may be the cumulative effect of many afferent inputs from the target organ onto the dendritic tree of one neuron which is necessary to initiate a postsynaptic response.

Within the NTSis, two types of axon terminals were identified. The first contained small round agranular vesicles and formed asymmetric synaptic contacts (RA) and the second type contained small pleomorphic agranular vesicles and formed symmetric contacts (PS). In the present survey RA synaptic terminals on dendrites made up the vast majority of the synapses and this is consistent with observations in the cat NTSis (Chazal et al., '91). However, Chazal et al. ('91) established two categories of RA synaptic terminals based on the size of the vesicles. In the rat no such distinction was evident although it was possible to find large and small round vesicles in most terminal profiles, but the vast majority of the vesicles were in the 30-60 μm range. Most other reports of synaptic terminals containing predominantly agranular round vesicles in subnuclei of the NTS are

consistent with the present observations in that they establish asymmetric synaptic contacts on dendrites and that these are the predominant synaptic arrangement. Furthermore, none of these other studies noted a second type of RA synaptic terminal based on the size of the vesicles contained in synaptic boutons (Chiba and Doba, '75, '76; Leslie et al., '82b; Kalia and Richter, '85, '88).

Axon terminals containing pleomorphic vesicles and forming symmetric synaptic contacts (PS) were rare, relative to RA synaptic terminals in the NTSis. PS synaptic terminals were found on small dendrites but also on proximal dendrites. Because of their low frequency in the NTSis it might be suggested that PS synaptic terminals play a relatively small role in the function of the subnucleus. However, the argument that proximal synapses have greater immediate influence on postsynaptic neurons also is consistent with the notion that the presence of PS synaptic terminals strategically located on proximal dendrites implies an important role in the modulation of the function of NTSis neurons. Interestingly, no PS synaptic terminals were labeled with HRP reaction product following pharyngeal or laryngeal injections. Therefore, they must originate from some other source, presumably elsewhere in the central nervous system, although little is known regarding central afferents to the NTSis (see chapter on PTN efferent connections). It has been reported that a correlation exists between the synaptic structure and the function of the synapse such that synapses of the RA type are excitatory and those of PS morphology are inhibitory (Eccles, '64; Uchizono, '65; Carlin et al., '80; Peters et al., '91). However, without knowledge of the identity of the neurotransmitter contained within the vesicles of a particular axon terminal and the effect of that transmitter at the postsynaptic site, one may only speculate as to whether inputs onto neurons in the NTSis are excitatory or inhibitory. However, it is generally accepted that primary afferents are excitatory. The NTSis contains catecholaminergic (i.e., dopamine, noradrenaline and adrenaline) neurons and fibers with noradrenaline being the most abundant monoamine present (Kalia et al., '85).

Interestingly, the present study did not reveal morphological differences among NTSis neurons which would suggest that they were neurochemically distinct. The presence of both neurons and terminals of the same neurochemistry in the NTSis raises the possibility of intrasubnuclear connections, the function of which is not readily apparent. Takahashi et al. ('80) identified noradrenaline terminals in the dorsal medial NTS which have similar morphological features to the RA synaptic terminals described in the NTSis. Neurons in the NTS which contain tyrosine hydroxylase contribute substantially to efferent pathways to the parabrachial nucleus (Malay et al., '87; Velley et al., '91) an area which receives projections from the NTSis (Herbert et al., '90). One other point should be noted and that is the presence of dense-cored vesicles in both RA and PS synaptic terminals. Dense-cored vesicles have been suggested as a storage site for enkephalins (Velley et al., '91) but not for catecholamines (Fuxe et al., '65), leading to a number of possibilities. The first possibility is that terminals in the NTSis containing dense-cored vesicles do not contain catecholamines. Alternatively, terminals with dense-cored vesicles might contain enkephalins, or both catecholamines and opioids. A fourth might be that dense-cored vesicles store other neurotransmitters or have different functions. The fourth possibility raises an interesting point, in light of the presence of profiles containing large numbers of dense-cored vesicles but not forming typical synapses in the NTSis. Another feature noted regarding dense-cored vesicles in RA and PS terminals was the tendency for these vesicles to be located some distance from the active zone. The presence of non-synaptic profiles containing dense-cored vesicles and dense-cored vesicles in RA and PS terminals have been taken to suggest that in some cases dense-cored vesicles undergo exocytosis at structurally non-specialized sites even when a typical synaptic zone is present (Zhu et al., '86). Substances (i.e., neurotransmitters or neurohormonal substances) released at non-synaptic sites are believed to function as general modulators or regulators at pre- and/or post synaptic membranes at one or more terminals in the immediate area (Zhu et al., '86).

The function of this mechanism, as it relates to primary afferents, which in this study also contained dense-cored vesicles is not readily apparent. It is conceivable that such a system could regulate the release of neurotransmitter at the afferent terminal under normal physiological circumstances. Nevertheless, if the hypothesis put forward by Zhu et al. ('86) is valid then dense-cored vesicles might very well serve a totally different function from that of the smaller, more abundant vesicles found in RA and PS synaptic terminals in the NTSis.

Axo-axonic and triplet arrangements were rare in the NTSis. The identification of axo-axonal synapses is dependent on classifying both structures as axonal, an issue which is often difficult to resolve, particularly when both structures are small. Axo-axonal contacts have been described elsewhere in the NTS, including the dorsal NTS (Kalia and Richter, '88), subnucleus commisuralis of the NTS (Chiba and Doba, '76), dorsal medial part of the NTS (Takahashi et al., '80) and NTSis of the cat (Chazal et al., '91). The present results indicate that synaptic terminals of RA or PS morphology can be the presynaptic element and that the postsynaptic terminal usually contains vesicles of different morphology from that in the presynaptic terminal. Chiba and Doba ('76) described a similar situation in the subnucleus commissuralis as that found in the NTSis in which either RA or PS synaptic terminals could form the presynaptic element. This is in contrast to the situation in the cat (Chazal et al. '91) where the presynaptic element in all axo-axonal arrangements corresponded to the RA type and a symmetrical synaptic contact was formed. Axo-axonal synapses in the rat NTSis had synaptic contacts (i.e., symmetric or asymmetric) consistent with the morphology of the vesicles (round versus pleomorphic) contained in the bouton. Presumably such axo-axonal relationships are involved either with the inhibition or enhancement of mediated transmission by the postsynaptic axon terminal. Axo-axonal arrangements have been implicated in presynaptic inhibition of primary afferent information where a PS terminal is presynaptic to a RA primary afferent terminal (Kalia and Richter,

'88). Axo-axonic contacts have been shown in other areas of the central nervous system to involve primary afferents including the dorsal column nuclei (Ellis and Rustioni, '81) and the superficial laminae of the spinal cord (Ralston and Ralston, '79). Pharyngeal and laryngeal primary afferents in the NTSis were not observed to participate in axo-axonic synaptic arrangements and, therefore, do not appear to be subject to presynaptic modulation.

Triplet arrangements involved two vesicle-containing profiles of different morphology and a third element which was dendritic. The function of synaptic triplets in the NTSis is not known. There is also considerable uncertainty at this time as to the origin of the participating elements in these triplets. However, the absence of labeled primary afferent terminals from these arrangements suggests a central origin, possibly local interneurons. Other locations from which the elements of triplets might arise include intranuclear connections (Loewy and Burton, '78; Morest, '67) or projections from forebrain autonomic centers including the paraventricular hypothalamic nucleus, lateral hypothalamic nucleus, central nucleus of the amygdala and bed nucleus of the stria terminalis (see Loewy and Spyer, '90 for review).

In the present study of pharyngeal and laryngeal primary afferents terminating in the NTSis, it was evident that both viscera had morphologically similar axon terminals and synaptic arrangements. Pharyngeal afferents are transmitted via the pharyngeal branch of the glossopharyngeal nerve while laryngeal afferents are contained in the superior laryngeal branch of the vagus nerve (Altschuler et al., '89). It has been previously noted by Mei et al. ('83) that the majority of axons in the central projection of the vagus nerve were small and unmyelinated. Our findings suggest that both primary pharyngeal and laryngeal afferents are predominantly unmyelinated. Vagal afferent terminations originating in the larynx are similar in morphology to vagal afferents and terminals in the medial NTS of the cat (Gwyn et al., '82). Based on the morphological and organizational similarities between

pharyngeal and laryngeal afferents terminating in the NTSis it seems reasonable to suggest that these afferents are functioning in a similar manner for both structures and that they might convey similar sensory modalities to the NTSis.

In summary, pharyngeal and laryngeal afferents are conveyed by cranial nerves IX and X respectively and terminate in a topographically overlapping manner in the subnucleus interstitialis of the NTS. Afferent axon terminals originating in either viscus are of similar morphology and form simple synaptic arrangements with one or more small dendritic profiles. Although the sensory modalities conveyed in primary afferents to the NTSis are not known, this information might play a role in the coordination of reflex activities related to gagging, deglutition, phonation, glottic closure, coughing and respiration which require the coordinated efforts of both the upper alimentary and respiratory tracts.

Technical Considerations

Because two different conjugates of HRP were used in the present study it is essential to address briefly the effectiveness of each tracer and comment on differences observed as a result of using one or the other.

The patterns of labeling produced by WGA- and CT-HRP showed no differences with regard to the location of retrograde or anterograde tracing in the medulla oblongata following peripheral injections. There was variation in the degree of labeling present in individual cases but this could not be correlated to one or the other of the HRP conjugates. The pharyngeal and laryngeal walls are extremely thin and this most certainly resulted in some tracer being accidentally deposited in the lumen of the structure. Within the lumen tracer could be diluted and/or washed away in the fluid milieu or be taken up and transported by more distal structures producing labeling in other locations in the brainstem. This possibility cannot be ruled out since it was impossible to be sure the pipette tip did not pierce the mucous membrane. In any event, tracer expelled into the lumen of the pharynx

or larynx is probably not available to the neuronal elements that lie in the mucosa and musculature of that structure and if it is, it has a greatly reduced concentration due to dilution. The only significant difference in labeling between WGA and CT-HRP was in the appearance of retrogradely labeled motor neurons. The somata of nucleus ambiguus neurons were equally well labeled with WGA and CT- HRP. However, CT-HRP produced extensive filling of proximal and secondary dendrites (Bieger and Hopkins , '87; Rinaman et al., '89; Rinaman and Miselis, '90).

Following histochemical procedures described in the methods, the appearance of reaction product was similar for both WGA-HRP and CT-HRP. This was confirmed at the electron microscopic level where crystals resulting from both conjugates were identical in morphology. The numbers of crystals and size present in a single terminal could vary considerably but this probably represents alterations which were made in the pH of the histochemistry used. Lower pH's produced smaller and more numerous crystalline structures while higher pH's such as those used in most cases in the present study produced larger more distinct crystals. The use of higher pH's provides two important advantages. The first is the ease with which the distinct HRP reaction product can be identified and the second is the better preservation of ultrastructure when techniques with pH's closer to physiological pH are used. HRP reaction product stabilized with ammonium molybdate was distinctively crystalline in appearance (Fig. 7B,11,12). HRP crystals produced according to the present methods retain their distinct shape and are difficult to mistake for any naturally occurring organelle. This contrasts with sections processed with DAB in which globular reaction product might be mistaken for lysosomal elements or cytoplasmic inclusions in the neuron. Of particular note is the ease with which these darkly-staining crystals could be identified even in the smallest (< 1.0 μm in diameter) axons and axon terminals. On rare occasions, profiles of labeled axon terminals were encountered in which the HRP crystal had disrupted the plasma membrane and

pierced adjacent structures. This was most prevalent when a pH of 5.0 or greater was used in the reaction medium. A higher pH in the reaction medium resulted in more numerous, large crystals with only a small decrease in overall sensitivity. In comparison to the diaminobenzidine method, the method used in the present study provides a clearer picture of the terminal complement of vesicles and synaptic junctions. Only in small terminals did reaction product develop so intensely that it occasionally perforated the plasma membrane or obscured the morphology of organelles within the terminal. There was no observable change in the ultrastructure of neurons or neuropil as a result of HRP histochemistry.

CHAPTER 4

ULTRASTRUCTURE AND SYNAPTOLOGY OF PRIMARY PHARYNGEAL AND LARYNGEAL AFFERENTS IN THE RAT PARATRIGEMINAL NUCLEUS.

INTRODUCTION

The spinal trigeminal tract overlying the rostral part of the spinal trigeminal nucleus pars caudalis and caudal two thirds of the pars interpolaris contains a diffuse group of neurons and neuropil referred to as the paratrigeminal nucleus (PTN) (Chan-Palay, '78a, b; Panneton and Burton, '85; Menétrey et al., '87; Menétrey and Basbaum, '87; Altschuler et al., '89). The PTN receives primary afferent input of somatic and visceral origin. Cranial nerves V, (Shigenaga et al., '86, '88; Pfaller and Arvidsson, '88; Panneton, '91) IX and X (Nomura and Mizuno, '83; Hamilton and Norgren, '84; Altschuler et al., '89) all have been shown to convey afferent fibers to the PTN in an overlapping pattern. In addition to cranial nerves, cervical dorsal root ganglia, as far caudal as C7, have terminal fields in the PTN (Abraham et al., '84; Neuhuber and Zenker, '89; Arvidsson and Pfaller, '90).

The PTN is particularly interesting because it is a rostral extra-solitary target for vago-glossopharyngeal afferents originating in the cervical viscera (Menétrey et al., '87; Altschuler et al., '89). In particular the PTN appears to be an equally prominent site to that of the NTSis with regard to afferents originating in the pharynx and larynx (Altschuler et al., '89).

Only a very limited amount of information is available in the literature pertaining to the cytoarchitecture of the PTN (Cajal, '09; Chan-Palay, '78a; Phelan and Falls, '89) and there is considerable ambiguity surrounding the uniqueness of the PTN as an anatomical and

functional entity (see Phelan and Falls, '89 for review). Other than an electron microscopic study in the monkey (Chan-Palay, '78a) there is a paucity of information regarding the fine structural detail of the PTN and the synaptology of afferent projections to the nucleus.

In the present study, the ultrastructure and synaptology of the PTN of the rat was characterized. In addition, the anterograde transport of WGA-HRP or CT-HRP was employed to study the synaptic organization of pharyngeal and laryngeal afferents terminating in the PTN.

MATERIALS AND METHODS

Subjects and Surgery

The subjects were 35 male Wistar rats (250-350g) which were anaesthetized with sodium pentobarbital (40-60 mg/kg) prior to all surgical procedures and at the time of sacrifice. Each rat also received 0.05 ml of atropine to minimize secretions during surgery.

The surgical approach to the pharynx and larynx was through a ventral midline incision made from the level of the hyoid bone down to the cranial border of the sternum. The skin was retracted with hemostats thereby exposing the underlying longitudinal muscles of the superficial neck. Each of the muscles was carefully dissected along fascial planes and then retracted laterally with loops of umbilical tape. Exposure of the pharynx and larynx was carried out in a manner so as to minimize vascular and neural damage which could result in spurious labeling following tracer injections. The anterior larynx was visualized by retracting the overlying sternohyoid and omohyoid muscles and, on either side of the larynx, the sternothyroid muscle which lies closely apposed to the larynx and trachea in the rat. The more lateral and posterior regions of the larynx were visualized following dissection of the esophagus to free it from the connective tissue binding it to the proximal end of the trachea and the larynx. The micropipette could then be placed in a position suitable for injection of tracer into the posterior aspects of the larynx. Surrounding muscles as well as the esophagus were isolated from the injection site by packing small strips of sterile gauze around or between these structures and the larynx. The pharynx was approached in a similar manner except that rather than dissecting free the esophagus from the overlying trachea and larynx a deeper, blunt dissection was carried out in order to free approximately 2 or 2.5 cm of the proximal esophagus from its fascial attachment to the posterior of the cervical neck cavity. After exposure of the esophageal segment a loop of umbilical tape was placed under the esophagus and trachea and both structures were

displaced lateral to the midline to expose the retropharyngeal space. This caudal approach to the pharynx made it possible to visualize the large inferior pharyngeal constrictor muscle and part of the middle constrictor. There is no identifiable superior constrictor muscle in rat (Cleaton-Jones, '72). The surrounding structures were isolated from the injection field with strategically placed sterile gauze. Despite the use of these precautions, in a small number of cases evidence was obtained in the form of retrograde and anterograde labeling patterns in the brainstem that tracer did on occasion spread from the injection site into surrounding tissues. Such spurious labeling was in most cases the result of tracer spread to the esophagus as evidenced by the retrograde labeling of neurons in the compact formation of the nucleus ambiguus and anterograde labeling in the subnucleus centralis of the NTS. Controls for the injection sites in the pharynx and larynx were based on comparison of the resulting retrograde and anterograde patterns of labeling in the present experiments with the comprehensive maps produced at the light level for the efferent motoneurons in the nucleus ambiguus innervating the striated musculature of the pharynx and larynx (Bieger and Hopkins, '87), as well as the afferent maps for each of these structures outlined in Altschuler et al. ('89).

Tracer Injections and HRP Histochemistry

A total of 31 rats received tracer injections. In 18 cases injections were made into the pharynx and in the remaining 13 cases the injections were in the larynx. Microinjections of two different conjugates of horseradish peroxidase (HRP) were used, wheat germ agglutinin-HRP (WGA-HRP, Sigma) (5% in distilled water) or cholera toxin beta subunit-HRP (CT-HRP, List Laboratories) (0.25-0.5% in distilled water).

Pressure injections of 2-8 μl were made via glass micropipettes affixed with dental sealing wax to either a 25 or 50 μl Hamilton syringe filled with light mineral oil. Tracer was administered at a series of sites along the target viscus in order to maximize coverage.

All injections were carried out with the visual aid of a surgical microscope. Visible leakage of tracer from the injection site was immediately removed with sterile cotton swabs.

After survival periods of 2-4 days (usually 3 days), each rat was deeply anesthetized and perfused transcardially with a prerinse of 500 ml of 0.15M phosphate buffer containing 0.1% sodium nitrite followed by 1 liter of aldehyde fixative (0.5% paraformaldehyde and 2.5% glutaraldehyde) in 0.15M phosphate buffer, giving a final osmolarity of 777-800 mosmol (pH 7.3, 20 °C) for 1 hour. Prior to craniotomy and removal of the brain and upper cervical spinal cord, each brain was left in situ for 1-2 hours. Brains were stored in cold (4 °C) 0.15M phosphate buffer prior to being sectioned. Vibratome sections (100 μm thick) were cut through the medulla from the cervical-medullary junction to the level of the parabrachial nucleus.

Sections were processed for HRP histochemistry with tetramethylbenzidine as the chromogen (Mesulam, '78). An initial incubation of twenty minutes was carried out in a medium containing the chromogen and was followed by a second incubation of twenty minutes in the same medium after the addition of substrate (1% H_2O_2). The development of the crystalline HRP reaction product was monitored (at 5 minute intervals) so that the reaction could be terminated, should large amounts of reaction product appear in the reaction medium and on the surface of the Vibratome section. Once developed, the reaction product was stabilized in 5% ammonium molybdate in acetate buffer (pH 5.0) (Marfurt et al., '86). Stabilization not only helped to retain labeling but also produced a mordant effect, thereby making it possible to visualize the crystalline label in toluidine blue stained sections under brightfield illumination. This was particularly effective with retrograde labeling but was also very useful with heavy anterograde labeling like that obtained in the present experiments.

Vibratome sections in which anterograde labeling in the PTN was intense enough to be identified visually were selected and the region of the dorsolateral medulla containing the

PTN was "blocked" to a size suitable for electron microscopic embedding procedures. Blocks were secondarily fixed in 1% osmium tetroxide in 0.15M phosphate buffer for 1-2 hours (20°C), stained *en bloc* with saturated aqueous uranyl acetate for 1 hour (4 °C), dehydrated through a graded acetone series (5 min. each) and embedded in TAAB resin (Marivac) for 48 hours at 60 °C. Semi-thin sections (1 μm) were cut with glass knives on a Reichert OMU3 ultramicrotome. Alternate 1 μm sections were stained with toluidine blue for the purpose of determining the orientation of the tissue block in the resin prior to ultrathin sectioning. Grey to silver sections were cut with a diamond knife and floated onto slotted copper grids coated with a support film of pioloform (1%, Marivac, R1275). Each grid was stained with Reynolds lead citrate at room temperature for 1-2 minutes. Electron microscopic observations were carried out on a Zeiss EM 10A electron microscope.

ABBREVIATIONS

D	dendrite
DCV	dense-cored vesicles
G	glial cell
NTS	nucleus of the tractus solitarius
NTSis	subnucleus interstitialis of the NTS
nu	nucleolus
P	profile
PS	pleomorphic symmetric
PTN	paratrigeminal nucleus
RA	round asymmetric
RER	rough endoplasmic reticulum
spVi	spinal trigeminal nucleus pars interpolaris

RESULTS

Light Microscopic Observations

Cytoarchitecture. The PTN had a rostral to caudal extent of approximately 1200-1400 μm and lay in close association with the medullary part of the spinal tract of the trigeminal nerve. The caudal one third of the PTN was located dorsolaterally to the spinal trigeminal nucleus pars caudalis (spVc). The caudal portion of the nucleus constituted the smallest part with regard to the amount of gray matter per equal cross section through the nucleus. In the caudal PTN, gray matter which extended into the spinal trigeminal tract and constituted the nucleus was continuous with the subjacent lamina I (marginal zone) of the spinal trigeminal nucleus pars caudalis. In the transverse plane, the caudal PTN consisted of thin bands or "cords" of gray matter comprised of a small number of neurons and a neuropil which permeated between the bundles of myelinated fibers forming the spinal trigeminal tract (Fig. 1). The remaining two thirds, including the most prominent part of the nucleus, lay dorsolateral to the spinal trigeminal nucleus pars interpolaris (spVi). In more rostrally located parts of the PTN, the nucleus was distinctly separate from the spinal trigeminal complex and lacked any continuities with the subjacent spinal trigeminal nucleus pars interpolaris.

The neuronal profiles seen in the rostral parts of the PTN were for the most part small and averaged 10 μm in diameter, although several larger (> 14 μm) neurons were seen in the caudal ventral part of the PTN. Neurons were typically round to fusiform in shape and generally showed very little discernible Nissl substance in 1 μm -thick sections. In the transverse plane the cords of neuropil took on a reticular appearance as a result of large bundles of myelinated trigeminal fibers which passed longitudinally through the nucleus as part of the spinal trigeminal tract. Immediately subjacent to the spinal trigeminal tract, groups of myelinated fibers ran longitudinally in the "deep bundles" described by Gobel

Fig. 1. Line drawings of photographs taken of 1-μm-thick plastic sections of the PTN cut in the transverse (A) and horizontal (B) planes. **A:** Note the reticulated appearance of the nucleus. The arrows indicate bundles of myelinated axons running parallel to the plane of section. **B:** In this plane of section the PTN appears as a sheet of neurons and neuropil traversed intermittently by small bundles of myelinated axons running perpendicular to the plane of section. Calibration bar: A,B 100 μm.

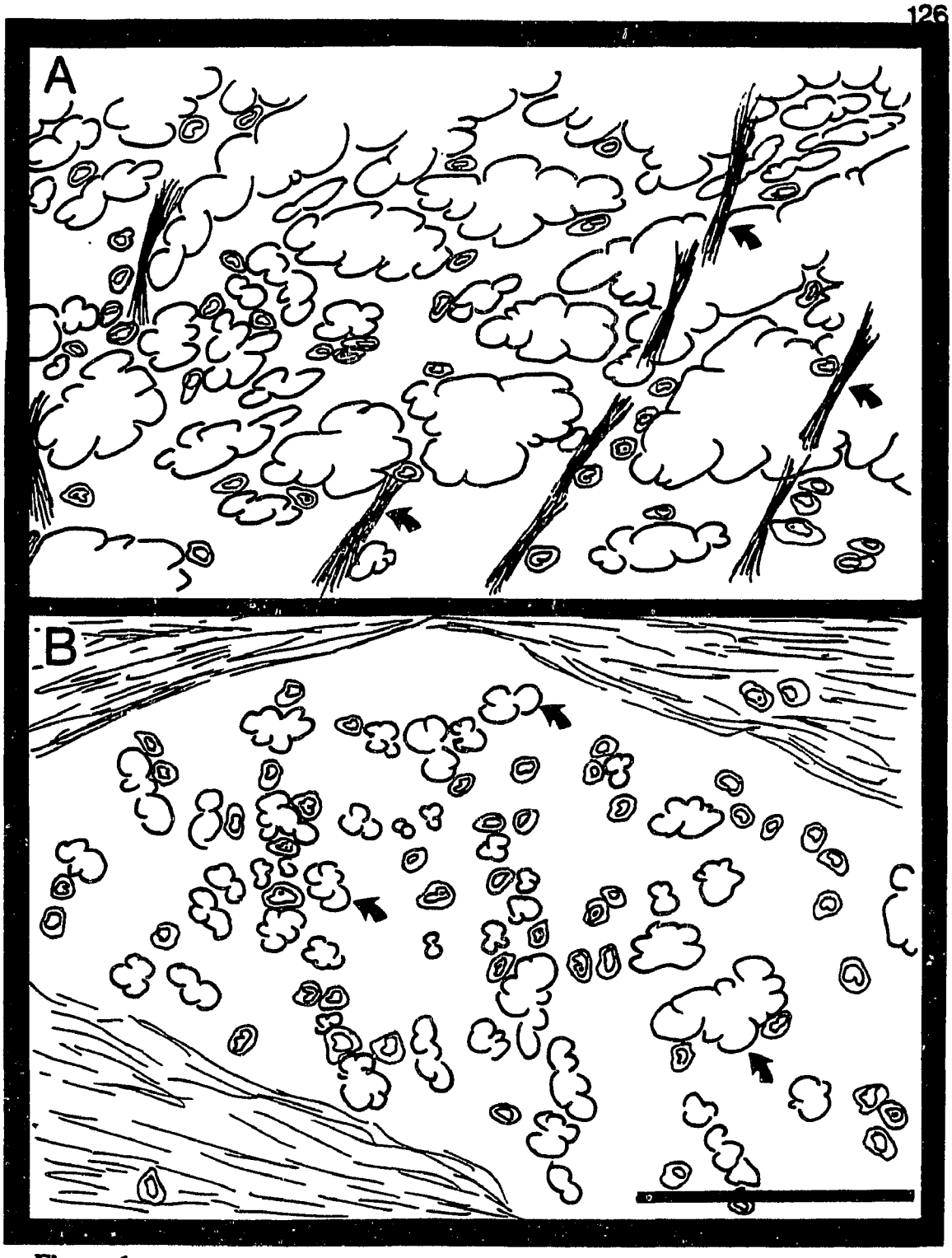

Figure 1

and Purvis ('72). The region between the deep bundles and the spinal trigeminal tract was relatively cell poor and those cells which were present were visibly larger than most of the cells in the nearby PTN.

Rostral to the obex at the approximate level where there was a transition from the spVc to the spVi, the PTN became more prominent. At this level, the neuropil and neurons making up the PTN were more extensive and gave the appearance of a distinct nucleus. Neurons at this level and in more rostrally located parts of the nucleus were remarkably similar in size with no particularly unique defining feature evident at the light microscopic level. When cut in an optimal horizontal plane the reticulated PTN appeared as a continuous sheet of gray matter with only a few small bundles of myelinated fibers dispersed in the field of view (Fig. 1). It was evident in the horizontal plane that the neurons of the PTN were dispersed throughout the nucleus. At it's most rostral extent, approximately at the level of the caudal end of the facial nucleus, the PTN rapidly decreased in size until it was no longer evident.

Neurons and Neuropil. The morphology of neurons throughout the length of the PTN was relatively homogeneous with only the occasional neuron that stood out by virtue of its larger size. Such large neurons were rare and tended to be located in more caudal parts of the PTN, in particular those areas overlying the spVc and, occasionally, the caudal spVi. Regardless of the plane of sectioning there were neuronal profiles which were round and others which were fusiform in shape. This fact, combined with the observation that round perikaryal profiles contained only a small amount of cytoplasm suggested that these neurons were also fusiform in shape but oriented perpendicular to the plane of section. The nuclear membrane usually contained a single invagination although multiple infoldings were regularly observed. The nucleus of each neuron contained a prominent nucleolus which was located centrally or eccentrically in the nucleus in equal proportions of neurons. In addition to the prominent nucleolus, nuclei were found which contained a second

element which was similar in appearance to the nucleolus. This "extranucleolar element" was separate from the nucleolus, but it was not possible at the light microscopic level to distinguish these two structures on the basis of morphology. Proximal dendrites were observed to originate from opposite poles of some neuronal profiles, in keeping with the fusiform appearance of many PTN neurons. The neuropil of the PTN presented a complex organization even at the light microscopic level. The processes that made up the neuropil were random in orientation with transverse, oblique and longitudinal profiles evident in both transverse and horizontal planes of section. Pale-staining profiles, presumably dendritic in nature, were numerous and variable in size and shape. Resolution at the light microscopic level did not permit the identification of other elements of the neuropil. Glial cell bodies were easily distinguished from neuronal somata by their smaller size and conspicuously darkly-stained cytoplasm and nucleus.

Electron Microscopic Observations

The ultrastructural and synaptic organization of the PTN was investigated in normal, unoperated (n=4) and experimental (n=31) rats. No apparent differences other than the presence of labeled afferent axons and terminals were observed between the results found in normal and experimental cases. To ensure that the neurons and neuropil studied were exclusively from the PTN, tissue blocks from normal animals were restricted to those regions of the PTN that were located lateral in the trigeminal tract. In experimental animals, the survey of neurons and neuropil was more extensive because the presence of anterogradely transported HRP delineated the boundaries of the nucleus. Neurons were considered to be in the PTN if the field in which they were viewed contained a labeled axon terminal.

Neurons. Neurons with minimum diameters greater than 10 μm were very rare. Measurements of neuronal profiles cut through the nucleolus indicated that the range for maximum diameter was 9-16 μm and minimum diameter 5-12 μm.

Based on the morphology and number of synaptic contacts on neuronal somata, three types of neurons were identified in the PTN. Until more is known about their connections and functions they will be designated arbitrarily as types A, B and C. Type A were the most numerous with the other two neuronal types (Type B and Type C) equally rare in the present survey. It is important to note that the region of the PTN which contained glossopharyngeal and vagal afferent terminations originating in the pharynx and larynx, respectively, was the focus of the present study. Consequently, the results may not be representative of the the caudal extreme of the PTN since afferent terminations from the above viscera are very light in the caudal PTN.

Type A neurons constituted greater than 90% of the neurons classified and were distinctly different from the other two neuronal types based on their size and morphology (Fig. 2). These neurons were elongate or fusiform in shape with an average maximum diameter of 13 μm. Each neuron contained an elongated nucleus with one or more deep nuclear invaginations. A prominent nucleolus and in some instances a separate distinct extranucleolar body was found (Fig. 2B). Sections through the long axis of a neuron revealed that only a small bridge of cytoplasm on either side of the nucleus connected the larger expanse of cytoplasm at either end of the cell (Fig. 2A). These cap regions of cytoplasm contained the bulk of the organelles in type A cells. Organelles within the cell included a distinctive rough endoplasmic reticulum (RER) in which the reticulum formed characteristically tortuous profiles (Fig. 2A). Long strands of loosely interconnected RER meandered through what was otherwise an organelle poor cytoplasm. Other than the RER and randomly distributed free ribosomes, other organelles were relatively sparse. Small numbers of mitochondria varying in shape and size tended to congregate near

Fig. 2. Electron micrographs of Type A neurons in the PTN. A: Section through a fusiform PTN neuron showing the invaginated nucleus, sparse rough endoplasmic reticulum (arrowheads) and a single proximal dendrite leaving the cell body (upper left hand corner). The arrow indicates a golgi apparatus. B: Cross section through a Type A neuron similar to that in (A) which is in close apposition (arrowheads) with a glial cell. The arrows indicate golgi apparatuses on opposite sides of the nucleus which contains two condensed nucleolar elements (nu_1 and nu_2). Calibration bars: A, 4 μm; B, 3 μm.

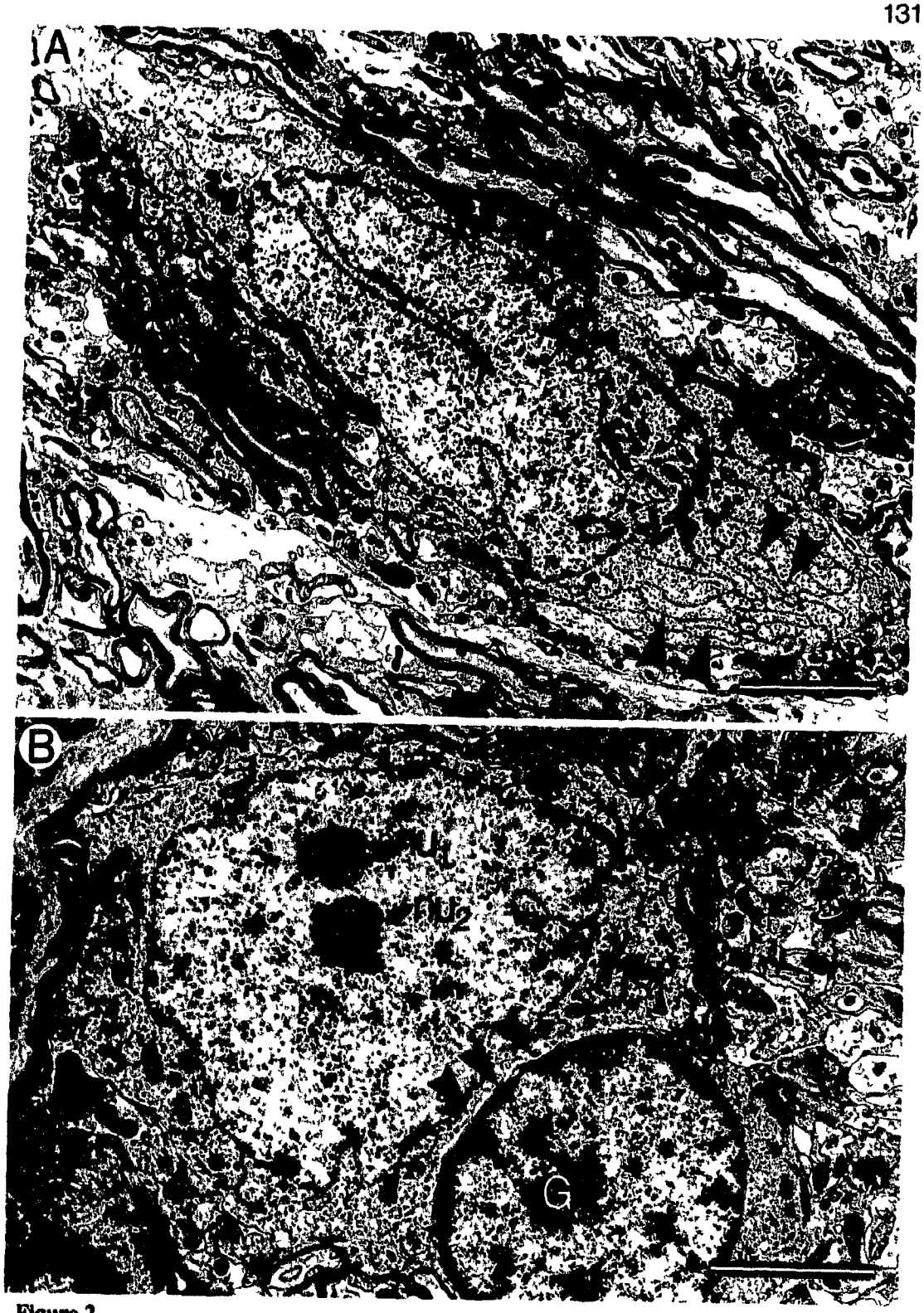

Figure 2

the nucleus (Fig. 2). The bridges of cytoplasm on either side of the nucleus also contained numerous free ribosomes and short segments of RER. Occasionally, an optimal section revealed two proximal dendrites at opposite ends of the soma. Proximal dendrites extended into the neuropil where they rapidly tapered to a diameter of less than 2 μm. Organelles including mitochondria, abundant free ribosomes and microtubules extended into the proximal dendritic process. Dark-staining membrane bound structures corresponding to lysosomes were common within the soma. With regard to synaptic contacts on the somata of Type A neurons, most profiles had none. However, in a small number of instances, one or possibly two axo-somatic synapses were seen. These synaptic contacts could be either RA or PS in morphology (see section on synaptology).

Type B neurons were typically round or oval in shape with an average maximum diameter of 10 μm. Each perikaryon contained a nucleus with a single deep nuclear membrane invagination that was often bifurcated (Fig. 3). The large and prominent nucleolus was generally located near the center of the nucleus and was surrounded by pale nucleoplasm containing only small amounts of condensed nuclear material. There was a full complement of cellular organelles present in the cytoplasm of each neuron. However, the organization of these organelles within the cell body was strikingly different from that of Type A neurons. Without exception, these neurons had some degree of stacked or organized Nissl substance (Fig. 3) rather than the reticulated strands typical of Type A neurons. There was an even distribution of small round or oval mitochondria and free ribosomes throughout the cytoplasm of the soma and into proximal dendrites (Fig. 3). Large darkly-staining lysosomal bodies also were common in the cytoplasm. Neuronal profiles with a single large proximal dendrite (> 2 μm in diameter) were common. Proximal dendrites tapered gradually and could only be followed for a few microns before disappearing out of the plane of section. In spite of the several differences in morphology between Type A and B neurons, they were similar with respect to axo-somatic synaptic

Fig. 3. Electron micrograph of a Type B neuron in the PTN. Note the round to oval shape, invaginated nucleus with a prominent nucleolus (nu), stacks of rough endoplasmic reticulum (Nissl substance, arrowheads) and absence of axo-somatic synaptic contacts. Calibration bar: 3 μm.

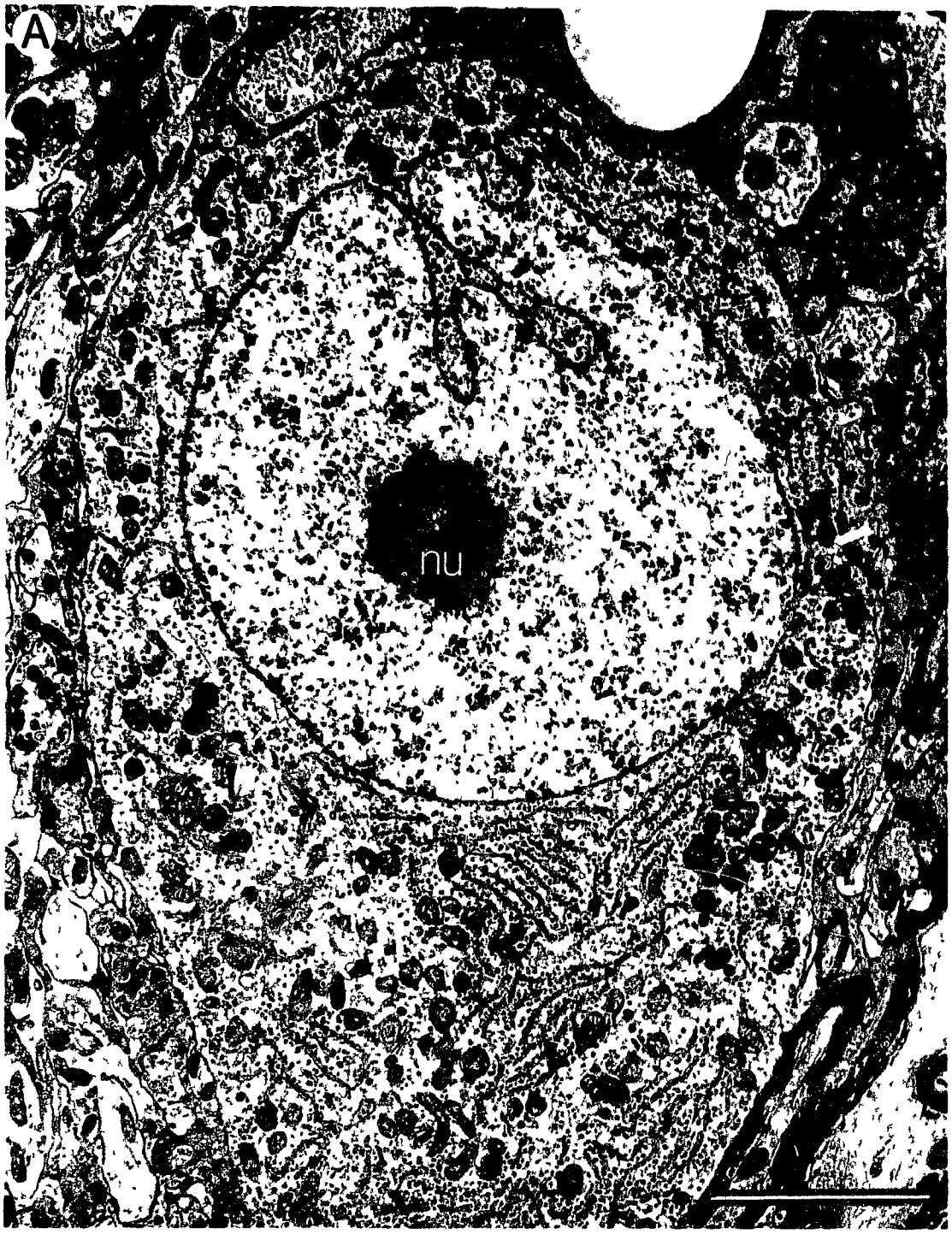

Figure 3

Fig. 4. Electron micrograph of a Type C neuron in the PTN. Note the similarity in size, shape and complement of cytoplasmic organelles to that in Type B neurons (Fig. 2). Axo-somatic contacts (arrowheads) cover much of the surface of the soma. Arrows indicate several Golgi apparatuses. Boxes are enlarged in Figure 5. Calibration bar: 3 μm.

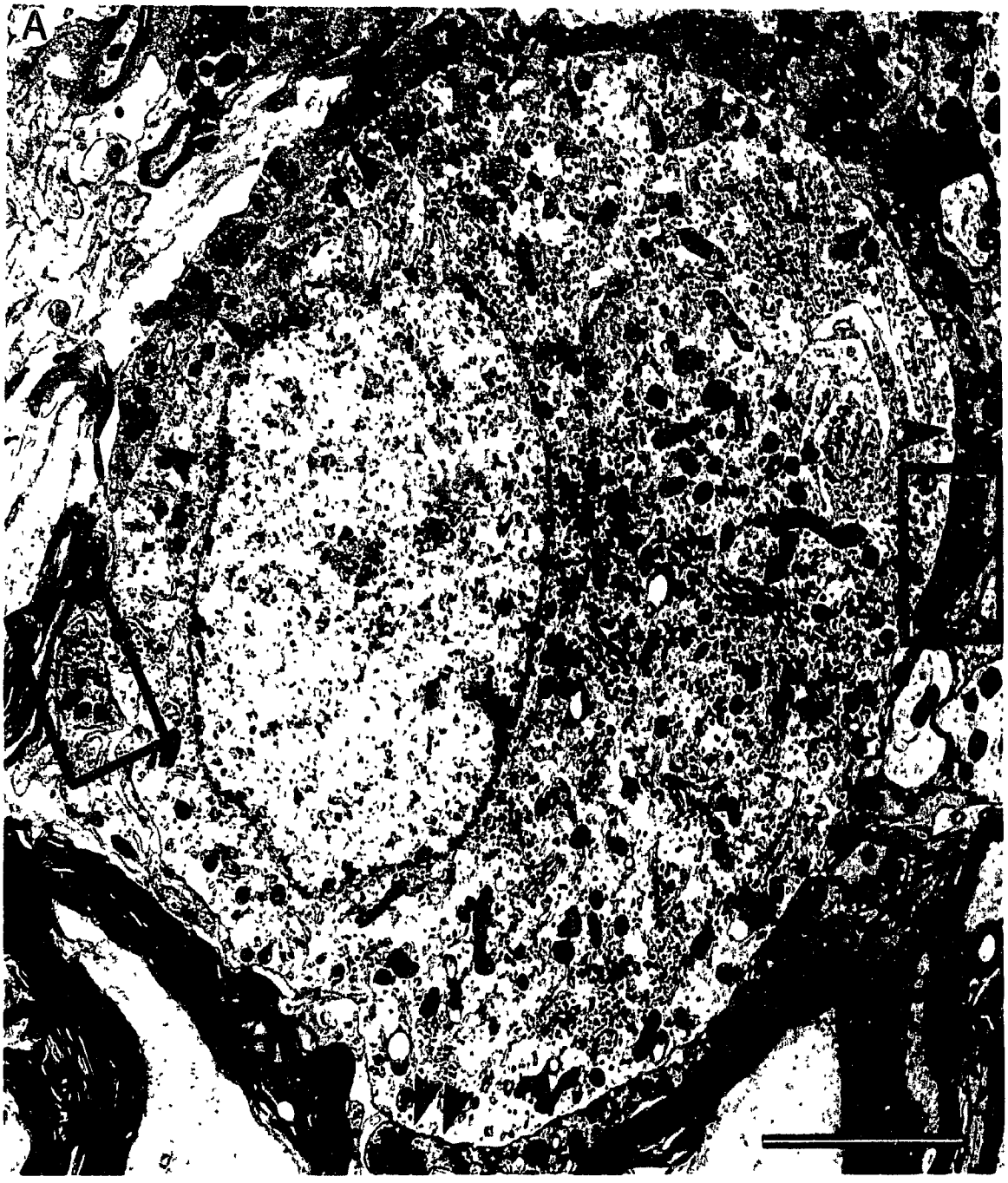

Figure 4

Fig. 5. Electron micrographs of higher magnifications of axo-somatic contacts enclosed in boxes in Figure 3. **A**: Axon terminal containing pleomorphic clear vesicles and making a symmetric synaptic contact (arrowheads) with a Type C neuron. **B**: Axon terminal containing pleomorphic clear vesicles and making two synaptic contacts with the surface of the soma (arrowheads). Calibration bars: A-B, 0.5 μm.

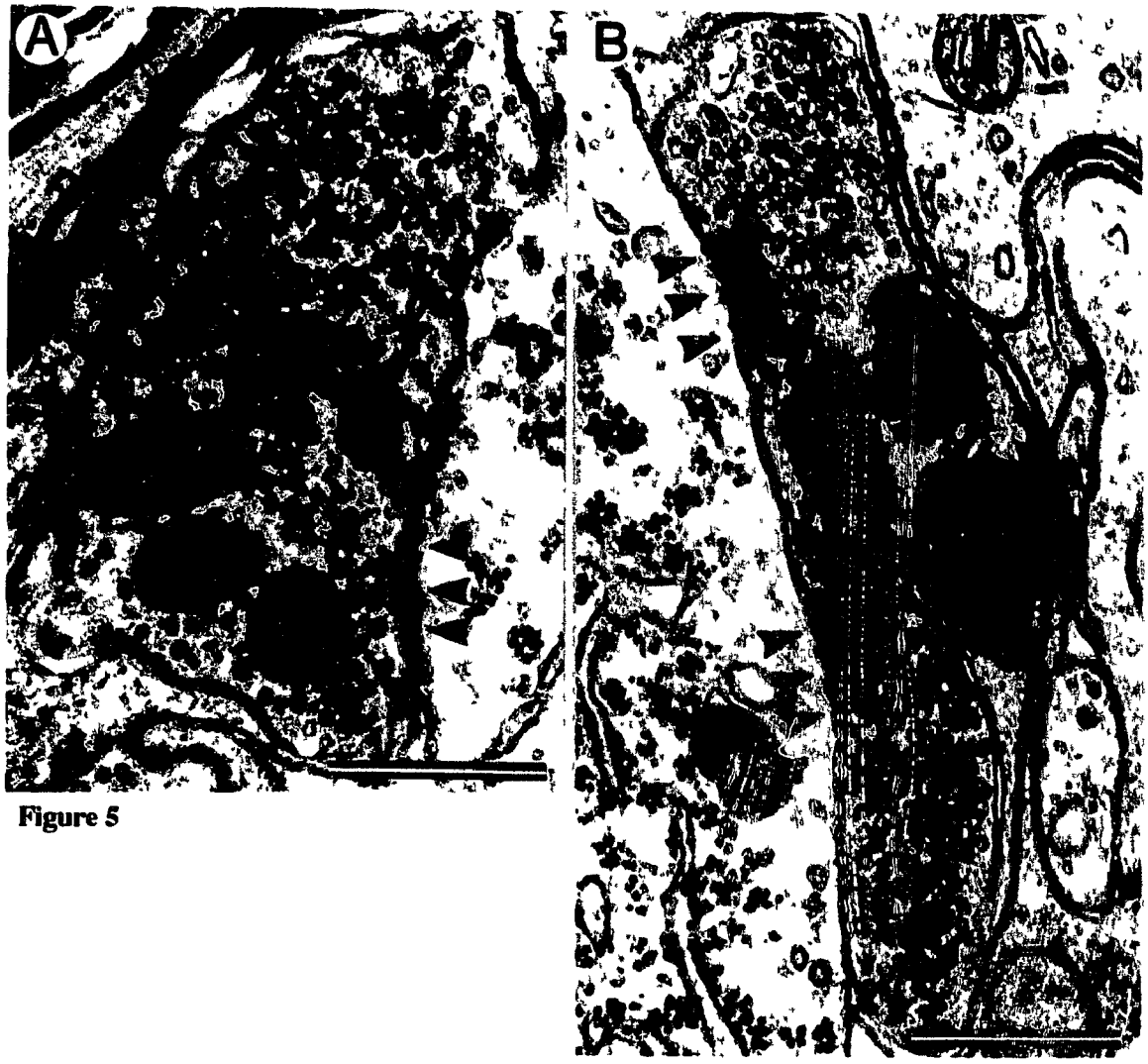

Figure 5

contacts. Both types of neurons rarely had axo-somatic synapses. There were, however, small numbers of synaptic contacts evident on proximal dendrites and these contained either agranular round or pleomorphic synaptic vesicles.

The third type of neuron (Type C) identified in the PTN was exceedingly rare and only four such neurons were encountered in the survey. These neurons shared many similarities with regard to morphology with Type B neurons with one important and defining difference. The feature which distinguished Type C neurons from Type B neurons was the number of axo-somatic synapses that were present on the soma of these neurons. Typically, the plasma membrane of the soma had a high density of synaptic boutons which abutted against one another along the soma surface (Fig. 4). Both RA and PS synaptic terminals were present although PS synaptic terminals were slightly more numerous (Figs. 4, 5). The cytoplasm of type C neurons contained a plethora of organelles. RER usually was in the form of short segments either occurring singly or in small stacked groups of 5 or 6 segments. Typically two or more Golgi apparatuses were present in the cytoplasm of each neuronal profile (Fig. 4). Lysosomes and mitochondria of various shapes and sizes and free ribosomes were also present (Fig. 4). In only one case was a large proximal dendrite found and it contained a similar complement of organelles. As mentioned above, small numbers of large fusiform neurons were observed in the 1 μm sections particularly in the caudal PTN, an area difficult to distinguish in normal tissue and these neurons may correspond to Type C neurons which were very rare at the electron microscopic level.

Neuropil. In keeping with the observations obtained from 1-μm-thick plastic sections, the neuropil of the PTN was comprised largely of unmyelinated axonal and dendritic profiles. Regardless of the plane of section through the PTN, profiles of processes were very heterogeneous in appearance, appearing as transversely, obliquely or longitudinally cut profiles which indicated that there was no preferred orientation within the nucleus.

Dendrites of various sizes and shapes were numerous and typically contained pale cytoplasm and numerous, relatively evenly distributed microtubules. In large dendrites there were many free ribosomes, short segments of RER and mitochondria. Small dendritic elements (<1 μm in diameter) had a pale cytoplasmic matrix and often contained one or two mitochondria and occasionally a small number of agranular, membrane-bound sacs corresponding to smooth endoplasmic reticulum. Ribosomes, the most definitive feature for identifying dendrites (Peters et al., '91), were often scarce or absent in small dendritic profiles and thus some of these profiles might correspond to dendritic appendages such as spines which characteristically contain morphologically undifferentiated cytoplasm and small amounts of smooth endoplasmic reticulum (Peters et al., '91) (Figs. 6A,13A). Many of the smaller dendrites were in close association with axon terminals, a major constituent of the neuropil (see section on synaptology).

Preterminal axons, most of which were less than 0.5 μm in diameter also contribute to the composition of the PTN neuropil. Preterminal axons were characterized by smooth contours, round shape, dark cytoplasmic matrix, and the presence of microtubules which appeared in less orderly arrays than those observed in dendrites. Considerable areas of the neuropil often were exclusively occupied by preterminal axons, some, but not all, containing vesicles. Axons in these regions were not oriented in an orderly fashion. In a number of cases, preterminal axons were found to contain small numbers of synaptic vesicles, usually in association with the plasma membrane, although no synaptic specializations were present. Vesicles in preterminal axons were typically agranular and round. Where two adjacent axonal profiles were closely apposed to one another they were often structurally associated by puncta adhaerentia.

Cell bodies and processes of glia were dispersed throughout the neuropil and were often in close association with neuronal somata (Fig. 2B). Glial cells were typically smaller than neuronal somata and contained a dark nucleus and a homogeneous cytoplasm.

The nucleus was round or oval in shape and contained a more or less continuous rim of condensed nuclear material adjacent to the inner nuclear membrane. The darkly-staining cytoplasm contained short cisternae of RER, numerous free ribosomes and a small number of small round mitochondria. Glial processes, were also dark in appearance and typically contained large numbers of filaments.

Synaptology. There was a rich complement of synaptic relationships among axon terminals of different morphologies and somata, dendrites and axon terminals in the PTN. Individual synaptic terminals were classified on the basis of the morphology of the synaptic vesicles present in the bouton and on the ultrastructure of the pre- and postsynaptic membranes at the site of synaptic contact. A terminal was considered to be making synaptic contact with a postsynaptic element if synaptic vesicles were clustered near the presynaptic membrane, if there was a distinct widening of the apposed membranes to form the synaptic cleft which contained dense intercellular material, and if there was a clear specialization of the postsynaptic membrane with dense material on the cytoplasmic side of the plasma membrane. The thickness of the postsynaptic membrane density was used as an additional criterion such that if densities were similar pre- and postsynaptically they were classified as a symmetric synaptic contact and if the postsynaptic density was thicker than that observed presynaptically the synapse was classified as asymmetric.

Based on the above criteria, two morphologically distinct synaptic types accounted for most of the identified synapses. A third classification was established to categorize unusual vesicle-containing profiles, some of which were synaptic and others which did not form any kind of synaptic contact. The third category included some terminals which made synaptic contacts, although the vesicle complement of these terminals was not classified with the two main terminal types because of the unusual numbers of dense-cored vesicles and the irregular shapes of many of the vesicles in the terminals (i.e., granular and agranular).

Fig. 6. Electron micrographs of RA type synaptic boutons in the neuropil of the PTN. **A**: A single small RA synaptic terminal containing round agranular vesicles clustered at the presynaptic membrane along the active zone (arrowheads) with a postsynaptic profile containing a small amount of smooth endoplasmic reticulum (arrow). **B**: Three RA terminals one of which contains small numbers of DCV of various sizes (large arrows). In one instance a small puncta adhaerens (small arrows) is found between two boutons containing predominantly agranular round vesicles. Calibration bars: A-B, 0.5 μm.

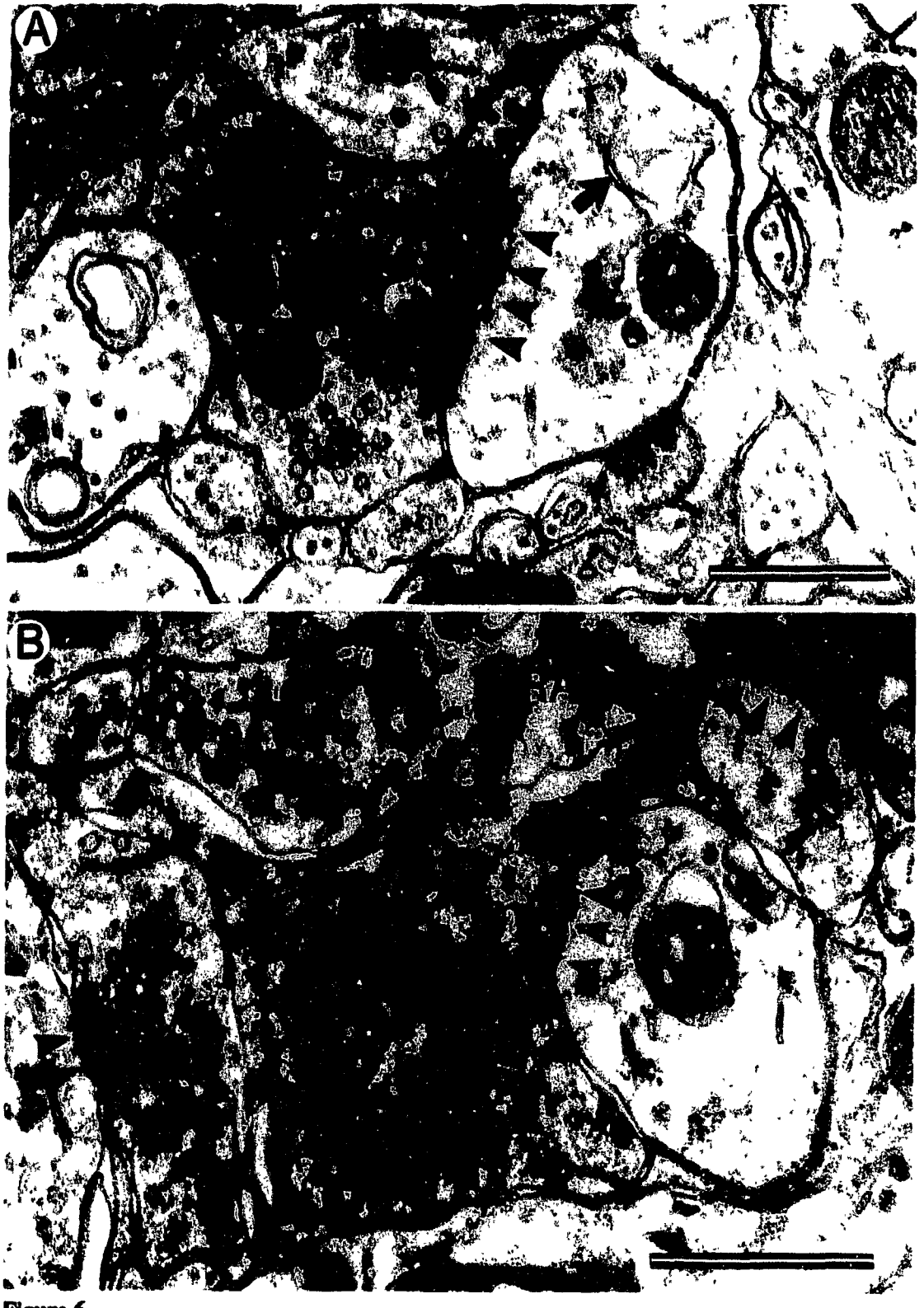

Figure 6

Fig. 7. Electron micrographs of two PS synaptic terminals and an RA terminal in the neuropil of the PTN. **A**: PS bouton containing many agranular pleomorphic vesicles and a single DCV (arrow) and making two synaptic contacts with a large dendrite (D). **B**: PS terminal contacting (arrowheads) a small dendritic profile. RA terminal synapsing on a dendrite (D). Note the subsynaptic dense bodies (arrowheads) and the close proximity of one of the DCV to the active zone (arrow). Calibration bars: A-B, 0.5 μm.

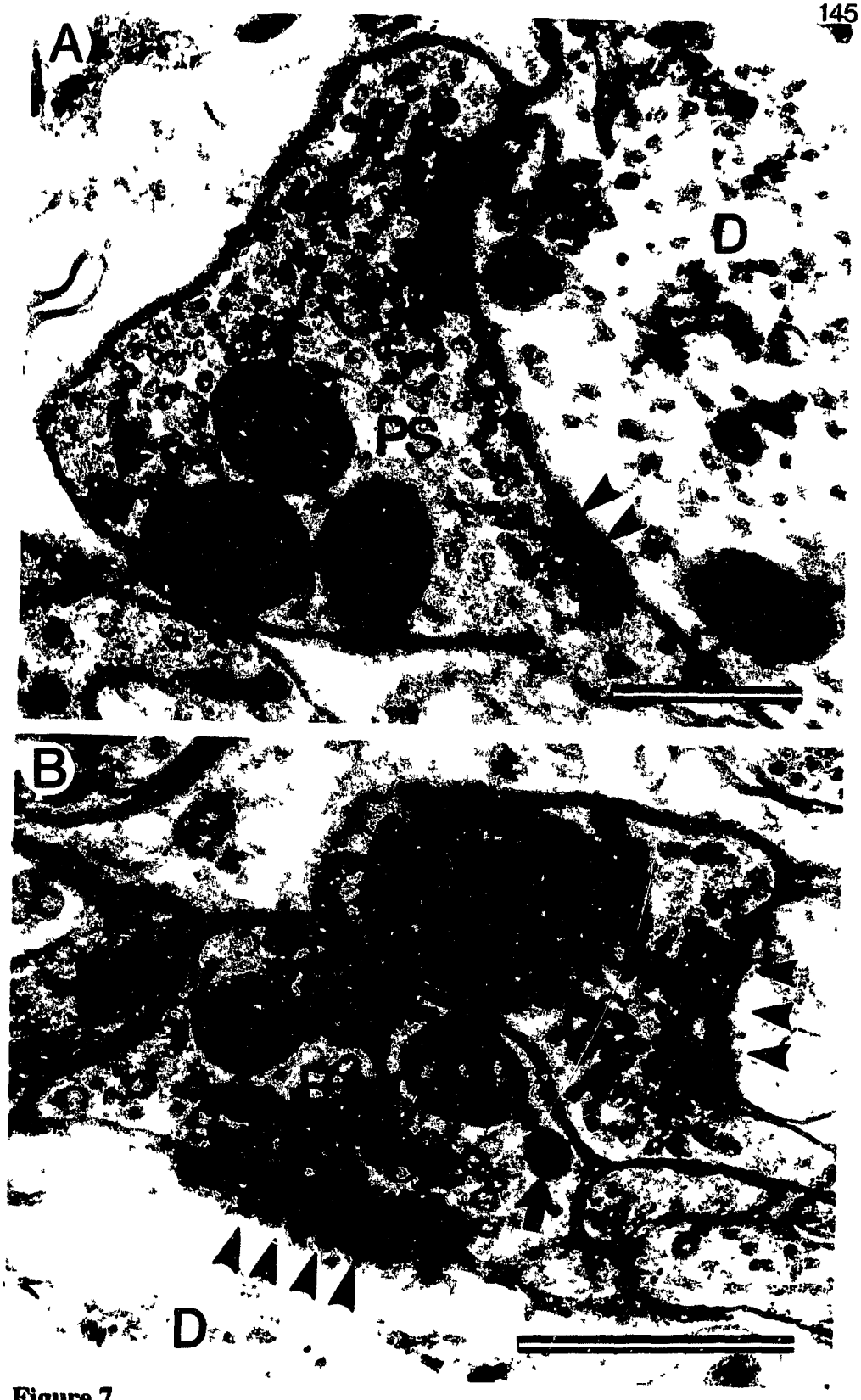

Figure 7

The first synaptic type contained predominantly small, round, agranular vesicles and formed asymmetric synaptic contacts (RA) with the postsynaptic element (Figs. 6, 7B, 10, 11). Subsynaptic dense bodies were common when RA synaptic contacts were formed with dendrites (Fig. 7B). The second terminal type identified contained a heterogeneous population of clear, agranular vesicles which varied from round to flattened and formed symmetric synaptic contacts with the postsynaptic element (PS) (Figs. 7). Although round vesicles were present, the predominant vesicle types were oval or flattened and these terminals were designated pleomorphic symmetric (PS). Dense-cored vesicles could be seen in both the RA and PS synaptic terminals and were typically larger (50-100 nm in diameter) than the more abundant small (30-60 nm in diameter) agranular vesicles . Dense-cored vesicles were found both in close approximation to the synaptic active zone and at considerable distances from the active zone with equal frequencies. (Figs. 6B, 7, 13B). The presence of dense-cored vesicles was not restricted to axon terminals and in a some instances small numbers, usually less than three, were seen in postsynaptic dendrites and in the cytoplasm of PTN neurons. These were indistinguishable from dense-cored vesicles found in preterminal axons and axon terminals.

Profiles resembling synaptic terminal-like structures and containing vesicles were encountered in the PTN. These profiles contained a large number of dense-cored vesicles relative to the numbers of smaller agranular vesicles. Another peculiarity of these profiles was that they were rarely encountered establishing true synaptic contacts although profiles were frequently encountered in the neuropil. Only 2 of 23 of these profiles were found to form synaptic contacts of any kind. In the small number of instances in which synaptic contacts were observed, contacts were always asymmetric (i.e., thick density on the postsynaptic membrane) and formed with a dendrite or second profile containing small numbers of granular and agranular vesicles (Fig. 8). The small agranular vesicles present in these terminals were heterogeneous in morphology and size (Fig. 8) which contrasts

Fig. 8. Electron micrograph showing two synaptic profiles (P_1, P_2) contacting a third profile (P_3) which contains a small number of vesicles. P_1 and P_2 form extensive asymmetric synaptic contacts (arrowheads) with P_3. Calibration bar: 0.5 μm.

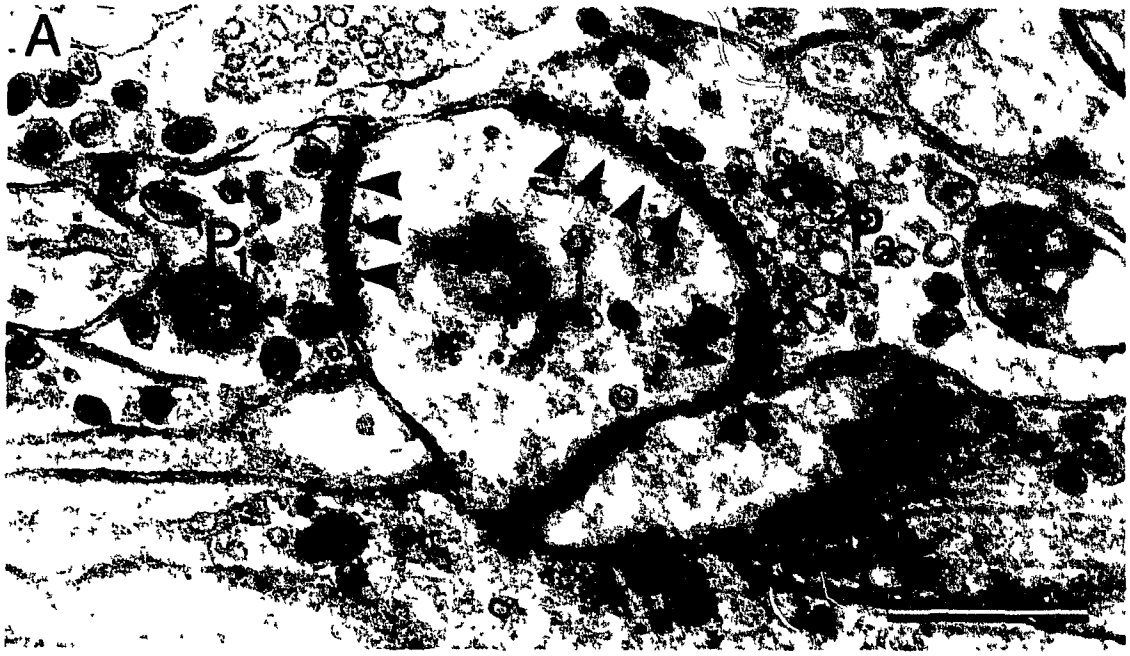

Figure 8

Fig. 9. Electron micrograph of a small diameter profile (P) containing numerous DCV but which does not form a synaptic specialization. Calibration bar: 0.5 μm.

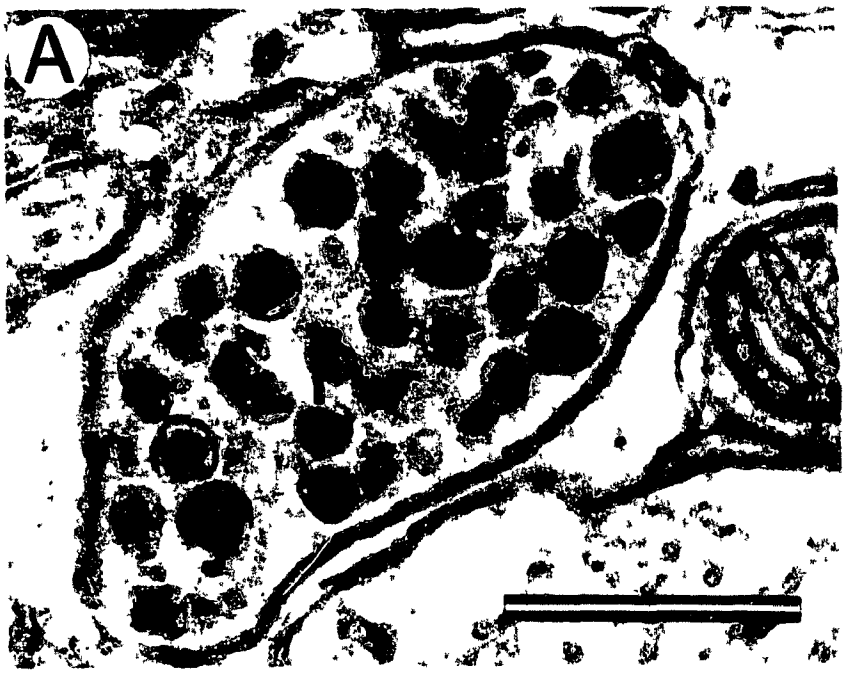

Figure 9

sharply with the vesicles of RA and PS synaptic terminals which were more uniform in size if not morphology (i.e., pleomorphic vesicles). Small profiles (< 1 μm in diameter) packed with dense-cored vesicles were encountered frequently during the survey of the PTN neuropil (Fig. 9). Serial sections through three such structures did not provide evidence for a typical synaptic relationship.

In addition to synaptic contacts, puncta adhaerentia were identified in surveys of the synaptic organization of the PTN. Occasionally such specializations occurred between two adjacent synaptic boutons with RA morphology (Figs. 6B, 10A, 14B). At the site of contact, the plasma membrane of the two adjacent boutons was parallel and closely apposed. On the cytoplasmic side of both terminals there was a symmetric accumulation of amorphous dense material. The space between the two adjacent plasma membranes was less dense in appearance although it did contain dense extracellular material. At no time were these puncta adhaerentia (Peters et al., '91) associated with an accumulation of vesicles and, thus, were presumably not synaptic in function. Rather they appeared to be related to the structural integrity of the terminal associations.

RA synaptic terminals were the most abundant synaptic type in the PTN and contributed the greatest variety of synaptic relationships. Axo-somatic contacts involving RA terminals were rare but sometimes did occur on both Type A and Type C neurons. When identified on Type A neurons one and no more than two contacts on one neuronal profile could be seen at any time, with most Type A neuronal somata exhibiting no axo-somatic contacts. Type C neurons on the other had numerous RA and PS axo-somatic synaptic contacts. Type B neurons were themselves rare and in the few cases (n=3) that were surveyed, no axo-somatic terminals were present, although in one case two RA synapses were found on the proximal dendrite close to the cell body. When the postsynaptic profile was a dendrite of small or medium size, RA synaptic terminals were

Fig. 10. Electron micrographs of examples of complex synaptic arrangements present in the PTN. **A**: Micrograph showing two RA synaptic terminals with a puncta adhaerens (arrows) formed between their adjacent plasma membranes. The RA on the left is making a synaptic contact with a dendritic profile containing pleomorphic vesicles. **B**: RA synaptic terminal containing a multivesicular body (arrow) and contacting (arrowheads) a dendritic profile containing pleomorphic vesicles. **C**: RA synaptic terminal with clustering of uniform round synaptic vesicles near the active zone (arrowheads) opposite the postsynaptic dendritic profile. The arrow indicates a segment of smooth endoplasmic reticulum. Calibration bars: A-C, 0.5 μm.

Figure 10

Fig. 11. Electron micrograph of two RA synaptic terminals (RA_1 and RA_2) participating in a synaptic triplet. RA_1 forms a synaptic contact (arrowheads) with RA_2 which in turn forms a synaptic contact (arrowheads) with a dendritic profile. Calibration bar: 0.5 μm.

Figure 11

common. However, small dendrites (<1.0 μm in diameter) were the most common site for RA synaptic contacts (Figs. 6, 7B, 13).

RA terminals also participated in synaptic arrangements that involved a second vesicle-containing profile (i.e., an axon or dendrite). In these arrangements, postsynaptic profiles contained either small, round, agranular vesicles or pleomorphic agranular vesicles (Figs. 10, 11). In most instances, a bouton containing round, agranular vesicles was the presynaptic element and it synapsed on a profile containing pleomorphic agranular vesicles (Fig. 10). Other than the uniqueness of the vesicle-containing postsynaptic profile in these arrangements, the presynaptic element was typically RA in morphology. The postsynaptic vesicle-containing element is referred to here as a profile (presumably dendritic in origin) as it was not possible, based on the ultrastructural features present in these small diameter (<1 μm) postsynaptic elements, to designate them conclusively in all instances as distinctly dendritic or axonic. In two instances a triplet synapse (Lieberman and Webster, '74) was observed where two terminals containing round agranular vesicles, one synapsing on the other and the second on a dendrite, were observed (Fig. 11). The photomicrograph in Figure 11 shows RA_1 synapsing on a second RA_2 profile but the contact is clearly symmetric. In the only other instance where this type of arrangement was observed the synaptic contact was asymmetric.

Another arrangement found in the PTN involved an RA terminal synapsing on a profile which contained pleomorphic clear vesicles (Fig. 10). In one instance the clustering of pleomorphic vesicles in the postsynaptic element was suggestive of a reciprocal synapse (Fig. 10A). A more frequent finding was that of postsynaptic clustering of pleomorphic vesicles away from the synaptic zone (Fig. 10B, C). Because of the small diameter of the profiles involved in these arrangements it was very difficult to find features such as ribosomes which might provide definitive identification, particularly for the postsynaptic element. Nevertheless, it was determined on the basis of the characteristic clustering of

vesicles and pale cytosol of these postsynaptic elements that they probably represented dendrites (Ralston, '71; Lieberman and Webster, '74). In an ideal situation, large diameter dendrites of irrefutable morphology and containing vesicles similar to those in the small would be identified. However, no such evidence was forthcoming.

PS terminals were rare relative to RA terminals and generally were restricted to contacts on somata and large diameter dendrites, i.e., proximal dendrites (Fig. 7A). It was very rare for PS terminals to be found on small (<1 μm in diameter) dendritic profiles (Fig. 7B). PS synaptic terminals on somata or large proximal dendrites typically made one or two synaptic contacts (Fig. 7). In no instances were postsynaptic dense bodies present at a PS synaptic site. The relative proportions of PS terminals on somata and proximal dendrites were approximately equal to that observed for RA terminals at the same sites, particularly on Type C neurons. Type A neurons were rarely found to have RA terminals while Type B neurons had small numbers on proximal dendrites and somata. The presence of PS terminals on small diameter dendrites was rare (Fig. 7B). Synaptic terminals were typically small (<1 μm in diameter) and contained numerous pleomorphic agranular vesicles. A single synaptic contact was the norm and they were occasionally seen synapsing on the same small dendrite adjacent to a synaptic terminal containing round agranular vesicles.

Pharyngeal and Laryngeal Afferent Synaptology

Light microscopic observations. Following the injection of WGA-HRP or CT-HRP into the musculature and mucosa of the pharynx or the larynx, afferent terminal labeling was located in three discrete regions of the medulla oblongata (Fig. 12). Labeling was present in the PTN overlying the dorsolateral spinal trigeminal nucleus pars caudalis and pars interpolaris. Two additional terminal sites in the NTS, the subnucleus interstitialis (see Chapter 3) and subnucleus intermedialis, received overlapping afferent projections from the pharynx and larynx.

Fig. 12. Photomicrograph of a 100-μm-thick vibratome section containing labeled pharyngeal primary afferent axons and axon terminals in the PTN, subnucleus interstitialis and subnucleus intermedialis (arrow) of the NTS.

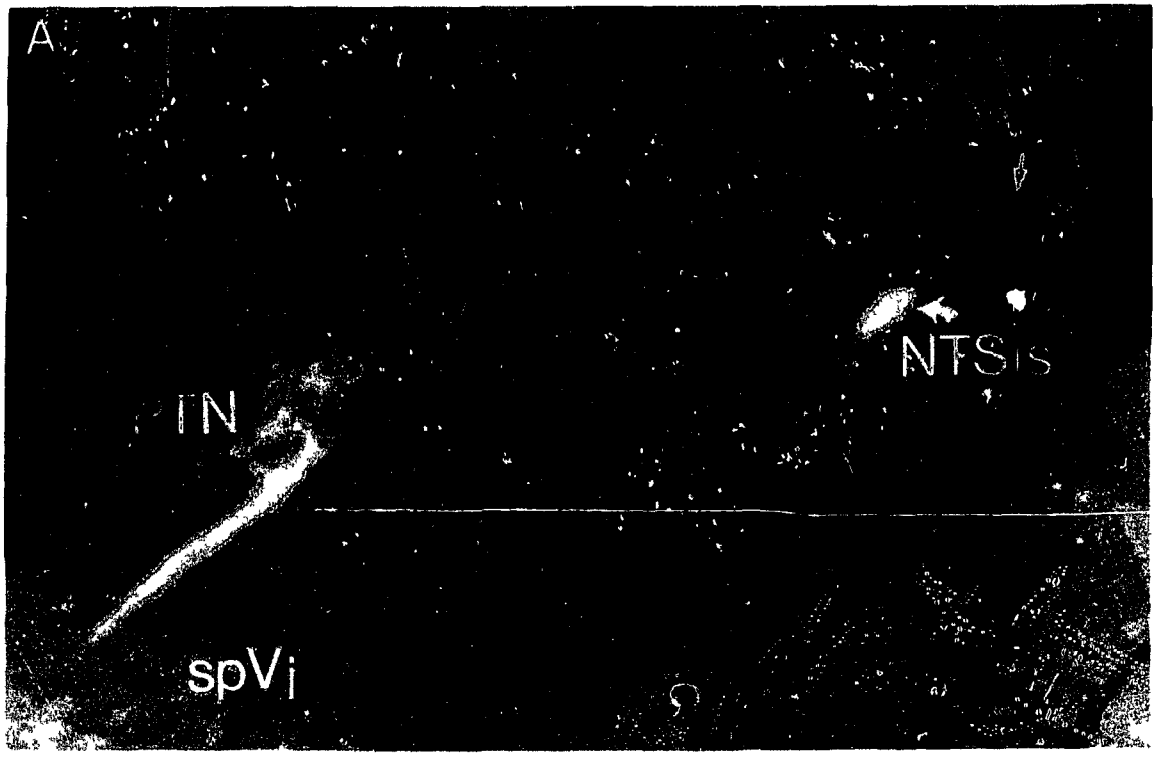

Figure 12

The PTN received a heavy primary afferent projection bilaterally following injections of either of the two conjugates of HRP into the pharynx or larynx. The primary afferent terminal fields of these two viscera were largely overlapping, with the laryngeal field extending approximately 50-100 μm more caudally in the PTN than did the pharyngeal afferent terminal field. The density of labeling in the PTN and subnucleus interstitialis of the NTS was roughly the same while labeling in the subnucleus intermedialis of the NTS was considerably lighter (Fig. 12). The anterograde labeling in figure 12 extends out into the reticulated network of the PTN and also ventrolaterally along the medial border of the spinal trigeminal tract. This ventrolateral extension in the present study was also considered part of the PTN, and in several cases such a ventrolateral extension was bracketed by the myelinated fibers of the spinal trigeminal tract.

Electron microscopic observations. The primary afferent labeling present in vibratome sections was confirmed in subsequent electron microscopic studies. Preterminal axons and numerous labeled synaptic boutons were found to contain HRP reaction product. Preterminal axons were unmyelinated and small in diameter (< 0.75 μm). Labeled terminals contained one or more darkly-staining crystalline structures typical of transganglionic transport of HRP (Figs. 13, 14). Crystals varied in size and shape, properties related to the pH of the histochemical procedure used and the orientation of crystals relative to the plane of section. For the most part, label appeared as a solid structure although it was not uncommon to find crystals with small to large perforations of irregular shape (Fig. 14A). Large HRP crystals seemed to be most likely to exhibit this appearance.

All labeled pharyngeal and laryngeal synaptic terminals were exclusively of the RA type and rarely exceeded 2.0 μm in diameter (Figs. 13, 14). Labeled boutons typically contained numerous round agranular vesicles with varying numbers of dense-cored vesicles (Fig. 13B), although the agranular vesicles were always more numerous.

Fig. 13. Electron micrographs of anterogradely labeled pharyngeal primary afferent terminals. **A**: RA synaptic terminal containing a large darkly-stained HRP crystal and contacting (arrowheads) a small dendritic profile containing smooth endoplasmic reticulum (arrow). **B**: RA synaptic terminal containing several DCV (arrows) one of which is close to the synaptic active zone (arrowheads). **C**: Labeled pharyngeal terminal synapsing (arrowheads) on a small dendritic profile containing a multivesicular body (curved arrow). Calibration bars: A-C, 0.5 μm.

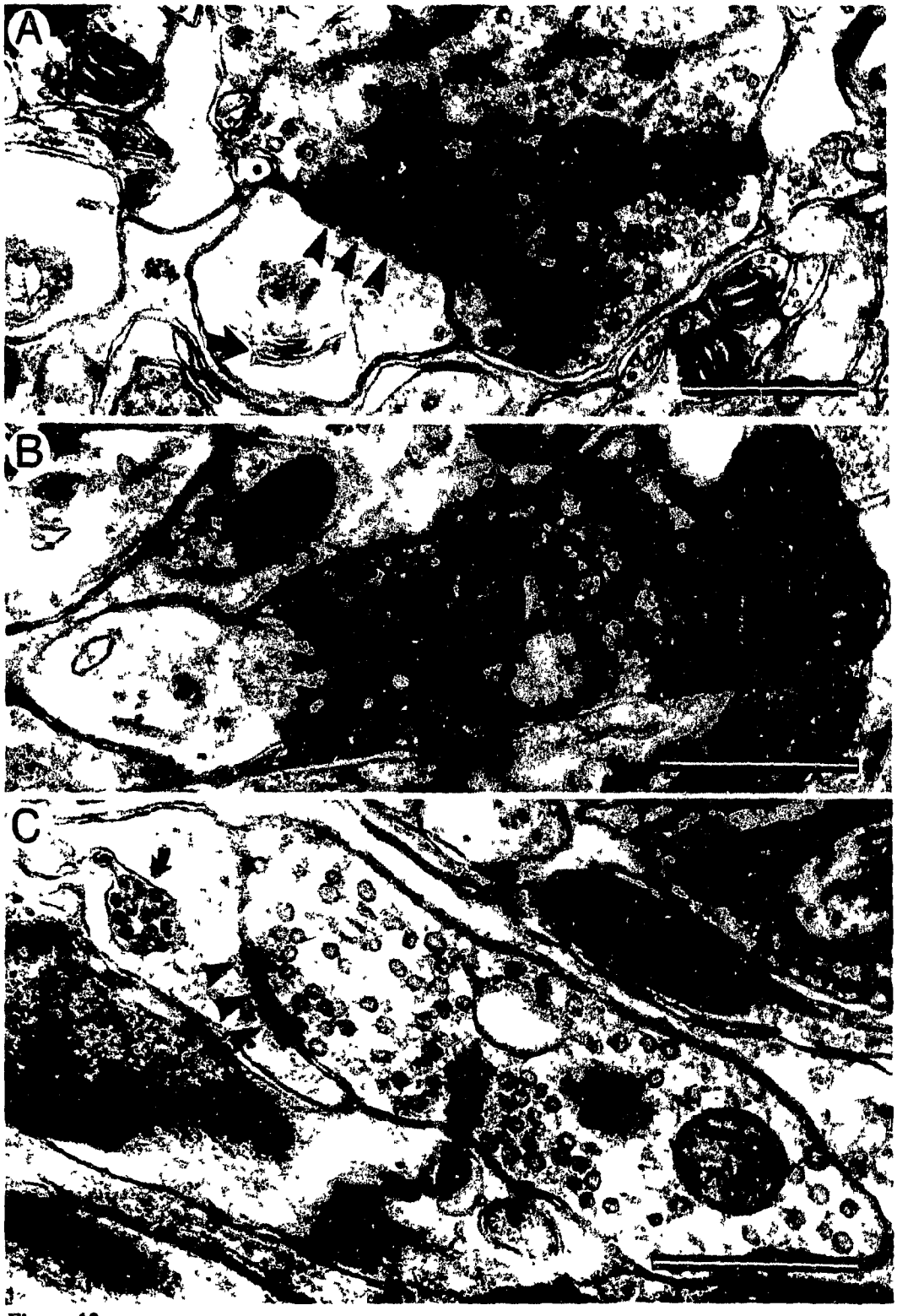

Figure 13

Fig. 14. Electron micrographs of labeled laryngeal primary afferent terminals. **A**: RA synaptic terminal containing HRP reaction product. Note the perforations in the crystalline reaction product. **B**: Labeled laryngeal synaptic terminal (arrowheads) on a dendritic profile. Note the distinct puncta adhaerens (arrows) between the labeled RA and an adjacent unlabeled RA synaptic terminal. Calibration bars: A-B, 0.5 μm.

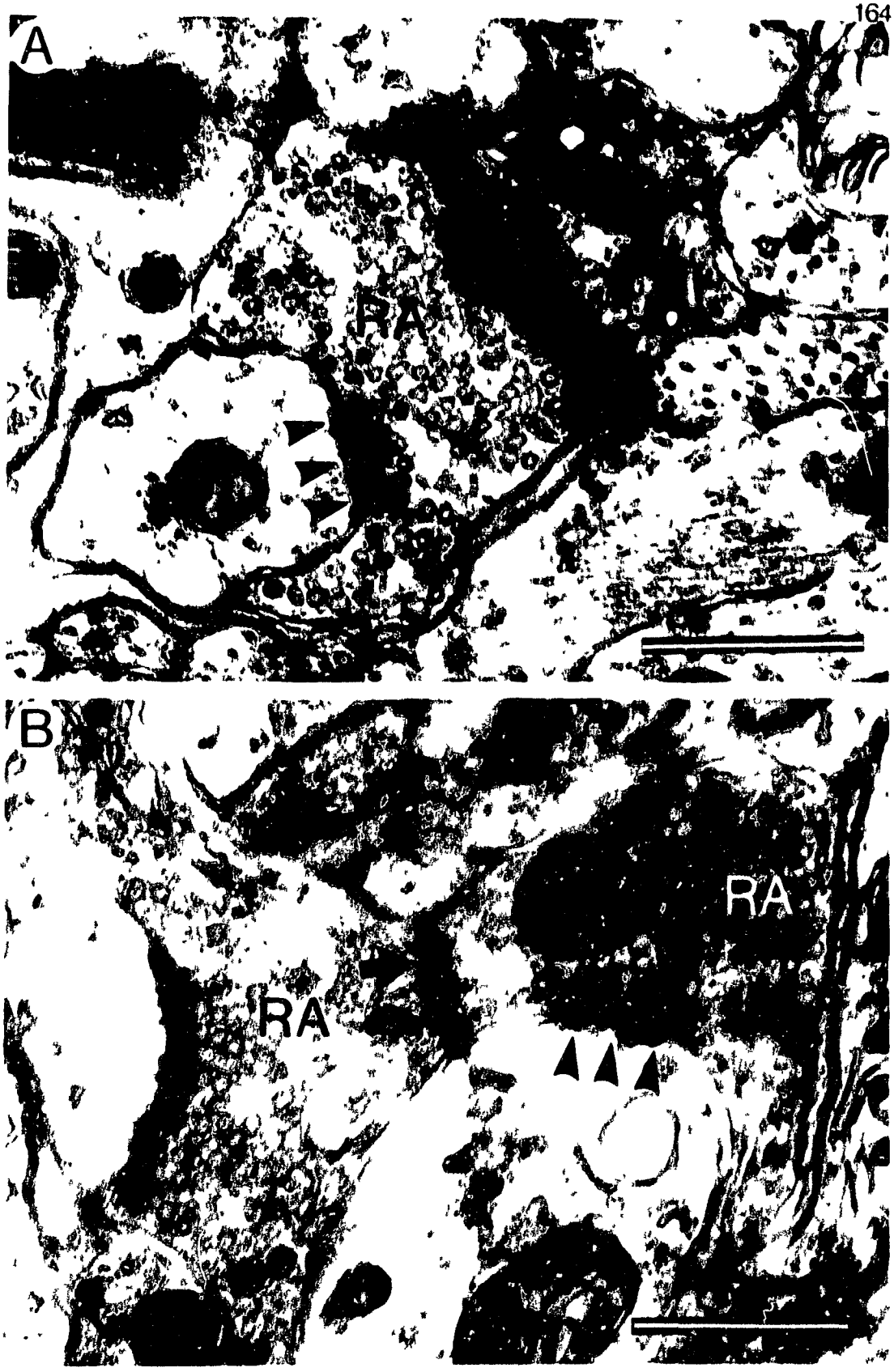

Figure 14

Fig. 15. Electron micrographs of two sections cut through the same labeled RA synaptic terminal showing the possible transsynaptic transport of WGA-HRP to the postsynaptic dendritic profile in B containing pleomorphic agranular vesicles. The survival time for this animal was five days. Calibration bars: A-B, 0.5 μm.

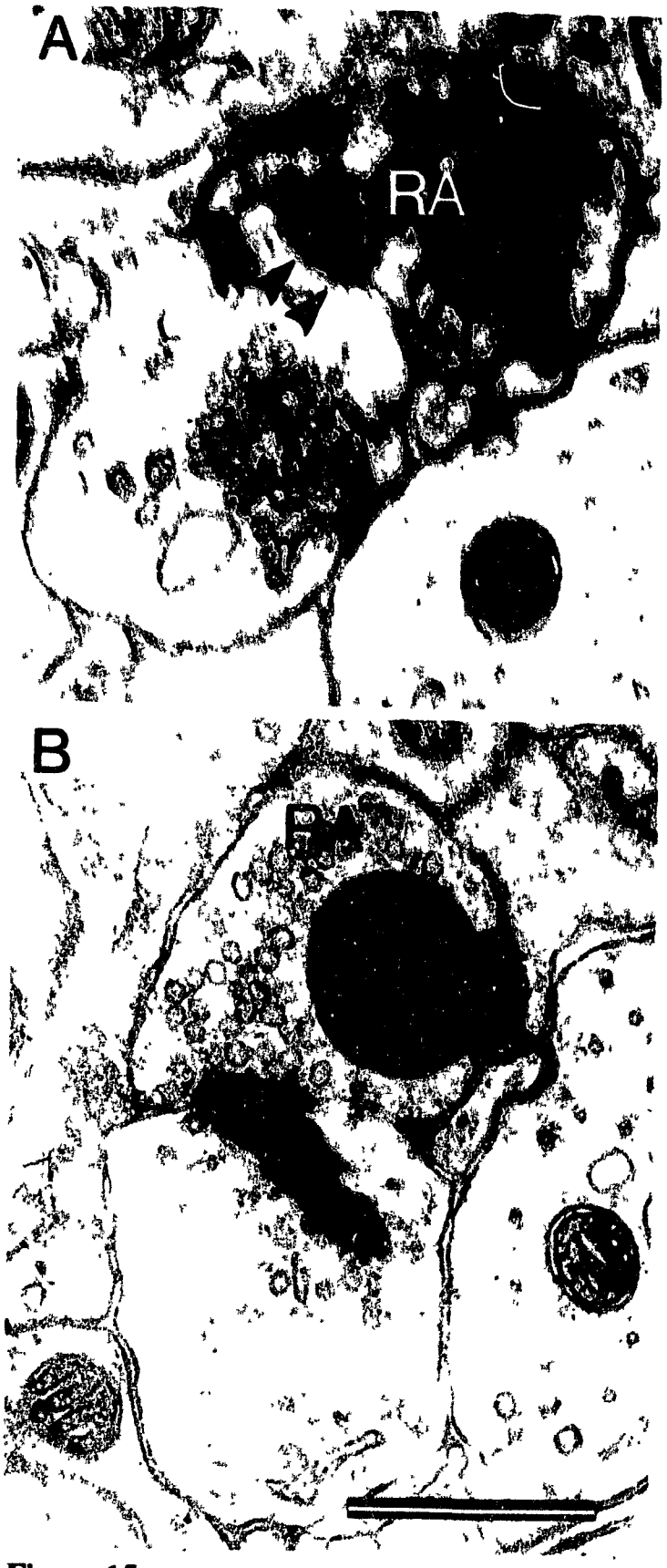

Figure 15

Synaptic junctions were clearly asymmetric and postsynaptic dense bodies were common. The postsynaptic element was always a small diameter (<1 μm) dendrite which occasionally contained a multivesicular body (Fig. 13C), mitochondria (Figs. 13A, B) and sometimes a number of small agranular membrane bound sacs (Fig. 13A). It is important to note that some small postsynaptic profiles have been designated as dendrites even though it is not entirely certain that these are dendrites proper, or possibly, dendritic spines. This ambiguity is attributed to the small size of the profiles and the relatively small amount of consistent evidence to suggest one or the other or both since characteristics of both dendrites and spines have been observed in the PTN (see technical considerations). In two instances a labeled RA terminal was seen to make contact with a vesicle-containing profile (Fig. 15) which raised the issue of the nature of the postsynaptic vesicle-containing profile. Was it dendritic or axonic? Serial sections through one such case did not resolve the issue because no defining characteristics were identified. Figure 15 shows two sections through the same labeled RA terminal and postsynaptic vesicle-containing profile (P) taken from an animal with a survival time of 5 days. Since the vesicles in the postsynaptic profile were pleomorphic it is assumed, based on the fact that no other profile containing pleomorphic vesicles was identified as containing HRP reaction product, that the labeled element identified as P (Fig. 14B) is the result of transsynaptic transport of the tracer. This result was never present in animals with survival times of 2-3 days. The presence of vesicles in the postsynaptic element in Figure 15 supports the observation that postsynaptic dendrites in the PTN do contain vesicles as reported earlier. This is in light of the fact that labeled afferent terminals synapse only on small diameter dendrites, some of which clearly contained ribosomes.

In summary, labeled primary afferents originating in the pharynx and larynx have overlapping terminal fields in the PTN. Furthermore, the ultrastructure of the synaptic

complexes formed by these primary afferent terminations within the PTN were morphologically similar.

DISCUSSION

Cajal ('09) appears to have been the first to detail the morphology of neurons lying within the spinal trigeminal tract in a nucleus he termed the cellules interstitielles. Since Cajal's Golgi studies numerous other investigators have identified a similar structure albeit by different nomenclatures in a number of different species. Interestingly, considerable variation exists in the delineation of this cell group (Fuse, '19; Åstrom, '53; Olszewski and Baxter, '54; Oswaldo-Cruz and Rocha-Miranda, '68; Gobel and Purvis, '72; Campbell et al., '74; Chan-Palay, '78a, b; Cechetto et al., '85). A recent light microscopic survey in the rat of cells lying lateral to the spinal trigeminal complex within the fibers of the spinal trigeminal tract by Phelan and Falls ('89) led these authors to divide the interstitial system into five anatomical regions. The paratrigeminal nucleus, which is one of the five subdivisions of the interstitial system, is the destination of numerous afferent fibers originating in visceral and somatic sites (Panneton and Loewy, '80; Panneton and Burton, '81; Arvidsson and Thomander, '84; Pfaller and Arvidsson, '88; Altschuler et al., '89; Arvidsson and Pfaller, '90; Panneton, '91). The present study reports on the fine structure of the PTN and the synaptology of primary visceral afferent projections to the nucleus.

The results of the electron microscopic survey of the PTN as they pertain to the termination sites of upper alimentary and respiratory tract primary afferent projections in the present study has revealed previously unreported data on the ultrastructure and synaptology of the PTN. It has been established that the PTN contains three distinct neuronal types and a complex synaptology involving axon terminals, somata, dendrites and vesicle-containing dendrites.

A number of investigators have described the morphology of neurons in the PTN based on Golgi preparations (Cajal, '09; Chan-Palay, '78a; Phelan and Falls, '89) Nissl stains (Phelan and Falls, '89) and electron microscopy (Chan-Palay, '78a,b). Unfortunately, the

descriptions vary because of the diversity of species: rabbit (Cajal, '09), rat (Phelan and Falls, '89) and monkey (Chan-Palay, '78a). However, since Phelan and Falls ('89) have presented results based on Golgi preparations in the rat, it is possible to make direct comparisons with results of the present ultrastructural study of the rat PTN. The present study established the presence of three unique neuronal groups within terminal fields of afferent projections originating in the pharynx and larynx. These neurons were elongate and fusiform in shape. By comparison, neurons identified in the Golgi preparations of Phelan and Falls ('89) were similar in shape and size to those in the present study. However, their results indicated that only two types of neurons existed in the PTN, based on the dendritic branching patterns. The present electron microscopic study permits the use of criteria such as the morphology of cellular organelles and the synaptic relationships of the cell soma that can not be utilized in Golgi and light microscopic studies. On the other hand, morphological features such as dendritic branching and dendritic spines are more easily described in Golgi preparations and thus the studies are complementary. It is clear from the present study that three neuronal types are present in the PTN, although two of the three types (i.e., Type B and C) are very rare in the region of the PTN which receives pharyngeal and laryngeal primary afferents. The rarity of these two cell types may have reduced the likelihood of identifying them in Golgi preparations because of the low percentage of cells revealed by the method. Another possibility is that the ultrastructural features that permitted the identification of three neuronal types in the present study do not translate into distinct morphological characteristics at the light microscopic level. This would seem very plausible since Type B and C neurons were very similar in size and shape and could only be distinguished one from the other based on the number of axo-somatic contacts and thus may have been identified as a single neuronal type by Phelan and Falls ('89). The presence of somatic spines in the PTN of rhesus monkey (Chan-Palay, '78a) and rat (Phelan and Falls, '89) could not be confirmed in the present study. It is interesting

to note that in Cajal's ('09) illustration and text regarding the PTN in rabbit there is no reference to somatic spines which might reflect species differences or possibly technical differences in the methods used in the three studies.

A light microscopic study (see Chapter 5) of the connections of the PTN and preliminary HRP retrograde results at the electron microscopic level suggest strongly that Type A neurons project primarily to the ipsilateral nucleus of the tractus solitarius and parabrachial nucleus and that these neurons extend throughout the PTN and are in continuity with neurons located in lamina I of the spinal trigeminal nucleus pars caudalis. Retrograde labeling in the PTN following injections in the ipsilateral rostral nucleus of the tractus solitarius or parabrachial nucleus revealed that most neurons in the PTN are labeled after such injections. In addition, double-labeling from the NTS and parabrachial nucleus showed many of the same neurons in the PTN project to both sites (see Chapter 5). Fluoro-gold filled neurons in the PTN following parabrachial nucleus injections appear morphologically very similar to Type I neurons (Phelan and Falls, '89) and the bipolar neurons described by Chan-Palay ('78a). Lastly, electron microscopic analyses of retrogradely labeled neurons in the PTN revealed them to be morphologically identical to Type A described in the present study (unpublished results).

Interestingly, it has been suggested that the interstitial system of the spinal trigeminal tract including the PTN represents extensions of the superficial laminae (i.e., I and II) of the spinal trigeminal nucleus pars caudalis (Torvik, '56). The widespread invocation of this statement by others warrants some discussion in light of the present ultrastructural study of the PTN and previous ultrastructural surveys of the marginal zone or lamina I (Kerr, '70a,b) and substantia gelatinosa or lamina II (Kerr, '66, '70a,b) of the spinal trigeminal complex. Kerr ('70 a,b) reported that the marginal zone in the cat was characterized by relatively few large neurons which he considered to correspond to Waldeyer neurons or marginal neurons. These marginal neurons were characterized by a

large nucleolus, abundant cytoplasm and large dendrites that run tangential to the spinal trigeminal tract. Most interestingly, marginal neurons receive a moderate number of axo-somatic synaptic contacts from axon terminals containing agranular vesicles. The present study identified a very small number of PTN neurons which were distinguished from surrounding neurons by the presence of axo-somatic contacts. It is possible that the small number of neurons with axo-somatic contacts in the PTN corresponds to neurons which are more plentiful or characteristic of the marginal zone. Support for this suggestion stems from the fact that a retrograde fluorescence study of neurons in the PTN following injections of Fluoro-gold into the contralateral thalamus (see Chapter 5) revealed that labeled neurons in the PTN tended to be larger than neurons retrogradely labeled with the same tracer following injection in the parabrachial nucleus. Furthermore, neurons in the PTN which projected to the thalamus tended to be topographically restricted to the most caudal parts of the nucleus overlying the spinal trigeminal nucleus pars caudalis and appeared to be continuous at more caudal levels with neurons of similar morphology in the crescent shaped lamina I of the pars caudalis. It is proposed that the very small number of these neurons observed in the present study is directly related to their location at more caudal levels of the PTN which was not investigated in detail in the present study. It is our hypothesis that at least at very caudal levels of the PTN, contributions are made by lamina I to the neuronal complement present in the PTN and that, based on morphological similarities, these neurons may be functionally similar to the marginal neurons mentioned by Kerr ('70a,b). To the extent that it is known that many lamina I neurons are responsive to noxious mechanical or noxious thermal stimuli (Christensen and Perl, '70; Price et al., '76) and that some of the neurons in lamina I project to the contralateral thalamus (Burton et al., '79; Hu et al., '81; Granum, '86), it is plausible that similar neurons in the caudal PTN may be involved in pain pathways. Future neuroanatomical tracer studies in which the morphology of retrogradely labeled neurons in the PTN and lamina I are correlated may

help to determine whether or not lamina I type neurons contribute to the neuronal composition of the PTN. It is important to note that although Kerr ('70a,b) identified the large marginal neuron as the characteristic neuron of lamina I he did make reference to a second neuronal type and referred to them as the gelatinosa neurons. No further discussion of these neurons was forthcoming and it is unclear how these might morphologically relate to the three types of neurons identified in the PTN.

The substantia gelatinosa or lamina II of the spinal trigeminal nucleus pars caudalis is considered to be similar to the substantia gelatinosa of the spinal cord, being essentially a rostral extension of the latter (Torvik , '56; Kerr, '66, '70a; Rustioni et al., '71; Gobel, '78a, b). Lamina II has also been implicated in contributing to the neuronal and neuropil composition of the PTN (Torvik, '56). With regard to the ultrastructure of the substantia gelatinosa, Kerr ('66, '70a) provided a description of the neurons which were characterized by having a large nucleus and only scant cytoplasm in a typically elongated soma. In addition, the nuclear envelope contained several invaginations, a scant complement of rough endoplasmic reticulum which was not organized into Nissl substance, and an absence of axo-somatic contacts. All of these characteristics are consistent with those found for the Type A neurons in the PTN. However, Phelan and Falls ('89) presented evidence based on Golgi and Nissl-stained material that neurons of the PTN were distinctly larger than those found in the substantia gelatinosa and that the dendritic arborizations also differ. Another point that argues strongly against Type A neurons in the PTN being similar to neurons in the substantia gelatinosa is the apparent difference between efferent connections for the two regions. Type A neurons are like the vast majority of neurons in the PTN, projection neurons (see Chapter 5 and Phelan and Falls, '89) and those of the substantia gelatinosa are considered to be local circuit or interneurons (Gobel, '76; Gobel and Hockfield, '77; Gobel, '78b) which have connections within the substantia gelatinosa and with neurons in the marginal zone (Gobel, '78b). The most compelling evidence for

the PTN not being a rostral extension of the substantia gelatinosa stems from connectivity studies of the PTN. The PTN has been shown to have considerable efferent projections (see Chapter 5) to the contralateral PTN and lamina I of the spinal trigeminal nucleus pars caudalis, nucleus of the tractus solitarius, parabrachial nucleus (Cechetto et al., '85; Menétrey and Basbaum, '87; Menétrey et al., '87) and the thalamus (see Chapter 5; Granum, '86). The substantia gelatinosa on the other hand is principally made up of interneurons which interconnect different laminae, and which are believed to be involved in the modulation of the activity of projection neurons (Gobel, '78b). It is interesting to note that the marginal zone or lamina I of the spinal trigeminal nucleus pars caudalis does, however, share many of the same efferent connections as the PTN. For instance the marginal zone has efferent projections to the nucleus of the tractus solitarius (Menétrey and Basbaum, '87), the parabrachial nucleus (Cechetto et al., '85; Menétrey et al., '87) and the thalamus (Burton et al., '79; Burton and Craig, '79; Craig and Burton, '81). This lends further support to the notion that lamina I might be homologous to the PTN. Clearly, the use of morphological characteristics as criteria for establishing the homology of a structure(s), in this instance lamina I and II of the spinal trigeminal nucleus pars caudalis is instructive. However, a more extensive and valid basis for establishing the similarities between two areas would include not only morphology but also data on the connectivity, and the physiology and neurochemistry of the region.

Although the neuropil of the PTN shares some morphological features with that of the marginal zone and the substantia gelatinosa of the spinal trigeminal nucleus pars caudalis there are also features which distinguish the PTN from these regions.

The PTN contains many pale-staining profiles of various sizes corresponding morphologically to dendrites. The only Golgi study of the PTN in the rat was carried out by Phelan and Falls ('89). Their findings suggest that proximal dendrites contain small numbers of dendritic spines and more distal dendritic segments contain slightly greater

numbers of spines. Dendritic spines have also been reported in the PTN of the monkey (Chan-Palay, '78a). In the present electron microscopic survey of the neuropil of the PTN dendritic spines could not be identified. Possible explanations for this might be related to the paucity of such structures and their distal location on small dendritic profiles. Gobel ('74) described the morphology of dendritic spines in the substantia gelatinosa of the cat spinal trigeminal nucleus pars caudalis. In his description, dendritic spines are pale, less than 1μm in diameter, devoid of microtubules, usually contain a fibrillar matrix and occasionally profiles of smooth endoplasmic reticulum, mitochondria and multivesicular bodies. In the present study these features were present in many of the small dendritic profiles of the PTN and so do not represent unique features which could be used to identify spines. Ribosomes, a standard feature for defining dendrites (Peters et al., '91), were often absent even from considerable lengths of small diameter dendrites. The presence of similar morphological features in many small diameter profiles presumably dendritic in origin, and the small numbers of spines reported in Golgi studies (Phelan and Falls, '89) may have contributed to our difficulty in the definitive identification of dendritic spines in the PTN. On the other hand, it is suprising that no examples of spines attached to dendritic shafts were encountered. The marginal zone in the cat has also been reported to contain dendritic profiles with small numbers of dendritic spines (Kerr, '70a,b). Gobel ('74) found marginal neurons in the cat which had variations in dendritic spine distribution depending on the laminar distribution of the dendrite. Those dendrites which did not extend beyond the marginal zone were relatively aspinous while dendrites extending from the marginal zone into the substantia gelatinosa contained many spines. The small numbers of dendritic spines in the marginal zone is consistent with the morphological similarities between this region and the PTN, even in light of species differences. Although there is no evidence of neurons in the PTN with dendrites extending into the subjacent layers (Phelan and Falls, '89) of the spinal trigeminal complex, a retrograde fluorescence study (see

Chapter 5) indicates that some neurons in the caudal PTN which project to the contralateral ventral basal complex do have a dendritic polarity that is directed toward the subjacent laminae. Interestingly, Gobel ('78b) described "stalked cells" which were located at the border of lamina I and II in the cat which are similar in dendritic morphology to some of the neurons in the caudal PTN projecting to the thalamus. However, stalked cells are considered local circuit neurons which synapse in lamina I (Gobel, '78a, b) while those described in the caudal PTN are clearly projection neurons.

One further point about dendritic morphology in the PTN and substantia gelatinosa relates to dendritic profiles containing synaptic vesicles. In the present study a number of profiles were found to contain pleomorphic clear vesicles and occasionally segments of smooth endoplasmic reticulum. These profiles were typically pale in appearance and the vesicles tended to be clustered rather than dispersed throughout the profile. Dendrites containing vesicles have been described elsewhere in the CNS including the thalamus (Morest, '71; Famiglietti, '70; Harding, '71), the substantia gelatinosa of the thoracic spinal cord (Zhu et al., '81) and the substantia gelatinosa of the spinal trigeminal nucleus (Gobel, '76). These vesicle-containing profiles often lacked distinguishing characteristics which would easily classify them as dendritic or axonal (see Famiglietti, '70 for review). However, one feature typical of vesicle-containing dendrites is the tight aggregation of vesicles in the cytoplasm which is in contrast to axon terminals which tend to have scattered and a more even distribution of synaptic vesicles within a given profile. In the present study, presumed dendrites containing vesicles were all of small diameter and lacking ribosomes, the most distinctive feature of dendrites which is in contrast to examples in the thalamus where proximal dendrites could be identified as containing synaptic vesicles. Based on the aggregation of vesicles and their similarity to vesicle-containing dendrites elsewhere in the CNS, it is probable that some of the profiles containing tight aggregations of pleomorphic synaptic vesicles in the PTN are in fact dendritic. It is also possible that

some of the small profiles containing vesicles in the PTN are dendritic spines. Dendritic spines containing vesicles have been identified in the substantia gelatinosa of the spinal trigeminal complex in glomerular synaptic arrangements characteristic of the region (Gobel, '74).

A number of different synaptic arrangements were encountered in the PTN including axo-somatic, axo-axonic, axo-dendritic as well as more complex three component triplet synapses. The only other electron microscopic study of the synaptic organization of the PTN was provided by Chan-Palay ('78a, b) in monkey. The following discussion of the synaptology of the PTN in the rat will be compared and contrasted with that of the synaptology described for the PTN in monkey.

In the present study axo-somatic synaptic contacts were present on Type A and Type C neurons in the PTN, although the synaptic contacts on Type A somata were rare. RA and PS axo-somatic synapses were found on Type A and C neuronal somata although axo-somatic terminals containing pleomorphic agranular vesicles were more numerous than axo-somatic contacts containing round agranular vesicles. Axo-somatic synaptic contacts were reported in the PTN of the monkey (Chan-Palay, '78a) and, as in the rat, both RA and PS synaptic types formed synapses with somata. In a subsequent study Chan-Palay ('78b) was able to identify terminals containing biogenic amines at the electron microscopic level in the PTN and correlate their presence with morphological features of the terminals in the nucleus. Indoleamine (i.e., serotonin) immunoreactive terminals were found to be of a number of different morphologies although those which formed axo-somatic contacts contained small round agranular vesicles and occasionally small numbers of dense-cored vesicles and formed symmetric contacts. In the present study Type A and C neuronal somata received axo-somatic inputs from terminals containing agranular round vesicles some of which contained small numbers of dense-cored vesicles. Chan-Palay ('78b) noted that the patterns of indoleamine , catecholamine and substance P immunoreactivity were

similar in both rat and monkey. Based on this similarity it might be suggested that the two species may also have the same distribution of these transmitters at the ultrastructural level. In keeping with this suggestion, two interesting possibilities relating to axo-somatic synapses can be proposed. The first is that at least some of the axo-somatic contacts in the rat PTN containing predominantly round agranular vesicles probably contain the neurotransmitter serotonin. The second relates to the putative neurotransmitter substance P, which Chan-Palay ('78b) found to be in 20-30% of neurons and in many processes of the PTN in the rat at the light microscopic level. Substance P- containing axons of intrinsic and extrinsic origin might also participate in axo-somatic or axo-dendritic synaptic contacts. However, the synaptic organization of substance P fibers in the PTN has not been investigated to date. In addition to the presence of substance P in the PTN (Chan-Palay, '78b; Del Fiacco and Cuello, '80; Jansco and Kiraly, '80; Shults et al., '84), there is autoradiographical evidence of a high density of neuropeptide Y binding sites in the PTN (Härfstrand et al., '86) which suggests that NPY might also be contained in terminals in the PTN. The presence of a number of these potential neurotransmitters including somatostatin, substance P (Chan-Palay, '78b; Fallon and Leslie, '86; Finley et al., '81), and enkephalin (Del Fiacco and Cuello, '80; Matthews et al., '89) within PTN neurons leads to the possibility of at least some of the fibers in the PTN of the same immunoreactivity being of intrinsic origin. The distribution of serotonin and enkephalin immunoreactivity has been shown to overlap in the PTN in the cat (Matthews et al.,'89). However, it is not clear where the origin for each of these neurotransmitters resides. In future experiments utilizing immunocytochemistry and electron microscopy it would be useful to look at the synaptic relationships of particular neurotransmitters.

Axo-dendritic synaptic contacts were the most frequently encountered synaptic arrangement in the neuropil of the PTN. This is consistent with observations in the monkey (Chan-Palay, '78a). In contrast to the results reported in the present study there

were, in addition to axo-dendritic synapses, considerable numbers of axo-spinous contacts in the monkey. Based on the Golgi studies of Phelan and Falls ('89), it is clear that small numbers of dendritic spines do occur in the rat PTN, although probably to a lesser degree than in the monkey. Consistent with results reported for the monkey, postsynaptic dendritic profiles were identified as containing small numbers of dense-cored vesicles. Most of the terminals involved in the axo-dendritic or axo-spinous synaptic contacts in the PTN of the rat and monkey were RA in morphology. In both species RA synapses contained small numbers of dense-cored vesicles. Chan-Palay ('78b) in her description of the distribution of indoleamine- and catecholamine-containing terminals stated that the dense indoleamine plexuses observed in the light microscope were involved in substantial numbers of synaptic contacts on perikarya, dendrites and dendritic spines and that these terminals were morphologically heterogeneous, some containing round clear vesicles and others with elliptical and flattened vesicles. The morphological diversity of indoleamine terminals has implications with regard to the axo-dendritic morphology observed in the rat PTN. Since indoleamine immunoreactivity can be localized both to terminals which correspond morphologically to RA and PS synaptic terminals and that this immunoreactivity appears at least at the light microscopic level (Chan-Palay, '78b) to be very similar in rat and monkey, it is possible that some of the RA and PS synaptic terminals described in the present study contain serotonin. Catecholaminergic fibers and terminals also showed similar patterns of distribution in rat and monkey (Chan-Palay, '78b). Although less common, catecholaminergic axons in the monkey contain pleomorphic vesicles and form synaptic contacts with distal dendrites. PS synaptic terminals in the PTN were not only less common than RA synaptic terminals in the rat but they were also found on proximal and distal dendrites. Presumably some of the PS synaptic terminals identified in the present study are catecholaminergic although it should be pointed out that synaptic contacts were always symmetric when pleomorphic vesicles were contained in the bouton

while both symmetric and asymmetric contacts were found for PS synaptic terminals synapsing on dendrites in the monkey.

Another type of axo-dendritic arrangement was identified in the PTN of the rat, in which an RA terminal made a contact with a dendritic profile which contained a tight aggregation of pleomorphic vesicles. Such a synaptic arrangement does not appear to occur in the monkey. However, Chan-Palay ('78a, b) shows photographic evidence of postsynaptic dendrites which contain small numbers of what appear to be round agranular vesicles and dense-cored vesicles. The tight aggregations of pleomorphic vesicles characteristic of postsynaptic dendrites in the present study are also found in dendrites of the substantia gelatinosa of the spinal trigeminal complex (Gobel, '74). In the present study postsynaptic dendrites containing vesicles were not seen to form a typical electron-dense synaptic contact with a third element. In one instance (Fig. 10A), the postsynaptic dendrite, by virtue of its clustering of vesicles near the membrane opposite the presynaptic terminal appears to be forming a reciprocal synaptic contact with the presynaptic terminal containing agranular round vesicles. Such reciprocal synapses should only be confirmed by serial sections, however, the extremely rare occurrence of these synaptic arrangements in the PTN made at this time their confirmation impractical. Presynaptic dendrites and reciprocal synapses have been described in the glomeruli of the substantia gelatinosa of the spinal trigeminal complex (Gobel, '74, '76), spinal cord (Zhu et al., '81), lateral geniculate nucleus (Famiglietti, '70; Lieberman and Webster, '74), and in the medial geniculate nucleus of the thalamus (Morest, '71). One interpretation of the feature in which an axon terminal containing agranular round vesicles synapses on a dendrite containing agranular pleomorphic vesicle might be that of a presynaptic excitatory input (i.e., if we assume that the presynaptic terminal represents an excitatory synapse based on morphology) (see Chapter 2) on the postsynaptic dendrite which will then release its vesicle contents either through classic chemical synaptic arrangements (not identified here) or via non-synaptic

means to affect other neuronal elements. However, without knowledge of the transmitters contained in the two synaptic elements and the function(s) of these transmitters it remains speculative as to the function of these arrangements. Dendro-axonic synapses have been described in glomeruli of the substantia gelatinosa of the spinal trigeminal nucleus (Gobel, '76) and these are primarily reciprocal in nature. With regard to the possibility of reciprocal synapses occurring in the PTN, we have identified situations which are very suggestive of such arrangements and feel that reciprocal synapses are likely to be present in the PTN. It seems reasonable to dismiss the possibility that both elements in the present synaptic arrangement are dendritic, since there is no evidence from our results that terminals containing uniform round agranular vesicles and forming asymmetric contacts are dendritic.

In the present study, axo-axonic synaptic contacts morphologically similar to those reported by Chan-Palay ('78a) were identified. Axo-axonic synapses consisted of an axon terminal which contained round agranular vesicles synapsing on a second terminal which contained vesicles that were of the same morphology (i.e., RA terminal contacting another RA terminal). In the rat, axo-axonic contacts were relatively rare. However, in most instances axo-axonic contacts were part of a more complex synaptic arrangement designated as a triplet synapse after the triplet synapses described by Jones and Powell ('69) and Lieberman and Webster ('74). The triplet synapse is a three component serial synapse in which a profile containing vesicles synapses on a second vesicle-containing profile which in turn makes a synaptic contact with a dendritic profile lacking vesicles. The term triad has also been used to describe a similar arrangement (Famiglietti and Peters, '72). However, the term triad should probably be reserved for arrangements associated with retinal ultrastructural studies where one of the components of the triad is always an axon terminal originating from a bipolar cell of the retina (for review see Lieberman and Webster, '74). The schematic summary of synaptic relationships found in Chan-Palay's ('78a) paper indicates that triplet arrangements similar to those illustrated in the present

study involving two components containing round clear vesicles are present in the monkey, although her description indicates that one of the two axon terminals typically contains numerous dense-cored vesicles as well as round clear vesicles. In the present study variable numbers of dense-cored vesicles in both RA and PC synaptic terminals were often found and serial sections through terminal profiles that lacked vesicles at one level through the terminal contained dense-cored vesicles elsewhere in the terminal.

One final point relates to the synaptic arrangements found in the PTN in comparison to that of the marginal zone (i.e., lamina I) and substantia gelatinosa (i.e., lamina II). In Kerr's ('66, '70a,b) description of lamina I of the cat, dendrites were predominantly contacted by terminals containing round clear vesicles which often contained dense-cored vesicles. Furthermore, his description includes axo-axonic contacts in which both terminals contain round agranular vesicles similar to those identified in the present study. A feature of the marginal zone that does not appear in the rat PTN is the apparent clustering of great numbers of axon terminals (Kerr, '66, '70a, b). There is also no indication that axon terminals make contact with dendrites containing vesicles in the marginal zone, suggesting a difference in the synaptology in the PTN and marginal zone . With regard to the substantia gelatinosa of the spinal trigeminal complex, there is at least one striking difference between the synaptology of that region and the PTN. The substantia gelatinosa has been described as containing a characteristic type of glomerulus which is unique to that layer (Kerr, '66, '70a,b; Gobel, '74,'76). These glomeruli are morphologically distinct structures which consist of an outer ring of small dendritic processes, some of which may contain pleomorphic vesicles, and a centrally located large axon terminal which makes synaptic contacts with the dendritic elements (Gobel, '74). In the present study no such glomerular structures were encountered in the survey of the rat PTN.

Vesicle-containing profiles, usually containing relatively large populations of dense-cored vesicles, were frequently encountered in the PTN. A peculiar feature of most of

these terminals was the absence of a classical synaptic contact, even in serial sections through the bouton. In those few instances where a clear synaptic contact was identified, the contact was clearly asymmetric and the postsynaptic element often contained small numbers of agranular and dense-cored vesicles. Because of the difficulty in determining conclusively whether small diameter structures are dendritic or axonal and the potential for dendrites to contain agranular and dense-cored vesicles, it was not possible to establish for certain if these were dendritic or axonal elements and for this reason were labeled as vesicle-containing profiles. The presence of non-synaptic boutons containing numerous dense-cored vesicles is consistent with results reported by Chan-Palay ('78b) in the monkey where both catecholamine and indoleamine immunoreactive axon terminals were found that did not form recognizable synaptic contacts. A difference between rat and monkey appears to be that the latter has a heterogeneous populations of non-synaptic boutons. In the rat non-synaptic terminals were all of similar morphology while in the monkey PTN, no less than ten types of synaptic and non-synaptic axon terminals of different morphologies were described as containing either indoleamines or catecholamines (Chan-Palay, '78b). Because of the likelihood that dendrites in the PTN contain vesicles, not all of the boutons identified by Chan-Palay are likely to be axons. In light of the fact that pleomorphic agranular vesicles in the monkey are associated with indoleamines and no indoleamine immunoreactive cells are found in the PTN (Chan-Palay, '78b), a question arises as to the origins of dendrites containing pleomorphic vesicles. There are two possibilities, the first being that these dendrites contain immunoreactivity for some other neurotransmitter as yet unidentified or these dendrites are serotonergic but originate from some extrinsic source to the PTN. Although only one type of non-synaptic bouton was characterized in the rat this morphology does compare favorably with the morphology of one of three serotonergic non-synaptic bouton types and one of two catecholaminergic non-synaptic bouton types in the monkey. It may be that, although there is greater diversity of

morphology with regard to non-synaptic boutons in the monkey, there are parallel structures in the rat that could represent indoleamine and catecholinergic terminals in this species. Those synaptic terminals containing dense-cored vesicles and forming asymmetric synapses may correspond to similar serotonergic boutons in the monkey (Chan-Palay, '78b) which form symmetric synaptic contacts with dendrites. Chan-Palay ('78b) hints in her summary of synapses that such boutons might form axo-axonic contacts but does not suggest the possibility of axo-dendritic synapses where the dendrite contains vesicles even though postsynaptic dendrites in the monkey (Chan-Palay, '78a) were reported to contain small numbers of dense-cored vesicles. In summary, it appears that there is less diversity with regard to synaptic types in the PTN of the rat compared to that of the monkey.

The peripheral afferent input to the PTN is diverse and originates from visceral and somatic sites. There is evidence that the PTN receives significant input which is conveyed in the glossopharyngeal and the vagus nerves (Torvik, '56; Panneton and Loewy, '80; Contreras et al., '82; Kalia and Sullivan, '82; Nomura and Mizuno, '82; Arvidsson and Thomander, '84; Sweazy and Bradley, '86; Housley et al., '87; Altschuler et al., '89). Of particular interest in the present study is the sensory innervation of the pharynx and larynx which is conveyed by the glossopharyngeal and vagus nerves, respectively.

The morphology of pharyngeal and laryngeal afferent terminals was identical and corresponded to RA synaptic terminals described in the ultrastructural survey of the PTN. Primary visceral afferents terminated on small diameter dendrites, presumably distal dendrites of PTN neurons. The morphology of primary afferents is consistent with the generally accepted concept that primary afferents are excitatory in function (Uchizono, '65). The function of primary afferents terminating in the PTN has not yet been established. However, based on responses of neurons in and around the PTN it is likely that information conveyed to the PTN is nociceptive, possibly thermal and/or mechanical (Price et al., '76; Salt et al., '83; Sessle et al., '86; Hayashi and Tabata, '89). Further

evidence of its potential role in thermal activity was suggested by Kilduff et al.,('82, '83, '84, '88, '90) based on the finding that the PTN has the highest ordinal ranking relative to other brain regions with regard to metabolic activity during early and deep hibernation in the ground squirrel.

Primary visceral afferents terminate on small diameter dendrites. Type C neurons which have many axo-somatic contacts therefore do not receive primary afferents of glossopharyngeal or vagal origin directly on their somata but may receive inputs on distal dendrites. The distal location of pharyngeal and laryngeal terminals provides no information as to whether or not a particular type of PTN neuron or all three types (i.e., A, B, and C) receive peripheral inputs. On the other hand, the vastly larger population of Type A neurons in the PTN where pharyngeal and laryngeal afferents terminate make them a primary candidate for being postsynaptic to primary afferents. Type B and C neurons might also receive pharyngeal and laryngeal inputs, but, because of their smaller numbers relative to Type A neurons are not likely to be the primary target. Having suggested Type A neurons are the primary target for these afferents, an interesting possibility is raised in light of the results of a recent retrograde electron microscopic study carried out in our lab. These results indicate that a large number of Type A neurons project to the parabrachial nucleus, an area intimately related to autonomic functions. This being the case, primary visceral afferent information relayed through the PTN to the parabrachial nucleus could provide the substrate for autonomic reflex changes in responses to nociceptive stimuli. Because of the considerable overlap of upper respiratory (Altschuler et al., '89; Panneton, '91) and alimentary tract (Altschuler et al., '89) inputs with terminal fields of somatic origin (Abrahams et al., '84; Arvidsson and Thomander, '84; Nishomori et al., '86; Pfaller and Arvidsson, '88; Shigenaga et al., '86, '88; Neuhuber and Zenker, '89; Arvidsson and Pfaller, '90) it is likely that individual PTN neurons might receive input from both visceral and somatic structures. Although the afferent modalities conveyed from visceral and

somatic structures are uncertain, the possibility of convergence of both types of information (visceral and somatic) onto the same neuron in the PTN might provide the anatomical substrate for mediating somatovisceral or viscerovisceral reflexes through PTN connections with the NTS (Menétrey and Basbaum, '87; Menétrey et al., '87) and parabrachial nucleus (Panneton and Burton, '85; Cechetto et al., '85). It might be possible in future experiments to retrogradely fill or immunocytochemically identify PTN neurons projecting to the parabrachial nucleus and identify primary pharyngeal and laryngeal afferent terminals synapsing on labeled PTN dendrites.

In two instances a labeled primary afferent terminal was identified synapsing on a profile deemed to be dendritic and containing pleomorphic agranular vesicles. This was obviously a rare occurrence even though unlabeled arrangements were found within the PTN. The paucity of labeled primary afferent terminals synapsing on dendrites containing vesicles may reflect the low frequency of such arrangements. The excitatory primary afferent input to the dendrite presumably would result in the release of vesicle contents from the postsynaptic dendrite at a synaptic junction on a third element or possibly, as Figure 10A would suggest, in reciprocal fashion back on the primary afferent terminal or both. The function of such arrangements is not clear. Because of the lack of information regarding the origin and chemospecificity of dendrites it is not possible to precisely identify the effect of reciprocal synapses as they pertain to the function of the PTN. However, since these arrangements appear to be associated with primary afferent terminals they might play some role in regulation of transmitter release and modulation of response.

Interestingly, primary afferent projections from the pharynx and larynx also terminate in the subnucleus interstitialis of the nucleus of the tractus solitarius (Altschuler et al., '89). Electron microscopic analysis (Chapter 3) of these afferent terminals reveals them to be morphologically identical to those found in the PTN (i.e., they contain agranular round vesicles and form asymmetric synaptic contacts with small diameter dendrites). The

question can be raised as to whether these projections arise from two separate populations of sensory neurons or whether they are collateralized projections. Study of the collateralization of primary afferent neurons as it pertains to this question is particularly difficult in light of the small size of the terminal sites and the close proximity of both and therefore the potential for labeling fibers of passage.

With respect to the issue as to whether the PTN represents a rostral extension of the marginal zone and substantia gelatinosa (Torvik, '56) a number of points can be made based on comparisons between the present study of primary afferents and those of primary afferents terminating in the subjacent spinal trigeminal complex. Anatomical analysis of the synaptic circuitry of the marginal zone (Kerr, '70a,b; Gobel and Hockfield, '77) and substantia gelatinosa (Gobel, '74; Gobel and Hockfield, '77) revealed differences between these areas and the PTN. The most striking difference between the synaptic circuitry in the PTN and that of the marginal zone and substantia gelatinosa is the absence of glomerular synaptic arrangements in the PTN, in which the central axon is of primary afferent origin (Gobel, '74). In the substantia gelatinosa the central axons are conspicuously large (2-9 μm diameter) and the glomeruli that they center are very common (Gobel, '74; Gobel and Hockfield, '77). Although less frequent, glomeruli are also present in the marginal zone as noted by Kerr ('70a,b). It was not until several years later that the central axons of glomeruli in the marginal zone were established as primary afferent in origin (Gobel and Hockfield, '77). The absence of such distinct synaptic arrangements in the PTN suggests that its synaptic organization is significantly different from that of the either the marginal zone or substantia gelatinosa of the spinal trigeminal complex.

The present study of the PTN in the rat has provided an ultrastructural analysis of the nucleus and identified many similarities with the same region in the monkey (Chan-Palay '78a, b). It has presented considerable morphological evidence that suggests that the PTN is a structure distinct from either the marginal zone or substantia gelatinosa of the spinal

trigeminal complex. The caudal PTN, which was not investigated extensively in this study, may contain features more closely resembling those of the marginal zone (Matthews et al., '89). Results of fluorescent retrograde studies (Chapter 5) suggest that the caudal PTN contains neurons projecting to the contralateral thalamus that are similar morphologically to those found in the marginal zone and also projecting to the thalamus. Further study of neurons in the caudal PTN at the electron microscopic level in combination with compatible retrograde neuroanatomical techniques should provide useful information about the caudal PTN and how it relates to the marginal zone.

Technical Considerations

In the preceding results section a number of technical issues have been touched on related to controls for injection site, survival times, transsynaptic transport of tracer and the identification of small diameter postsynaptic structures.

Although care was taken to prevent the spread and or leakage of tracers into surrounding structures, the close anatomical proximity and continuity between the pharynx and larynx and the pharynx and esophagus make total exclusion of this possibility difficult. However, the patterns of labeling resulting from injection of each of these structures is characteristically different particularly with regard to the distribution of efferent projections (see Bieger and Hopkins, '87) so that the degree of spread, if any, could be evaluated. Spread of tracer to the esophagus did occur following pharyngeal injection as evidenced by the patterns of afferent and efferent labeling in the brainstem but this was not a concern because afferent labeling from the esophagus is restricted in the subnucleus centralis of NTS (Altschuler et al., '89, see Chapter 2). There was the possibly of some tracer spread to the trachea from the larynx. Since the trachea apparently also projects lightly to the same regions of the brainstem as the pharynx and larynx (Altschuler et al., '89; Kalia and Mesulam, '80b), it is possible that the trachea did contribute in a minor way to labeling in

the PTN. However, since the results indicate that all labeled primary afferents in the PTN are of similar morphology it is likely that the ultrastructure of any primary afferents of tracheal origin were the same as those from the pharynx and larynx.

There was a possibility that transsynaptic transport of WGA-HRP evident in one animal following a postoperative survival time of 5 days. The transport of WGA and WGA-HRP transsynaptically is well documented but typically requires extended survival times in most systems, i.e., 72 hours or more (Trojanowski, '83; Trojanowski and Schmidt, '84; Fabin and Coulter, '85). Two to three days resulted in excellent transport of tracers in the anterograde direction with no evidence of transsynaptic transport. In the one case where possible transsynaptic transport occurred (Fig. 15) it was evident that such labeling would be troublesome in the present system particularly in light of the presence of postynaptic dendrites containing vesicles. For this reason the animal with a postoperative survival time of five days was not considered further for the study of primary afferents.

Certain postsynaptic elements were simply designated as profiles (P) as a consequence of the difficulty in determining the true nature of these structures. In many instances these postsynaptic structures were identified as dendritic as a result of finding ribosomes following serial section. However, the small size (often <1 μm in diameter) (Figs. 6, 7, 13, 14) and the lack of Nissl substance or ribosomes, and presence of small irregular agranular membranous sacs in some profiles suggest that some of these structures might represent dendritic spines. Ribosomes, which are known to penetrate into even the farthest regions of the dendritic tree, do so in an ever decreasing manner as the distance from the cell body increases and are rare in narrow terminal dendrites or dendritic spines (Peters et al., '91). This makes the distinction between small dendrites and dendritic spines difficult. The presence of small amounts of agranular endoplasmic reticulum in and of itself is not enough to establish the identity since both small distal dendrites and dendritic spines can contain such cytoplasmic organelles. It should be noted that, in Golgi preparations, Chan-

Palay ('78a) and Phelan and Falls ('89) did describe dendritic spines in the PTN in the monkey and rat, respectively. Postsynaptic elements containing clusters of pleomorphic vesicles were also difficult to identify with certainty as being dendritic or axonal in nature since neither ribosomes nor other distinct morphological features were present in these small profiles. In two instances, serial sections were cut although this did not resolve the question. Based on the above considerations, it was decided that in ambiguous instances rather than making an arbitrary classification of the postsynaptic elements in the present study, that it would be more appropriate to identify them as postsynaptic profiles. Further investigations, with respect to the neurochemistry of the neuropil and the other afferent inputs to the PTN at the EM level, might shed more light on the exact nature of these profiles.

CHAPTER 5

EFFERENT AND COLLATERAL ORGANIZATION OF NEURONS IN THE PARATRIGEMINAL NUCLEUS : AN ANTEROGRADE AND RETROGRADE FLUORESCENT NEUROANATOMICAL TRACER STUDY IN THE RAT.

INTRODUCTION

Although a considerable body of literature exists regarding the primary afferent inputs to the PTN, there is only sparse literature describing the efferent connections of the PTN. Much of what is known about the central connections of the PTN is derived from retrograde neuroanatomical tracer studies exploring the central connections of the NTS, (Menétrey et al., '87; Menétrey and Basbaum, '87) parabrachial nucleus (Cechetto et al., '85; Panneton and Burton, '85; Herbert et al., '90) and thalamus (Burton et al., '79; Burton and Craig, '79; Panneton and Burton, '85; Granum, '86). Although these studies have revealed the general patterns of efferent connections for the PTN, they lack specificity and do not adequately address the possibility of collateral projections to different levels of the neuraxis.

In the present study the specifics of efferent projections from the PTN and the collateralizations of these projections were investigated. A new neuroanatomical anterograde tracer, tetramethylrhodamine (TMR) was used to study the distribution of PTN efferent projections in the brainstem and thalamus. The collateralization of the PTN was addressed through the use of different fluorescent retrograde tracers in a double-labeling study.

MATERIALS AND METHODS

The subjects were 59 male Wistar rats weighing 250-350-grams. Prior to surgery each rat was anaesthetized with sodium pentobarbital (Somnitol), (40-60 mg/kg, i.p.).

Anterograde Tracing Experiments

Subjects and surgery. Eighteen rats received stereotaxic injections (0.03-0.1 μl) of 2-5% tetramethylrhodamine (TMR) (D-1817, Molecular Probes, OR.) in distilled water into the paratrigeminal nucleus. TMR was selected over more conventional anterogradely transported neuroanatomical tracers such as WGA-HRP or PHA-L because of its ease of application, small injection sites, and high resolution anterograde labeling (see technical considerations and Nance and Burns, '90).

Rats were placed in a Kopf stereotaxic apparatus and the neck was flexed to facilitate opening the space between the occipital bone and the atlas for exposure of the dorsal medulla. The skin and muscle of the neck were incised along the midline from the nuchal crest down to the upper cervical vertebrae. The dorsal musculature of the neck was bluntly dissected to expose the occipital bone and the atlanto-occipital membrane. With the visual aid of a Zeiss surgical microscope the occipital bone over the posterior cerebellum and the atlanto-occipital membrane were removed using fine bone rongeurs. Once the dorsal medulla was visualized, the outer meningeal coverings were lifted with a pair of fine forceps and reflected with the aid of a sharp hypodermic needle. This permitted access to the dorsal and dorsolateral surface of the caudal medulla oblongata.

The tracer was pressure injected using a 0.5 or 1.0 μl Hamilton syringe mounted in a modified Kopf stereotaxic holder and fitted with a glass micropipette (tip diameter 25-65 μm) filled with light mineral oil. Before lowering the tracer-laden glass micropipette to the surface of the brainstem, the posterior part of the cerebellum overlying the medulla was

gently pushed anteriorly with a sterile Q-tip to prevent it from interfering with the vertical path of the pipette. The pipette was lowered under visual guidance initially and with the help of a surgical microscope once the pipette was near the surface of the brainstem. After penetration to the desired coordinates (Paxinos and Watson, '86) the pipette was left in place for 5 minutes to allow the brain tissue to settle around the pipette tip. The desired amount of tracer was administered in 2 to 4 aliquots with 5 minute intervals between each. After the tracer was expelled, the pipette was left in place for a further 5 minutes and then removed. The dorsal muscles of the neck were reapposed and sutured along the midline and to the posterior border of the temporalis muscle. The skin was closed with surgical staples and the wound sprayed with an antibacterial (Anaspray).

Animals were allowed to survive for 5 to 7 days before they were perfused transcardially with 500 ml of prerinse (0.15 M phosphate buffer, pH 7.3-7.4) containing 0.1% sodium nitrite, followed by 1000 ml of fixative (4% paraformaldehyde) in the same buffer. The fixed brains were left in situ for 1-2 hours after which the entire brain and upper cervical spinal cord were removed and placed in 30% sucrose in phosphate buffer (pH 7.4) overnight. Subsequently, 40-μm-thick frozen sections were cut in the transverse plane, collected in dilute (0.01 M) phosphate buffer and mounted on microscope slides within 24 hours. Sections were rinsed in dilute phosphate buffer (0.01M), floated onto chrome alum-coated slides and allowed to dry at room temperature for 12 hours. Slides were treated in one of two ways prior to coverslipping. They were either dehydrated briefly in a graded series of alcohols and then cleared in xylene or dipped in 100% xylene for 15 to 20 seconds. All sections were coverslipped with Fluoromount mountant (Gurr) and studied with an Olympus fluorescence microscope.

Retrograde Tracing Experiments

Subjects. In eleven rats stereotaxic injections of 0.02-0.06 μl of Fluoro-gold (FG) (Fluorochrome INC, CO.) were made into either the parabrachial nucleus (n=3) or ventral basal complex (n=3) using a Kopf stereotaxic apparatus. Stereotaxic injections of fluorescent latex beads were made into the rostral NTS of 5 rats. Subsequent processing of tissue for fluorescence microscopy was the same as that outlined in the anterograde methods section.

Retrograde Double-labeling Experiments

Subjects and Tracers. Thirty rats received stereotaxic injections of combinations of two different retrograde tracers.

Because of the diversity of PTN efferent sites identified by anterograde tracing and the small size of the PTN relative to other sensory nuclei in the immediate area, the question arose as to whether or not the PTN contained neurons that projected to more than one of these sites. Three combinations of sites were studied: 1) ventral basal complex and nucleus of the tractus solitarius, (n=7), 2) parabrachial nucleus and nucleus of the tractus solitarius, (n=15), 3) ventral basal complex and parabrachial nucleus (n=8). Several combinations of retrograde tracers were tested to determine optimum combinations of neuroanatomical tracers. The combinations of tracers tested were as follows : 1) Diamidino yellow (DY) (Sigma) (2% in dH_2O) and True Blue (TB) (Sigma) (2% in dH_2O), 2) Fluoro-Gold (04 % in dH_2O) and red latex beads (Luma Fluor Inc., NY.) (undiluted), 3) Fluoro-Gold (04 % in dH_2O) and DiI (Molecular Probes, OR.) (5% in 100% ethanol or a suspension in dH_2O, DiIs). The advantages and disadvantages of each tracer combination within the context of the present experiments will be discussed in the results and discussion section. The objective was to obtain combinations of tracers which permitted

superior double-labeling which could be photographed to provide documentary evidence of clear double-labeling in the PTN.

DY and TB were made up as 2% weight per volume solutions, although these tracers do not dissolve completely in dH_2O and therefore a suspension was obtained. DiI was also made up into a fine particulate suspension in dH_2O. First, the DiI was dissolved in 100% ethanol to the desired 5% per 20 μl volume. Once dissolved, the liquid was transferred to an Eppendorf microcentrifuge tube, and a small volume (0.5-1.0 μl) of dH_2O was added to the solution. Addition of the dH_2O immediately resulted in the precipitation of DiI in a fine particulate form. A brief (5-10 min.) spin in a clinical centrifuge at medium to high speed collected the DiI particles in the bottom of the microcentrifuge tube. The clear supernatant of alcohol was then drawn off without disturbing the DiI clumped at the bottom of the tube, and an equal volume of dH_2O was added to the tube. The DiI was suspended in the dH_2O just prior to use by rapidly agitating the tube on a mechanical vortex agitator (Fisher Vortex Genie 2) at high speed.

Because DY, TB, and DiI in water are all suspensions composed of particles of various sizes , microinjections were made with glass micropipettes with large tip diameters (50-100 μm). The dissolved forms , DiI, FG, and the fine suspension of Lumofluor latex beads were all injected with glass micropipettes (tip diameter 25-65 μm). The volume of tracer injected varied with the tracer, depending on its form (dissolved or suspended), the size of the structure being injected, and previous documented information and personal experience with that particular tracer. Following injection of the tracers, the animals were allowed to survive for 3-5 days for the combination of DY and TB and 5-7 days for the other two combinations of tracers. They were then perfused and processed as described in the anterograde methods section.

ABBREVIATIONS

cc	central canal
cl	central lateral subnucleus of the PBN
cNTS	caudal nucleus of the tractus solitarius
DMV	dorsal motor nucleus of the vagus nerve
exl	external lateral subnucleus of the PBN
exm	external medial subnucleus of the PBN
mcp	middle cerebellar peduncle
MeV	mesencephalic nucleus of the trigeminal
mV	motor nucleus of the trigeminal
PBN	parabrachial nucleus
PBNm	medial subnucleus of PBN
PrV	principal nucleus of the trigeminal
PTN	paratrigeminal nucleus
rNTS	rostral nucleus of the tractus solitarius
scp	superior cerebellar peduncle
sp V_C	nucleus caudalis of the trigeminal

lam I	lamina I of the sp V_C
TS	tractus solitarius
vest	vestibular complex
vl	ventral lateral subnucleus of the PBN
VPM	ventroposteromedial nucleus
Vtr	trigeminal tract
XII	hypoglossal nucleus

RESULTS

The results will be presented in three parts. In the first part, the distribution of terminal fields of efferent projections from the PTN will be described as revealed by the anterograde tracing experiments. In the second part, the results obtained with fluorescent retrograde tracers will confirm anterograde tracing results and demonstrate optimum combinations of tracers used in the study of PTN collaterals. In a number of instances the results of both anterograde and retrograde tracing studies will be presented in parallel in order to emphasize the topography and overlap of PTN efferent projections with distinct neuronal populations in various regions of the brain. This parallel presentation also helps to define the borders of the nucleus as they relate to anterograde and retrograde experiments. In the third part, the results from the double-labeling experiments will be presented.

Anterograde Tracing Experiments

Of the 18 cases in which the PTN was injected with TMR, in 3 cases the injection site was confined to the PTN with little or no involvement of the underlying spinal trigeminal nucleus. As a consequence, the following results are based primarily on these three cases.

The injections were placed so as to involve the PTN at the level where it is anatomically most extensive; between 1.5 to 2.0 mm rostral to the obex. TMR injection sites produced following slow pressure injections were discrete (Fig. 1A) and did not spread far from the focal area of the pipette penetration relative to other tracers like FG of equal volume . When TMR spread was evident it tended to follow the reticulated pattern of the neuropil of the PTN passing primarily in the interstices of the spinal trigeminal tract and did not appear to stain the large myelinated fibers of the tract. Injection sites appeared as small brightly fluorescent red areas in the dorsolateral medulla oblongata when viewed under optics suitable for visualizing rhodamine fluorescence. Occasionally, individual neuronal somata

Fig. 1. Fluorescence photomicrographs of a typical TMR injection site in the PTN (A) and a neuron in the ipsilateral spinal trigeminal nucleus pars caudalis retrogradely labeled with TMR. **A**: Illustrates the small size of the injection site and the degree of tracer spread within the unmyelinated neuropil of the nucleus. **B**: Illustrates a neuron containing punctate fluorescent cytoplasmic inclusions that extended into the proximal dendrites. The arrowhead indicates a pericyte which has also taken up the dye. Calibration bars: A 100 μm, B 25 μm.

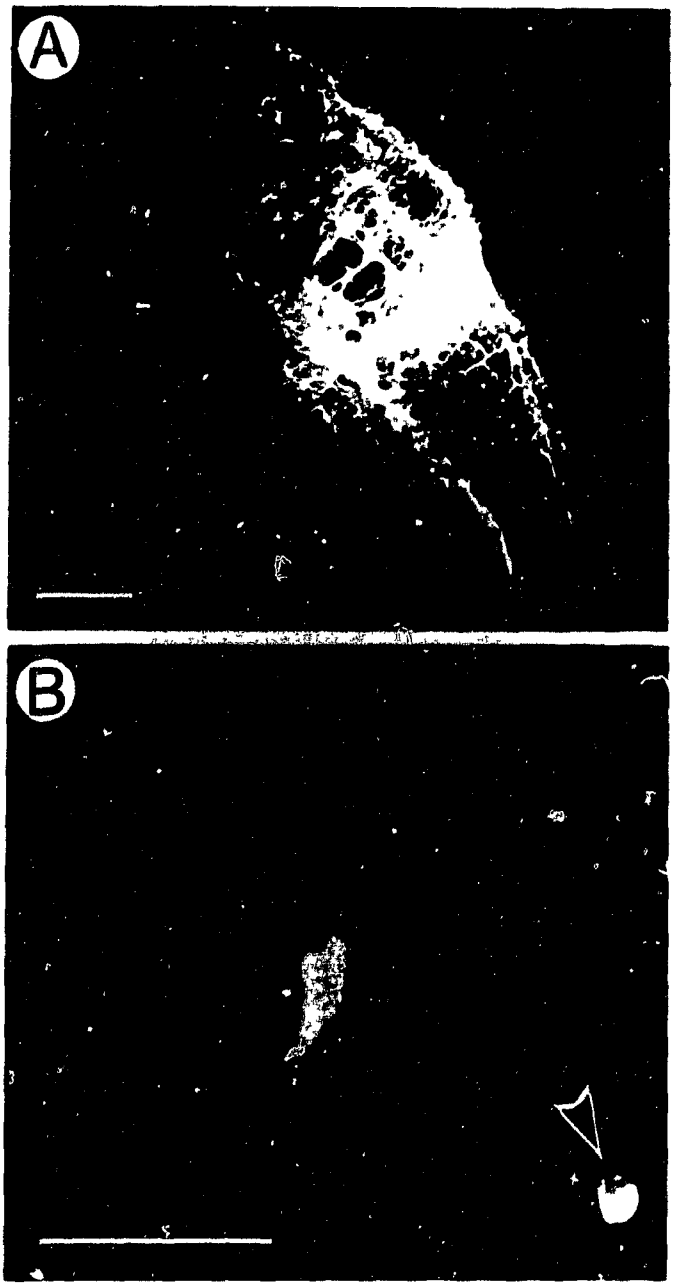

Figure 1

near the edge of the injection site could be seen to contain brightly fluorescent granular inclusions. However, it was not clear whether these somata took the label up directly or if they transported the tracer retrogradely from the injection site. Although TMR is primarily an anterograde tracer, a very small numbers of neurons appear to be able to pick up the tracer and transport it back to the cell body (Fig. 1B).

After small stereotaxic injections of TMR into the PTN, anterogradely labeled axons and presumed axon terminals were located in several nuclei in the brainstem and in the thalamus. Anterogradely-labeled fibers exhibited a homogeneous, intensely red fluorescence. Axonal labeling consisted of short or long axonal segments while presumed terminal labeling appeared as brightly fluorescent enlargements or swellings at the end of or along the path of a single uniformly labeled axon (Figs. 2A, 3). Punctate labeling was also apparent but could not be differentiated as axonal or terminal at the light microscopic level because transverse sections through labeled axons could also be expected to produce profiles similar to that of labeled terminals.

Spinal trigeminal nucleus and PTN. Caudal brainstem structures containing PTN efferent terminal fields included lamina I of the contralateral spinal trigeminal nucleus pars caudalis and PTN (Fig. 2). Fiber and terminal labeling was found as far caudal as the spinal-medullary junction in the contralateral lamina I of the spinal trigeminal complex. Typically, PTN efferent input to the contralateral lamina I of spinal trigeminal nucleus pars caudalis extended in a continuum dorsoventrally, close to the medial edge of the spinal trigeminal tract. The heaviest labeling in lamina I was located dorsolateral and just caudal to the caudal limit of the PTN in a region corresponding to the paramarginal nucleus described by Phelan and Falls ('89) (Fig. 1A). The labeling in the paramarginal nucleus was continuous ventrally along the medial edge of the spinal trigeminal tract with labeling in lamina I. Labeling in lamina I and the paramarginal nucleus overlapped with neurons projecting to the dorsolateral pons or to the thalamus (Figs. 2A-D). Although the

Fig. 2. Fluorescence photomicrographs comparing anterograde labeling after TMR injections into the PTN and retrograde labeling after FG injections into the PBN or VPM. PTN efferent labeling in the caudal medulla oblongata (left column: A, C, E) and retrogradely labeled neurons in regions corresponding to those shown on the left. **A**: Anterogradely labeled fibers in lamina I of the spinal trigeminal nucleus pars caudalis. Insert is a higher magnification of labeling in A showing the PHA-L-like filling of axons. Arrowhead indicates a common landmark in the two photomicrographs. **B**: Neurons retrogradely labeled with FG following injection of tracer in the thalamus. **C**: PTN efferent labeling in small ventral interstitial regions of the spinal trigeminal tract and subtrigeminal region. Arrows indicate TMR labeled fibers interstitial in the ventral spinal trigeminal tract. **D**: Neurons projecting to the thalamus located in similar regions to that of PTN efferent labeling in (C). Arrowhead indicates a retrogradely labeled neuron lying in the ventral spinal trigeminal tract. **E**: Anterograde TMR labeling in the PTN overlying the spinal trigeminal nucleus pars interpolaris. **F**: Labeled neurons projecting to the caudal one third of the PBN. Calibration bars: 50 μm.

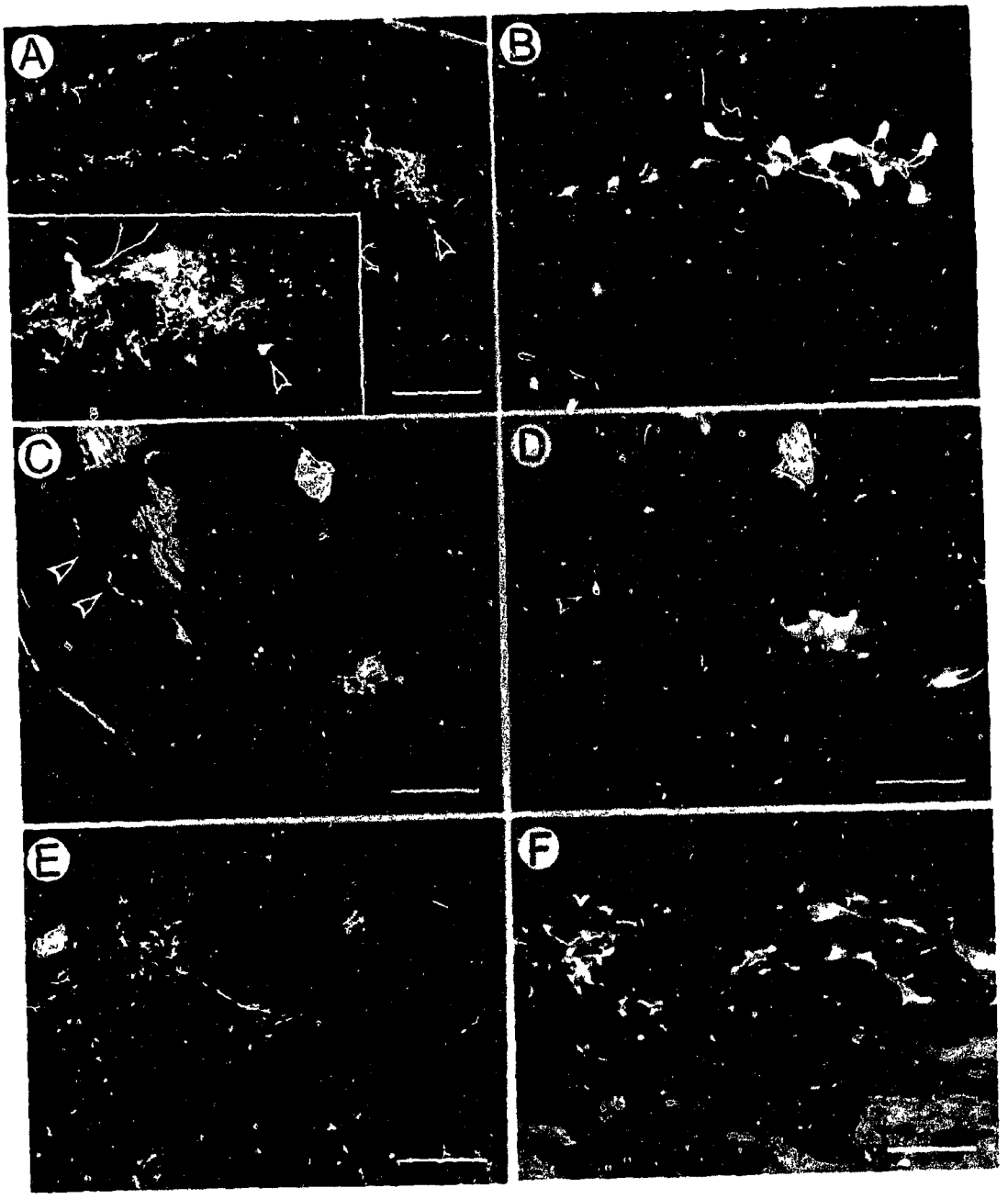

Figure 2

paramarginal nucleus has been considered a separate part of the spinal trigeminal interstitial system (Phelan and Falls, '89), it is not clear in the present study whether or not this is valid and for this reason the paramarginal nucleus will be considered part of lamina I (i.e., marginal zone). In spite of the dense contralateral labeling in lamina I of the spinal trigeminal nucleus pars caudalis it was difficult to identify individual fibers crossing from the injection site to contralateral cell groups.

Rostral to labeling in lamina I, a distinct region of anterograde labeling was characterized by thin strands of gray matter extending into the spinal trigeminal tract overlying the contralateral rostral pole of the spinal trigeminal nucleus pars caudalis (Fig. 4A). These interstitial cords of gray matter represented the caudal extent of the PTN. The contralateral labeling in the PTN extended throughout the nucleus from just caudal to the obex to its rostral extent which is located approximately 2/3 of the distance moving caudal to rostral along the spinal trigeminal nucleus pars interpolaris. Overlying the spinal trigeminal nucleus pars interpolaris, the PTN appears as an accumulation of neurons and neuropil situated in the dorsolateral aspect of the spinal trigeminal tract containing large numbers of PTN efferent fibers while the underlying spinal nucleus remained virtually void of any labeling (Figs. 2E-F). PTN efferent labeling in the contralateral PTN was continuous with labeling in lamina I. Injections of FG into the PTN indicated that the innervation of the contralateral PTN originated from a relatively small number of the total population of neurons in the nucleus.

Retrograde tracing experiments indicated that efferent fibers in the PTN overlap neurons within the nucleus which had different projection terminal fields in the medulla oblongata, pons, and thalamus. Caudally in the PTN, overlap occured between efferent projections from the PTN with neurons projecting to the nucleus of the tractus solitarius and parabrachial nucleus as well as with neurons which had terminal fields in contralateral

Fig. 3. Line drawings (A, B) and photomicrographs (C, D) illustrating ipsilateral (B, D) and contralateral (C, D) anterograde labeling in the caudal NTS and dorsal motor nucleus of the vagus nerve following TMR injection in the PTN. **A**: Illustrates fibers crossing the midline (arrowheads) to the contralateral NTS and DMV. **B**: Illustrates fibers in the ipsilateral NTS and DMV at a level 120 μm rostral to that shown in (A). **C-D**: Photomicrographs of boxed areas in (A) and (B) illustrating anterograde labeling in and around the tractus solitarius. Calibration bars: 50 μm.

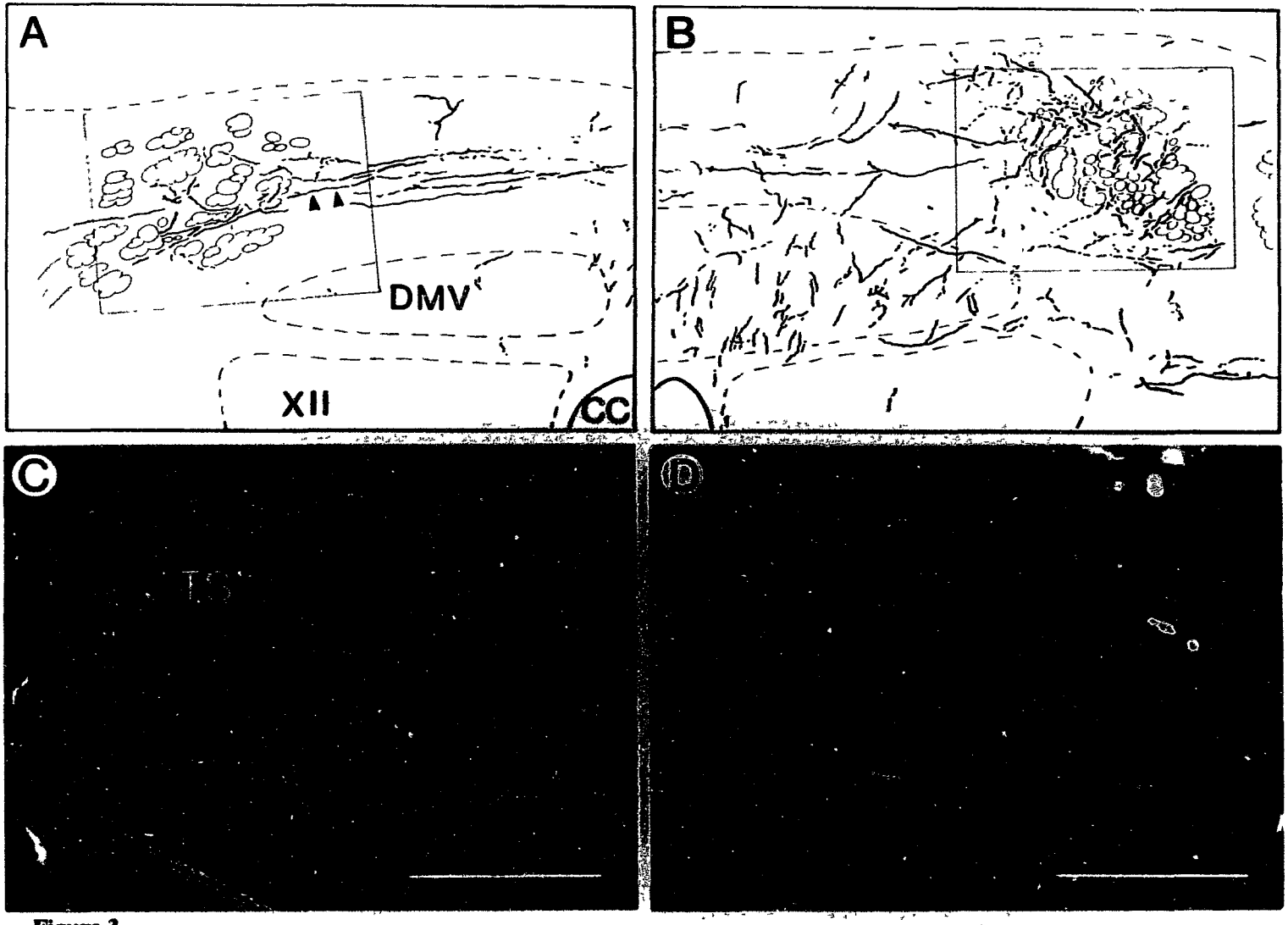

Figure 3

Fig. 4. Fluorescence photomicrographs illustrating the correspondence of regions of anterograde and retrograde labeling in the PTN. **A**: Labeled PTN efferent fibers in the contralateral caudal PTN overlying the spinal trigeminal nucleus pars caudalis. **B**: Large neurons in the PTN retrogradely labeled with FG following injections in the contralateral thalamus. **C**: PTN efferent fibers in the contralateral PTN overlying the spinal trigeminal nucleus pars interpolaris. **D**: Retrogradely labeled neurons in the contralateral PTN following FG injection in the PTN. Note the size differences between the neurons in (B) and (D). Calibration bars: 50 μm.

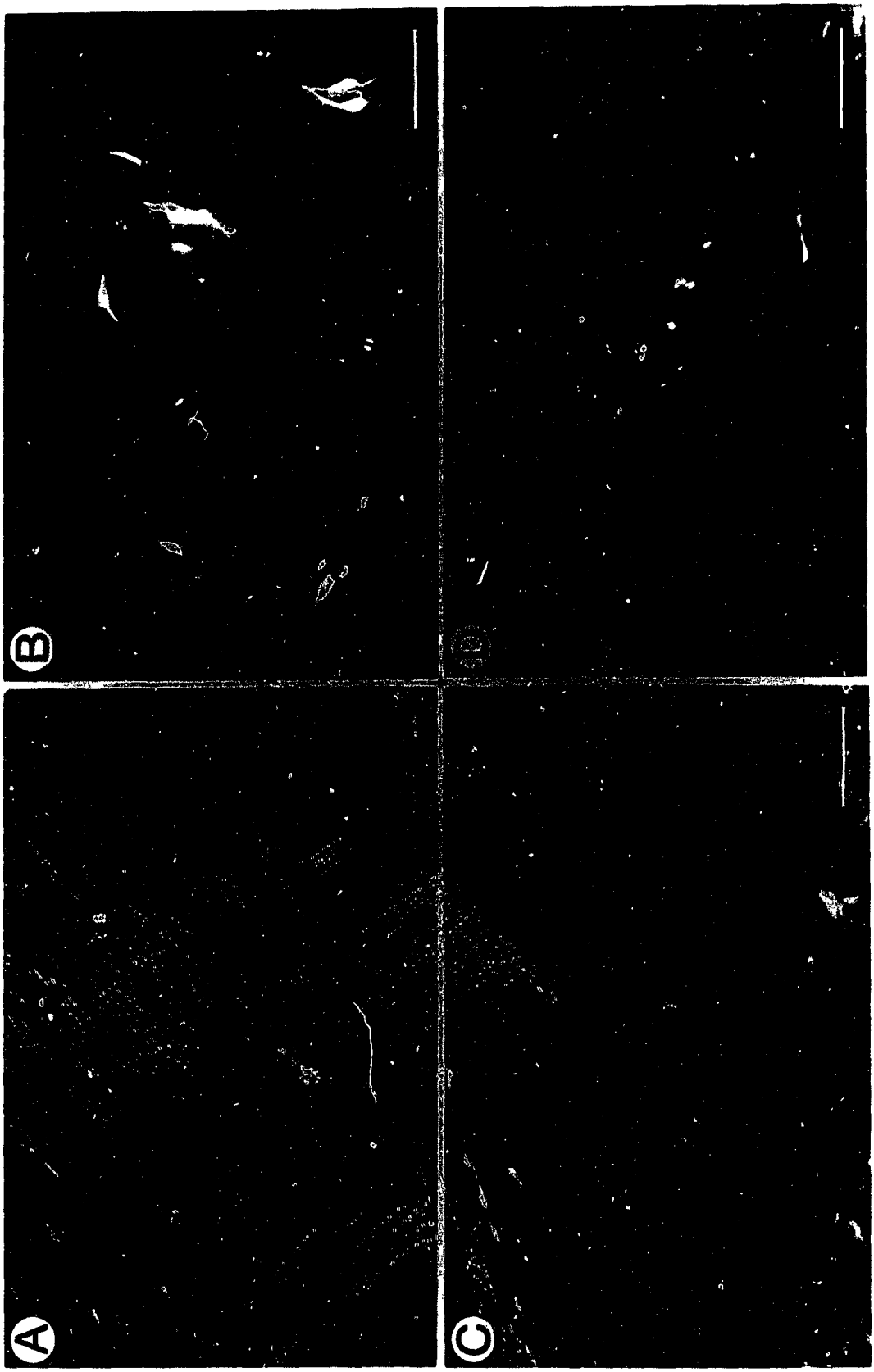

Figure 4

PTN and thalamus (Figs. 3-5). Similarly, in the rostral PTN where neurons projecting to the NTS and PBN predominated there were efferent fibers from the contralateral PTN.

Dorsal vagal complex. Bilateral anterograde labeling of the nucleus of the tractus solitarius and dorsal motor nucleus of the vagus nerve (DMV) was evident following TMR injection into the PTN (Figs. 3, 5). The commissural subnucleus of the nucleus of the tractus solitarius contained a small number of labeled fibers ipsilaterally and in two cases these fibers were found to extend into the contralateral half of the nucleus. Labeled fibers in the nucleus of the tractus solitarius rostral to the subnucleus commissuralis were not restricted exclusively to an individual subnucleus (Fig. 3). The subnucleus interstitialis of the nucleus of the tractus solitarius did receive distinct bilateral innervation from the PTN (Fig. 3). Fiber and presumed terminal boutons were evident passing between the myelinated bundles of the tractus solitarius and terminating in the subnucleus interstitialis. Retrograde FG experiments indicate that the distribution of PTN efferents in the nucleus of the tractus solitarius overlap with many neurons with terminal fields in the parabrachial nucleus (Fig. 5). Although numerous medium and fine caliber fibers could be seen leaving the injection site and passing into the dorsal part of spinal trigeminal nucleus pars caudalis these rarely were seen to produce characteristic terminal swellings. Small numbers of labeled efferent axons from the PTN were seen running in a predominantly dorsal ventral orientation in the dorsal motor nucleus of the vagus nerve (Fig. 3).

The rostral (gustatory) part of the nucleus of the tractus solitarius (rNTS) was labeled bilaterally. The ipsilateral rNTS contained many labeled preterminal and presumed axon terminal profiles throughout its neuropil (Fig. 5C). Labeling in the contralateral rNTS was light but extended throughout the nucleus with the same distribution as in the more heavily labeled ipsilateral nucleus. Subjacent to the rNTS the parvocellular reticular formation received a sparse projection from the PTN. As was the case for the caudal (visceral) NTS,

Fig. 5. Fluorescence photomicrographs of afferent labeling in the ipsilateral caudal (A) and rostral (C) NTS after injection of TMR into the PTN compared with retrograde labeling in comparable regions of the NTS after injections of FG into the PBN. Calibration bar: 50 μm.

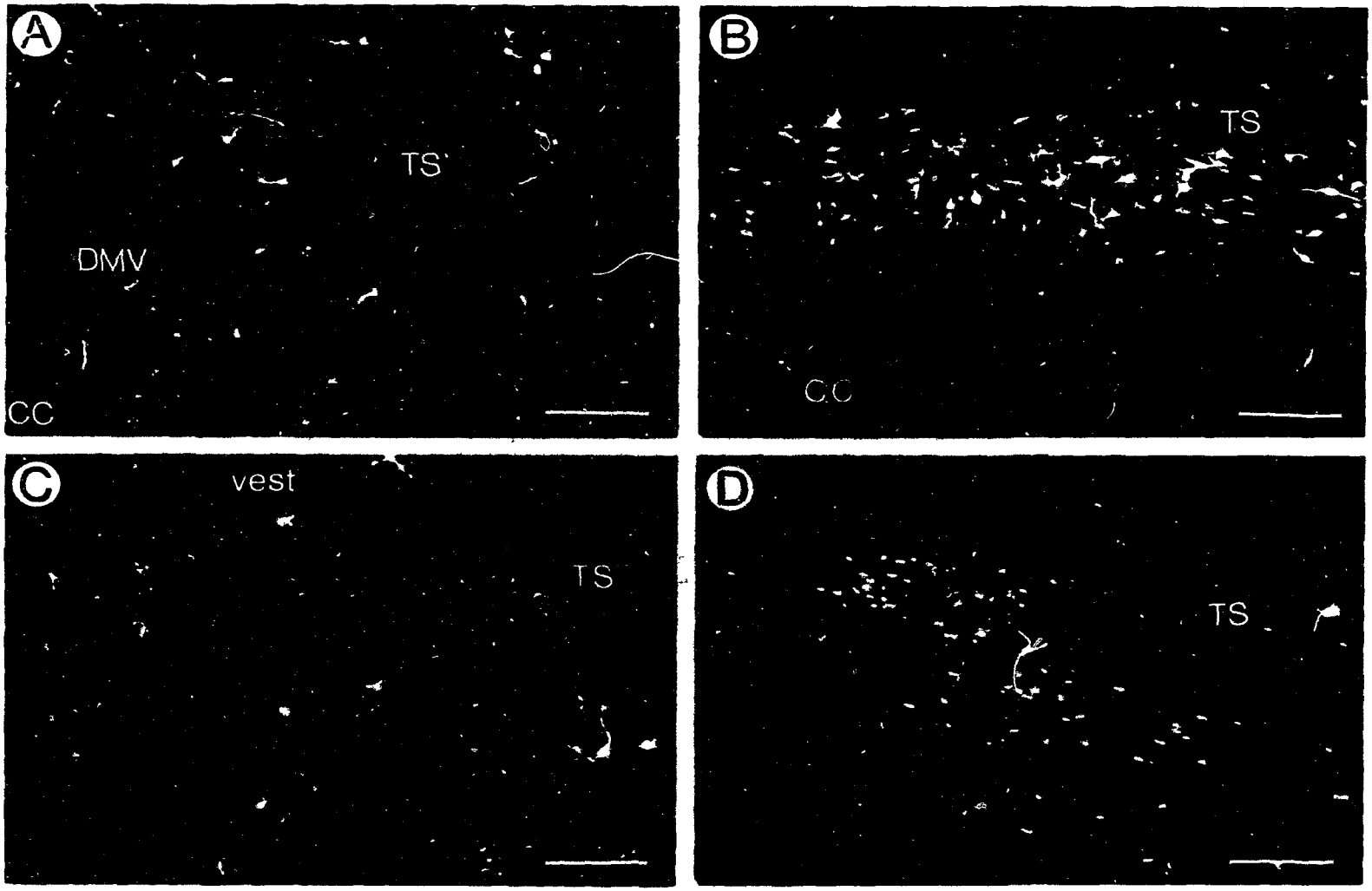

Figure 5

Fig. 6. Fluorescence photomicrographs of labeled PTN efferent axons in the ipsilateral principal trigeminal nucleus (A) and (B) and an area located between the caudal pole of the superior cerebellar peduncle and the dorsal part of the principal trigeminal nucleus (C). **A:** Illustrates a number of thick axons (arrowheads) leaving the spinal trigeminal tract to arborize in the principal trigeminal nucleus (PrV). **B:** Moderately heavy afferent labeling curving over the dorsal cap of PrV (arrowheads). **C:** Numerous labeled axons located between the superior cerebellar peduncle (upper left) and the dorsal part of the PrV. Note the two long axons (arrowheads) extending toward the medial subnucleus of the PBN. Calibration bars: 50 μm.

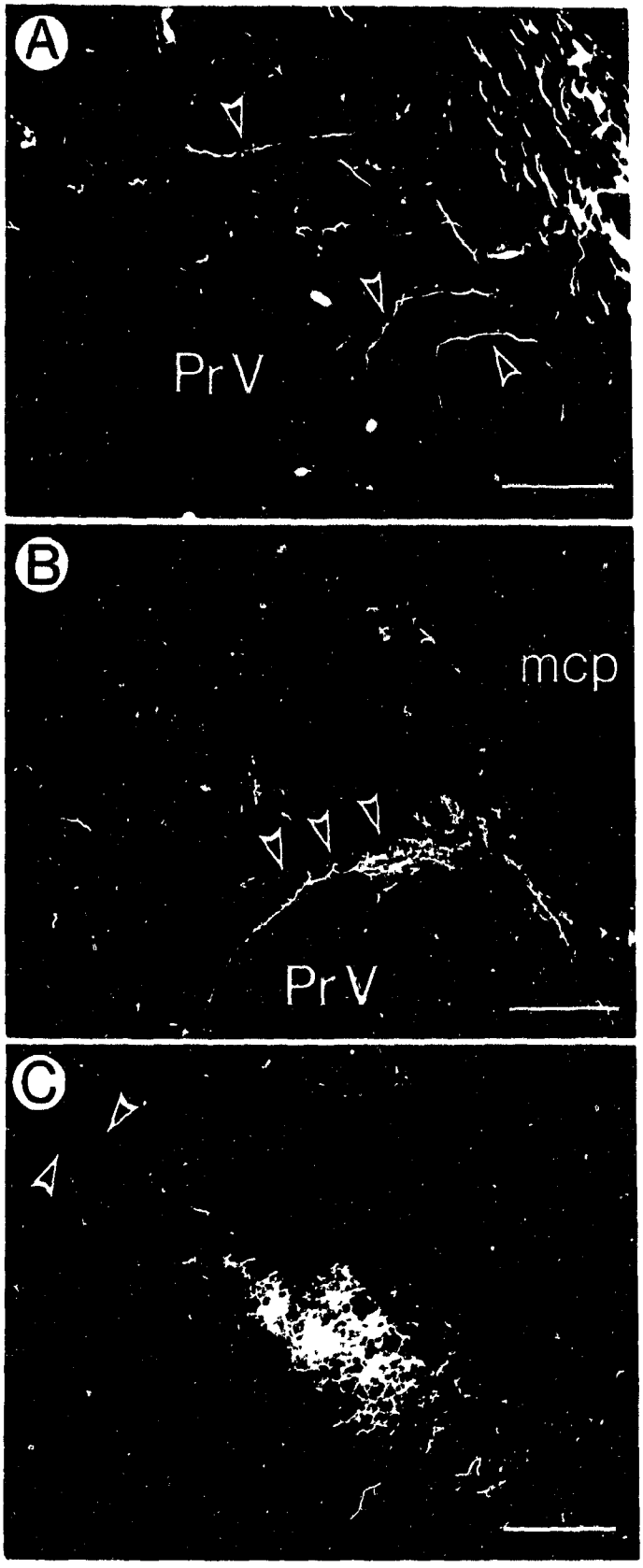

Figure 6

efferent fibers from the PTN overlapped extensively in the rNTS with neurons projecting to the ipsilateral parabrachial nucleus (Figs. 5C-D).

The spinal trigeminal complex rostral to the injection site also received a number of projections. However, the number of axons entering the spinal trigeminal nuclei was greater when the injection site included a substantial part of the underlying spinal trigeminal nuclei. The spinal trigeminal tract contained numerous labeled fibers in the dorsolateral part of the tract from the level of the injection site as far rostral as the principal trigeminal nucleus (Fig. 6A). Moderate numbers of fibers leaving the tract and entering the pars interpolaris, pars oralis and principal trigeminal nucleus were largely confined to the dorsal part of the nuclei along the border with the spinal trigeminal tract (Figs. 6A, B). There was a PTN terminal field at the level of the appearance of the superior cerebellar peduncle (Fig. 6C). This area of heavy labeling was interposed between the superior cerebellar peduncle and the dorsal principal trigeminal nucleus. Because of its extreme caudal location in the parabrachial region it did not appear to fit any of the established parabrachial subdivisions (Fulwiler and Saper, '84) or subdivisions of the trigeminal system (Paxinos and Watson, '86). Occasionally fibers were seen extending from this area in a dorsomedial direction toward the caudal part of the medial subnucleus of the parabrachial nucleus (Fig. 6C).

Parabrachial nucleus. At the level of the pons, the parabrachial nucleus was labeled bilaterally, with an ipsilateral predominance. The following description of the distribution of PTN efferent projections to different regions of the parabrachial nucleus utilizes the subnuclear parcellation of the parabrachial nucleus presented in the paper by Fulwiler and Saper ('84). Anterograde labeling in the parabrachial region following injection of tracer into the PTN was most prominent in the caudal one half of the nucleus. Several parabrachial subnuclei including the medial, external medial, external lateral, central lateral, ventrolateral and waist area, all contained anterograde labeling. Beginning caudally in the parabrachial nucleus, the first subnucleus found to contain anterograde

Fig. 7. Line drawing of a coronal section through the caudal parabrachial region (A) and a fluorescence photomontage (B) of the boxed area in (A). **B**: Labeled PTN efferent fibers extending along the middle cerebellar peduncle (mcp) and then coursing dorsomedially into the medial subnucleus (PBMm) adjacent to the superior cerebellar peduncle (scp). The arrowheads indicate labeled fibers in the neuropil between autofluorescent mesencephalic trigeminal nucleus (MeV) neurons (arrow). Calibration bar: 50 μm.

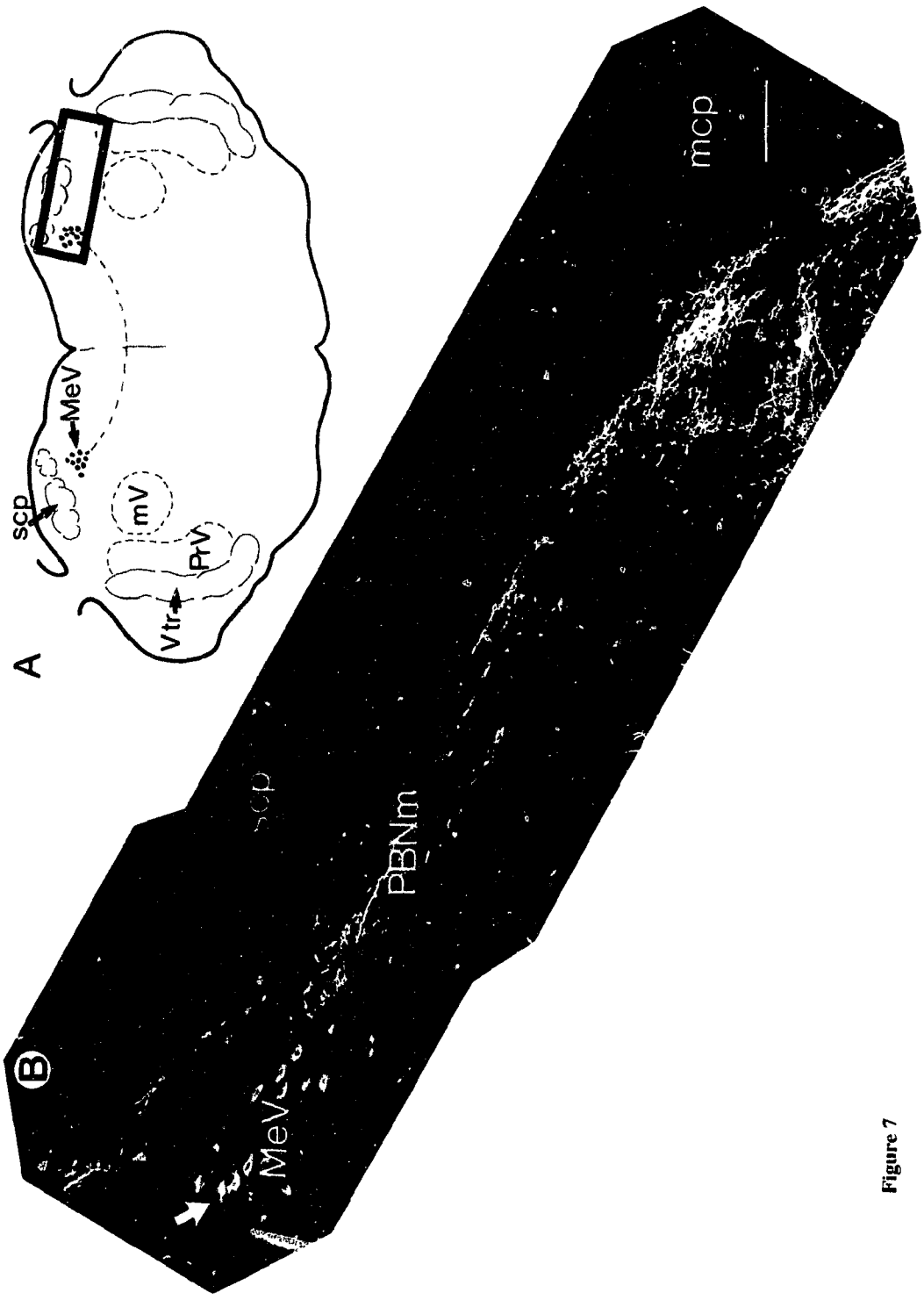

Figure 7

Fig. 8. Fluorescence photomicrographs of coronal sections through the ipsilateral PBN showing anterograde labeling after injection of TMR into the PTN. **A**: Anterograde labeling in the waist area (arrowheads) and fibers (arrows) leaving the PBNm in the direction of the MeV. **B**: Heavy anterograde labeling in the external medial subnucleus (exm) of the PBN which is continuous dorsolaterally with light labeling in the external lateral subnucleus (exl) . **C**: Anterograde labeling in the ventral lateral (vl) and central lateral (cl) subnuclei of the PBN. **D**: Heavy anterograde labeling in the vl adjacent to the superior cerebellar peduncle (scp). Note the paucity of labeling in the medial subnucleus of PBN at this level. Calibration bars: 50 μm.

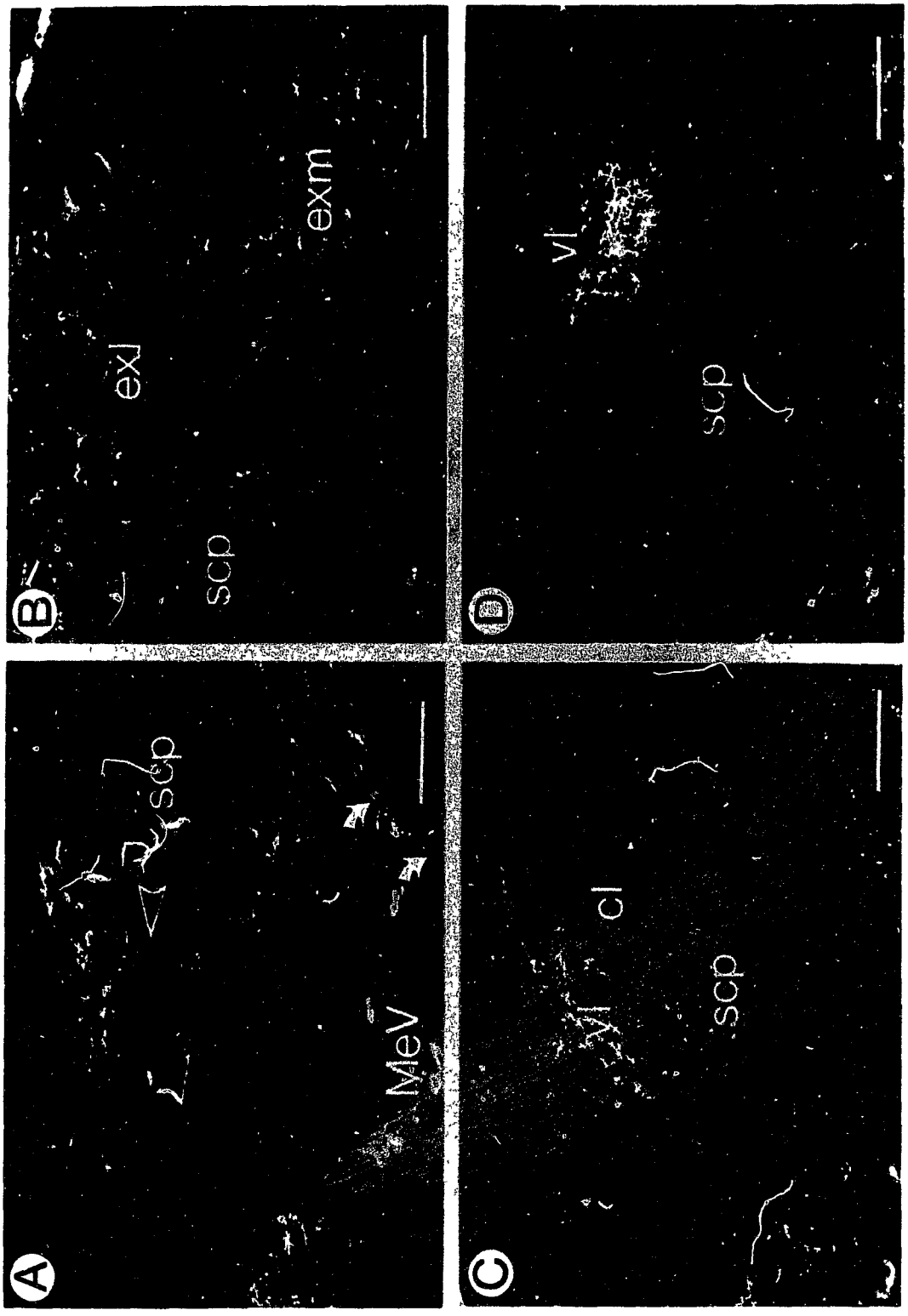

Figure 8

Fig. 9. Line drawings from fluorescence photomontages illustrating the overall pattern of anterograde labeling as seen in coronal sections through the ipsilateral dorsolateral pontine region following injection of TMR in the PTN. **A-B**: Sections taken from the caudal half of the PBN. Details are illustrated in Fig. 8. **C**: Section through the caudal pole of the PBN and dorsal PrV. Details are illustrated in Fig. 7.

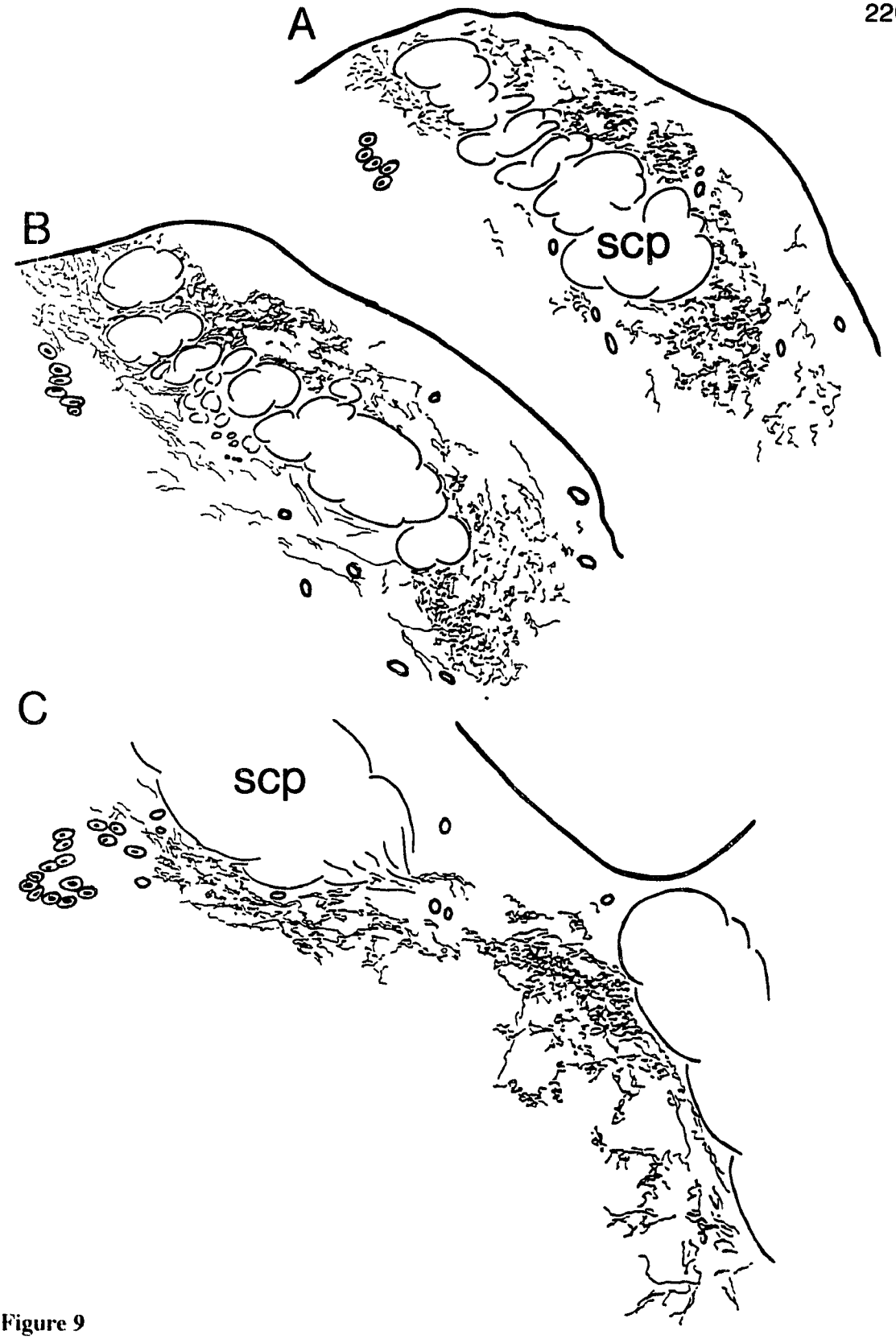

Figure 9

labeling was the medial subnucleus (Figs. 7, 8A, 9). Labeled fibers coursed along the medial edge of the middle cerebellar peduncle and then followed a dorsomedial trajectory as they passed over the dorsal cap of the principal trigeminal nucleus and into the medial subnucleus of the parabrachial nucleus (Figs. 7, 9). Labeling in the medial subnucleus was most pronounced in the region immediately adjacent to the medial border of the superior cerebellar peduncle where it lay in close proximity to the border of the fiber bundle in the transverse plane (Fig. 7). A small number of labeled fibers were found to leave the medial subnucleus and enter the lateral extent of the mesencephalic nucleus of V and pass between the large neurons which exhibited slight autofluorescence (Figs. 7, 8A, C). The waist area of the parabrachial nucleus, located at the narrowing of the superior cerebellar peduncle, consists of two small, circumscribed regions on either side of the peduncle which are connected by thin strands of gray matter which also contained anterogradely labeled fibers (Figs. 8A, 9). The next region of the parabrachial nucleus to exhibit heavy fiber labeling was the external medial subnucleus located around the ventral pole of the superior cerebellar peduncle. Simultaneous with the appearance of dense labeling in the external medial subnucleus was moderate amounts of fiber and terminal labeling in the lateral parabrachial nucleus adjacent to the lateral border of the superior cerebellar peduncle in a region corresponding to the external lateral subnucleus (Figs. 8B, 9). The lateral parabrachial nucleus contained two other subnuclei innervated by efferent fibers of PTN origin, these being the ventral lateral and central lateral subnuclei. The ventral lateral subnucleus received a substantial input from the PTN while the central lateral subnucleus contained only very sparse anterograde labeling (Figs. 8C, D).

Contralateral labeling in the parabrachial nucleus mirrored that of the ipsilateral described above; however, the degree of labeling present was greatly reduced. Labeling rostral to the level of the caudal one half of the parabrachial nucleus rapidly diminished with no further labeling evident in the brainstem.

Fig. 10. Fluorescence photomicrographs of retrogradely labeled neurons following injection of FG into the contralateral thalamus (A-C) and the ipsilateral PBN (D). **A**: Cluster of large neurons located dorsal in lamina I of the spinal trigeminal nucleus pars caudalis. **B**: Retrogradely labeled neurons in the caudal PTN overlying the rostral spinal trigeminal nucleus pars caudalis. **C**: Retrograde labeling in the caudal nucleus pars interpolaris and in the PTN (arrowheads) following thalamic injections of FG . **D**: Large neuron (arrowhead) among more numerous small neurons in the caudal, ipsilateral PTN after FG injection in the PBN. Calibration bars: A, B, D 50 μm, C 100 μm.

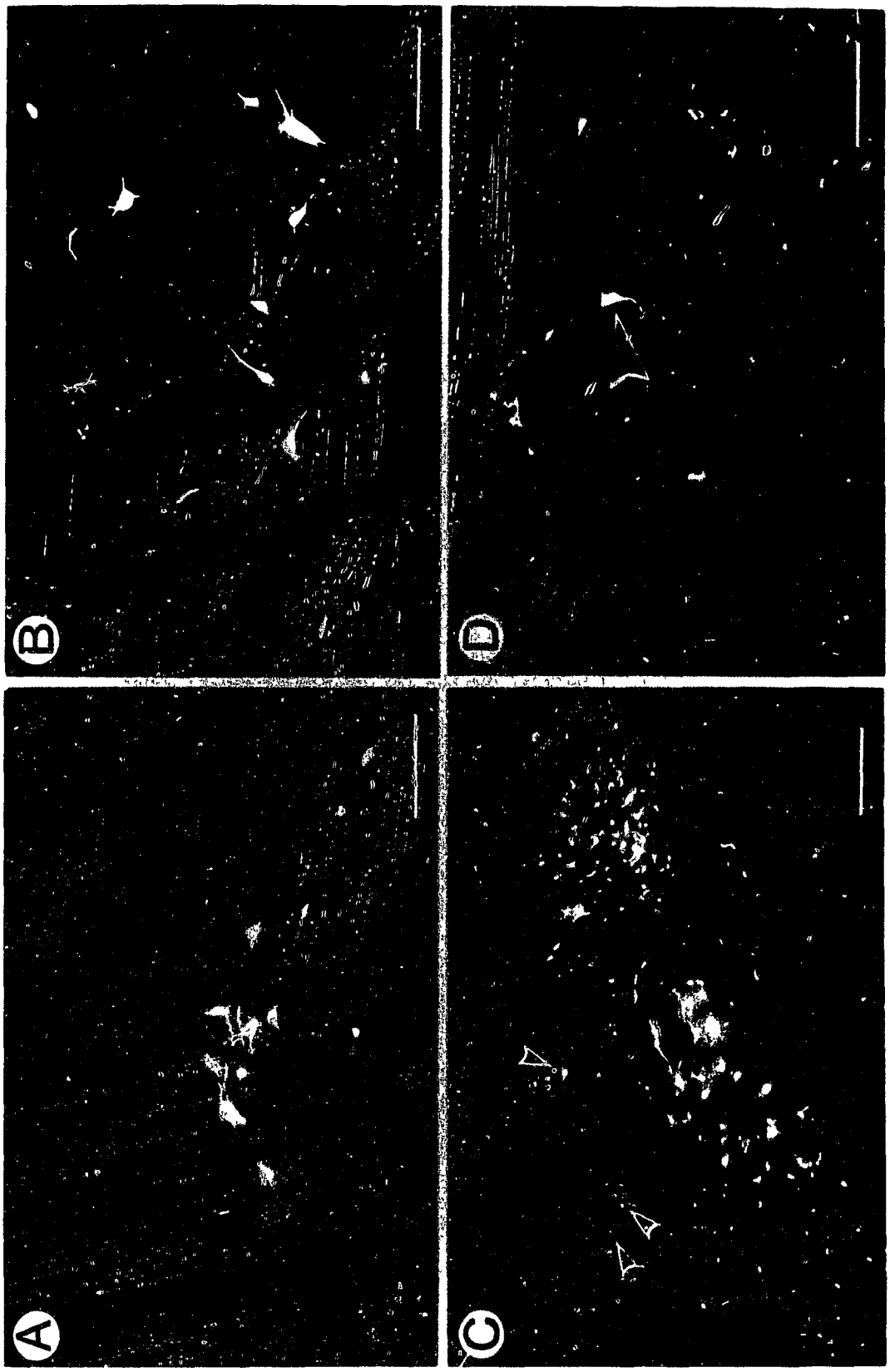

Figure 10

Fig. 11. A: Diagram of a coronal section showing the region in the ventroposteromedial nucleus (hatched area) from which the fluorescence photomicrograph in (B) was taken. In B the arrowhead indicates a pericyte containing TMR fluorescence. Calibration bar: 25 μm

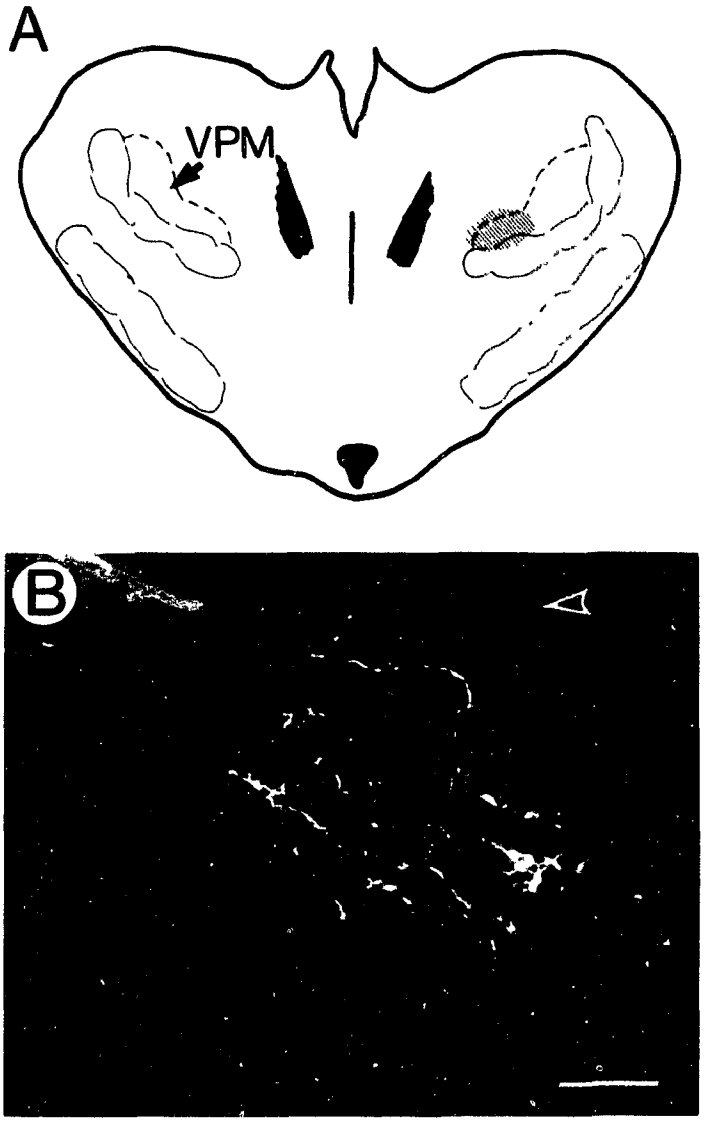

Figure 11

Thalamus. The thalamus was studied in only two cases with TMR injections in the PTN. In both cases, very light contralateral labeling was found in the ventromedial region of the ventral basal complex corresponding to the medial extension of the ventroposteromedial nucleus of the thalamus (Fig. 11). Just caudal to the ventral basal complex small numbers of fluorescent fibers were found running obliquely just dorsal to the medial lemniscus and medial to the medial geniculate nucleus but the course of these fibers caudal to this level could not be determined. No labeling was evident in the ipsilateral thalamus.

Control injections of TMR into the underlying spinal trigeminal nucleus pars caudalis produced fiber labeling throughout the rostro- caudal extent of the spinal trigeminal complex and principal trigeminal nucleus confirming previously established intranuclear pathways between these nuclear groups. There were differences in the distribution compared to that seen after PTN injections. Fibers could be found in the dorsolateral pons but to a much diminished extent compared to that following PTN injection. No labeled axons were observed in the contralateral PTN provided the injection site did not involve any part of the PTN. Fibers were observed in small numbers to enter the ipsilateral nucleus of the tractus solitarius at the level of the injection site but were rapidly diminished at more rostral levels of the nucleus of the tractus solitarius. A small number of retrogradely labeled neurons were evident within the ipsilateral spinal trigeminal complex indicating a tendency for a small population of neurons to transport TMR in a retrograde direction (for details see technical considerations section). This retrograde labeling was very rare. Pericytes near small capillaries were occasionally found to fluoresce red in a characteristic manner similar to that of anterogradely labeled TMR axons.

In summary, following injections of TMR into the PTN, axonal labeling was evident in the contralateral lamina I and PTN and in the visceral and gustatory nuclei of the tractus solitarius bilaterally. Bilateral labeling was also present in the dorsal lateral pons in the

parabrachial nucleus. The contralateral thalamus was the most rostrally located site containing anterogradely labeled fibers following injection into the PTN.

Retrograde Tracing Experiments

Rostral NTS injections. The fourth major efferent termination site indicated by anterograde tracing was the rostral nucleus of the tractus solitarius (rNTS). Lumofluor latex beads were injected into the rostral nucleus of the tractus solitarius in order to confirm PTN efferent projections to this area and to establish topographical relations in the PTN relative to parabrachial and thalamic projecting neurons. Because the rNTS is very small, injections were made with latex beads to produce small injection sites with less spread of the tracer to surrounding structures. Nevertheless, most injection sites were not confined entirely to the rNTS but included parts of the overlying vestibular nuclei and/or underlying reticular formation. Case 211-91 is representative of rNTS injections and will be used to describe the pattern of retrograde labeling observed in the medulla as far caudal as the spinal-medullary junction. Lumofluor latex beads have a characteristic granular appearance inside of retrogradely filled neuronal somata and proximal dendrites (Figs. 13D, F, H). The greatest number of retrogradely labeled neurons was found in the ipsilateral PTN and the ipsilateral nucleus of the tractus solitarius caudal to the injection site. Neurons in the PTN were located throughout the rostral caudal extent of the nucleus and were morphologically indistinguishable from neurons labeled in lamina I of spinal trigeminal nucleus pars caudalis. Numerous neurons in various subnuclei of the nucleus of the tractus solitarius as far caudal as the obex were retrogradely labeled. Caudal to the obex, retrogradely labeled neurons in the subnucleus commissuralis of the nucleus of the tractus solitarius were few in number and confined to the ipsilateral half of the subnucleus. Contralaterally fewer neurons were found in the PTN and lamina I of caudalis. Neurons in lamina I of pars caudalis were most abundant in the dorsal half of the nucleus. No

retrogradely filled neurons were seen in the area postrema. The numbers of cells labeled and the topography of these cells were remarkably similar to the pattern observed following injection of FG into the parabrachial nucleus.

Controls were provided by the data from three rats in which the injection sites did not involve the rNTS but involved structures adjacent to the nucleus of the tractus solitarius. In the first case the tracer was injected into the overlying vestibular complex including the medial vestibular and spinal vestibular nuclei. In the second instance the injection site was in the subjacent parvocellular reticular formation but also involved the dorsal part of the spinal trigeminal nucleus pars oralis and spinal trigeminal tract. In a third case the pipette passed deep to the nucleus of the tractus solitarius and the tracer deposit was in the parvocellular reticular formation beneath the nucleus of the tractus solitarius. Without identifying the cell groups retrogradely labeled after each of these injections, suffice it to note that only a very small number (< 10) labeled neurons per case were identified in the PTN, suggesting that the large number of retrogradely labeled neurons observed following rNTS injections resulted primarily from the uptake of the tracer in the nucleus of the tractus solitarius which is in strong confirmation of the results of the anterograde tracing experiments with TMR.

Parabrachial injections. Fluoro-Gold was injected into the dorsal lateral pons in three rats. In all cases the injection site included not only the medial and lateral division of the parabrachial nucleus but also a small dorsal part of the principal nucleus of the trigeminal nerve and in one case the mesencephalic trigeminal nucleus. Retrogradely labeled neurons were observed in numerous brainstem locations but only those areas which were targets of efferent projections from the PTN will be described in detail. Among the areas labeled following tracer deposit in the caudal one third of the parabrachial nucleus were the nucleus of the tractus solitarius, PTN, lamina I of the spinal trigeminal nucleus pars caudalis, subtrigeminal region and the ventrolateral medulla.

One representative case will serve to illustrate the results. The injection site in case 276-91 included the medial, external medial, external lateral, central lateral and ventral lateral subnuclei of the parabrachial nucleus and a small dorsal portion of the principal trigeminal nucleus. In the spinal trigeminal complex as far caudal as the spinal-medullary junction, the majority of retrogradely labeled neurons were located superficially, primarily ipsilaterally. Small numbers of labeled cells were also identified in deeper layers. Labeled neurons in lamina I were most numerous at the level of the obex where they were at times clustered dorsally along the border between the spinal trigeminal nucleus pars caudalis and the spinal trigeminal tract. Small numbers of cells of similar morphology to those in dorsal lamina I extended ventrally along the medial border of the spinal trigeminal tract. Labeled cells were identified in the PTN at the level of the rostral part of the pars caudalis. This pattern extended rostrally over the caudal 2/3 of the spinal trigeminal nucleus pars interpolaris. Most of these cells, like those of lamina I, were fusiform in shape although their dendritic orientation was not as restricted as that of pars caudalis neurons which were oriented parallel to the interface between the nucleus and the spinal trigeminal tract. Labeled neurons in the most caudal part of the PTN formed a continuum with those neurons of lamina I of pars caudalis. Labeling in the superficial laminae of the spinal trigeminal nuclei gradually disappeared at more rostral levels over nucleus pars interpolaris where the PTN is most distinct (Fig. 12D). Generally there tended to be fewer cells labeled in the spinal trigeminal nucleus pars interpolaris relative to caudalis except for the PTN which contained many neurons labeled with FG (Fig. 2F). Small numbers of retrogradely labeled neurons were also found over the same rostral-caudal extent on the contralateral side of the brainstem in lamina I and PTN. Small numbers of retrogradely labeled neurons were present bilaterally in the deep parts of the spinal trigeminal complex and medullary reticular formation.

The heaviest retrograde labeling in the medulla following parabrachial nucleus injections of FG was in the nucleus of the tractus solitarius and the area postrema. Labeled neurons in the nucleus of the tractus solitarius and area postrema were bilaterally situated with ipsilateral predominance. All subnuclei of the nucleus of the tractus solitarius except the subnucleus centralis were found to contain FG labeled neurons. When FG injections in the parabrachial nucleus were centered at more rostral levels (i.e., rostral two thirds of parabrachial nucleus) the number of labeled cells in the PTN and lamina I of the spinal trigeminal complex was considerably diminished.

Thalamic injections. FG injections in the ventral basal complex, primarily in the ventral posteriomedial nucleus were made in order to identify the location of neurons in the PTN that provided the small efferent input to the ventral posteriomedial nucleus identified in the anterograde tracing experiments. It was also of interest to compare the topography of the neurons projecting to the thalmus relative to those projecting to the parabrachial nucleus especially in light of the presence of the small number of large fusiform neurons similar in morphology to thalamic projection neurons observed in the caudal PTN after parabrachial nucleus injections (Figs. 10D, 12A). In each of the three cases there was some spread of the tracer to the ventral posterolateral nucleus laterally and to the posterior thalamic nuclear group medially. In one case tracer spread impinged on the parafascicular thalamic nucleus. A number of areas including the contralateral cuneate, gracile, spinal trigeminal complex, PTN (Fig. 10C), principal trigeminal nucleus, ipsilateral parabrachial nucleus and nucleus of the tractus solitarius contained retrogradely filled neurons. The distribution of labeled neurons in lamina I of the pars caudalis followed the medial border of the spinal trigeminal tract (Figs. 2B, 2D, 14E). These neurons were variable in size and usually fusiform in shape with the long axis of the cell oriented along the curvature of the lamina in the transverse plane (Fig. 10A). Although neurons could be found throughout the dorso-ventral extent of lamina I there was in all cases, a tendency for cells to be congregated in the

dorsal region, especially at more rostral levels of the spinal trigeminal nucleus pars caudalis (Fig. 10A). With regard to the contralateral PTN a small number of neurons was consistently seen, but these neurons were located only in the most caudal parts of the PTN overlying the caudal spinal trigeminal pars interpolaris and rostral pars caudalis (Figs. 4B, 10B, C, 14B). Within the PTN overlying the caudal part of the spinal trigeminal nucleus pars interpolaris, neurons projecting to the thalamus were most commonly found in the ventral lateral part of the PTN either as single cells or small clusters which appeared continuous with more ventral neurons lying in lamina I (Fig. 13G). The primary and occasionally secondary dendrites were filled with FG. When dendritic filling was extensive it was possible to find labeled dendritic profiles in more rostral parts of the PTN although labeled somata were extremely rare. In one instance, a uniform small diameter process, possibly a labeled axon or axon collateral, was observed leaving a group of labeled neurons and extending into the subjacent spinal trigeminal nucleus pars caudalis. In all but one case in which FG was injected into the thalamus, a small group of retrogradely labeled neurons was observed in the ipsilateral nucleus of the tractus solitarius medial to the TS at the level of the area postrema. Other areas exhibiting retrograde labeling of neurons were the ipsilateral parabrachial nucleus, medial and lateral to the superior cerebellar peduncle and contralateral principal trigeminal nucleus.

To summarize the results of the retrograde experiments, the PTN has efferent connections with the contralateral PTN and VBC and with the NTS and PBN bilaterally, but with ipsilateral predominance.

Retrograde Double-Labeling Experiments

Combinations of tracers. Although the literature contains many reports of double-labeling experiments and combinations of tracers, considerations such as the size of nuclei to be injected and the size of neurons being investigated made it prudent to test a number of

different combinations of tracers. In order to determine whether efferent projections from the PTN originate from separate neurons or represent neurons with collateral projections to several sites, injections of FG, Lumofluor latex microspheres, True Blue (TB), and Diamidino Yellow (DY) were injected into sites confirmed by anterograde and retrograde tracing studies as being target sites for PTN projections. In preliminary experiments, comparisons were made to identify which neuroanatomical tracers provided optimal results in terms of size of injection, ease of application, transport times and photography.

The nuclear stain, Diamidino Yellow was used in combination with TB, a cytoplasmic stain. TB produced a large injection site relative to the volume injected when compared with the DY injection site. Retrograde labeling of neurons following TB injections was extensive following both thalamic and parabrachial injections, but retrograde labeling following DY application was variable and produced fewer labeled cells than TB. Even in the best case, only a small number of cells showed fluorescent nuclear label. Following TB injection into the ventral basal complex and DY injection into the parabrachial nucleus, many cells were identified as projecting to the thalamus from the appropriate nuclei and similarly, DY labeled neurons were present in all previously described areas following parabrachial nucleus injection of FG but only in small numbers. Double-labeled neurons were indicated only when a bright yellow nucleus and a pale blue cytoplasm were present in the same cell. Both DY and TB were viewed under UV light which is an advantage for viewing and for photography. However, for many double-labeled cells the size, brightness of the two tracers and leaching of DY into the cytoplasm often made it difficult to be absolutely sure that cells were double-labeled and made photographic presentation of the results difficult. This was especially evident for most PTN and spinal trigeminal nucleus pars caudalis lamina I labeled neurons which had a large nucleus to cytoplasm ratio. In such cases it was difficult to be sure that the cell was double-labeled at all because flare from the nucleus resembled cytoplasmic labeling and often obscured cytoplasmic labeling if

present. These drawbacks required that other combinations be explored for study of the collateral organization of projections from the PTN.

Preliminary studies of different combinations of retrograde tracers revealed FG and Lumofluor latex beads as the best suited combination for double-labeling experiments. Therefore, latex beads impregnated with dyes which were fluorescent under rhodamine or FITC filters were used. The fluorescent beads yielded small, discrete injection sites suitable for those double-labeling experiments involving the rostral nucleus of the tractus solitarius. Spread of the beads from the injection site was largely limited to the immediate area around the tip of the micropipette. The resulting retrogradely labeled neurons were brightly fluorescent under the appropriate fluorescent filters. Because the labeling with FG and Red or Green beads was viewed under different filter combinations the identification of double-labeled neurons was much more reliable than the combination of DY and TB and was not affected by the cell size. In the case of the rhodamine latex beads, there was a large difference in wavelength of light for illumination of the beads versus the FG, making "bleed-through" of little consequence. However, the FG/Green (FITC) beads combination under the wide range FITC filter used in the present study did in some cases produce bleed through images in which heavily labeled FG neurons occasionally appeared as faint images that were easily distinguished from the bright FITC fluorescence of neurons labeled with latex beads because labeling with beads resulted in a characteristic granular appearance (Figs. 13G, H). The drawbacks associated with the latex beads were: 1) small necrotic areas in the injection sites in a small number of cases, and 2) degree of retrograde labeling varied from case to case even when the injection volume and location were apparently very similar. When a large structure was injected, a number of penetrations were required because single injections of large volumes of beads did not spread readily from the focal injection site but did cause larger areas of tissue damage. Advantages of the latex beads included, 1) their ease of application, 2) small circumscribed injection sites obtained, and 3)

distinctive, granular labeling in the cytoplasm. Aqueous suspensions of latex beads did not plug even small diameter pipettes (< 30 μm). FG and latex bead labeled neurons were easy to distinguish whether they were single or double-labeled. Beads were easy to photograph and resistant to fading when repeatedly observed and photographed. Storage of slides at 4°C in the dark not only prolonged fluorescence quality, but also appeared to reverse partially the fading that occurred during prolonged exposure to fluorescent light. This was true to a greater extent for the rhodamine beads which were not only more resistant to fading after light exposure but also appeared to show significant recovery of fluorescence after storage. With all factors taken into account, the combination of FG and latex beads was deemed superior, particularly where one injection site was small, (i.e., rostral nucleus of the tractus solitarius) and the other site larger (i.e., parabrachial nucleus or ventral basal complex).

The advantages of latex beads in this system were a drawback when applied to another system. The small injection sites produced by latex beads even at large volumes made it less attractive when injections were required in relatively large sites such as the parabrachial nucleus and ventral basal complex. Consequently, another tracer which would combine suitably with FG had to be identified. It was preferable to find a tracer which fluoresced some distance in the color spectrum from FG to facilitate identification of double-labeled cells. This led to the use of DiI, a lipid soluble red fluorescent carbocyanine dye. When DiI was injected stereotaxically into the ventral basal complex, retrogradely labeled neurons were identified in the same sites in the brainstem as after FG injections. No anterograde transport of DiI was observed in the brainstem. Because DiI is soluble in absolute alcohol and xylene it was not possible to dehydrate in alcohols and coverslip the sections with xylene-based mountants because the DiI would leach out into the overlying medium making photography virtually impossible. However, both the FG and DiI photographed well uncoverslipped and it was therefore not necessary to coverslip (Fig. 14). Double

exposures of the same section showing double-labeled neurons were also possible (Fig. 14C). Sections with FG and DiI labeled cells retained good fluorescence for more than four months when stored at 4 °C in the dark.

In one animal the DiI was delivered in a 100% ethanol vehicle. DiI is very soluble in 100% ethanol and such a mixture permits the use of small diameter micropipettes. When aqueous suspensions were used micropipettes of slightly larger diameter were used to avoid plugging of the pipette opening. DiI in ethanol produced smaller injection tracks; however, significant necrosis at the site was characteristic of this type of administration of the tracer. The damage to the cells and neuropil was extensive and retrograde transport, although present, was not as good as in animals in which the DiI was delivered in an aqueous suspension.

rNTS and PBN. The following results are based on Case 183-91 which is representative of those cases in which injection sites were centered on the rostral nucleus of the tractus solitarius and the parabrachial nucleus. Injection of red latex beads into the rostral nucleus of the tractus solitarius and FG into the caudal parabrachial nucleus revealed two main features of the relationship of their afferent inputs. First, labeled neurons in the PTN projecting to either the ipsilateral rNTS or parabrachial nucleus occupied the same region of the nucleus. That is to say, there was overlap in the locations of cells of origin that projected to these two sites (Fig. 12). Neurons which projected from the contralateral PTN to the rNTS and PBN were few in number but distributed in the same areas as those retrogradely labeled neurons in the ipsilateral PTN. Neurons projecting to the rNTS and parabrachial nucleus were found throughout the entire extent of the PTN and were continuous with labeled neurons in lamina I of spinal trigeminal nucleus pars caudalis. Labeled neurons were located in the PTN and in lamina I overlying the caudal spinal trigeminal nucleus pars interpolaris retrogradely (Figs. 12A, B). More rostrally, neurons were localized in the PTN lying within the spinal trigeminal tract (Figs. 12C, D) with only

Fig. 12. Fluorescence photomicrographs of retrogradely labeled neurons in the PTN following injection of FG into the PBN and red latex beads into the rNTS ipsilaterally. **A-B**: The caudal PTN and superficial laminae of the subjacent nucleus pars caudalis showing the high degree of overlap of retrograde labeling and double-labeled neurons which are collateralized to the ipsilateral rNTS and PBN. A few examples of double-labeled neurons are indicated by arrowheads. **C-D**: The rostral PTN showing the topography of rNTS and PBN efferent neurons in the nucleus and neurons collateralized to the rNTS and PBN (arrowheads). Note the paucity of labeled neurons in the subjacent spinal trigeminal nucleus pars interpolaris. Calibration bars: 25 μm.

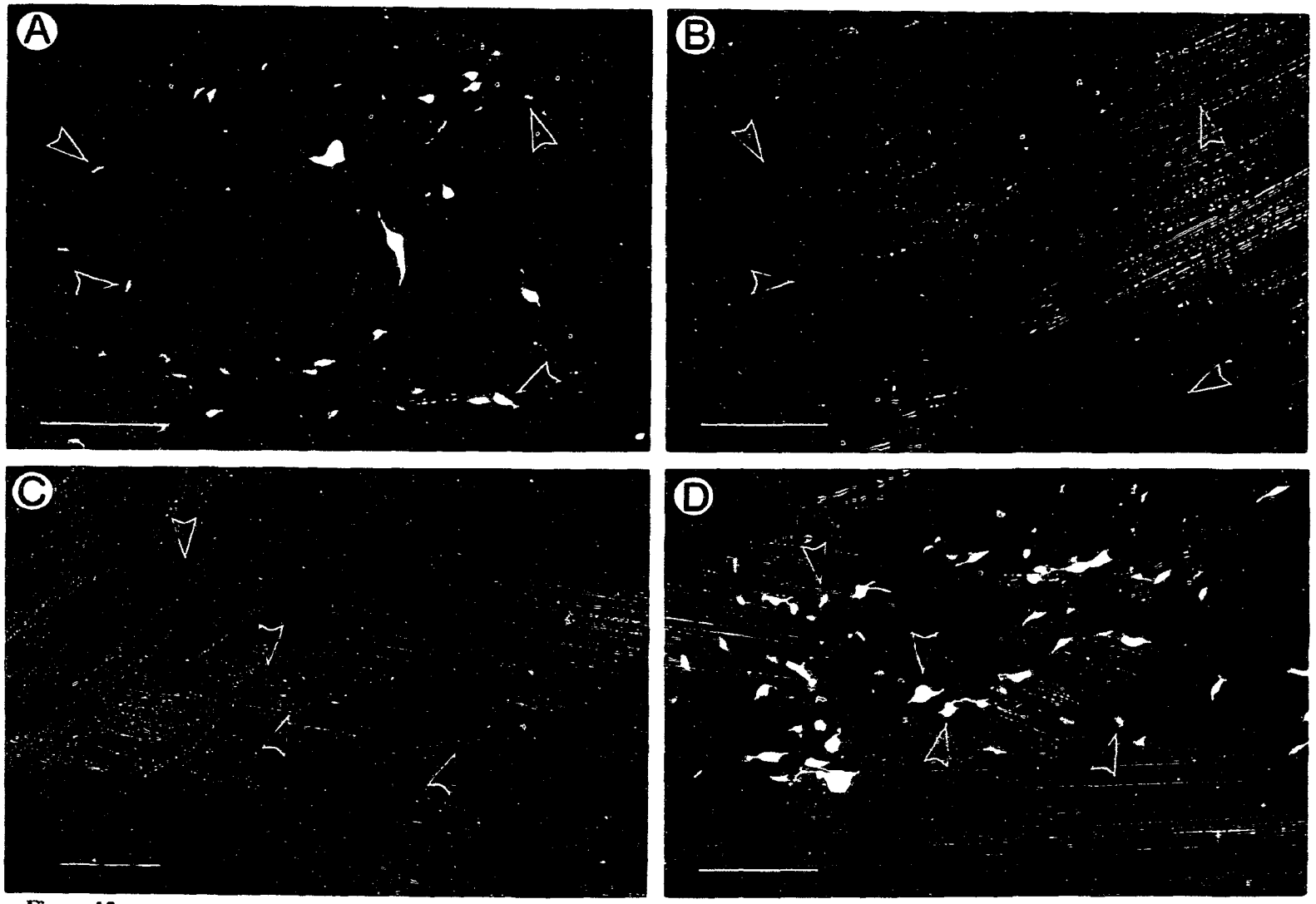

Figure 12

the occasional neuron labeled in the subjacent laminae of the spinal trigeminal region. Occasionally a labeled neuron (FG or latex beads) was observed in the deeper layers of the spinal trigeminal complex and reticular formation ipsilaterally. Retrogradely labeled neurons were also found in the nucleus of the tractus solitarius caudal to the injection site in the rNTS. The pattern of retrograde labeling after the parabrachial injection was the same as that obtained when FG alone was injected.

In summary, the topography of the neurons projecting to the rNTS and parabrachial nucleus overlapped in the lamina I of the spinal trigeminal nucleus pars caudalis, caudal pars interpolaris and also in the PTN. Retrogradely labeled neurons were found bilaterally in the area postrema following injection in the parabrachial nucleus but no neurons were identified in the area postrema after rNTS injection.

Double-labeling of neurons was observed in a number of areas of interest in the present study including the ipsilateral PTN, nucleus of the tractus solitarius, lamina I of the spinal trigeminal nucleus pars caudalis and contralateral PTN and lamina I. The degree of double-labeling was not quantified because of variables related to efficacy of tracer and size of injection sites. However, there was variability in the number of cells labeled following what appeared to be equivalent injections of latex beads into the rNTS although in every case it was clear that many more neurons were double-labeled ipsilaterally. Double-labeled neurons in the rostral half of the PTN (i.e., most extensive part of the PTN) overlying the spinal trigeminal nucleus pars interpolaris made up a significant proportion of the total number of labeled neurons (Figs. 12C, D). In some sections up to 70% of the cells were double-labelled. Double-labeled neurons in the caudal half of the PTN were present in smaller absolute numbers relative to the more rostral levels of the nucleus. The spinal trigeminal complex, particularly lamina I of the nucleus pars caudalis, contained double-labeled neurons as far caudally as the medullary-spinal junction. Sections caudal to this level were not studied in the present experiments. Labeling was bilateral in lamina I of

spinal trigeminal nucleus pars caudalis with the same predominance of double-labeled neurons ipsilaterally as was observed for the PTN. Contralaterally, neurons which were double-labeled were small in number and all were located in the dorsal aspect of spinal trigeminal nucleus pars caudalis, unlike those on the ipsilateral side which extended dorsoventrally in lamina I along the medial border of the spinal trigeminal tract. Double-labeled neurons observed in the contralateral PTN and lamina I of spinal trigeminal nuclei were morphologically indistinguishable from their more numerous counterparts in the ipsilateral PTN.

VBC and rNTS. In eight rats injections of FG were made into the ventral basal complex at one or more stereotaxic sites on the right side of the brain, while green fluorescent latex beads were injected on the left side in the rostral nucleus of the tractus solitarius in order to provide a comprehensive map of double-labeled neurons in the medulla. Results of one representative case are presented to illustrate the results in which FG was injected into the ventral basal complex and green latex beads into the rNTS.

Retrogradely labeled cells containing FG and latex beads were found in several locations in the medulla oblongata. Double-labeled neurons were identified only on the ipsilateral side of the brainstem in the PTN and lamina I of spinal trigeminal nucleus pars caudalis. Those neurons in the PTN that were double-labeled were restricted to the caudal one half of the nucleus overlying the caudal pole of spinal trigeminal nucleus pars interpolaris and rostral pole of spinal trigeminal nucleus pars caudalis. A second topographical arrangement was apparent within the PTN such that, double-labeled neurons were found almost exclusively in the ventral lateral part of the PTN (Fig. 13). The numbers of double-labeled neurons in the PTN were small and this might be expected since only small numbers of neurons in the PTN were found to project to the thalamus. Immediately caudal to the PTN there were double-labeled neurons in lamina I of spinal trigeminal nucleus pars caudalis, particularly the dorsal part along the medial border of

spinal trigeminal tract (Figs. 13 A, B, E, F). Interestingly, when compared to the same section (Figs. 12A ,B) the distribution of the neurons in the caudal PTN projecting to the rNTS overlaps with neurons projecting to the thalamus. Close inspection of the distribution of rNTS and thalamic projection neurons in the subjacent superficial laminae of the spinal trigeminal nucleus pars caudalis revealed that thalamic neurons occupied a more or less restricted area of lamina I immediately adjacent to the spinal trigeminal tract while those projecting to the rNTS were found in substantial numbers not only in lamina I but also in deeper layers where thalamic neurons were conspicuously absent (Figs. 13A, B). In other cases small numbers of neurons projecting to the thalamus were found in the deep layers of the spinal trigeminal nucleus pars caudalis but none of these neurons were double-labeled. Although it is difficult to measure accurately the size of neurons labeled with two different fluorescent tracers because of the error introduced as a result of the differences in the fluorescent halos, it is possible to qualitatively compare cell sizes within a single field of view. When double-labeled neurons were compared with neurons which were single labeled for either FG or green latex beads the double-labeled neurons appeared to be larger than those neurons projecting only to the rostral nucleus of the tractus solitarius (Figs. 13A, B). When compared to neurons retrogradely filled with FG following thalamic injection, double-labeled neurons were similar in size or were generally larger than neurons retrogradely labeled only with green latex beads. In other words, neurons which were double-labeled were typically more similar in size to neurons projecting to the contralateral thalamus than to neurons projecting to the rNTS.

Fig. 13 Fluorescence photomicrographs of retrogradely labeled neurons following FG and green latex bead injections into the contralateral thalamus and ipsilateral rNTS, respectively. **A-B**: Double-labeled neurons in the caudal PTN (arrows) and superficial lamina I of the spinal trigeminal nucleus pars caudalis (arrowheads). **C-F**: High magnification of double-labeled neurons indicated in A and B. Note the granular appearance of neurons containing latex beads (D and F). **G**: FG labeled neurons in the caudal PTN and dorsal lamina I of the spinal trigeminal nucleus pars caudalis . Arrowhead indicates a neuron which is double-labeled. **H**: High magnification of double labeled neuron in (G) (arrowhead). Note the bleed-through of FG ventral to neuron labeled by latex beads. Although bleed-through occurs, the absence of any granular labeling indicates that the neuron is not double-labeled. Calibration bars: A-B 50 μm, C-D 10 μm, E-F 20 μm, G 50 μm, H 20 μm.

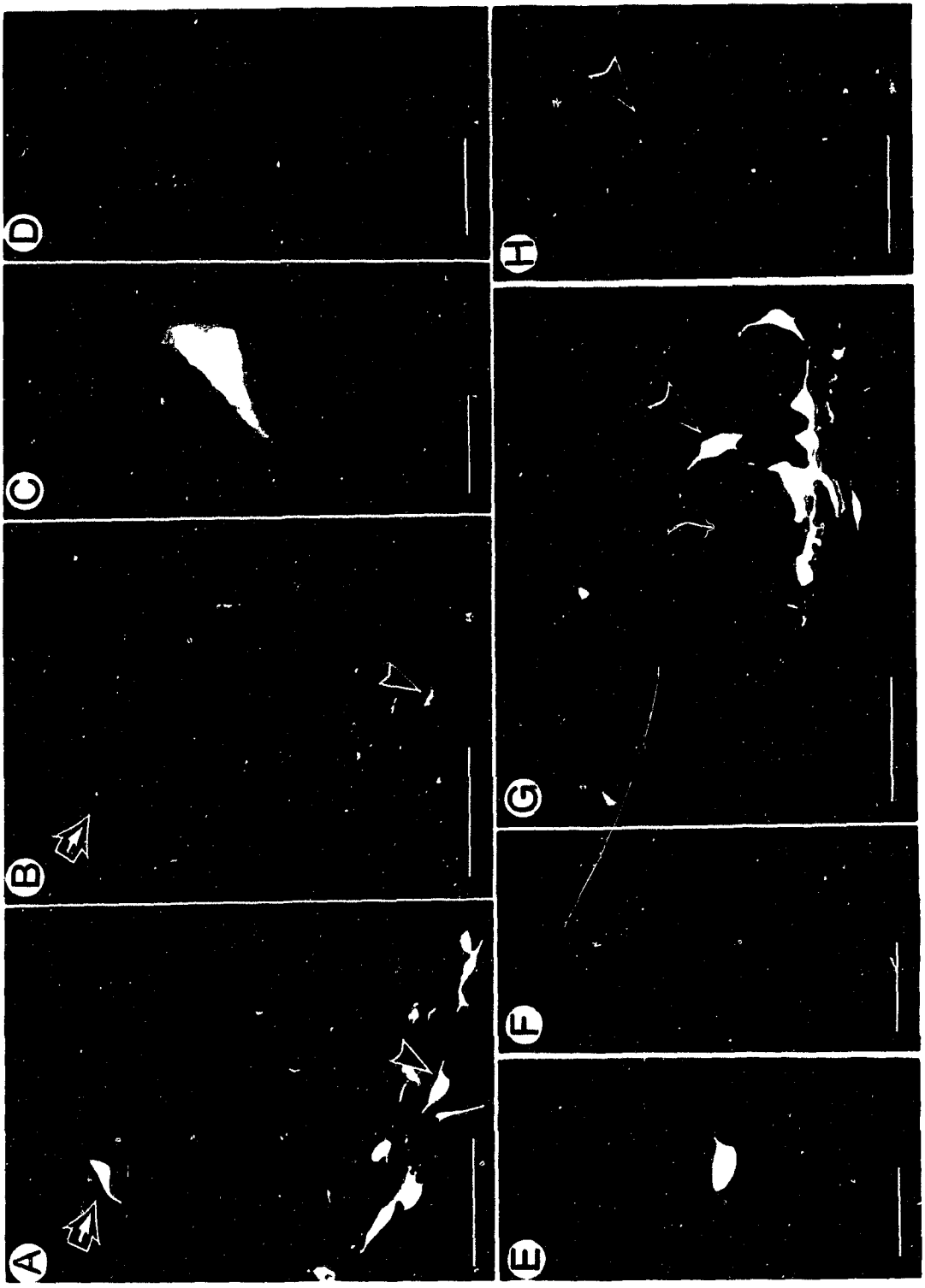

Figure 13

PBN and VBC. Injections into the parabrachial nucleus on the left side and ventral basal complex on the right side of the brain were made in eleven rats. There was some variability in the relative numbers of labeled cells after ventral basal complex injection of DiI. This variability probably resulted from differences in the size of the effective injection sites (i.e., a single large stereotaxic site versus three sites). In all cases where a single large injection of DiI was placed in the ventral basal complex the number of retrogradely labeled neurons found in the brainstem was less than when three small injections were made at stereotaxic sites in the ventral basal complex.

The distribution of PTN neurons projecting to the parabrachial nucleus and ventral basal complex was distinct for each neuronal group. As described above, PTN neurons projecting to the contralateral ventral basal complex were located predominantly in the caudal one half of the nucleus. These neurons were continuous caudally with labeled neurons in lamina I of spinal trigeminal nucleus pars caudalis. PTN neurons projecting to the ipsilateral parabrachial nucleus were found throughout the rostral caudal extent of the PTN. However, in the caudal PTN it was apparent from the present results that there is only a slight overlap in the PTN of neurons projecting to the parabrachial nucleus and ventral basal complex (Figs. 14A-C). More caudally in the spinal trigeminal nucleus pars caudalis neurons retrogradely filled from both the parabrachial nucleus and ventral basal complex were found in lamina I in an overlapping distribution (Figs 14D,E). At the interface between the caudal PTN and lamina I of spinal trigeminal nucleus pars caudalis double-labeled neurons were found in the ventral lateral part of the PTN (Figs. 14A-C). Also at this level and more caudally there were numerous double-labeled neurons in lamina I of spinal trigeminal nucleus pars caudalis. Double-labeled neurons were most numerous in the dorsal part of lamina I. However, they were found elsewhere in small numbers along the medial border of the spinal trigeminal tract. Double-labeled neurons were seen as far caudal as the spinal-medullary junction. Double-labeled neurons were never found in

Fig. 14. Fluorescence photomicrographs of the caudal PTN and superficial laminae of the spinal trigeminal nucleus pars caudalis following injections of FG into the PBN and DiI into the VPM respectively. **A-B**: Single exposures with double-labeled neurons indicated by arrowheads. **C**: Double exposure with double-labeled neurons indicated by arrowheads. **D-E**: Lamina I of the spinal trigeminal nucleus caudalis showing double-labeled neurons (arrowheads) and overlapping topography of neurons projecting to the PBN and VPM.
Calibration bars: 50 μm.

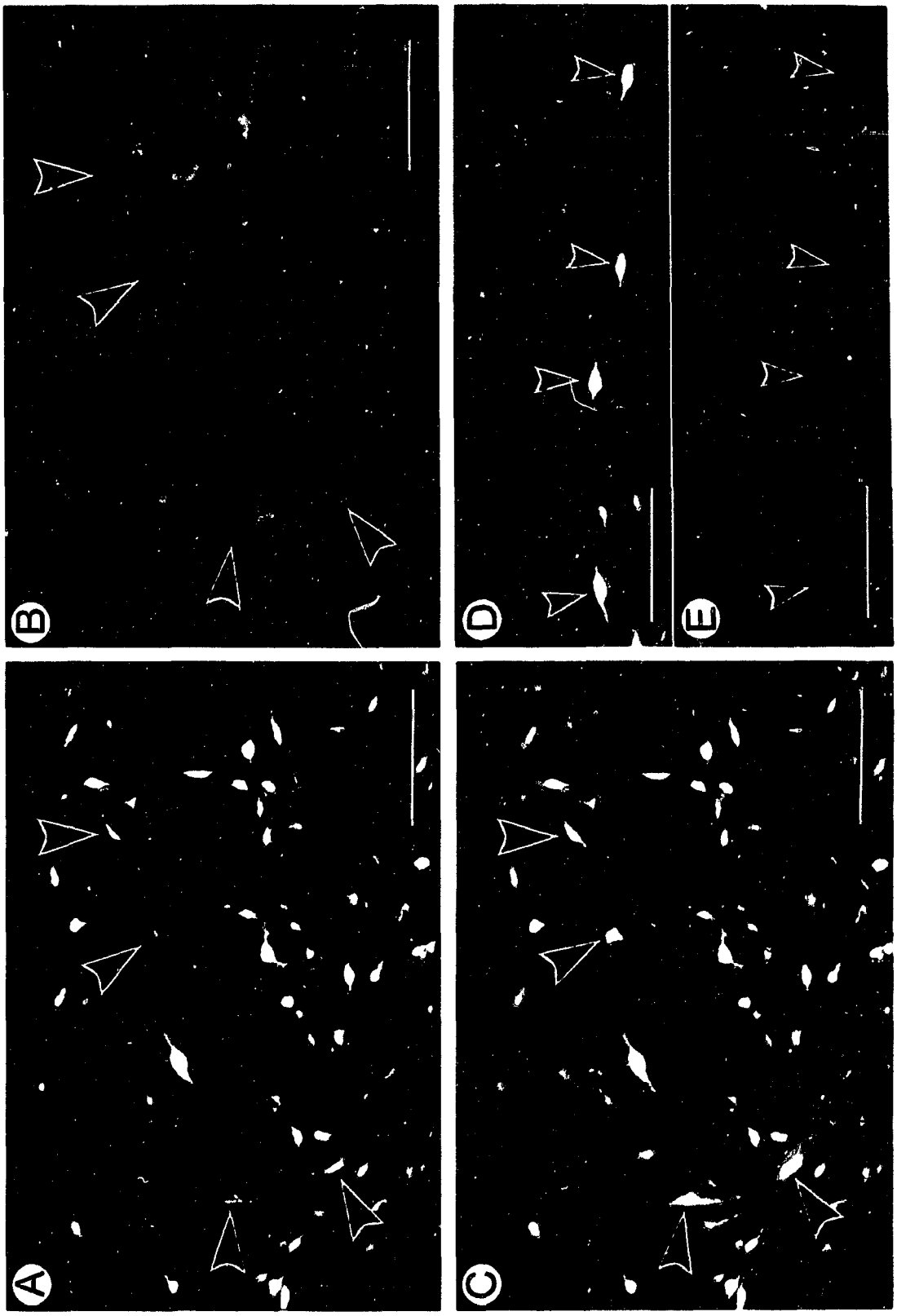

Figure 14

the deeper layers of the spinal trigeminal complex. The wide separation in excitation wavelengths for FG and DiI made identification of single and double-labeled neurons very reliable. The resistance of FG and DiI to fading under illumination made it possible to use a double exposure of a single section in order to record single and double-labeled neurons simultaneously (Fig. 14C).

DISCUSSION

Efferent Connections of the PTN

Using tetramethylrhodamine dextran (TMR) it has been possible for the first time to make very small injections of a highly sensitive anterograde tracer into the PTN. This contrasts with previous studies (Burton et al., '79; Craig and Burton, '81; Hockfield and Gobel, '82; Cechetto et al., '85; Jacquin et al., '90a, '90b; Yoshida et al., '91) in which other neuroanatomical tracers were used and which inevitably spread at the injection site to involve many nuclear structures. This is particularly relevant with regard to injections into the spinal trigeminal complex where individual laminae are small and close together and thus it is inevitable that more than one lamina is involved in the injection site. It is for this reason that the above mentioned studies could not provide precise information relevant to the laminar organization of the efferent projections. In the present study we have investigated the efferent connections of the PTN as well as the collateral projectons of the neurons in this nucleus to different nuclei in the brainstem and thalamus using anterograde and retrograde tracing techniques.

The PTN has been reported to have a number of ascending projections (Burton et al., '79; Somana and Walberg, '79; Craig and Burton, '81; Cechetto et al., '85; Panneton and Burton, '85; Granum, '86; Hayashi and Tabata, '89; Yoshida et al., '91). In addition, a descending projection to the contralateral lamina I of spinal trigeminal nucleus pars caudalis has been identified in the present study. This descending PTN efferent projection to the contralateral lamina I overlaps with neurons projecting to the thalamus and PBN. The significance of the relay of information from the PTN to the contralateral lamina I of spinal trigeminal nucleus pars caudalis is not known. It is however known that lamina I is a site for the termination of primary afferents (Kerr, '70b; Gobel and Hockfield, '77; Jacquin et al., '83; Pfaller and Arvidsson, '88; Jacquin et al., '90a), and has been implicated in pain

pathways (Price et al., '76; Dostrovsky and Hellon, '78; Burton et al., '79; Bennett et al., '80; Hu et al., '81; Shigenaga et al., '86). A crossed connection within the medullary dorsal horn has been reported although specifics about the precise location of origin of these projections as they relate to laminae was lacking (Burton et al., '79; Hockfield and Gobel, '82; Jacquin et al., '90a). The present results suggest that at least part of the contralateral afferent input to the superficial lamina I of spinal trigeminal nucleus pars caudalis consists of fibers crossing the midline from the PTN. Unlike previous studies these connections were evident for some distance caudal to the level of the injection site throughout the crescent shaped lamina I of spinal trigeminal nucleus pars caudalis. Hockfield and Gobel ('82) identified a number of different populations of neurons in the medullary dorsal horn that projected to the contralateral dorsal horn and they suggested that these projections mediated contralateral inhibition of homologous receptive fields which were excitatory on the ipsilateral side. This inhibition was most powerfully produced when noxious stimuli were applied, although innocuous stimuli also produced an affect but to a lesser extent.

Neurons located in the superficial lamina of the medullary dorsal horn and in the dorsal horn of the spinal cord are known to have projections to the periaquaductal gray (Panneton and Burton, '85) and thalamus (Burton et al., '79; Craig and Burton, '81; Bennett et al., '80; Sessle et al., '86) both of which are considered significant in the appreciation of pain. However, no such projection to the periaquaductal gray could be identified in the present study of the PTN. The absence of a PTN projection to the periaqueductal gray, a terminal locus for lamina I projections, might be taken to indicate that lamina I was not significantly involved in the injection site. Neurons projecting to the PBN (Cechetto et al., '85; Panneton and Burton, '85) from the PTN and lamina I of the spinal trigeminal nucleus pars caudalis were overlapped by efferent fibers originating in the contralateral PTN. Similarly the distribution of neurons projecting to the thalamus overlap with those projecting to the

PBN (Cechetto et al., '85; Panneton and Burton, '85) and thus are also in the terminal field of projections crossing the midline from the PTN. Outside the PTN, the heaviest anterograde labeling is concentrated over the dorsal part of lamina I where the greatest number of ventral basal complex projection neurons reside (Figs. 2A-D). Although PTN efferent labeling overlapped with neurons in lamina I , it was in the PTN that the most prominent overlap occurred (Figs. 2E-F). The existence of a crossed PTN efferent connection with lamina I of spinal trigeminal nucleus pars caudalis, an area implicated in pain mechanisms, suggest that information conveyed from the PTN might play a role in modifying or modulating pain mechanisms. Neurons projecting to the parabrachial nucleus from lamina I may also receive input from the PTN on the contralateral side which modifies their function, possibly related to autonomic function and reflexes mediated through the parabrachial nucleus.

Retrograde tracing techniques confirmed that the dense crossing connection from the PTN to contralateral PTN is provided by a relatively small number of cells distributed throughout the PTN. These cells are generally smaller in size relative to neurons projecting to the thalamus found in the caudal parts of the PTN (Fig. 4B) and more closely related in morphology to PTN neurons which project to the nucleus of the tractus solitarius and parabrachial nucleus (Figs. 2F, 12B-C).

The PTN is the site of termination of both primary visceral afferents conveyed mainly via the glossopharyngeal and vagus nerves (Jansco and Kiraly, '80; Nomura and Mizuno, '83; Bradley et al., '85; Housley et al, '87; Altschuler et al., '89) and primary somatic afferents (Arvidsson and Thomander, '84; Shigenaga et al., '86; Pfaller and Arvidsson, '88; Arvidsson and Pfaller, '90; Panneton, '91). With regard to the convergence of visceral and somatic information in the PTN it has been suggested that incoming information is integrated in the PTN and then, through connections with the nucleus of the tractus solitarius and parabrachial nucleus, influences autonomic reflexes (Cechetto et al.,

'85; Menétrey et al., '87; Menétrey and Basbaum, '87), possibly related to cardiovascular and cardiopulmonary function (Menétrey et al., 87). Furthermore, the NTS and PBN have connections with other significant autonomic centers such as the spinal intermediolateral cell column, ventrolateral medulla, paraventricular hypothalamus and basal forebrain. Through these connections the PTN may indirectly affect autonomic function (Menétrey et al., '87; Saper and Loewy, '80; Cechetto et.al, '85). Thus, the primary afferent information relayed in the PTN might be necessarily transferred in some form to the contralateral PTN where integration with information in that nucleus provides for modulating affects prior to relay to autonomic centers including the NTS and PBN.

A small number of neurons in the PTN were identified as projecting to the ventral basal complex of the thalamus. Based on the present evidence from anterograde tracing, these neurons project to the medial extension of the contralateral ventroposteromedial nucleus. Typically small numbers of neurons in the caudal one third of the PTN were retrogradely labeled following injection of FG into the ventroposteromedial nucleus. Other studies have also reported retrogradely labeled neurons in the contralateral PTN following thalamic injections (Burton et al., '79; Burton and Craig, '79; Craig and Burton, '81; Panneton and Burton, '85; Granum, '86) however, they did not discuss the distribution of these neurons in the PTN. Surprisingly, Phelan and Falls ('91a) did not report retrogradely labeled neurons in the PTN following injection of WGA-HRP into the thalamus. This is likely a reflection of the effective size of the injection site. Our results indicate that only a very small part of the medial ventroposteromedial nucleus, which is caudally located in the ventral basal complex, receives a projection from the PTN. It should be noted that retrograde tracing studies from the nucleus submedius (Yoshida et al., '91) indicate a predominantly contralateral projection from the medullary dorsal horn including the PTN and it is possible that their HRP injections in the nucleus submedius may have spread to the ventroposteromedial nucleus. Neurons in the PTN which project to the contralateral

thalamus are similar in morphology to those labeled in lamina I of spinal trigeminal nucleus pars caudalis. Neurons in lamina I of the spinal dorsal horn have been reported to be large and fusiform in shape, similar to those retrogradely labeled in the caudal PTN and lamina I of the spinal trigeminal nucleus pars caudalis following injections of FG into the ventroposteromedial nucleus. Spinothalamic neurons of the superfical layers of the spinal cord receive nociceptive primary afferent inputs (Light et al., '79) and have been implicated in pain transmission. Electrophysiological studies in rat and cat brainstem, including the PTN have produced evidence that certain neurons in this region are responsive to nociceptive as well as innocuous stimuli (Salt et al., '83; Burton et al., '79; Hayashi and Tabata, '89).

The next significant brainstem region to receive substantial innervation from the PTN is the dorsal vagal complex. Previous retrograde tracing studies have reported that neurons in the PTN and in lamina I of the nucleus pars caudalis project to the caudal NTS (Menétrey and Basbaum, '87; Menétrey et al., '87). Although the study indicated bilateral labeling it was not possible to establish whether this was truly a bilateral projection because the injections were relatively large and involved structures on both sides of the midline. The present study is the first to describe the nature and distribution of PTN prjections to the dorsal vagal complex. An unexpected finding was the existence of a moderate bilateral projection to the dorsal motor nucleus of the vagus nerve.

The efferent projection to the dorsal motor nucleus of the vagus nerve is of particular interest because it reveals an anatomical substrate by which visceral and somatic afferent inputs can have a relatively direct influence on autonomic motor function. This projection, like that to the NTS, was bilateral with an ipsilateral predominace. The dorsal motor nucleus of the vagus nerve is known to provide parasympathetic motor innervation to the gastrointestinal tract, particularly the stomach (Leslie et al., '82a; Gwyn et al., '85; Rinaman et al., '89; Rinaman and Miselis, '90). It could be speculated that information

related to upper alimentary and respiratory structures and their status received in the PTN and relayed to the DMV provides information about ingested materials which will shortly reach the stomach.

The nucleus of the tractus solitarius receives a bilateral projection from the PTN with an ipsilateral dominance. Within the caudal one half of the nucleus of the tractus solitarius, PTN efferents tended to be concentrated around the TS in the region of the subnucleus interstitialis (NTSis), a site for the termination of primary visceral afferents originating in the soft palate, pharynx and larynx (Altschuler et al., '89). The PTN also receives dense innervation from primary afferents from each of the above structures. The modalities conveyed by these primary afferents are not known and it is not clear whether these afferents are collaterals to the NTSis and the PTN. However, primary afferents terminating in the caudal 2/3 of the nucleus of the tractus solitarius are related to visceral autonomic function (Norgren, '78; Menetrey and Basbaum, '87; Altschuler et al., '89; Herbert et al., '90; Loewy and Spyer, '90). The PTN projection to the contralateral NTS appears to be diffuse and takes a path through the NTS to the contralateral side. This might also be a path for PTN efferents to the contralateral PTN as a number of fibers could be seen passing out of the NTS with a trajectory consistent with passage to the PTN of the opposite side. Although not evident in the present study, there is a report of a projection from the nucleus of the tractus solitarius to the PTN in the monkey (Beckstead et al., '80). The absence of this projection might reflect differences directly related to the species used in each study.

The rostral, or gustatory NTS, receives primary afferents from cranial nerves VII, IX and X and is densely innervated by the PTN. The entire ipsilateral rNTS contained many PTN efferent fibers. A similar pattern of labeling although not as heavy is present contralaterally in the rNTS. The rNTS, like most of the nucleus of the tractus solitarius, projects heavily to the ipsilateral parabrachial nucleus where taste information is believed to be integrated with somatic and visceral information. Convergence of information in the

PBN is believed to influence autonomic responses mediated through the parabrachial nucleus (Travers et al., '87). The heavy projection of the PTN to the rNTS which in turn projects to the parabrachial nucleus, particularly the external medial subnucleus (Herbert et al., '90), implicates the PTN in the possible modulation of taste perception. Moreover, the PTN also gives rise to direct projections to the external medial subnucleus of the PBN. This connection provides a parallel anatomical substrate to effect functions in the external medial subnucleus. Clearly, through its direct connections with the NTS (i.e., rostral and caudal) there is a great potential for the modulation of general and specific NTS functions in response to primary afferent input to the PTN, most likely to be nociception or thermal sensations which are of somatic and visceral origin. It could be envisioned that nociceptive (thermal, chemical or mechanical) information conveyed to the PTN and then superimposed on innocuous stimuli, possibly taste, could modify or inhibit a response to the taste stimulus under circumstances where stimuli have the potential for damaging tissue.

The spinal trigeminal nucleus pars oralis and principal trigeminal nucleus also received projections from the PTN. The projection to the pars oralis was sparse but present in all instances where distinct labeling occurred in the principal trigeminal nucleus, the latter receiving a moderate projection largely restricted to the dorsal part of the nucleus. These projections tended to be most evident when the PTN injection site included part of the subjacent spinal trigeminal nucleus. It is possible that the PTN has ipsilateral efferent projections to these nuclei, however, the differences in the densities of this efferent projection appear to depend on the degree to which the underlying spinal trigeminal complex is encroached upon by the injection site. This suggests that these efferent fibers are at least partially derived from intratrigeminal connections. There are numerous accounts in the literature documenting extensive intranuclear connections within the spinal trigeminal complex and between the spinal trigeminal nuclei and the principal nucleus of the trigeminal nerve (see Jacquin et al., '90b for review). This is particularly true of the caudal two

subdivisions of the spinal trigeminal complex where intranuclear connections to more rostral parts of the trigeminal complex originate primarily from local circuit neurons and to a lesser extent cells projecting to more rostral structures like the midbrain and the diencephalon (Jacquin et al., '90b). Jacquin et al. ('90b) showed through reconstruction of intranuclear axons that the majority of such axons terminate in all levels of the trigeminal complex. It is therefore likely that some, but not necessarily all of the labeled fibers observed leaving the spinal trigeminal tract at the level of the nucleus pars oralis and the principal trigeminal nucleus represent intersubnuclear projections of second order neurons in the spinal trigeminal complex located ventral to the PTN. In support of this, there appear to be no references in the literature to neurons in the PTN being retrogradely labeled following injection of retrograde tracers into the nucleus pars oralis or principal trigeminal nucleus. However, it is possible in light of the ambiguity surrounding the anatomical uniqeness of the PTN that cells were labeled in the PTN but were considered to be part of the superfical laminae of the spinal trigeminal complex.

Although the parabrachial region has been investigated extensively with regard to cytoarchitecture (Fulwiler and Saper, '84), connectivity (Saper and Loewy, '80; King, '80; Herbert et al., '90) and neurochemistry (Herbert and Saper, '90) there are undoubtedly some aspects of its extent and subdivisional cytoarchitecture which remain to be elucidated. At the level of the caudal superior cerebellar peduncle a rather dense terminal field lies medial to the middle cerebellar peduncle, dorsal to the principal trigeminal nucleus and ventrolateral to the superior cerebellar peduncle. This region did not correspond to any of the conventional regions described in Paxinos and Watson ('86). It appears to be close to the Kölliker-Fuse nucleus (Fulwiler and Saper, '84) but, close analysis reveals it to be caudal to the Kölliker-Fuse nucleus. It is possible that this unidentified region which receives a dense innervation from the PTN, is part of the parabrachial nucleus, possibly another subdivision previously not identified. On the other hand, it may represent a caudal

extension of another already established subdivision of the parabrachial nucleus although the present data does not permit the identification of that subdivision.

The dorsolateral pons, in particular the parabrachial region, receives a dense afferent projection from the PTN. Previously reported results based on the retrograde and anterograde transport of WGA-HRP established the presence of efferent connections between the PTN and the parabrachial nucleus (Cechetto et al., '85; Herbert et al., '90). However, specific information regarding the subdivisional regions of the parabrachial nucleus innervated by PTN efferents was largely established based on injections in the dorsolateral medulla and included much of the medullary dorsal horn. With the injection of a sensitive anterograde tracer such as TMR into PTN, a more precise and detailed picture of the projection from the PTN to the specific sites within the parabrachial nucleus in which PTN efferents terminate was obtained. Interestingly, many of the sites innervated in the parabrachial nucleus by the PTN also received projections from individual subnuclei in the NTS. The general notion that the rostral (gustatory) NTS innervates the medial subdivision of the parabrachial nucleus and that the caudal (visceral) NTS projects to the lateral parabrachial nucleus (Norgren, '78; Ricardo and Koh, '78) has been well accepted. However, more recently, the relationship of projections from specific NTS subnuclei to parabrachial subnuclei have been worked out with considerable precision (Herbert et al., '90). In light of the overlap of PTN terminal fields in the parabrachial nucleus (Cechetto et al., '85; present study) with a number of terminal fields originating in subnuclei of the NTS it is evident that there is a system of parallel inputs from the NTS and PTN to the PBN which have their origin in primary afferents related to the same visceral structures (Altschuler et al., '89).

It is important to reiterate that at present the modalities of the primary afferents terminating in the PTN are largely unknown and that the exact functional significance of information being relayed through the PTN to the nucleus of the tractus solitarius or

parabrachial nucleus is not known. There is, however, evidence based on capsaicin studies in the rat that chemosensitive primary afferent neurons have afferent terminations in the PTN (Janscó and Király, '80) and that such fibers are carried in the IXth and Xth cranial nerves innervating the mucous membranes of pharyngo-laryngeal tissues (Janscó-Gábor and Szolcsányi, '72). Physiological studies of the PTN region in the cat by Hayashi and Tabata ('89) indicated that neurons in the PTN are nociceptive specific (i.e., responsive to noxious mechanical or thermal stimuli) and that some of these neurons projected to the PBN. With regard to possible thermal aspects of the PTN, Kilduff et al.('83, '84, '90) using ^{14}C-2-deoxyglucose autoradiography identified the PTN as a significant brainstem structure involved in the entrance and during hibernation in the golden mantle ground squirrel. The PTN is also activated during induced hypothermia in ground squirrels, further supporting the possible role of the PTN in thermal sensory systems (Kilduff et al., '84, '90). There are also reports of neurons in the superficial medullary dorsal horn responsive to innocuous cutaneous thermal as well as noxious thermal and mechanical stimulation (Christensen and Perl, '70; Price et al., '76). Clearly the complexity of inputs, should they all be relayed to the parabrachial nucleus, might have profound effects on functions mediated by the parabrachial nucleus.

Proceeding in a caudal to rostral fashion the first subdivision of the parabrachial nucleus to exhibit afferent labeling originating in the PTN is the medial subdivision. The medial parabrachial subnucleus is known to receive efferent projections from the rostral (gustatory) NTS (Norgren, '78; Ricardo and Koh, '78) and adjacent parvicellular reticular formation (Herbert et al., '90). The rNTS receives gustatory information via the facial, glossopharyngeal and vagus nerves (Torvik, '56; Contreras et al., '82) as well as somatosensory input from the trigeminal nerve relaying information from the tongue and oral cavity (Jacquin et al., '83; Hamilton and Norgren, '84; Pfaller and Arvidsson, '88; Travers et al., '87). The overlap of PTN efferent projections in the parabrachial nucleus

with gustatory information and parvicellular reticular input is suggestive of a role for information relayed through the PTN in the function of oral motor reflexes possibly in response to gustatory and/or somatic and visceral nociceptive input. Convergence of information from the PTN, NTS and parvicellular reticular formation in the PBN may affect long-term behavioral responses related to taste through efferent connections between the parabrachial nucleus and higher levels of the neuraxis particularly the basal forebrain (Ricardo and Koh, '78; Travers et al., '87).

The PTN projects to the waist area (Fulwiler and Saper, '84) of the caudal PBN. This part of the parabrachial nucleus has been identified physiologically as a site for the convergence of vagal, hepatic and gustatory afferent input relayed from the NTS (Hermannn and Rogers, '85). It was proposed that the integration of visceral and gustatory afferent information within the brainstem may effect changes in behavior and autonomic function (Hermann and Rogers, '85). Direct visceral-vagal modulation of taste perception might also have superimposed on it the information relayed by the PTN to further modulate such responses. There is also evidence of efferent input from the caudal two thirds of the nucleus of the tractus solitarius (visceral) to the dorsal part of the waist area (Herbert et al., '90). The parabrachial nucleus has connections with limbic structures, hypothalamus and cortex (Saper and Loewy, '80; Voshart and van der Kooy, '81; Fulwiler and Saper, '84). These connections might provide the anatomical substrate whereby convergent information in PBN can be further integrated and influence long term behavioral patterns, possibly related to feeding, learned taste aversion and taste preference (Hermann and Rogers, '85).

Two other subnuclei of the PBN receive PTN efferent fibers. The first is the external medial subnucleus which receives a moderate to heavy projection from the PTN. Labeling in the external medial subnucleus is contiguous with more diffuse labeling in the external lateral subnucleus of the parabrachial nucleus. The external medial subnucleus can be

divided into a lateral and medial division based on the basis of efferent projections from the nucleus of the tractus solitarius (Herbert et al., '90). The lateral part of the external medial subnucleus receives input from the caudal two thirds of the NTS and the adjacent area postrema. The medial part of the subnucleus has reciprocal connections with the periambigual region, rostral ventrolateral reticular nucleus and the ventrolateral, intermediate and commissural subnuclei of the NTS as well as a projection originating in the gustatory/oral somatosensory rostral NTS. In general, the external medial subnucleus of the parabrachial nucleus receives diverse convergent input from viscera, somatosensory and gustatory second-order neurons. The complexity of the inputs to this region is further added to by the projections from the PTN which convey afferent information of visceral (Altschuler et al., '89; 'Panneton, '91) and somatic (Marfurt, '81; Panneton and Burton, '81; Arvidsson and Thomander, '84; Nishimori et al., '86; Shigenaga et al., '86, '88; Pfaller and Arvidsson, '88; Neuhuber and Zenker, '89; Arvidsson and Pfaller, '90) origin. Since PTN efferent projections do not distinguish between medial and lateral parts of the external medial nucleus it can be suggested that it is equally important to both regions. The PTN may indirectly, through the external medial nucleus connections with the insular, lateral and infralimbic cortex as well as with the ventromedial basal thalamic nucleus (Fulwiler and Saper, '84), influence complex integrated information related to autonomic and behavioral patterns.

PTN efferent labeling adjacent to the lateral edge of the superior cerebellar peduncle in the caudal parabrachial nucleus in an area corresponding to the external lateral nucleus was light. Labeling extended into the centrolateral and ventrolateral subnuclei at more rostral levels of the parabrachial nucleus. The external lateral nucleus receives brainstem inputs from the medial part of the NTS and the adjacent area postrema (Herbert et al., '90). The external lateral subnucleus has efferent connections with the substantia innominata, zona incerta, lateral hypothalamus, periventricular and preoptic nuclei and the central nucleus of

the amygdala (Saper and Loewy, '80; Voshart and van der Kooy, '81; Fulwiler and Saper, '84) all of which have been implicated to some degree in autonomic and/or behavioral functions.

Two rostrally located parabrachial subnuclei, the central lateral subnucleus and ventral lateral subnucleus also receive projections from the PTN. The central lateral subnucleus interposed between the external lateral and ventrolateral subnuclei contains a small PTN terminal field. Projections from the NTS to the central lateral subnucleus emanate primarily from the caudal two thirds of the medial part of the nucleus (Herbert et al., '90). Respiratory regions such as the ventrolateral, intermediate and commissural subnuclei of the NTS and rostral ventrolateral reticular nucleus have reciprocal connections with the central lateral parabrachial subnucleus (Herbert et al., '90). Efferent connections of the central lateral parabrachial nucleus terminate in the median preoptic nucleus, hypothalamic paraventricular nucleus and the bed nucleus of the stria terminalis; areas which have been implicated in emotional, behavioral and autonomic functions (Saper and Loewy, '80; Fulwiler and Saper, '84). Based on the relatively light projection to the central lateral subnucleus the information relayed from the PTN may not play an important role in influencing respiratory functions beleived to be mediated by that subnucleus. The ventral lateral subnucleus of the PBN on the other hand receives a dense PTN input. The ventral lateral subnucleus has been implicated through connections with the rostral (gustatory) NTS and adjacent parvicellular reticular area in gustatory and oral somatosensory functions. The dense projection from the PTN to the central lateral subnucleus suggests that the visceral and somatic information relayed via the PTN might provide important input to the parabrachial nucleus affecting the responses to gustatory and somatosensory stimuli related to oral and upper respiratory and alimentary structures as well as somatic regions of the head and neck.

Fig. 15 Diagrams of the efferent connections (A) and collateral organization (B) of neurons in the PTN. The relative densities of PTN efferent projections are indicated by the thickness of the lines in A.

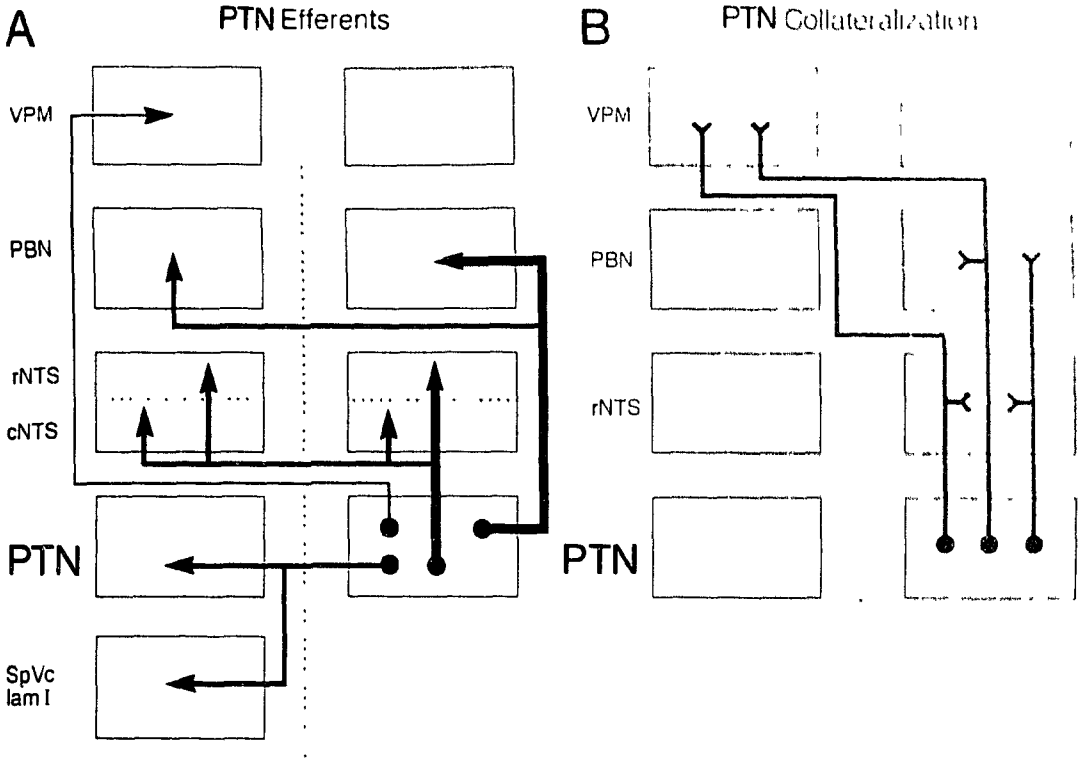
A
PTN Efferents
VPM
PBN
rNTS
cNTS
PTN
SpVc
lam I
B
PTN Collateralization
VPM
PBN
rNTS
PTN

Figure 15

It would seem, based on the high degree of connectivity between the PTN and parabrachial nucleus, that the PTN plays a role not only in the transmission of visceral and somatic information but through connections of the PBN with higher levels of the neuraxis may affect any number of important autonomic or behavioral changes.

Rostral to the level of the parabrachial nucleus only one other terminal site, the contralateral medial limb of the ventroposteromedial thalamic nucleus was identified as receiving a small PTN efferent input. Although the function of such a small projection is not clear, it is known that this region of the thalamus contains both somatosensory and gustatory responsive neurons (Lasiter and Glanzman, '83). Whether or not PTN efferents contact these neurons has not been established but projections to the thalamus from the PTN presents the possibility of information of visceral and somatic origin having a direct affect on gustatory or somatosensory mechanisms at the thalamic level.

Collateral Organization of the PTN

PTN efferent projections reach a number of different target sites (Fig. 15). With the small size of the nucleus and the considerable overlap of retrograde labeling following injections of retrograde tracers into each of these target sites it seemed reasonable that some of the neurons in the PTN would provide collateral projections to more than one target. The greatest overlap in distribution with regard to PTN efferent neurons was between the ipsilateral rNTS and PBN projection neurons. Injection of two different tracers produced closely overlapping populations of neurons in the lamina I of the spinal trigeminal nucleus pars caudalis, pars interpolaris and the PTN. Within the PTN a subpopulation of neurons (60-70%) were double-labeled indicating a considerable degree of divergent collaterals. Double-labeled neurons were similar in morphology to those which contained only one of the tracers. This might be interpreted in two ways: 1) that only a select group of neurons are collateralized or 2) that injections inevitably did not label all the possible collateralized

axons in each target area and that the degree of collateralization reported here is actually an underestimation. The collateralization of PTN projections coupled with the convergence of visceral and somatic inputs suggest a rather general modulatory function for the PTN rather than retention of modality specific information unless there is neurochemical coding as suggested for the NTS by Mantyh and Hunt ('84). Although the present study did not establish collateralization of PTN neurons to the caudal NTS and the PBN, the PTN efferent study suggests that there is potential for such collateralization.

The overlapping populations of projection neurons to the NTS and PBN extended throughout the rostral to caudal extent of the PTN and was continuous with neurons in lamina I of the spinal trigeminal nucleus pars caudalis and overlapped with caudally located PTN neurons projecting to the contralateral ventroposteromedial nucleus of the thalamus. Further collateralization of the PTN neurons was suspected due to the overlap between NTS and PBN projection neurons with PTN neurons projecting to the contralateral ventroposteromedial nucleus. As the results indicate, the caudal PTN and lamina I of the spinal trigeminal nucleus pars caudalis contained neurons which were collateralized not only to the ventroposteromedial nucleus and rNTS but also to the ventroposteromedial nucleus and PBN. The number of neurons projecting to both these sites were small and this might be expected since the number of retrogradely labeled neurons in the PTN following retrograde tracing experiments from the ventroposteromedial nucleus were very small. The collateral organization revealed in the present study raises the question as to whether or not there are neurons in the PTN which collateralize to more than two sites. It is not unreasonable to suggest that there may be PTN neurons which project to the NTS, PBN and the thalamus.

To our knowledge there is no reference in the literature to collateralized connections from lamina I of the spinal trigeminal nucleus pars caudalis and PTN neurons to the rNTS and contralateral VPM. Neurons with collateralized projections to these two sites were

similar in size and shape to neurons retrogradely labeled after injections in the ventroposteromedial nucleus. Double-labeled neurons were located in the caudal part of the PTN. If the neurons in the caudal PTN which project to the contralateral thalamus are of homologous function and connections as spinal trigeminal nucleus pars caudalis lamina I neurons, as their similarity in size and shape would suggest, then these neurons may well be implicated in a role in the processing of nociception since lamina I neurons of the medullary dorsal horn have been shown to respond to noxious stimuli (Price et al., '76; Hu et al., '81; Salt et al., '83; Panneton and Burton, '85; Sessle et al., '86). Direct physiological support for the involvement of PTN neurons in nociception has been presented by Hayashi and Tabata ('89) for the cat and by Salt et al.('83) for the rat. Although the distributions of PTN neurons projecting to the NTS and those projecting to the thalamus are overlapping, those projecting to the NTS extend deeper into lamina I of the spinal trigeminal nucleus pars caudalis than thalamic projection neurons which are located exclusively adjacent to the spinal trigeminal tract in lamina I.

It was particularly surprising to find a collateral organization with regard to lamina I of the spinal trigeminal nucleus pars caudalis and PTN efferent connections with the ipsilateral parabrachial nucleus and contralateral ventroposteromedial nucleus since this contradicts a similar study carried out in the cat (Panneton and Burton, '85). In their study the combination of FB and NY were used to retrogradely label neurons in lamina I of the medullary dorsal horn. No double-labeled neurons were observed although they did report a topographical distribution for neurons such that neurons projecting to the medial thalamus were located more superficially in the medullary dorsal horn than neurons projecting to the dorsolateral pons. Panneton and Burton ('85) also point out that double-labeled neurons may have been masked by either of the tracers used. The topographical organization of PTN neurons projecting to the PBN and thalamus in the present investigation was similar to that observed for neurons projecting to the NTS and thalamus. This would be expected

since neurons projecting to the NTS and PBN overlap extensively throughout the PTN and lamina I of the spinal trigeminal nucleus pars caudalis. The only difference between the overlap of PTN neurons projecting to the PBN and NTS was that neurons projecting to the PBN tended to extend farther caudally in lamina I of spinal trigeminal nucleus pars caudalis. This may reflect differences related to the injection sites within the PBN (i.e., caudal) and the NTS (i.e., rostral) as neither nucleus was totally covered by any one injection. The presence of double-labeled neurons in the caudal PTN and lamina I of pars caudalis indicated collateral projections to the PBN and contralateral thalamus. Typically double-labeled neurons were fusiform in shape and large relative to the more numerous single labeled neurons projecting to the ipsilateral PBN. However, small double-labeled profiles were seen (Fig. 14). These smaller profiles might represent a different class of neuron in the PTN carrying the same or different information to that of larger neurons which were morphologically similar to neurons which project to the thalamus. In fact, electron microscopic survey of the PTN has revealed three different types of neurons in the PTN (see Chapter 4) based on morphology and axosomatic contacts. The differences between the cat study (Panneton and Burton, '85) and the present study in the rat might be explained simply as species differences but technical limitations related to the tracers used, size and location of injection sites probably played a significant role in the discrepancies between the two studies. Since little is known about the function of the PTN the significance of a collateral organization to the parabrachial nucleus and ventroposteromedial nucleus is uncertain. It can be hypothesized that the information collected by neurons having projections to both the PBN and thalamus provide similar information to both nuclei, and that this information can be used to modulate functions mediated within each nucleus in unique ways or in a parallel manner. This type of collateral organization might prove particularly important in specific physiological states such as hibernation or hypothermia. In the golden mantle ground squirrel, lamina I of the spinal trigeminal

nucleus pars caudalis and the PTN are metabolically very active during the entrance into and while in deep hibernation, a state of profound physiological and autonomic change (Kilduff et al., '82,'83, '84, '88, '90). Of utmost importance to the animal is the monitoring of ambient temperature so that if changes occur autonomic and behavioral responses can be implemented. Primary afferent inputs to the PTN from regions of the head and neck (Marfurt, '81; Panneton and Burton, '81; Arvidsson and Thomander, '84; Shigenaga et al., '86, '88; Arvidsson and Pfaller, '90; Panneton, '91) as well as from the upper respiratory and alimentary tracts (Altschuler et al., '89; Panneton, '91) may convey thermal sensory information to the PTN. These areas could act as monitoring centers for the external environment (i.e., somatic inputs) while core and perhaps brain temperatures might be reflected more accurately by sensory input from the pharynx and larynx. The PTN may well convey crucial information about these environments which then can be relayed to the parabrachial nucleus, a region implicated in autonomic control of cardiorespiratory function that could mediate autonomic changes in responses to slight changes in the external or internal environment. In the event of dangerously low temperatures it may be important for behavioral alternatives, such as arousal, to occur which require measures that can only be mediated through higher levels of the neuraxis and thus connections with the thalamus and ultimately the cortex may be essential. Lamina I and PTN neurons projecting to both the parabrachial nucleus and thalamus could provide the anatomical substrate for these responses to certain environmental stimuli in the ground squirrel. If this is in fact the case it raises the question of the role of such a system in a non-hibernating animal. It is known that the rat (a non-hibernator) will show a similar metabolic pattern in lamina I and the PTN under induced hypothermic conditions (Kilduff et al., '88, '90). *This does not necessarily mean there is a functional homology in the* hibernator and non-hibernator, but rather that the PTN may respond to thermal challenges in both by increasing metabolic activity relative to surrounding brain structures.

Technical Considerations

Early neuroanatomical studies utilized retrograde and anterograde degeneration to determine neural connections. More recently a variety of neuroanatomical tracers have been developed to take advantage of the properties of axonal transport to map the connectivity of the brain. Most of these techniques have one or more limitations which must be taken into account when designing experiments and interpreting results. Tracers exhibiting both retrograde and anterograde axonal transport such as HRP may produce results that can be at times difficult to interpret due to ambiguity between terminal, axonal and dendritic labeling at the light microscopic level, particularly if reciprocal connections are present. The introduction of Phaseolus vulgaris leucoagglutinin (PHA-L), an anterograde neuroanatomical tracer, for tracing efferent connections with high resolution has helped greatly in confirming or elaborating information regarding the connectivity of many brain regions. Although PHA-L has been used with great success, the introduction of new retrograde and anterograde neuroanatomical tracers, particularly fluorescent tracers has vastly increased our knowledge of neural connectivity. Fluorescent tracers (Kuypers et al., '80) made it possible to double-label neurons easily and reliably thus establishing a means for studying the collateral organization of efferent projections from particular regions of the brain.

These fluorescent tracers, as do HRP and PHA-L, utilize the unique properties of neurons to take up and subsequently transport via axonal transport exogenous compounds to distant parts of the neuron thus revealing the distribution and origins of terminal fields. Because of their simplicity of use and generally high sensitivity, retrograde neuroanatomical fluorescent tracers have been used to a much greater degree. These retrograde tracers find their most useful application in combination, to establish whether

individual neurons give rise to collaterals to two or more destinations (Kuypers et al., '80; van der Kooy et al., '78; Takeuchi et al., '85; Tomney et al., '85).

Tetramethylrhodamine Dextran: In an attempt to develop anterograde tracers which circumvent some of the tedious processing and capricious results related to immunocytochemical processing necessary with the PHA-L techniques investigators have tested numerous fluoresent dyes (Nance and Burns, '90; Schmued et al., '90). As a result of these studies, a new fluorescent tracer, tetramethylrhodamine dextran (TMR) was identified as an anterograde neuroanatomical tracer.

TMR (10,000 MW) also called Fluoro-Ruby by Schmued et al. ('90) is visualized with a filter system (wavelength 530-560 nm) suitable for rhodamine. This tracer offers a number of distinctly favorable characteristics relative to PHA-L. For example, TMR can be applied using pressure injections rather than ionophoretic injection procedures essential to the effective delivery of PHA-L. The anterograde labeling of axons can be visualized without the immunocytochemical processing needed for PHA-L. TMR produces small and discrete injection sites following slow injection of relatively large volumes (0.2 μl) of tracer.

At the TMR injection site neuronal cell bodies and neuropil are intensely fluorescent. Interestingly, analysis of the PTN injection sites revealed the tracer to diffuse through the neuropil of the nucleus while being blocked by the heavily myelinated fiber bundles which characteristically run rostral caudal through the PTN as part of the spinal trigeminal tract. As reported by Nance and Burns ('90), optimal results were obtained when pressure injections of small to moderate volumes were administered slowly. When large volumes of tracer were used two undesirable outcomes occurred: 1) some of the tracer was forced up along the outer surface of the micropipette and spilled out onto the surface of the brainstem and 2) there is a large necrotic center present at the time of sectioning. It is important to

minimize damage at the injection site because of its potential role in facilitating the uptake of tracer by damaged fibers of passage (Nance and Burns, '90; Schmued et al., '90).

Previous reports indicate that 10 000 MW dextrans are transported predominantly anterogradely and those of greater molecular weights (70 000) only in the retrograde direction (Schmued et al., '90; Fritzsch and Wilm, '90; Heimer et al., '90). The present results suggest that 10 000 and 40 000 MW dextrans produce predominantly anterograde labeling while 70 000 MW dextrans producing less effective anterograde labeling than both 10 000 and 40 000 MW markers. In the present experiments a small number of retrogradely labeled neuronal somata were identified with all three dextrans. With respect to anterograde labeling, the most notable difference was the qualitatively more intense appearance of fibers labeled following application of the 40 000 MW dextran. This could possibly be explained by the larger dextran molecule being more highly substituted with rhodamine thereby giving it a more intense fluorescence. The reason for the 70 000 MW dextran not transporting well in either the anterograde or retrograde direction in the two cases attempted is not known. One possibility may be related to the tracer composition, in particular, the degree of substitution of lysine molecules which allow for formalin-fixation of the tissue and therefore low background fluorescence (Glover et al., '86) might have exceeded the upper limit of approximately four molecules per dextran chain reported by Gimlich and Braun ('85). A dextran molecule substituted with more than four lysine molecules per dextran chain produces a toxic molecule (Gimlich and Braun, '85). Since only a single lot of 70 000 MW dextran was used and it is not uncommon for variation to occur among commercially available tracers the present results are not sufficient to dismiss the 70 000 MW dextrans as suitable retrograde tracers.

Neurons retrogradely labeled with TMR were identified in the present study. These neurons contained brightly fluorescent granules in the cytoplasm of the soma and in the proximal trunks of the dendrites. Surprisingly, no labeled axons were identified in

relationship to retrogradely labeled neurons. The difference in labeling in axons (i e., homogeneous filling) and that of neuronal somata (i.e., granular) and the absence of labeled axons contiguous with labeled somata suggests that different as yet unidentified mechanisms are involved in the two types of transport and resultant labeling.

Brightly fluorescent non-neuronal elements which appeared in this study have been previously described as perivascular cells (Nance and Burns, '90; Schmued et al., '90) In both studies, these labeled non-neuronal cells were most evident near or in the lumen of small blood vessels and easily distinguished from retrogradely labeled neurons by their lack of dendritic processes. Our results suggest that these perivascular cells can be found at great distances from the injection site. For example lightly labeled perivascular cells were observed in the ventral basal complex following injection of the PTN. Labeling of non-neuronal elements may be the result of movement of the tracer into the microcirculation of the brain and subsequent sequestering of the tracer by fixed cells closely related to blood vessels (i.e., pericytes). This is supported by the fact that these cells appear less heavily labeled at progressively greater distances from the injection site which would be consistent with the inevitable dilution of the tracer as it moved away from the injection site. Another possibility is that circulating lymphocytes or macrophages accumulate the tracer at or near the injection site or from the blood and move to distant areas where the cell lodges and is fixed during tissue processing. Schmued et al. ('90) reported that TMR did not diffuse from labeled structures even after 12 months of storage in the dark at 4°C. In the present experiments sections have been stored up to 24 months after which time axonal and terminal labeling was found to be robust.

The mechanism by which TMR is taken up and transported is not known. However, similar physical and chemical factors as discussed for FG (Schmued and Fallon, '86) are likely to play a role in the transport of these molecules by neurons. It has been speculated

that the charge, lipid solubility, polarity and molecule size all play a role in the uptake and subsequent axonal transport.

Fluoro-gold: FG (excitation wavelength 340-380 nm) is now well established as a superior retrograde marker for tracing efferent connections in both the central as well as peripheral nervous system (Schmued et al., '90). The intense fluorescence given off by retrogradely labeled cells make them easily identified even when lightly labeled. Schmued and Fallon ('86) demonstrated that FG resulted in brightly fluorescent retrogradely labeled neurons and in most cases dendritic filling out to branching points of proximal dendrites. The present results on the other hand indicate that within retrogradely labeled neurons FG produces variable degrees of somal and dendritic filling even when similar survival periods are used. Typically neurons projecting to the parabrachial nucleus from lamina I , PTN and NTS appeared to have an accumulation of bright granules in their cytoplasm while those neurons projecting from lamina I and PTN to the contralateral ventral basal complex typically were more evenly filled and the dendritic labeling was more extensive. This might reflect some difference in the uptake, either the rate or absolute amounts in each of the two systems or the rate of transport of FG back to the cell body. It seems reasonable to assume that FG is transported by similar mechanisms in most neurons and thus it is unlikely that this accounts for the obvious differences in appearance mentioned above. However, it is possible that neurons projecting to the parabrachial nucleus only terminate in a small number of terminations while those projecting to the thalamus terminate with numerous endings thus allowing for a greater uptake of tracers per unit time. Another possible explanation for the difference in appearance of labeled neurons might reflect a difference in bulk pinocytotic events at the terminal end of axons with neurons projecting to the ventral basal complex being the more active than those projecting to the parabrachial nucleus and thus taking up more of the tracer for a given unit of time.

Fluorescent Latex Microspheres: The use of fluorescent latex microspheres commonly referred to as "latex beads" for retrograde axonal transport in the nervous system both in vivo and vitro was first demonstrated by Katz et al. ('84). A number of considerations led to utilization of latex beads in combination with FG in experiments investigating the collateralization of the PTN. Before addressing the advantages these particular tracers offer, it is worth noting why the more traditional combinations of nuclear yellow (NY) or diamidino yellow (DY) and true blue (TB) were not found suitable for the present study.

Although double-labeling was obtained with the combinations NY and TB or DY and TB, the preliminary experiments yielded unsatisfactory results. The stated advantage of these combinations, to view and photograph with a single UV filter system (Kuypers et al., '80), appeared to be a disadvantage in the viewing of PTN neurons. The reason for this is that the vast majority of PTN neurons are small with a high nucleus to cytoplasm ratio. Therefore, nuclear markers like NY and DY may mask or be masked by a cytoplasmic dye such as TB and as a consequence, it is difficult to conclude unequivocally whether or not a small cell is double-labeled. Furthermore, NY can diffuse from the labeled nucleus into the surrounding cytoplasm where it can mask cytoplasmic labeling. NY has also been noted to leak from the labeled neuron and subsequently label neuronal and non-neuronal glial structures in the immediate vicinity (Kuypers et al., '80; Bentivoglio et al., '80). As a consequence these tracers were deemed inadequate because of the difficulty in making definitive identification of double-labeled neurons and the difficulty of producing convincing photographic evidence of double-labeling. In addition to the problem of interpretation the application of these dyes (i.e. NY, DY and TB) is technically difficult due to the relatively high insolubility of all three tracers in vehicles like distilled water or phosphate buffer. Because of their insolubility these tracers were mixed as suspensions which necessitated the use of large-bore glass micropipettes which ultimately resulted in

greater damage to tissue in and around the pipette tip. In contrast the combination of FG with rhodamine- or fluorescein-labeled latex microspheres produced reliable patterns of retrograde labeling without many of the difficulties mentioned above. FG was used for those injections into the parabrachial nucleus or ventral basal complex while the latex microspheres were injected into the rostral gustatory portion of the nucleus of the tractus solitarius. Latex microspheres have diameters no greater than 0.2 μm (Katz et al., '84) and this permitted the use of small diameter (30-50 μm) glass micropipettes and pressure injections that were optimally confined to regions as small as the rostral nucleus of the tractus solitarius. Katz et al. ('84) showed that the injection sites did not change dimensions over time and, therefore the effective injection site is closely related to the area of bright fluorescence as viewed under rhodamine or FITC filter systems. It has been suggested that the hydrophobic surfaces of the latex beads tend to stick to cell membranes and that this is the reason beads remain localized in the injection site over time (Katz et al., '84).

DiI: Because experiments in which the ventral basal complex and the parabrachial nucleus were injected required large injections to provide maximal labeling, the small injection sites produced by latex beads were not adequate. The carbocyanine dye DiI or 1,1'- dioctadecyl-3, 3, 3',3'- tetramethylindocarbocyanine perchlorate has previously been shown to be retrogradely and anterogradely transported in cells in vitro and vivo (Honig and Hume, '89; Berthoud et al., '90). This particular fluorophore has an excitation spectrum similar to rhodamine and is easily visualized using green rhodamine filters. A number of technical problems had to be overcome before DiI could be used in the study of PTN collatral projections. The first hurdle to be overcome when using DiI is its virtual insolubility in aqueous media. Berthoud et al. ('90) successfully injected DiI dissolved in 100% alcohol in the dorsal motor nucleus of the vagus nerve, obtaining good axonal transport, but also noted considerable necrosis associated with injection sites. Therefore a

less toxic vehicle was desirable, preferably one that was largely aqueous. By dissolving DiI in 100% alcohol and precipitating it out slowly by the addition of a small amount of water a fine suspension of particulate DiI was obtained which could be injected via glass micropipettes. The dark red color of the dye at the injection site was visible during sectioning which made it possible to assess the approximate location of the injection prior to further processing. DiI injections resulted in patterns of retrogradely labeled neurons which corresponded to those after FG injections although there were usually a smaller number of neurons labeled following DiI applications. This was most likely due to the general tendency of FG to spread out from the injection site.

Visualization of DiI fluorescence was complicated because it is highly soluble in organic solvents such as xylene or toluene which are used in most standard mountants. When coverslipped with standard mountants DiI will over time (2-6 hours) diffuse into the medium and produce levels of background fluorescence that will prevent observation or photography. Equally problematic was dehydration of sections prior to coverslipping. This step had to be eliminated to prevent leaching out of the dye in the alcohol baths. The best solution to this conundrum was to photograph non-dehydrated and uncoverslipped sections. Under these conditions labeling was robust enough to enable excellent photographic documentation. DiI in neurons fluoresce a bright orange-red with a resolution that included retrogradely filled somata and proximal dendrites. The bright fluorescence of DiI was found to be highly resilient even after long periods of illumination. Background fluorescence was minimal, a feature particularly attractive when photomicrography is desired. Of particular note with regard to the present results with DiI was the absence of anterograde labeling, since anterograde labeling has been reported in the literature to occur in mammals including the rat (Thanos and Bonhoeffer, '87; O'Leary anaTerashima, '88; Berthoud et al., '90).

The exact nature of the uptake and transport of DiI in neurons is not known. However, a number of the unique characteristics of DiI are known and these probably play a considerable role in the uptake and transport of the dye. The DiI molecule contains two long fatty acyl chains which confer lipophilic properties on the molecule. It is the lipophilic nature of the DiI molecule which makes it insoluble in water but able to insert into the lipid fraction of the plasma membranes (Sims et al., '74; Jacobson et al., '81). Once inserted the dye can move by lateral diffusion through the lipid membrane or be taken into the cell during the course of normal membrane turnover (Honig and Hume, '89). It is unclear whether or not all neurons can take up and transport DiI from the extracellular space by bulk pinocytosis (Godement et al., '87). The present results do indicate that DiI produces similar patterns of retrograde labeling in the CNS to that of FG following thalamic injections. It is important to note that neurons are not the exclusive target of the dye as it will enter other cell types and it is therefore the physical and physiological properties of neurons which ultimately determine the rates of internalization and transport of the carbocyanine dyes. DiI has been reported to be transported in neurons at rates comparable with fast axonal transport (Godement et al., '87)

Fibers of Passage. The tracer TMR has been reported to be taken up by a subset of axons and transported in both the anterograde and retrograde direction (Schmued et al., '90). Injections into fiber tracts provided no insight into whether or not these axons took up the tracers as result of damage or by some other mechanism (Schmued et al., '90). Our results suggest that heavily myelinated fibers like those of the spinal trigeminal tract which travel through the PTN injection site (Fig. 1A) tend to remain unlabeled while the neurons and unmyelinated neuropil at the injection site fluoresce brightly. Fritzsch and Wilm ('90) reported that dextrans are only taken up by cut or damaged neuronal profiles, while Nance and Burns ('90) reported TMR to be taken up and transported by both intact and damaged profiles at the injection site. The likelihood of producing an injection site without some

kind of physical disruption of structures in the immediate area is very low and it is therefore reasonable to assume that some transport may have resulted from damaged fibers of passage although the degree to which this occurred was not assessed.

Considerable evidence in the literature suggests that FG is not taken up and transported by undamaged fibers of passage, however, damaged or cut axons do take up this tracer and transport it retrogradely (see Schmued and Fallon, '86 for review). Similarly latex microspheres are taken up and transported by damaged but not undamaged fibers of passage (Katz et al., '84). Our results indicate that the best transport was achieved when only a small necrotic center was present suggesting that cell processes in the immediate area of injection take up the tracer and transport it.

DiI, because of its unique lipophylic properties, gains access to cell membranes and moves via intracellular transport mechanisms in vivo once it has been internalized. Carbocyanine dyes can also move by lateral diffusion in the membrane of both unfixed or fixed tissue (Honig and Hume, '89; Fritzsch and Wilm, '90). It is probable that DiI can enter all membranes whether damaged or undamaged, however, this does not necessarily mean that in vivo where rapid transport appears to be largely dependent on internalization of the dye in membrane bound vesicles, fibers of passage in which the dye may insert is taken up to a sufficient degree and transported by these axons. Observations reported by Berthoud et al. ('90) suggest that DiI is taken up by damaged but not intact axons of passage.

In the present study there was no evidence for transneuronal labeling by any of the tracers which is consistent with other reports (Katz et al., '84; Schmued and Fallon, '86; Schmued et al., '90). However, DiI has been reported to produce transneuronal labeling in fixed tissue (Fritzsch and Wilm, '90) and thus there is the possibility that transneuronal labeling could occur in the in vivo situation.

CHAPTER 6

GENERAL SUMMARY

The preceding four chapters present the results of a series of experiments designed to investigate the synaptology in the medulla oblongata of primary visceral afferents originating in the upper alimentary and respiratory tracts. The two brainstem locations investigated were the nucleus of the tractus solitarius and the paratrigeminal nucleus both of which receive dense afferent projections from upper alimentary and respiratory viscera. During the course of investigating these two regions, questions arose regarding the connectivity of the PTN so a fluorescent retrograde and anterograde tracing study was carried out to elucidate the connections and collateral organization of PTN efferent projections.

The first part of this thesis (Chapters 2 and 3) deals with primary afferents originating in the upper alimentary and respiratory tracts and terminating in the NTS. Numerous studies over the past number of decades have centered on the NTS and its relationship to gustatory and autonomic function. It is a generally accepted fact that because of its important role as the primary site for the termination of primary afferents originating in visceral structures of the thorax and abdomen, particularly those related to cardiorespiratory function, the NTS is a crucial link between peripheral and central control of many homeostatic functions. In addition, the upper respiratory and alimentary tracts contain structures which have afferent links to the NTS and particularly to the subnucleus centralis (esophagus) and subnucleus interstitialis (pharynx and larynx). It is in these subnuclei that afferent projections terminate in a roughly topographical fashion. In the NTScen, esophageal afferents terminate in an overlapping fashion with more cranial parts of the esophageal tube giving rise to terminal fields that extend slightly more

rostral in the subnucleus and overlap caudally with thoracic and abdominal parts. In the NTSis and PTN pharyngeal and laryngeal afferent terminal fields overlap extensively. Such convergence of afferent information whether in the NTScen from different levels of the esophagus or in the NTSis from the anatomically and functionally linked pharynx and larynx is likely to be intimately linked to coordinated movements and functions of these structures. Examples of activities which may rely on convergent afferent input are the reflex closure of the glottis during deglutition or the smooth rostral to caudal peristaltic waves characteristic of esophageal swallowing. It has yet to be determined exactly how afferent information is processed in these subnuclei or how it is integrated to influence physiological responses in visceral structures. However, neuroanatomical, physiological and pharmacological studies are gradually providing answers to these functional questions.

The present neuroanatomical studies of primary visceral afferents and their related NTS subnuclei yielded a number of interesting results. Three points deserve particular note. The first is the observation that neurons of the NTScen and NTSis were morphologically very similar to each other and to NTS neurons described in other subnuclei of the NTS. The second point of interest is the unusual cytoarchitectural arrangement in the NTSis as compared to the NTScen. In the NTSis neurons are located around a core of unmyelinated neuropil while in the NTScen, neurons are clustered in the center of the nucleus and are surrounded by a cell-poor region of unmyelinated neuropil. The third point relates to the primary afferents terminating in the two subnuclei. The morphology of synaptic terminals of esophageal afferents in the NTScen was morphologically very similar to primary afferent terminations of pharyngeal and laryngeal origin synapsing in the NTSis. In each case, the primary afferent terminal contained predominantly round agranular vesicles and formed asymmetric synaptic contacts with small-diameter dendrites or dendritic spines. Although it is not known

what modalities are conveyed via these primary afferents to the NTS, it has been speculated that structure/function correlates exist such that terminal morphologies like those reported herein are excitatory in function. The similarity in neuronal morphology between the NTSis and the NTScen might suggest similar functions for neurons in these two areas. However, as pointed out in a previous discussion, the connectivity of these two subnuclei differs. The NTScen projects to the ventrolateral medulla where esophageal motor neurons are located while the NTSis has efferent projections not only to the ventrolateral medulla but also to the parabrachial nucleus of the dorsolateral pons. The difference in connectivity does not preclude the possibility that neurons in the NTScen and NTSis function in similar fashion, it does emphasize that these two nuclei have dissimilar efferent relay pathways. The interesting contrast in cytoarchitectonic arrangement of neurons and neuropil in the NTScen and NTSis has been noted although no clear reason for such organization is apparent. One possible interpretation of this organization might be that neurons in each of these areas are developmentally restricted such that neurons in the NTScen, because of their close proximity to one another produce dendrite arbors that extend in a radial fashion producing the cell-poor zone around a core of neurons, while neurons of the NTSis are restricted by the tractus solitarius which encircles the subnucleus and thus they produce dendritic arbors which concentrate in a central core region. There may also be functional consequences of these arrangements, however, further knowledge of the underlying mechanisms and how these relate to the organization of these subnuclei await elucidation.

The second part of this thesis (Chapters 4 and 5), deals with the primary afferent inputs and efferent connectivity and collateralization of neurons of the paratrigeminal nucleus. Located dorsolaterally in the spinal trigeminal tract, overlying the rostral spinal trigeminal nucleus pars caudalis and caudal two thirds of the spinal trigeminal nucleus pars interpolaris, the PTN receives afferent input from somatic and visceral sites, in

particular the pharynx and larynx. The PTN is a poorly understood region of the brainstem which has been incorrectly considered a rostral extension of the superficial laminae (lamina I and II; or the marginal zone and substantia gelatinosa, respectively) in many accounts in the literature. The present results suggest that the ultrastructural features and the connectivity of the PTN are unique and different from that of the marginal zone and the substantia gelatinosa of the spinal trigeminal complex. Although all three areas receive primary afferent inputs, the synaptic glomeruli characteristic of the substantia gelatinosa and the marginal zone are not evident in the PTN. Furthermore, the substantia gelatinosa is believed to be composed primarily of local circuit neurons with connections to other laminae while the PTN is clearly a projection nucleus. It is somewhat less clear how the PTN may relate to the marginal zone. Based on retrograde and anterograde studies of the PTN reported herein, it has been suggested that neurons in the caudal PTN may intermingle with neurons which are characteristic of the marginal zone. This particular aspect requires further investigation before a more conclusive statement can be made regarding the marginal zone's contribution to the neuronal and neuropil complement of the PTN. The present results report an absence of synaptic glomeruli, but the presence of complex triplet synaptic arrangements that involve axon terminals, dendrites containing vesicles and nonvesicle containing dendrites is evident. These triplets, unlike synaptic glomeruli did not appear to involve primary afferent terminals and certainly not to the extent reported for the substantia gelatinosa and marginal zone. Although the significance of synaptic triplets in the PTN is unknown, such complex interactions between neurons has implications regarding the function of the nucleus.

In light of the diverse inputs to and the paucity of information regarding the efferent connectivity of the PTN it was of interest to investigate how the PTN was related to other brain regions. Of particular note was a previously unreported projection from the PTN to

the contralateral PTN and marginal zone of the spinal trigeminal nucleus pars caudalis. Another interesting connection was the PTN projection to the region of the NTSis and to the rostral "gustatory" part of the NTS. The PTN projection to the NTSis is particularly intriguing since the NTSis also receives a dense primary afferent projection from the pharynx and larynx. The interaction between the PTN and its efferent targets such as the NTS, parabrachial nucleus and thalamus and the collateralization of these projections to two and possibly more of these sites raises questions about how the PTN influences functions in each of these efferent sites. Because of the autonomic implications associated with the NTS and parabrachial nucleus, it would be of interest to know how the PTN influences autonomic function.

Very little is known about the function of the PTN other than there are neurons located in the PTN which respond to noxious thermal and mechanical stimuli applied cutaneously and that some of these neurons project to the parabrachial region. The PTN has also been implicated in the regulation of hibernation in mammals, a process intimately linked to autonomic regulation. Although a function has not as yet been specifically attributed to the PTN, it seems reasonable to suggest, based on its diverse primary afferent input (i.e., somatic and visceral) and its widely collateralized efferent connections to autonomic centers, that the PTN is to some degree involved in the modulation of autonomic responses to external as well as internal afferent temperature or pain stimuli.

REFERENCES

Abrahams, V.C., F.J. Richmond, and J. Keane (1984) Projections from C2 and C3 nerves supplying muscles and skin of the cat neck: A study using transganglionic transport of horseradish peroxidase. J. Comp. Neurol. *230:* 142-154.

Aimi, Y., M. Fujimura, S.R. Vincent, and H. Kimura (1991) Localization of NADPH-diaphorase-containing neurons in sensory ganglia of the rat. J. Comp. Neurol. *306:* 382-392.

Allen, G.V., and D.A. Hopkins (1989) Mamillary body in the rat: Topography and synaptology of projections from the subicular cortex, prefrontal cortex, and midbrain tegmentum. J. Comp. Neurol. *286:* 311-336.

Allen, G.V., and D.A. Hopkins (1990) Topography and synaptology of mamillary body projections to the mesencephalon and pons in the rat. J. Comp. Neurol. *301:* 214-231.

Altschuler, S.M., X. Bao, D. Bieger, D.A. Hopkins, and R.R. Miselis (1989) Viscerotopic representation of the upper alimentary tract in the rat: Sensory ganglia and nuclei of the solitary and spinal trigeminal tracts. J. Comp. Neurol. *283:* 248-268.

Armstrong, D.M., V.M. Pickel, T.H. Joh, D.J. Reis, and R.J. Miller (1981) Immunocytochemical localization of catecholamine synthesizing enzymes and neuropeptides in area postrema and medial nucleus tractus solitarius of rat brain. J. Comp. Neurol. *196:* 505-517.

Armstrong, D.M., C.A. Ross, V.M. Pickel, T.H. Joh, and D.J. Reis (1982) Distribution of dopamine-, noradrenaline-, and adrenaline-containing cell bodies in the rat medulla oblongata: Demonstration by the immunocytochemical localization of catecholamine biosynthetic enzymes. J. Comp. Neurol. *212:* 173-187.

Arvidsson, J., and K. Pfaller (1990) Central projections of C4-C8 dorsal root ganglia in the rat studied by anterograde transport of WGA-HRP. J. Comp. Neurol. *292:* 349-362.

Arvidsson, J., and L. Thomander (1984) An HRP study of the central course of sensory intermediate and vagal fibres in peripheral facial nerve branches in the cat. J. Comp. Neurol. *223:* 35-45.

Åstrom, K.E. (1953) On the central course of afferent fibers in the trigeminal, facial, glossopharyngeal, and vagal nerves and their nuclei in the mouse. Acta Physiol. Scand. (Suppl.) *106:* 209-320.

Bandler, R., and I. Tork (1987) Midbrain periaqueductal grey region in the cat has afferent and efferent connections with solitary tract nuclei. Neurosci. Lett. *74:* 1-6.

Beckstead, R.M., and R. Norgren (1979) An autoradiographic examination of the central distribution of the trigeminal, facial, glossopharyngeal, and vagus nerves in the monkey. J. Comp. Neurol. *184:* 455-472.

Beckstead, R.M., J.R. Morse, and R. Norgren (1980) The nucleus of the solitary tract in the monkey: Projections to the thalamus and brain stem nuclei. J. Comp. Neurol. *190:* 258-282.

Bell, F.R., and A.M. Lawn (1955) Localization of regions in the medulla oblongata of sheep associated with rumination. J. Physiol. (Lond.) *128:* 577-592.

Bennett, G.J., M. Abdelmoumene, H. Hayashi, and R. Dubner (1980) Physiology and morphology of substantia gelatinosus neurons intracellularly stained with horseradish peroxidase. J. Comp. Neurol. *194:* 809-827.

Bennett-Clarke, C.A., N.L. Chiaia, M.F. Jacquin, and R.W. Rhoades (1992) Parvalbumin and calbindin immunocytochemistry reveal functionally distinct cell groups and vibrissa-related patterns in the trigeminal brainstem complex of the adult rat. J. Comp. Neurol. *320:* 323-338.

Bentivoglio, M., H.G.J.M. Kuypers, C.E. Catsman-Berrevoets, H. Loeve, and O. Dunn (1980) Two new fluorescent retrograde neuronal tracers which are transported over long distances. Neurosci. Lett. *18 :* 25-30.

Berthoud, H.-R., A. Jedrzejewska, and T.L. Powley (1990) Simultaneous labeling of vagal innervation of the gut and afferent projections from the visceral forebrain with DiI injected into the dorsal vagal complex in the rat. J. Comp. Neurol. *301:* 65-79.

Bieger, D. (1984) Muscarinic activation of rhombencephalic neurones controlling oesophageal peristalsis in the rat. Neuropharmacology *23:* 1451-1464.

Bieger, D., and D.A. Hopkins (1987) Viscerotopic representation of the upper alimentary tract in the medulla oblongata in the rat: The nucleus ambiguus. J. Comp. Neurol. *262:* 546-562.

Björklund, A., and T. Hökfelt (1985) Handbook of Chemical Neuroanatomy. Vol. 4: GABA and neuropeptides in the CNS, Part I. Elsevier Science Publishers B.V.

Blessing, W.W., P.R.C. Horne, T.H. Joh, J.R. Oliver, and J.O. Willoughby (1986) Distribution of tyrosine hydroxylase and neuropeptide Y-like immunoreactive neurons in rabbit medulla oblongata, with attention to colocalization studies, presumptive adrenaline-synthesizing perikarya, and vagal preganglionic cells. J. Comp. Neurol. *:248:* 285-300.

Bradley, R.M., C.M. Mistretta, C.A Bates, and H.P. Killackey (1985) Transganglionic transport of HRP from the circumvallate papilla of the rat. Brain Res. *361:* 154-161.

Burton, H., A.D. Craig, Jr., D.A. Poulos, and J.T. Molt (1979) Efferent projections from the temperature sensitive recording loci within the marginal zone of the nucleus caudalis of the spinal trigeminal complex in the cat. J. Comp. Neurol. *183 :* 753-778.

Burton, H., and A.D. Craig, Jr. (1979) Distribution of trigeminothalamic projection cells in cat and monkey. Brain Res. *161:* 515-521.

Cajal, S.R. (1909) Histologie du Système Nerveux de l'Homme et des Vertébrés, Vol. I, Madrid: Instituto de Ramón y Cajal, (reprint 1972).

Campbell, S.K., T.D. Parker, and W. Welker (1974) Somatotopic organization of the external cuneate nucleus in albino rats. Brain Res. *77:* 1-23.

Carlin, R.K., D.J. Grab, R.S. Cohen, and P. Siekevitz (1980) Isolation and characterization of postsynaptic densities from various brain regions: Enrichment of different types of postsynaptic densities. J. Cell Biol. *86:* 831-832.

Cechetto, D.F., and F.R. Calaresu (1985) Central pathways relaying cardiovascular afferent information to amygdala. Am. J. Physiol. *248:* R38-R45.

Cechetto, D.F., D.G. Standaert, and C.B. Saper (1985) Spinal and trigeminal dorsal horn projections to the parabrachial nucleus in the rat. J. Comp. Neurol. *240:* 153-160.

Chan-Palay, V. (1978a) The paratrigeminal nucleus. I. Neurons and synaptic organization. J. Neurocytol. *7:* 405-418.

Chan-Palay, V. (1978b) The paratrigeminal nucleus. II. Identification and inter-relations of catecholamine axons, indoleamine axons, and substance P immunoreactive cells in the neuropil. J. Neurocytol. *7:* 419-442.

Chazal, G. , A. Bande, A. Barbe, and J.J. Puizillout (1991) Ultrastructural organization of the interstitial subnucleus of the nucleus of the tractus solitarius in the cat: Identification of vagal afferents. J. Neurocytol. *20:* 859-874.

Chiba, T., and N. Doba (1975) The synaptic structure of catecholaminergic axon varicosities in the dorso-medial portion of the nucleus tractus solitarius of the cat: Possible roles in the regulation of cardiovascular reflexes. Brain Res. *84:* 31-46.

Chiba, T., and N. Doba (1976) Catecholaminergic axo-axonic synapses in the nucleus of the tractus solitarius (pars commissuralis) of the cat: Possible relation to presynaptic regulation of baroreceptor reflexes. Brain Res. *102:* 255-265.

Christensen, B.N., and E.R. Perl (1970) Spinal neurons specifically excited by noxious or thermal stimuli: Marginal zone of the dorsal horn. J. Neurophysiol. *33:* 293-307.

Christensen, J. (1984) Origin of sensation in the esophagus. J. Physiol. *246:* G221-G225.

Ciriello, J., A.W. Hrycyshyn, and F.R. Calaresu (1981) Glossopharyngeal and vagal afferent projections to the brainstem of the cat: A horseradish peroxidase study. J. Auton. Nerv. Syst. *4:* 63-79.

Ciriello, J., and M.M. Caverson (1986) Bidirectional cardiovascular connections between ventrolateral medulla and nucleus of the solitary tract. Brain Res. *367:* 273-281.

Clarke, G.D.,and J.S. Davison (1978) Tension receptors in the esophagus and stomach of the rat. J. Physiol. (Lond) *244:* 41-42.

Cleaton-Jones, P. (1972) Anatomical observations in the soft palate of the albino rat. Anat. Anz. *131:* 419-424.

Clerc, N., and M. Condamin (1987) Selective labeling of vagal sensory nerve fibres in the lower esophageal sphincter with anterogradely transported WGA-HRP. Brain Res. *424:* 216-224.

Cohen, M.I. (1979) Neurogenesis of respiratory rhythm in the mammal. Physiol. Rev. *59:* 1105-1173.

Coil, J.D., and R. Norgren (1979) Cells of origin of motor axons in the subdiaphragmatic vagus of the rat. J. Auton. Nerv. Syst. *1:* 203-210.

Connors, N.A., J.M. Sullivan, and K.S. Kubb (1983) An autoradiographic study of the distribution of fibers from the dorsal motor nucleus of the vagus to the digestive tube of the rat. Acta. Anat. *115:* 266-271.

Contreras, R.J., R.M. Beckstead, and R. Norgren (1982) The central projections of the trigeminal, facial, glossopharyngeal and vagus nerves: An autoradiographic study in rat. J. Auton. Nerv. Syst. *6:* 303-322.

Cottle, M.K. (1964) Degeneration studies of primary afferents of IXth and Xth cranial nerves in the cat. J. Comp. Neurol. *122:* 329-345.

Craig, A.D., Jr., and H. Burton (1981) Spinal and medullary lamina I projection to nucleus submedius in medial thalamus: A possible pain center. J. Neurophysiol. *45:* 443-466.

Cunningham, E.T., Jr., and P.E. Sawchenko (1989) A circumscribed projection from the nucleus of the solitary tract to the nucleus ambiguus in the rat: Anatomical evidence for somatostatin-28-immunoreactive interneurons subserving reflex control of esophageal motility. J. Neurosci. *9:* 1668-1682.

Cunningham, E.T., Jr., and P.E. Sawchenko (1990) Central neural control of esophageal motility: A review. Dysphagia *5:* 35-51.

Danielsen, E.H., D.J. Magnuson, and T.S. Gray (1989) The central amygdaloid nucleus innervation of the dorsal vagal complex in rat: A phaseolus vulgaris leucoagglutinin lectin anterograde tracing study. Brain Res. Bull. *22:* 705-715.

Del Fiacco, M., and A.C. Cuello (1980) Substance P- and enkephalin-containing neurones in the rat trigeminal system. Neuroscience *5:* 803-815.

Diamant, N.E. (1989) Physiology of esophageal motor function. Gastro. Clin. North Am. *18:* 179-194.

Dostrovsky, J.O., and R.F. Hellon (1978) The representation of facial temperature in the caudal trigeminal nucleus of the cat. J. Physiol. (Lond.) *277:* 29-47.

Eccles, J.C. (1964) The physiology of synapses. New York: Academic Press.

Ellis, L.C., and Rustioni, A. (1981) A correlative HRP, Golgi, and EM study of the intrinsic organization of the feline dorsal column nuclei. J. Comp. Neurol. *197:* 341-367.

Fabin, R.H., and J.D. Coulter (1985) Transneuronal transport of lectins. Brain Res. *344:* 41-48.

Fallon, J.H., and F.M. Leslie (1986) Distribution of dynorphin and enkephalin peptides in the rat brain. J. Comp. Neurol. *249:* 293-336.

Famiglietti, E. V. Jr. (1970) Dendro-dendritic synapses in the lateral geniculate nucleus of the cat. Brain Res. *20:* 181-191.

Famiglietti, E.V. Jr.,.and A. Peters (1972) The synaptic glomerulus and the intrinsic neuron in the dorsal lateral geniculate nucleus of the cat. J. Comp. Neurol. *144:* 285-334.

Finley, J.C.W., J.L. Maderdrut, L.J. Roger, and P. Petrusz (1981) The immunocytochemical localization of somatostatin-containing neurons in the rat nervous system. Neuroscience *7:* 2173-2192.

Fritzsch, B., and C. Wilm (1990) Dextran amines in neuronal tracing. Trends Neurosci. *12:* 14.

Fryscak, T., W. Zenker, and D. Kantner (1984) Afferent and efferent innervation of the rat esophagus. A tracing study with horseradish peroxidase and nuclear yellow. Anat. Embryol. *170:* 63-70.

Fulwiler, C.E., and C.B. Saper (1984) Subnuclear organization of the efferent connections of the parabrachial nucleus in the rat. Brain Res. Rev. *7:* 229-259.

Fuse, G. (1919) Beitrage zur normalen Anatomie des der spinalen Trigeminuswurzel ngehorigen Graves, von allem der Substantia gelatinosa Rolands bein Menschen. Arb. a.d. Anat. Inst. d. Kaiserlich- Japanicker Univ. Zu Sendai. *: 2:* 87-189.(cited by Phelan and Falls, '89)

Fuxe, K., T. Hökfelt, and O. Nilsson (1965) A fluorescence microscopical and electron microscopic study on certain brain areas rich in monoamine terminals. Amer. J. Anat. *117:* 33-46.

Gerlinda, E.H., and R.C. Rogers (1985) Convergence of vagal and gustatory afferent input within the parabrachial nucleus of the rat. J. Auton. Nerv. Syst. *13:* 1-17.

Getz, B., and T. Sirnes (1949) The localization within the dorsal motor vagal nucleus. An experimental investigation. J. Comp. Neurol. *90:* 95-110.

Gimlich, R.L., and J. Braun (1985) Improved fluorescent compounds for tracing cell lineage. Dev. Biol. *109:* 509-514.

Glover, J.C., G. Petursdottir, and J.K.S. Jansen (1986) Fluorescent dextran-amines used as axonal tracers in the nervous system of the chicken embryo. J. Neurosci. Meth. *18:* 255-268.

Gobel, S. (1974) Synaptic organization of the substantia gelatinosa in the spinal trigeminal nucleus of the adult cat. J. Neurocytol. *3:* 219-243.

Gobel, S. (1976) Dendro-axonic synapses in the substantia gelatinosa glomeruli in the spinal trigeminal nucleus of the cat. J. Comp. Neurol. *167:* 165-176.

Gobel, S. (1978a) Golgi studies of the neurons in layer I of the dorsal horn of the medulla (trigeminal nucleus caudalis). J. Comp. Neurol. *180:* 375-394.

Gobel, S. (1978b) Golgi studies of the neurons in layer II of the dorsal horn of the medulla (trigeminal nucleus caudalis). J. Comp. Neurol. *180:* 395-414.

Gobel, S., and Purvis (1972) Anatomical studies of the organization of the spinal V nucleus: The deep bundles and the spinal V tract. Brain Res. *48:* 27-44.

Gobel, S., and S. Hockfield (1977) An anatomical analysis of the synaptic circuitry of layers I, II and III of trigeminal nucleus pars caudalis in the cat. In *Pain in the trigeminal region.* D.J. Anderson and B. Matthews, ed., pp. 203-211. Elsevier/North-Holland, Amsterdam.

Godement, P., J. Vanslow, S. Thanos, and F. Bonhoeffer (1987) A study in developing visual system with a new method of staining neurons and their processes in fixed tissue. Development *101:* 697-713.

Gonatas, N.K., S.U. Kim, A. Stieher, and S.J. Avrameas (1977) Internalization of lectins in neuronal Gerl. J. Cell Biol. *73:* 1-13.

Granum, S.L. (1986) The spinothalamic system of the rat. I. Locations of cells of origin. J. Comp. Neurol. *247:* 159-180.

Gray, E.G. (1969) Electron microscopy of excititory and inhibitory synapses: A brief review. Prog. in Brain Res. *31:* 141-155.

Green, T., and G.J. Dockray (1987) Calcitonin gene-related peptide and substance P in afferents to the upper gastrointestinal tract in the rat. Neurosci. Lett. *76:* 151-156.

Groves, P.M., and J.C. Linder (1983) Dendro-dendritic synapses in substantia nigra: Descriptions based on analysis of serial sections. Exp. Brain Res. *49:* 209-217.

Gwyn, D.G., P.H. Wilkinson, and R.A. Leslie (1982) The ultrastructural identification of vagal terminals in the solitary nucleus of the cat after anterograde labeling with horseradish peroxidase. Neurosci. Lett. *28:* 139-143.

Gwyn, D.G., R.A. Leslie, and D.A. Hopkins (1979) Gastric afferents to the nucleus of the solitary tract in cat. Neurosci. Lett. *14:* 13-17.

Gwyn, D.G., R.A. Leslie, and D.A. Hopkins (1985) Observations on the afferent and efferent organization of the vagus nerve and the innervation of the stomach in the squirrel monkey. J. Comp. Neurol. *239:* 163-175.

Hamilton, R.B., and R. Norgren (1984) Central projections of gustatory nerves in the rat. J. Comp. Neurol. *222:* 560-577.

Hamilton, R.B., H. Ellenberger, D. Liskowsky, and N. Schneiderman (1981) Parabrachial area as mediator of bradycardia in rabbits. J. Auton. Nerv. Syst. *4:* 261-281.

Hanamori, T., and D.V. Smith (1986) Central projections of the hamster superior laryngeal nerve. Brain Res. Bull. *16:* 271-279.

Hanamori, T., and D.V. Smith (1989) Gustatory innervation in the rabbit: Central distribution of sensory and motor components of the chorda tympani, glossopharyngeal, and superior laryngeal nerves. J. Comp. Neurol. *282:* 1-14.

Harding, B.N. (1971) Dendro-dendritic synapses, including reciprocal synapses, in the ventrolateral nucleus of the monkey thalamus. Brain Res. *34:* 181-185.

Härfstrand, A., K. Fuxe, L.F. Agnati, F. Benfenati, and M. Goldstein (1986) Receptor autoradiographical evidence for high densities of ^{125}I-neuropeptide Y binding sites in the nucleus of the tractus solitarius of the normal male rat. Acta. Physiol. Scand. *128:* 195-200.

Hashim, M.A., and D. Bieger (1987) Excititory action of 5-HT on deglutitive substrates in the rat solitary complex. Brain. Res. Bull. *18:* 355-363.

Hayashi, H. and T. Takata (1989) Physiological properties of sensory neurons of the interstitial nucleus in the spinal trigeminal tract. Exp. Neurol. *105*: 219-220.

Heimer, L., S. Zahm, and L.C. Schmued (1990) The basal forebrain projection to the nuclei gemini in the rat: A combined light and electron microscopic study employing HRP and fluorescent tracers. Neuroscience *34:* 707-731.

Henderson, Z., F. Igielman, and F.E. Sherriff (1991) Organisation of the visceral solitary tract nucleus in the ferret as defined by the distribution of choline acetyltransferase and nerve growth factor immunoreactivity. Brain Res. *568:* 35-44.

Herbert, H., M.M. Moga, and C.B. Saper (1990) Connections of the parabrachial nucleus with the nucleus of the solitary tract and the medullary reticular formation in the rat. J. Comp. Neurol. *293:* 540-580.

Hermann, G.E., and R.C. Rogers (1985) Convergence of vagal and gustatory afferent input within the parabrachial nucleus of the rat. J. Auton. Nerv. Syst. *13:* 1-17.

Hockfield, S., and S. Gobel (1982) An anatomical demonstration of projections to the medullary dorsal horn (trigeminal nucleus caudalis) from rostral trigeminal nuclei and the contralateral caudal medulla. Brain. Res. *252:* 203-211.

Honig, M.G., and R.I. Hume (1989) DiI and DiO: Versatile fluorescent dyes for neuronal labeling and pathway tracing. Trends Neurosci. *12:* 333-341.

Hopkins, D.A., and G. Holstege (1978) Amygdaloid projections to the mesencephalon, pons and medulla oblongata in the cat. Exp. Brain Res. *32:* 529-547.

Housley, G.D., R.L. Martin-Body, N.J. Dawson, and J.D. Sinclair (1987) Brain stem projections of the glossopharyngeal nerve and its carotid sinus branch in the rat. Neuroscience *22:* 237-250.

Hu, J.W., J.O. Dostrovsky, and B.J. Sessle (1981) Functional properties of neurons in cat trigeminal subnucleus pars caudalis (medullary dorsal horn). I. Responses to oral-facial noxious and nonnoxious stimuli and projections to the thalamus and subnucleus oralis. J. Neurophysiol. *45:* 173-192.

Hwang, K. (1954) Mechanism of transportation of the content of the esophagus. J. Appl. Physiol. *6:* 781-796.

Itoh, K., A. Konishi, S. Nomura, N. Mizuno, Y. Nakamura, and T. Sugimoto (1979) Applications of coupled oxidation reaction to electron microscopic demonstration of horseradish peroxidase: Cobalt-glucose oxidase method. Brain Res. *175:* 341-346.

Jacobson, K., Y. How, Z. Derzko, J. Wojcleszyn, and D. Organisciak (1981) Lipid lateral diffusion in the surface membrane of cells and in multibilayers formed from plasma membrane lipids. Biochemistry *20:* 5268-5275.

Jacquin, M.F., K. Semba, M.D. Egger, and R.W. Rhoades (1983) Organization of HRP-labeled trigeminal mandibular primary afferent neurons in the rat. J. Comp. Neurol. *215:* 397-420.

Jacquin, M.F., N.L. Chiaia, J.H. Haring, and R.W. Rhoades (1990a) Trigeminal projections to contralateral dorsal horn: Central extent, peripheral origin, and plasticity. Somatos. Mot. Res. *7:* 153-183.

Jacquin, M.F., N.L. Chiaia, J.H. Haring, and R.W. Rhoades (1990b) Intersubnuclear connections with the rat trigeminal brainstem complex. Somatosens. Mot. Res. *7:* 399-420.

Janscó, G., and E. Kiraly (1980) Distribution of chemosensitive primary sensory afferents in the central nervous system of the rat. J. Comp. Neurol. *190:* 781-792.

Janscó-Gábor, A., and J. Szolcsányi (1972) Neurogenic inflammatory response. J. Dent. Res. Suppl. No. 2 *651:* 264-269.

Jean, A. (1984) Control of the central swallowing program by inputs from the peripheral receptors. A review. J. Auton. Nerv. Syst. *10:* 225-233.

Jean, A., and A. Car (1979) Inputs to the swallowing medullary neurons from the peripheral afferent fibers and the swallowing cortical area. Brain Res. *178:* 567-572.

Jennes, L., W.E. Stumpf, and P.W. Kalivas (1982) Neurotensin: Topographical distribution in rat brain by immunohistochemistry. J. Comp. Neurol. *210*: 211-224.

Jones, E.G., and T.P.S. Powell (1969) Electron microscopy of synaptic glomeruli in the thalamic relay nuclei of the cat. Proc. Royal Soc. *172:* 153-171.

Kalia, M., and D. Richter (1985) Morphology of physiologically identified slowly adapting lung stretch receptor afferents stained with intra-axonal horseradish peroxidase in the nucleus of the tractus solitarius of the cat. II. An ultrastructural analysis. J. Comp. Neurol. *241:* 521-535.

Kalia, M., and D. Richter (1988) Rapidly adapting pulmonary receptor afferents: II. Fine structure and synaptic organization of central terminal processes in the nucleus of the tractus solitarius. J. Comp. Neurol. *274:* 574-594.

Kalia, M., and J.M. Sullivan (1982) Brainstem projections of sensory and motor components of the vagus nerve in the rat. J. Comp. Neurol. *211:* 248-264.

Kalia, M., and K. Fuxe (1985) Rat medulla oblongata. I. Cytoarchitectonic considerations. J. Comp. Neurol. *233:* 285-307.

Kalia, M., and K. Fuxe, and M. Goldstein (1985) Rat medulla obglongata. II. Dopaminergic, noradrenergic (A1 and A2) and adrenergic neurons, nerve fibers, and presumptive terminal processes. J. Comp. Neurol. *233:* 308-332.

Kalia, M., and M.-M. Mesulam (1980a) Brain stem projections of sensory and motor components of the vagus complex in the cat: I. The cervical vagus and nodose ganglion. J. Comp. Neurol. *193:* 435-465.

Kalia, M., and M.-M. Mesulam (1980b) Brain stem projections of sensory and motor components of the vagus complex in the cat: II. Laryngeal, tracheo-bronchial, pulmonary, cardiac and gastrointestinal branches. J. Comp. Neurol. *193:* 467-508.

Kalia, M., K. Fuxe, T. Hökfelt, and A. Härfstrand (1984a) Somatostatin produces apnea and is localized in medullary respiratory nuclei: A possible role in apneic syndromes. Brain Res. *296:* 339-344.

Kalia, M., K. Fuxe, T. Hökfelt, O. Johanson, R. Lang, D. Ganten, C. Cuello, and L. Terenius (1984b) Distribution of neuropeptide immunoreactive nerve terminals within the subnuclei of the nucleus tractus solitarius of the rat. J. Comp. Neurol. *222*: 409-444.

Katz, L.C., A. Burkhalter, and W.J. Dreyer (1984) Fluorescent latex microspheres as a retrograde neuronal marker for in vivo and in vitro studies of visual cortex. Nature (London) *310:* 498-500.

Kawai, Y., K. Takami, S. Shiosaka, P.C. Emson, C.J. Hillyard, S. Girgis, I. MacIntyre, and M. Tohyama (1985) Topographic localization of calcitonin gene-

related peptide in the rat brain: An immunohistochemical analysis. Neuroscience *15:* 747-763.

Kerr, F.W.L. (1962) Facial, vagal, and glossopharyngeal nerves in the cat. Afferent connections. Arch. Neurol. *6:* 264-281.

Kerr, F.W.L. (1966) The ultrastructure of the spinal tract of the trigeminal nerve and the substantia gelatinosa. Exp. Neurol. *16:* 359-376.

Kerr, F.W.L. (1970a) The fine structure of the nucleus caudalis of the trigeminal nerve. Brain Res. *23:* 129-145.

Kerr, F.W.L. (1970b) The organization of primary afferents in the subnucleus caudalis of the trigeminal: A light and electron microscopic study of degeneration. Brain Res. *23:* 147-165.

Kerr, F.W.L., N. Herdler, and P. Bowron (1970) Viscerotopic organization of the vagus. J. Comp. Neurol. *138:* 279-290.

Kilduff, T.S., F.R. Sharp, and H.C. Heller (1982) [^{14}C]2-Deoxyglucose uptake in ground squirrel brain during hibernation. J. Neurosci. *2:* 143-157.

Kilduff, T.S., F.R. Sharp, and H.C. Heller (1983) Relative 2-deoxyglucose uptake of the paratrigeminal nucleus increases during hibernation. Brain Res. 262: 117-123.

Kilduff, T.S., F.R. Sharp, and H.C. Heller (1988) Progressive activation of paratrigeminal nucleus during entrance to hibernation. Am. J. Physiol. *255:* R178-R181.

Kilduff, T.S., H.C. Heller, and F.R. Sharp (1984) Paratrigeminal nucleus: A previously unrecognized thermal relay? In *Thermal Physiology*, J.R.S. Hales. ed., pp. 101-104. Raven Press, New York.

Kilduff, T.S., J.D. Miller, C.M. Radeke, F.R. Sharp, and H.C. Heller (1990) ^{14}C-2-deoxyglucose uptake in the ground squirrel brain during entrance to and arousal from hibernation. J. Neurosci. *10:* 2463-2475.

King, G.W. (1980) Topography of ascending brainstem projections to nucleus parabrachialis in the cat. J. Comp. Neurol. *191:* 615-638.

Knyihár, E., and B. Csillik (1977) Regional distribution of acid phosphatase positive axonal systems in the rat spinal cord and medulla representing central terminals of cutaneous and visceral nociceptive neurons. J. Neurol. Transm. *40:* 227-234.

Kubota, Y., S. Inagaki, S. Shiosaka, H.J. Cho, K. Tateishi, E. Hashimura, T. Hamaoka, and M. Tohyama (1983) The distribution of cholecystokinin octapeptide-like structures in the lower brain stem of the rat: An immunohistochemical analysis. Neuroscience *9*: 587-604.

Kuypers, H.G.J.M., M. Bentivoglio, C.E. Catsman-Berrevoets, and A.T. Bharos (1980) Double retrograde neuronal labeling through divergent axon collaterals using two fluorescent tracers with the same excitation wavelength which label different features of the cell. Exp. Brain Res. *40:* 383-392.

Lasiter, P.S. and D.L. Glanzman (1983) Axon collaterals of positive taste area neurons project to the posterior ventromedial thalamic nucleus and to the gustatory neocortex. Brain Res. *58:* 299-304.

Lemann, W., C.B. Saper, D.B. Rye, and B.H. Wainer (1985) Stabilization of the TMB reaction product for electron microscopic retrograde and anterograde fiber tracing. Brain Res. *14:* 277-281.

Leslie, R.A. (1985) Neuroactive substances in the dorsal vagal complex of the medulla oblongata: Nucleus of the tractus solitarius, area postrema, and dorsal motor nucleus of the vagus. Neurochem. Int. *7:* 191-211.

Leslie, R.A., D.G. Gwyn, and D.A. Hopkins (1982a) The central distribution of the cervical vagus nerve and gastric afferent and efferent projections in the rat. Brain Res. Bull. *8:* 37-43.

Leslie, R.A., D.G. Gwyn, and D.A. Hopkins (1982b) The ultrastructure of the subnucleus gelatinosus of the nucleus of the tractus solitarius in the cat. J. Comp. Neurol. *206:* 109-118.

Lieberman, A.R. (1973) Neurons with presynaptic perikarya and presynaptic dendrites in the rat lateral geniculate nucleus. Brain Res. *59:* 35-59.

Lieberman, A.R., and K.E. Webster (1974) Aspects of the synaptic organization of intrinsic neurons in the dorsal lateral geniculate nucleus: An ultrastructural study of the normal and of the experimentally deafferented nucleus in the rat. J. Neurocytol. *3:* 677-710.

Light, A.R., D.L. Trevino, and E.R. Perl (1979) Morphological features of functionally defined neurons in the marginal zone and substantia gelatinosa of the spinal dorsal horn. J. Comp. Neurol. *186:* 151-172.

Loewy, A.D., and H. Burton (1978) Nuclei of the solitary tract: Efferent projections to the lower brain stem and spinal cord of the cat. J. Comp. Neurol. *181:* 421-450.

Loewy, A.D., and K.M. Spyer (1990) Central Regulation of Autonomic Functions. Oxford University Press, New York. pp. 68-208.

Lucier, G.E., and R. Egizii (1986) Central projections of the ethmoidal nerve of the cat as determined by the horseradish peroxidase tracer technique. J. Comp. Neurol. *247:* 123-132.

Maley, B.E., B.W. Newton., K.A. Howes, L.M. Herman, C.L. Oloff, K.C. Smith, and R.P. Elde (1987) Immunohistochemical localization of substance P and enkephalin in the nucleus tractus solitarii of the Rhesus monkey, *Macaca mulatta*.. J. Comp. Neurol. *260:* 483-490.

Mantyh, P.W., and S.P. Hunt (1984) Neuropeptides are present in projection neurones at all levels in visceral and taste pathways: From periphery to sensory cortex. Brain Res. *299:* 297-311.

Marfurt, C.F. (1981) The central projections of trigeminal primary afferent neurons in the cat as determined by the transganglionic transport of horseradish peroxidase. J. Comp. Neurol. *203:* 785-798.

Marfurt, C.F., E.M. Zaleski, C.E. Adams, and C.L. Welter (1986) Sympathetic nerve fibers in the rat orofacial and cerebral tissues as revealed by the HRP-WGA tract tracing technique: A light and electron microscopic study. Brain Res. *366:* 373-378.

Matthews, M.A., T.V. Hernandez, K.D. Hoffmann, A.I. Romanska, and S.L. Liles (1989) Synaptic substrates for enkephalinergic and serotonergic interactions with dental primary afferent terminals in trigeminal subnucleus interpolaris: An immunocytochemical study using peroxidase and colloidal gold. Synapse *4:* 175-195.

Meessen, H., and J. Olszewski (1949) A Cytoarchitectonic Atlas of the Rhombencephalon of the Rabbit. S. Karger, Basel-New York.

Mei, N. (1983) Sensory structures in the viscera, In: D. Ottoson (Ed.), *Progress in sensory physiology*, Vol. IV. Springer, Berlin. pp. 1-42.

Mei, N. (1985) Intestinal chemosensitivity. Physiol. Rev. *65:* 211-237.

Melander, T., T. Hökfelt, and A. Rökaeus (1986) Distribution of galanin-like immunoreactivity in the rat central nervous system. J. Comp. Neurol. *248:* 475-517.

Menétrey, D., and A.I. Basbaum (1987) Spinal and trigeminal projections to the nucleus of the solitary tract: A possible substrate for somatovisceral and viscerovisceral reflex activation. J. Comp. Neurol. *255:* 439-445.

Menétrey, D.J., J. Leah, and J. de Pommery (1987) Efferent projection of the paratrigeminal nucleus in the rat. Neurosci. Lett. *73:* 48-52.

Mesulam, M.-M. (1978) Tetramethyl benzidine for horseradish peroxidase neurochemistry: A non-carcinogenic blue reaction-product with superior sensitivity for visualizing neural afferents and efferents. J. Histochem. Cytochem. *26:* 106-117.

Miller, A.J. (1982) Deglutition. Physiol Rev. *62:* 129-172.

Miller, A.J. (1986) Neurophysiological basis of swallowing. Dysphagia *1:* 91-100.

Morest, K.D. (1967) Experimental study of the projections of the nucleus of the tractus solitarius and the area postrema in the cat. J. Comp. Neurol. *130:* 277-300.

Morest, K.D. (1971) Dendrodendritic synapses of cells that have axons: The fine structure of the golgi type II cell in the medial geniculate body of the cat. Z. Anat. Entwickl.-Gesch. *133:* 216-246.

Moyles, M.R., and D.A. Hopkins (1988) Fine structure and synaptology of esophageal motor neurons in the rat. Neurosci. Abstr. *14:* 338.

Nance, D.M., and J. Burns (1990) Fluorescent dextrans as sensitive anterograde neuroanatomical tracers: Applications and pitfalls. Brain Res. Bull. *25:* 139-145.

Nazruddin, S. Suemune, Y. Shirana, K. Yamauchi, and Y. Shigenaga (1989) The cells of origin of the hypoglossal afferent nerves and central projections in the cat. Brain Res. *490:* 219-235.

Nelson, J.B., and J.E. Richter (1989) Upper esophageal motility disorders. Gastro. Clin. North Am. *18:* 195-217.

Neuhuber, W. (1987) Sensory vagal innervation of the rat esophagus and cardia: A light and electron microscopic anterograde tracing study. J. Auton. Nerv. Syst. *20:* 243-255.

Neuhuber, W.L., and W. Zenker (1989) Central distribution of cervical primary afferents in the rat, with emphasis on proprioceptive projections to vestibular, perihypoglossal, and upper thoracic spinal nuclei. J. Comp. Neurol. *280:* 231-253.

Nishimori, T., M. Sera, S. Suemune, A. Yoshida, K. Tsuru, Y. Tsuiki, T. Akisaka, T. Okamoto, Y. Dateoka, and Y. Shigenaga (1986) The distribution of muscle primary afferents from the masseter nerve to the trigeminal sensory nuclei. Brain Res. *372:* 375-381.

Nomura, S., and N. Mizuno (1982) Central distribution of afferent and efferent components of the glossopharyngeal nerve: An HRP study in the cat. Brain Res. *236:* 1-13.

Nomura, S., and N. Mizuno (1983) Central distribution of efferent and afferent components of the cervical branches of the vagus nerve: A HRP study in the cat. Anat. Embryol. *166:* 1-18.

Norgren, R. (1976) Taste pathways to hypothalamus and amygdala. J. Comp. Neurol. *166:* 17-30.

Norgren, R. (1978) Projections from the the nucleus of the solitary tract in the rat. Neuroscience *3:* 207-218.

Norgren, R. (1985) Taste and the autonomic nervous system. Chem. Senses *10:* 143-161.

O'Leary, D.D.M., and T. Terashima (1988) Cortical axons branch to multiple subcortical targets by interstitial axon budding: Implications for target recognition and "Waiting Periods". Neuron *1:* 901-910.

Ogawa, H., T. Hayama, and S. Ito (1982) Convergence of input from tongue and palate to the parabrachial nucleus neurons of rats. Neurosci. Lett. *28:* 15-20.

Olszewski, J., and D.W. Baxter (1954) Cytoarchitecture of the human brainstem. Philadelphia and Montreal: J.B. Lippincott Co.

Oswaldo-Cruz, E, and C.E. Rocha-Miranda (1968) The brain of the opossum (*Didelphis marsupialis*): A cytoarchitectonic atlas in stereotaxis coordinates. Rio de Janeiro: Instituto de Biofisica.

Panneton, W.M. (1991) Primary afferent projections from the upper respiratory tract in the muskrat. J. Comp. Neurol. *308:* 51-65.

Panneton, W.M., and H. Burton (1981) Corneal and periocular representation within the trigeminal sensory complex in the cat studied with transganglionic transport of horseradish peroxidase. J. Comp. Neurol. *199:* 327-344.

Panneton, W.M., and H. Burton (1985) Projections from the paratrigeminal nucleus and the medullary and spinal dorsal horns to the peribrachial area of the cat. Neuroscience *3:* 779-797.

Panneton, W.M., and A.D. Loewy (1980) Projections of the carotid sinus nerve to the nucleus of the solitary tract. Brain Res. *191:* 239-244.

Papez, J.W. (1929) Comparative Neurology. Thomas Y. Crowell Co., New York.

Paxinos, G. (1990) *The Human Nervous System.* Academic Press, Inc. San Diego.

Paxinos, G., and C.Watson (1986) *The rat brain in stereotaxic coordinates.* New York, Academic Press,

Peters, A., S.L. Palay, and H. deF. Webster (1991) *The fine structure of the nervous system: Neurons and their supporting cells.* New York, Oxford University Press. pp. 3-199.

Pfaller, K., and J. Arvidsson (1988) Central distribution of trigeminal and upper cervical primary afferents in the rat studied by anterograde transport of horseradish peroxidase coupled to wheat germ agglutinin. J. Comp. Neurol. *268:* 91-108.

Phelan, K.D., and W.M. Falls (1989) The interstitial system of the spinal trigeminal tract in the rat: Anatomical evidence for morphological and functional heterogenecity. Somatosens. Motor Res. *6:* 367-399.

Phelan, K.D., and W.M. Falls (1991) A comparison of the distribution and morphology of thalamic, cerebellar and spinal projection neurons in rat trigeminal nucleus interpolaris. Neuroscience *40:* 497-511.

Price, D.D., R. Dubner, and J.W. Hu (1976) Trigeminothalamic neurons in the nucleus caudalis responsive to tactile, thermal, and nociceptive stimulation of monkey's face. J. Neurophysiol. *39:* 936-953.

Ralston, H.J. III (1971) Evidence for presynaptic dendrites and a proposal of their mechanism of action. Nature *230:* 585-587.

Ralston, H.J. III, and D.D. Ralston (1979) The distribution of dorsal root axons in laminae I, II and III of the macaque spinal cord: A quantitative electron microscopic study. J. Comp. Neurol. *184:* 643-684.

Ramon-Moliner, E. (1977) The reciprocal synapses of the olfactory bulb: Questioning the evidence. Brain Res. *128:* 1-20.

Reiner, P.B., R.E. Shapiro, R. Miselis, and S.R. Vincent (1986) Subnuclear organization of the nucleus of the tractus solitarius: Immunohistochemical and tract-tracing studies. Anat. Rec. *214:* 106A-107A.

Reiner, P.B., and S.R. Vincent (1986) The distribution of tyrosine hydroxylase, dopamine-ß-hydroxylase, and phenylethanolamine-N-methyltransferase immunoreactive neurons in the feline medulla oblongata. J. Comp. Neurol. *248:* 528-531.

Rhoton, A.L., Jr., J.L. O'Leary, and J.P. Ferguson (1966) The trigeminal, facial, vagal, and glossopharyngeal nerves in the monkey. Arch. Neurol. *14:* 530-540.

Ricardo, J.A., and E.T. Koh (1978) Anatomical evidence of direct projections from the nucleus of the solitary tract to the hypothalamus, amygdala, and other forebrain structures in the rat. Brain Res. *153:* 1-26.

Rinaman, L., and R.R. Miselis (1990) Thyrotropin-releasing hormone-immunoreactive nerve terminals synapse on the dendrites of gastric vagal motoneurons in the rat. J. Comp. Neurol. *294:* 235-251.

Rinaman, L., J.P. Card, J.S. Schwaber, and R.R. Miselis (1989) Ultrastructural demonstration of a gastric monosynaptic vagal circuit in the nucleus of the solitary tract in rat. J. Neurosci. *9:* 1985-1996.

Rodrigo, J. J. DeFilipe, E.M. Robles-Chillida, J.A. Perez-Anton, I. Mayo, A. Gomez (1982) Sensory vagal nature and anatomical access paths to the esophagus laminar nerve endings in myenteric ganglia: Determination by surgical degeneration methods. Acta. Anat. *112:* 47-57.

Ross, C.A., D.A. Ruggerio, and D.J. Reis (1985) Projections from the nucleus tractus solitarii to the rostral ventrolateral medulla. J. Comp.Neurol. *242:* 511-534.

Rustioni, A., S. Sanyal, and H.G.J.M. Kuypers (1971) A histochemical study of the distribution of the trigeminal divisions in the substantia gelatinosa of the rat. Brain Res. *32:* 45-52.

Salt, T.E., R. Morris, and R.G. Hill (1983) Distribution of substance P-responsive and nociceptive neurons in relation to substance P-immunoreactivity within the caudal trigeminal nucleus of the rat. Brain Res. *273:* 217-228.

Saper, C.B., A.D. Loewy, L.W. Swanson, and W.M. Cowan (1976) Direct hypothalamo-autonomic connections. Brain Res. *117:* 305-312.

Saper, C.B., and A D. Loewy (1980) Efferent connections of the parabrachial nucleus in the rat. Brain Res. *197:* 291-317.

Schmued, L., K. Kyriakidis, and L. Heimer (1990) In vivo anterograde and retrograde axonal transport of the fluorescent rhodamine-dextran-amine, Fluoro-Ruby, within the CNS. Brain Res. *526:* 127-134.

Schmued, L.C., and J.H. Fallon (1986) Fluoro-Gold: A new fluorescent retrograde axonal tracer with numerous unique properties. Brain Res. *377:* 147-154.

Schultzberg, M., T. Hökfelt, G. Nilsson, L. Terenius, J.F. Rehfeld, M. Brown, R. Elde, M. Goldstein, and S. Said (1980) Distribution of peptide- and catecholamine-containing neurons in the gastro-intestinal tract of the rat and guinea-pig: Immunohistochemical studies with antisera to substance P, vasoactive intestinal polypeptide, enkephalins, somatstatin, gastrin/cholecystokinin, neurotensin and dopamine ß-hydroxylase. Neuroscience *5:* 689-744.

Sessle, B.J., J.W. Hu, N. Amano, and G. Zhong (1986) Convergence of cutaneous, tooth pulp, visceral, neck and muscle afferents onto nociceptive and non-nociceptive neurons in trigeminal subnucleus caudalis (medullary dorsal horn) and its implication for referred pain. Pain *27:* 219-235.

Shapiro, R.E., and R.R. Miselis (1985) The central neural connections of the area postrema of the rat. J. Comp. Neurol. *234:* 344-364.

Shigenaga, Y., I.C. Chen, and S. Suemune (1986) Oral and facial representation within the medullary and upper cervical dorsal horns in the cat. J. Comp. Neurol. *243:* 388-406.

Shigenaga, Y., M. Sera, T. Nishimori, S. Suemune, M. Nishimura, A. Yoshida, and K. Tsuru (1988) The central projection of masticatory afferent fibers to the trigeminal sensory nuclear complex and upper cervical spinal cord. J. Comp. Neurol. *268:* 489-507.

Shults, C.W., R.Quirion , B. Chronwall, T. N. Chase, and T. L. O'Donohue (1984) A comparison of the anatomical distribution of substance P and substance P receptors in the rat central neurvous system. Peptides *5:* 1097-1128.

Shults, R. C., A. R. Light, and S. Donaghy (1985) Interstitial nucleus of the spinal trigeminal tract : A specific nociceptive relay for oral and peri-oral structures ? Neurosci. Abstr. *11:* 578.

Siggins, G.R., and D.L. Gruol (1986) Mechanisms of transmitter action in the vertebrate central nervous system. In Bloom F.E. (ed): *The Nervous System: Intrinsic Regulatory Systems of the Brain.*. Bethesda, MD: Am. Physio. Soc. pp 1-114.

Sims, P.J., A.S. Waggoner, C.-H. Wang, and J.F. Hoffman (1974) Studies on the mechanism by which cyanine dyes measure membrane potential in red blood cells and phosophatidylcholine vesicles. Biochemistry. *13:* 3315-3330.

Skofitsch, G., and D.M. Jacobowitz (1985) Immunohistochemical mapping of galanin-like neurons in the rat central nervous system. Peptides *6:* 509-546.

Skofitsch, G., N. Zamir, C.J. Helke, J.M. Savitt, and D.M. Jacobowitz (1985) Corticotropin releasing factor-like immunoreactivity in sensory ganglia and capsaicin sensitive neurons of the rat central nervous system: Colocalization with other neuropeptides. Peptides *6:* 307-318.

Somana, R., and F. Walberg (1979) The cerebellar projection from the paratrigeminal nucleus in the cat. Neurosci. Lett. *15:* 49-54.

Sweazy, R.D., and R.M. Bradley (1986) Central connections of the lingual-tonsillar branch of the glossopharyngeal nerve and the superior laryngeal nerve in lamb. J. Comp. Neurol. *245:* 471-482.

Taber, E. (1961) The cytoarchitecture of the brain stem of the cat. I. Brain stem nuclei of cat. J. Comp. Neurol. *116:* 27-69.

Takahashi, Y., M. Tohyama, K. Satoh, T. Sakumoto, A. Kashiba, and N. Shimizu (1980) Fine structure of noradrenaline nerve terminals in the dorsomedial portion of the nucleus tractus solitarii as demonstrated by a modified potassium permanganate method. J. Comp. Neurol. *189:* 525-535.

Takeuchi, Y., G.V. Allen, and D.A. Hopkins (1985) Transnuclear transport and axon collateral projections of the mamillary nuclei in the rat. Brain Res. Bull. *14:* 453-468.

Thanos, S., and F. Bonhoeffer (1987) Axonal arborization in the developing chick retinotectal system. J. Comp. Neurol. *261:* 155-164.

Tomney, P.A., D.A. Hopkins, and J.A Armour (1985) Axonal branching of canine sympathetic postganglionic cardiopulmonary neurons. A retrograde fluorescent labeling study. Brain Res. Bull. *14:* 443-452.

Torvik, A. (1956) Afferent connections to the sensory trigeminal nuclei, the nucleus of the solitary tract and adjacent structures: An experimental study in the rat. J. Comp. Neurol. *106:* 51-142.

Travers, J.B., S.P. Travers, and R.Norgren (1987) Gustatory neural processing in the hindbrain. Ann. Rev. Neurosci. *10:* 595-632.

Travers, S.P., and D.V. Smith (1984) Responsiveness of neurons in the hamster parabrachial nuclei to taste mixtures. J. Gen. Physiol. *84:* 221-250.

Trojanowski, J.Q. (1983) Native and derivatized lectins for in vitro studies of neuronal connectivity and neuronal cell biology. J. Neurosci. Meth. *9:* 185-204.

Trojanowski, J.Q., and M.L. Schmidt (1984) Interneuronal transfer of axonally transported proteins: Studies with HRP and HRP conjugates of wheatgerm

agglutinin, cholera toxin and the B subunit of cholera toxin. Brain Res. *331:* 366-369.

Uchizono, K. (1965) Charateristics of excititory and inhibitory synapses in the central nervous system of the cat. Nature *207:* 642-643.

van der Kooy, D., H.G.J.M. Kuypers, and C. Catsman-Berrevoets (1978) Single mammillary body cells with divergent axon collaterals. Demonstration by a simple fluorescent retrograde double labeling technique in the rat. Brain Res. *158:* 189-196.

van der Kooy, L.Y. Koda, J.F McGinty, C.R Gerfen, and F.E. Bloom (1984) The organization of projections from the cortex, amygdala, and hypothalamus to the nucleus of the solitary tract in rat. J. Comp. Neurol. *224:* 1-24.

Velley, L., T.A. Milner, J. Chan, S.F. Morrison, and V.M. Pickel (1991) Relationship of Met-enkephalin-like immunoreactivity to vagal afferents and motor dendrites in the nucleus of the solitary tract: A light and electron microscopic dual labeling study. Brain Res. *55 :* 298-312.

Von Euler, C., J.N. Hayward, I. Martilla, and R.J. Wyman (1973) Respiratory neurons of the ventrolateral nucleus of the solitary tract in the cat: Vagal input, spinal connections and morphological identification. Brain Res. *61:* 1-22.

Voshart, K., and D. van der Kooy (1981) The organization of the efferent projections of the parabrachial nucleus to the forebrain in the rat: A fluorescent double-labeling study. Brain Res. *212:* 271-286.

Whitehead, M.C. (1988) Neuronal architecture of the nucleus of the solitary tract in the hamster. J. Comp. Neurol. *276:* 547-572.

Whitehead, M.C., and M.E. Frank (1983) Anatomy of the gustatory system in the hamster: Central projections of the chorda tympani and the lingual nerve. J. Comp. Neurol. *220:* 378-395.

William, R.G., and G.J. Dockray (1983) Distribution of enkaphalin-related peptides in rat brain: Immunohistochemical studies using antisera to met-enkephalin and met-enkephalin $Arg^{6}Phe^{7}$. Neuroscience *9:* 563-586.

Willett, C.J., D.G. Gwyn, J.G. Rutherford, and R.A. Leslie (1986) Cortical projections to the nucleus of the tractus solitarius: An HRP study in the cat. Brain Res. Bull. *16:* 497-505.

Willett C.J., J.G. Rutherford, D.G. Gwyn, and R.A. Leslie (1987) Projections between the hypothalamus and the dorsal vagal complex in the cat: An HRP and autoradiographic study. Brain Res. Bull. *18:* 63-71.

Yoshida, A., J.O. Dostrovsky, B.J. Sessle, and C.Y. Chiang (1991) Trigeminal projections to the nucleus submedius of the thalamus of the rat. Neurol. *307:* 609-625.

Zhu, C.G., C. Sandri, and K. Akert (1981) Morphological identification of axoaxonic and dendro-dendritic synapses in the rat substantia gelatinosa. Brain Res. *230:* 25-40.

Zhu, P.C., A. Thureson-Klein, and R.L. Klein (1986) Exocytosis from large dense cored vesicles outside the active synaptic zones of terminals within the trigeminal subnucleus caudalis: A possible mechanism for neuropeptide release. Neuroscience *19:* 43-54.